

# Deposit & Copying of Dissertation Declaration



UNIVERSITY OF  
CAMBRIDGE

Board of Graduate Studies

Please note that you will also need to bind a copy of this Declaration into your final, hardbound copy of thesis - this has to be the very first page of the hardbound thesis.

1	Surname (Family Name)	Forenames(s)	Title
	Ho	Hin Chung Jonathan	Mr.
2	Title of Dissertation as approved by the Degree Committee		
	Computational study of hydro-environmental processes of Poyang Lake, China		

In accordance with the University Regulations in *Statutes and Ordinances* for the PhD, MSc and MLitt Degrees, I agree to deposit one print copy of my dissertation entitled above and one print copy of the summary with the Secretary of the Board of Graduate Studies who shall deposit the dissertation and summary in the University Library under the following terms and conditions:

## 1. Dissertation Author Declaration

I am the author of this dissertation and hereby give the University the right to make my dissertation available in print form as described in 2. below.

My dissertation is my original work and a product of my own research endeavours and includes nothing which is the outcome of work done in collaboration with others except as declared in the Preface and specified in the text. I hereby assert my moral right to be identified as the author of the dissertation.

The deposit and dissemination of my dissertation by the University does not constitute a breach of any other agreement, publishing or otherwise, including any confidentiality or publication restriction provisions in sponsorship or collaboration agreements governing my research or work at the University or elsewhere.

## 2. Access to Dissertation

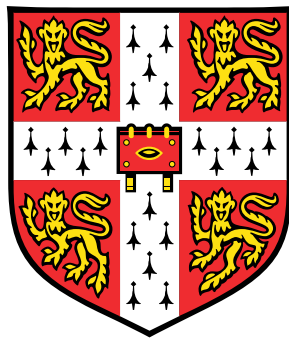
I understand that one print copy of my dissertation will be deposited in the University Library for archival and preservation purposes, and that, unless upon my application restricted access to my dissertation for a specified period of time has been granted by the Board of Graduate Studies prior to this deposit, the dissertation will be made available by the University Library for consultation by readers in accordance with University Library Regulations and copies of my dissertation may be provided to readers in accordance with applicable legislation.

3	Signature	Date
		28th October 2019

## Corresponding Regulation

Before being admitted to a degree, a student shall deposit with the Secretary of the Board one copy of his or her hardbound dissertation and one copy of the summary (bearing student's name and thesis title), both the dissertation and the summary in a form approved by the Board. The Secretary shall deposit the copy of the dissertation together with the copy of the summary in the University Library where, subject to restricted access to the dissertation for a specified period of time having been granted by the Board of Graduate Studies, they shall be made available for consultation by readers in accordance with University Library Regulations and copies of the dissertation provided to readers in accordance with applicable legislation.

# Computational study of hydro-environmental processes of Poyang Lake, China



**Jonathan Hin Chung Ho**

Department of Engineering

University of Cambridge

This dissertation is submitted for the degree of

*Doctor of Philosophy*

Christ's College

September 2018



*To my dearest mother*



## Declaration

I hereby declare that except where specific reference is made to the work of others, the contents of this dissertation are original and have not been submitted in whole or in part for consideration for any other degree or qualification in this, or any other University. This dissertation is the result of my own work and includes nothing which is the outcome of work done in collaboration, except where specifically indicated in the text. This dissertation contains less than 65,000 words including appendices, bibliography, footnotes, tables and equations and has less than 150 figures.

Jonathan Ho  
September 2018



Computational study of hydro-environmental processes of Poyang Lake, China

Jonathan Hin Chung Ho

## **Abstract**

Poyang Lake, the largest freshwater lake in China, plays a key role in regulating the hydrology, water quality and ecosystem in the middle reaches of the Yangtze River. Recent industrial development and urbanization in Jiangxi province have driven rapid increase in water consumption and deterioration of water quality, exerting pressure on water utilization in the Poyang Lake basin. In order to set up an integrated water management framework for the protection of Poyang Lake's ecosystem and surrounding communities, an accurate and representative evaluation of the hydraulic and environmental challenges is vital. In this research, a numerical model is developed and utilized to simulate the hydrodynamics and water quality of Poyang Lake and its surrounding river networks. The study couples an in-house 1-D river network hydrodynamic and mass transport model together with a 2-D MIKE hydrodynamic and water quality model. The model is validated against field-measured data from the local water authorities. The impact of the proposed downstream barrage on Poyang Lake's hydrodynamics and water quality is then investigated. It is concluded that: the established integrated model is capable of simulating the hydrodynamic and water-quality processes of the Poyang Lake to satisfactory degrees; and the operation of proposed barrage has large effects on the nutrients distribution and water resources availability. The findings of the study contribute to a better understanding of the fate of Poyang Lake's pollutants and the influence of the proposed hydraulic projects on the lake's flow and ecosystem. Many of these findings are relevant to large freshwater lakes in other developing countries and could contribute to the fields of water engineering and water management.



## Acknowledgement

I would like to express my sincerer gratitude to my PhD supervisor, Dr Dongfang Liang, for his tremendous guidance, support and encouragement over the last few years. His helpful advice and suggestions for research directions often shed beams of light during the hardest days. I am forever thankful for the many opportunities and learning experience that he offered me over the course of my PhD. It has been a true honor to learn from Dr Liang and to complete this research under his guidance and advice.

I would also like to thank my advisor Professor Richard Fenner for his continuous support over my times in Cambridge, long from my year as a MPhil student under his Engineering for Sustainable Development course to the many turbulence and obstacles that he has guided me through in my early PhD years. I am also grateful for the support and advice from Ms Sian Owen, Professor Peter Guthrie and Professor Lord Robert Mair in the Department of Engineering. I would like to thank Dr Guoxian Huang and Professor Tiejian Li for their assistance in providing field measured results, numerical simulation framework and computational resources during my research exchange at the Department of Hydraulic Engineering in Tsinghua University.

To my dearest mother, for her endless love and care and her long-term support of my studies abroad in the United Kingdom. She has been and will always be my anchor in life. To my uncles, aunts and cousins for their encouragement, critical advice and financial support that make this journey a lot more comfortable and smoother than it could have been. I am utterly grateful for everything that my family has done for me.

I would like to express particular thanks to Dr Helena Browne and Professor Martin Johnson from Christ's College for their kind encouragement and care in terms of my welfare and mental health over the course of my PhD. I am also grateful for all the administrative help from Ms Louise Yirrell and Ms Dee Kunze at the Tutorial Office in Christ's College.

I thank Croucher Foundation Hong Kong for sponsoring a large portion of my PhD with their full scholarship. I am grateful for their generous support over the past years. I am also thankful for the British Council Newton Funds for supporting my exchange to Tsinghua University in Beijing and the various travel grants and studentships given by the Department of Engineering, Christ's College and the Cambridge Philosophical Society.

Last but not least, I would like to thank my friends who all have made this journey enjoyable and worthwhile. Special thanks to Weiling Teh, Jonathan Mak, Niki Leung, Wendy Wen, Edwin Lee, Tammy Tong, Elaine Wong, Stephen Chan, Michael Lau, Justin Chan, Benny Wong, Carrie Hau, Annie Chiu, Fan Yang, Didi Hu, Tiana Ng, Ivan Chan, James Fan, Ruby Yeung, Calvin Lui, Carmen Ho, Raymond Cheng, Nicola Tsang, Zhonglu Lin, Ivy Choi, Clara Cheung, Heather Lim, Lina Chun, Hovy Wong, Anson Cheung, Calvin Chan, Kenneth Li and last but not least, Karcy Chan. They have gone through the highs and lows with me at different stages of my PhD and I could not have made it without them.



# Table of Contents

<b>List of Figures</b>	<b>xv</b>
<b>List of Tables</b>	<b>xix</b>
<b>Nomenclature</b>	<b>xxvii</b>
<b>1 Introduction</b>	<b>1</b>
1.1 Background . . . . .	1
1.2 Research Question . . . . .	4
1.3 Report Structure . . . . .	7
<b>2 Literature Review</b>	<b>8</b>
2.1 Studies of Lakes and Rivers . . . . .	9
2.1.1 Hydraulic Modeling . . . . .	10
2.1.2 Water Quality Modeling . . . . .	16
2.2 Poyang Lake: Background and Challenges . . . . .	21
2.2.1 Hydrodynamics and Hydrology . . . . .	24
2.2.2 Impact of Three Gorges Project . . . . .	29
2.2.3 Existing Research on Hydrodynamics of Poyang Lake . . . . .	31
2.2.4 Poyang Lake Barrage . . . . .	37
2.2.5 Water Quality . . . . .	40
2.2.6 Existing Research on Water Quality of Poyang Lake . . . . .	45
2.2.7 Improvement of Data Collection . . . . .	52
2.2.8 Extension of Monitoring Network . . . . .	53
2.2.9 Economic and Social Impact . . . . .	54
2.3 Chapter Summary . . . . .	55
<b>3 Methodology</b>	<b>58</b>
3.1 Part 1 - Hydrodynamics . . . . .	60
3.1.1 3-D Hydrodynamic Governing Equations . . . . .	60

## Table of Contents

---

3.1.2	3-D Solute Transport Governing Equations . . . . .	62
3.1.3	2-D Hydrodynamic Governing Equations . . . . .	64
3.1.4	2-D Solute Transport Governing Equations . . . . .	65
3.1.5	2-D and 3-D Numerical Methods . . . . .	65
3.1.6	1-D Hydrodynamic Governing Equations . . . . .	80
3.1.7	1-D Numerical Methods for Hydrodynamics . . . . .	82
3.1.8	1-D Solute Transport Governing Equations . . . . .	86
3.1.9	1-D Numerical Methods for Solute Transport . . . . .	87
3.2	Part 2 - Water Quality . . . . .	89
3.2.1	Dissolved Oxygen Process . . . . .	89
3.2.2	Nitrogen Cycle . . . . .	95
3.2.3	Phosphorus Cycle . . . . .	101
3.2.4	Temperature Process . . . . .	105
3.2.5	Solving Methods . . . . .	105
3.3	Chapter Summary . . . . .	107
<b>4</b>	<b>Models Development</b>	<b>108</b>
4.1	1-D Simulation Setup . . . . .	109
4.1.1	Study Regions and Resources . . . . .	109
4.1.2	Models Parameters . . . . .	111
4.2	1-D Model Validation . . . . .	114
4.2.1	1-D Hydrodynamic Validation . . . . .	114
4.2.2	1-D Water Quality Validation . . . . .	119
4.3	Multi-Dimensional Simulation Setup . . . . .	122
4.3.1	Study Regions and Resources . . . . .	122
4.3.2	Boundary Conditions . . . . .	130
4.3.3	Model Parameters and Control - Hydrodynamic . . . . .	133
4.3.4	Model Parameters and Control - Water Quality . . . . .	140
4.3.5	Model Parameters and Control - 3-D Model . . . . .	149

## Table of Contents

---

4.3.6	Parallel Computing . . . . .	150
4.3.7	Management of Simulations . . . . .	151
4.3.8	2-D and 3-D Simulation Comparison . . . . .	152
4.4	2-D Model Validation . . . . .	157
4.4.1	2-D Hydrodynamic Validation . . . . .	157
4.4.2	2-D Water Quality Validation . . . . .	165
4.5	Chapter Summary . . . . .	175
<b>5</b>	<b>Potential Barrage Water Management Schemes for Poyang Lake</b>	<b>177</b>
5.1	Introduction . . . . .	177
5.2	Operational Schemes . . . . .	178
5.3	Barrage Effect on Lake Hydrodynamics . . . . .	183
5.4	Barrage Effect on Water Quality . . . . .	191
5.4.1	Impact on DO Concentration . . . . .	191
5.4.2	Impact on NH <sub>3</sub> -N Concentration . . . . .	195
5.4.3	Impact on Phosphorus Concentration . . . . .	201
5.4.4	Effect of Water Levels on Water Quality Variables . . . . .	211
5.5	Chapter Summary . . . . .	215
<b>6</b>	<b>Conclusions</b>	<b>216</b>
6.1	Overview . . . . .	216
6.1.1	Problems and Modeling in Freshwater Environment . . . . .	217
6.1.2	Developing the Coupled Numerical Model . . . . .	218
6.1.3	Evaluating the Engineering Control of the Barrage . . . . .	220
6.2	Discussion and Remarks . . . . .	222
6.2.1	Data and Simulation Validity . . . . .	222
6.2.2	Accuracy of Data and Assumptions . . . . .	223
6.2.3	Modeling the Environment of the Lake . . . . .	224
6.3	Future Work . . . . .	225
	<b>References</b>	<b>229</b>

# List of Figures

2.1	Location of Poyang Lake in China . . . . .	22
2.2	Poyang Lake natural and historical environments . . . . .	23
2.3	Poyang Lake water surface environment in July during wet season . . . . .	26
2.4	Poyang Lake water surface environment in January during dry season . . . . .	27
2.5	Annual average water level at Xingzi of Poyang Lake for 1953-2013 (Source: Wang et al., 2015) . . . . .	31
2.6	Comparison of observed (solid line) and simulated (dotted line) lake water levels for 2006–2008 by Li et al., (2014) . . . . .	33
2.7	Time series validation of inundation area between MODIS images ex- tracted and simulation by Lu et al. (2015) . . . . .	35
2.8	Time series of water age differences at Hukou station and spatial pattern of water age differences on Dec 2 2009 between the barrage project case and the non-project case by Qi et al. (2016) . . . . .	35
2.9	Location of potential barrage in Poyang Lake (Source: CCTV China) . . . . .	38
2.10	Proposed barrage design in Poyang Lake (Source: WWF China) . . . . .	38
2.11	Vertical profiles of the average content of phosphorus in Poyang Lake sediments (Source: Xiang and Zhou, 2011) . . . . .	47
2.12	Concentration data of total nitrogen (TN) in the sediments of the Yangtze River basin from studies conducted from 1990 to 2013 (Source: Yang et al., 2017) . . . . .	48
2.13	Measured and simulation of chlorophyll <i>a</i> using Artificial Neural Network at Kangshan of Poyang Lake (Source: Huang et al., 2015a) . . . . .	51
3.1	Principle of meshing for the 3-D case (Source: DHI) . . . . .	67

## List of Figures

---

3.2	Cross section of vertical sigma mesh and hybrid sigma/z-level mesh, with interface indicated between sigma level and z-level (Source: DHI) . . . . .	69
3.3	Vertical distribution of layers for a water column in sigma mesh . . . . .	70
3.4	Discretization of spatial derivative in Preissmann scheme . . . . .	83
3.5	Mass and energy conservation of channels at junction $N$ . . . . .	85
3.6	Four potential flow directions in one river section . . . . .	88
3.7	Nitrogen cycle (modified from the Queensland Government) . . . . .	96
4.1	1-D simulation area of the middle and lower reach of Yangtze River . . . . .	110
4.2	1-D simulation area and cross-sections of Poyang Lake basins . . . . .	112
4.3	1-D hydrodynamic model validation locations . . . . .	115
4.4	Measured water surface elevations compared with 1-D river model predictions at Hukou, Duchang and Wucheng . . . . .	117
4.5	Measured water surface elevations compared with 1-D river model predictions at Tangyin, Kangshan and Boyang . . . . .	118
4.6	1-D water quality model validation locations . . . . .	120
4.7	Measured $\text{NH}_3\text{-N}$ compared with 1-D model predictions at stations across Poyang Lake . . . . .	123
4.8	Measured TP compared with 1-D model predictions at stations across Poyang Lake . . . . .	124
4.9	Measured DO compared with 1-D model predictions at stations across Poyang Lake . . . . .	125
4.10	Measured TEMP concentration compared with 1-D model predictions at stations across Poyang Lake . . . . .	126
4.11	Poyang Lake 2-D unstructured mesh . . . . .	128
4.12	Sections of 2-D unstructured mesh . . . . .	129
4.13	Locations of the 16 boundary conditions in Poyang Lake . . . . .	131
4.14	Bed roughness across simulation domain in Poyang Lake . . . . .	136

## List of Figures

---

4.15	Surface elevation comparison of two simulation periods at Xingzi, Boyang and Kangshan . . . . .	153
4.16	Water quality comparison of two simulation periods of DO at Duchang, NH <sub>3</sub> -N at XinjiangWest and PO <sub>4</sub> -P at XinjiangWest . . . . .	154
4.17	Surface elevation comparison of 2-D and 3-D simulation at Xingzi, Boyang and Kangshan . . . . .	155
4.18	Water quality comparison of 2-D and 3-D simulation of DO at Kangshan, NH <sub>3</sub> -N at XinjiangWest and PO <sub>4</sub> -P at Boyang . . . . .	156
4.19	Measured water surface elevations compared with 2-D hydrodynamic model predictions at Hukou, Duchang and Wucheng . . . . .	159
4.20	Measured water surface elevations compared with 2-D hydrodynamic model predictions at Tangyin, Kangshan and Boyang . . . . .	160
4.21	Water surface elevations compared with total water depth from 2-D simulation at Duchang and Tangyin . . . . .	161
4.22	Comparison of the simulated and field measured water level in Poyang Lake for 2008 (Source: Hu et al., 2012b) . . . . .	161
4.23	Comparison of satellite captured water coverage and model generated flow field of Poyang Lake during wet season . . . . .	163
4.24	Comparison of satellite captured water coverage and model generated flow field of Poyang Lake during dry season . . . . .	164
4.25	2-D water quality model validation locations . . . . .	166
4.26	Comparison of the simulated and field measured monthly-averaged TIN and TP in Poyang Lake for 2010 (Source: Hu et al., 2012b) . . . . .	169
4.27	Measured NH <sub>3</sub> -N compared with 2-D water quality model predictions at stations across Poyang Lake . . . . .	170
4.28	Measured TP compared with 2-D water quality model predictions at stations across Poyang Lake . . . . .	171
4.29	Measured DO compared with 2-D water quality model predictions at stations across Poyang Lake . . . . .	172

## List of Figures

---

4.30	Measured TEMP compared with 2-D water quality model predictions at stations across Poyang Lake . . . . .	173
5.1	Water levels at the proposed barrage location under different operational schemes . . . . .	181
5.2	Scheme comparison of water levels at Xingzi, Wucheng, Kangshan and Boyang . . . . .	184
5.3	Scheme 0 surface elevation spatial distribution in 2007 . . . . .	188
5.4	Scheme 1 surface elevation spatial distribution in 2007 . . . . .	189
5.5	Scheme 4 surface elevation spatial distribution in 2007 . . . . .	190
5.6	Scheme comparison of DO at Boyang, XiuheMouth and Xingzi . . . . .	193
5.7	Scheme 0 DO spatial distribution in 2007 . . . . .	196
5.8	Scheme 1 DO spatial distribution in 2007 . . . . .	197
5.9	Scheme 4 DO spatial distribution in 2007 . . . . .	198
5.10	Scheme comparison of NH <sub>3</sub> -N at Boyang, XiuheMouth and Xingzi . . . . .	200
5.11	Scheme 0 NH <sub>3</sub> -N spatial distribution in 2007 . . . . .	202
5.12	Scheme 1 NH <sub>3</sub> -N spatial distribution in 2007 . . . . .	203
5.13	Scheme 4 NH <sub>3</sub> -N spatial distribution in 2007 . . . . .	204
5.14	Scheme comparison of TP at Boyang, XiuheMouth and Xingzi . . . . .	206
5.15	Scheme 0 PO <sub>4</sub> -P spatial distribution in 2007 . . . . .	208
5.16	Scheme 1 PO <sub>4</sub> -P spatial distribution in 2007 . . . . .	209
5.17	Scheme 4 PO <sub>4</sub> -P spatial distribution in 2007 . . . . .	210
5.18	Distribution of monthly-averaged TIN and TP in dry and fiat period of Poyang Lake (Source: Hu et al., 2012b) . . . . .	212
5.19	Comparison of water depth (z) against water quality variables (DO, NH <sub>3</sub> -N and TP) under different barrage operational schemes at Xingzi and Boyang . . . . .	214

# List of Tables

2.1	Examples of open-source hydrodynamic models . . . . .	14
2.2	Inflow pollutant contribution from rivers into Poyang Lake in 2013 . . .	42
4.1	List of model parameters for 1-D water quality simulation . . . . .	113
4.2	Locations of boundary condition and their input types . . . . .	132
4.3	List of 2-D hydrodynamic model parameters . . . . .	139
4.4	List of 2-D water quality model constants . . . . .	144
4.5	Annual mean area and annual budget of water balance of Poyang Lake basin for 2006-2010 (Source: Liu et al., 2013) . . . . .	175
5.1	Proposed barrage operational schemes . . . . .	180
5.2	Water surface area and volume of Poyang Lake under Scheme 0-5 . . .	187

# Nomenclature

## Abbreviations

AD	advection-dispersion
BOD	biochemical oxygen demand
CFL	Courant-Friedrichs-Lewy
DEM	digital elevation map
DHI	Danish Hydraulic Institute
DO	dissolved oxygen
EFDC	environmental fluid dynamics code
FDM	finite difference method
FEM	finite element method
FVM	finite volume method
GPU	graphic processing unit
MPI	message passing interface
ON	organic nitrogen
OP	organic phosphorus
PI	permanganate index
PP	particulate phosphorus
SOD	sediment oxygen demand
SWAT	soil and water assessment tool
SWE	shallow water equations
TDMA	tridiagonal matrix algorithm
TEMP	temperature
TP	total phosphorus
WASP	water quality analysis simulation program

## Nomenclature

---

### Greek Symbols

$\alpha_{CCHL}$	carbon-to-chlorophyll ratio
$\alpha_{NC}$	nitrogen-to-carbon ratio in phytoplankton
$\alpha_{OC}$	oxygen to carbon ratio
$\alpha_{PC}$	phosphorus to carbon ratio in phytoplankton
$\Delta\Gamma_j$	length or area of cell interface $j^{th}$
$\eta$	free surface elevation
$\Gamma_i$	boundary of $i^{th}$ cell
$\kappa$	von Kármaán constant
$\lambda$	integration variable with respects to $A_i$
$\nu_h$	horizontal eddy viscosity
$\nu_t$	vertical eddy viscosity
$\Omega$	water surface area of streams' intersection point
$\omega$	angular rate of revolution
$\phi$	geographic latitude
$\psi$	surface control parameter for vertical mesh
$\rho$	water density
$\rho_0$	reference water density
$\sigma_c$	equidistant distribution and stretch distribution weight factor
$\sigma_i$	number of sigma level
$\sigma_T$	Prandtl number
$\tau$	actual time of day related to noon
$\theta$	temporal weighting coefficient
$\Theta_1$	temperature coefficient for photosynthetic respiration rate
$\Theta_2$	temperature coefficient for respiration rate of bacteria
$\Theta_3$	temperature coefficient for biomass degradation constant
$\Theta_4$	temperature coefficient for conversion rate of ammonia to nitrite
$\Theta_5$	temperature coefficient for conversion rate of nitrite to nitrate
$\Theta_6$	temperature coefficient for denitrification rate
$\Theta_7$	temperature coefficient for conversion rate of PP to OP
$\Theta_{83}$	temperature coefficient for organic phosphorus minerlization

## Nomenclature

---

$\Theta_8$	temperature coefficient for rate of adsorption of OP
$\Theta_{SOD}$	temperature coefficient for SOD
$\vec{\tau}_b$	bottom stress
$\vec{\tau}_s$	surface wind stress

## Roman Symbols

$\bar{c}$	depth averaged scalar quantity
$\bar{s}$	depth averaged salinity
$\bar{T}$	depth averaged temperature
$\bar{u}, \bar{v}$	depth averaged velocities
$\mathbf{n}_j$	unit outward normal vector at $j^{th}$ side
$\Delta z_b$	distance above riverbed or seabed
$\hat{E}$	evaporation rate
$\hat{H}$	source term due to atmospheric heat exchange
$\hat{P}$	precipitation rate
DO	dissolved oxygen concentration
DP	dissolved phosphorus concentration
HS <sub>BOD</sub>	half saturation oxygen concentration for BOD
HS <sub>NH3</sub>	half saturation concentration for nitrogen uptake by bacteria
HS <sub>nitr</sub>	half saturation concentration for nitrification
HS <sub>PO4</sub>	half saturation concentration for phosphorus uptake by bacteria
HS <sub>SOD</sub>	half saturation concentration for SOD
NH <sub>3</sub> -N	ammoniacal nitrogen concentration
NO <sub>2</sub>	nitrite concentration
NO <sub>3</sub>	nitrate concentration
ON	organic nitrogen concentration
OP	organic phosphorus concentration
PC	phytoplankton carbon concentration
PO <sub>4</sub> -P	orthophosphate concentration
PP	particulate phosphorus concentration
UN <sub>p</sub> , UN <sub>b</sub>	ammonia uptake by plants and bacteria

## Nomenclature

---

$UP_p, UP_b$	phosphorus uptake by plants and bacteria
$A$	coefficient matrix
$B$	vector with explicit variables
$F$	flux vector function
$n$	unit onward normal vector along boundary
$S$	vector of source term
$U$	vector of conserved variables
$\vec{u}_b$	flow velocity above the bottom layer
$A$	river channel wetted cross sectional area
$a$	actual relative day length
$A_i^k$	average cross sectional area in $i^{th}$ control volume at $k^{th}$ time step
$A_i$	cell area or volume
$A_N$	storage area of river junction $N$
$A_T$	ambient air temperature
$B$	river channel wetted perimeter
$b$	bottom control parameter for vertical mesh
$b_0$	bed roughness length scale
$C$	Chezy number
$c$	concentration
$c_f$	drag coefficient
$c_p$	specific heat of water
$C_s$	saturation level for oxygen in water
$c_s$	concentration at source
$D$	segment depth
$d$	still water depth
$D_h$	horizontal turbulent diffusion coefficient
$D_v$	vertical turbulent diffusion coefficient
$D_x, D_y, D_z$	dispersion coefficients
$D_j$	average depth of channel segment $j$
$D_{P1}$	phytoplankton death and respiration rate
$ds$	integration variable along boundary

## Nomenclature

---

$E$	surface heat exchange coefficient
$f$	Coriolis parameter
$F_1(h)$	light dampening function
$f_{D7}$	fraction of dissolved organic nitrogen
$f_{D8}$	fraction of dissolved organic phosphorus
$f_{ON}$	fraction of dead phytoplankton recycled to the organic nitrogen food
$f_{OP}$	fraction of dead phytoplankton recycled to organic phosphorus pool
$Fr$	Froude number
$g$	gravitational acceleration
$G_{P1}$	specific phytoplankton growth rate
$h$	water depth
$h_\sigma$	fixed fraction of total sigma layer depth
$h_{dry}$	drying depth
$h_{flood}$	flooding depth
$h_{wet}$	wetting depth
$I_s$	saturation light intensity for phytoplankton
$k$	light extinction coefficient
$k_p$	linear decay rate
$k_s$	roughness height
$k_{1C}$	phytoplankton growth rate constant
$k_{1D}$	non-predatory phytoplankton death rate
$k_{1G}$	grazing rate on phytoplankton per unit zooplankton population
$k_{1R}$	phytoplankton respiration rate
$K_2$	reaeration rate
$K_3$	biomass degradation rate
$K_4$	conversion rate of ammonia to nitrite
$K_5$	conversion rate of nitrite to nitrate
$K_6$	denitrification rate
$k_{71}$	organic nitrogen mineralization rate
$K_7$	conversion rate of PP to OP
$k_{83}$	mineralization rate of dissolved organic phosphorus

## Nomenclature

---

$K_8$	rate of adsorption of OP
$k_{BOD}$	half saturation constant of BOD for O <sub>2</sub> limitation
$k_{DS}$	decomposition rate of CBOD in sediment
$K_d$	decay factor
$k_d$	deoxygenation rate for CBOD
$k_{MNG}$	half saturation constant of nitrogen for phytoplankton growth
$K_{mN}$	half saturation constant for nitrogen
$k_{mPc}$	half saturation constant for phytoplankton limitation
$k_{MPG}$	half saturation constant of phosphorus for phytoplankton growth
$k_{NIT}$	half saturation constant of nitrogen for O <sub>2</sub> limitation
$K_{NO_3}$	Michaelis constant for denitrification
$k_{OND}$	decomposition rate of organic nitrogen in sediment
$k_{OPD}$	decomposition rate of organic phosphorus in sediment
$k_{PZD}$	decomposition rate constant for phytoplankton in sediment
$k_{qj}$	flow induced reaeration rate
$L$	lateral discharge momentum
$l$	characteristic length
$m$	total number of streams linked to river junction $N$
$n$	Manning roughness coefficient
$N_\sigma$	number of layers in sigma domain
$NS$	number of sides of discretization cell
$P$	photosynthesis respiration production
$p_a$	atmospheric pressure
$P_{max}$	maximum production of photosynthesis at noon
$P_{NH_3}$	preference for ammonia uptake term
$Q$	flow discharge
$q$	lateral discharge per unit channel length
$Q_a$	absolute value of flow discharge
$Q_n$	surface net heat flux
$r$	respective number of streams linked to river junction $N$
$R_1$	photosynthetic respiration rate

## Nomenclature

---

$R_2$	respiration rate of bacteria
$S$	point source discharge magnitude
$s$	salinity
$s_e$	slope due to local head loss
$s_f$	friction slope
$s_s$	salinity of source
$S_2$	resuspension rate for inorganic particulates
$S_3$	sedimentation rate for inorganic particulates
$S_c$	external source and sink term
$S_{ij}$	deformation rate for eddy viscosity
$S_k$	kinetic source term due to chemical reaction
$s_{xx}, s_{xy}, s_{yx}, s_{yy}$	radiation stress tensor
$STC$	specific thermal capacity of seawater
$T$	water temperature
$t$	time
$T_s$	temperature of source
$t_{up}, t_{down}$	actual relative day length
$u$	flow velocity in $x$ direction
$u_b$	magnitude of main streamline lateral flow velocity in river channel
$U_{\tau_b}$	friction velocity associated with bottom stress
$U_{fc}$	friction velocity
$u_s, v_s$	water discharge velocities
$V$	flow velocity in 1-D river channel
$v$	flow velocity in $y$ direction
$v_j$	average velocity in channel segment $j$
$v_{s3}$	organic matter settling velocity
$v_{s4}$	net settling velocity of phytoplankton
$v_{s5}$	inorganic sediment settling velocity
$w$	flow velocity in $z$ direction
$W_v$	wind speed
$x$	river channel distance

## Nomenclature

---

$x, y, z$	Cartesian coordinates
$Y$	state of system in numerical method
$Y_i$	yield factor of oxygen consumed in nitrification
$Y_2$	phosphorus content in organic matter
$Y_{BOD}$	nitrogen content in organic matter
$Z$	water surface elevation
$z_0$	specified depth for vertical mesh
$T_e$	evaporation temperature
$T_p$	precipitation temperature

### Subscripts

0	initial condition
$i, j, k$	vector components
$N$	river channels junction number
$s$	source term
$x, y, z$	direction components

### Superscripts

$I$	inviscid fluxes
$V$	viscous fluxes



# Chapter 1

## Introduction

### 1.1 Background

Water is one of the most essentials of all natural resources. All vital processes of value to mankind require water as a fundamental element. Although 70% of the earth's surface is covered by water, freshwater only accounts for approximately 2.5%. Of that small fraction, the majority is in the form of permanent ice and snow, or groundwater that are inaccessible to human beings. In the end only 0.3% of freshwater is available and renewable as runoff and surface flows (National Geographic, 2010; UN POPIN, 1994), making it as a finite and precious resource globally. Demand for clean water supply, on the other hand, is unlimited. Rapid population growth, extensive urban development and intense socio-economic expansion over recent decades have driven the increase of water demand across municipal, agricultural and industrial sectors (MET Office, 2013). From basic drinking, irrigation to industrial cooling, demands from various sectors are escalating and competing with one another. Rising standards of living and urbanization have placed tremendous stress on the already critical freshwater shortage situation. The issue is further aggregated because water resources are in general unevenly distributed temporally and spatially, making access and storage of water difficult in nature. Ensuring the present and future generations an adequate and

## Introduction

---

sustainable water supply (i.e. water security) has become one of the most pressing global issues.

The impact of urbanization and human activities on water resources is not limited to a problem of quantity, but also extends to that of quality. Freshwater is often polluted during sanitation, from industrial wastes removal and in agricultural runoff. Sewage, sludge and toxic pollutants are occasionally dumped directly into water bodies. Furthermore, construction of infrastructure such as dams and landfills near freshwater resources would disturb the flow patterns and contribute towards water pollution through the disturbance of sediments and soil nutrients. The chemical properties and compositions of water are altered in these processes. In some cases untreated water may even heighten the risk of water-borne diseases. Alongside adequate water supply, concurrent maintenance of a safe and potable water base and environment also becomes part of the challenge.

An additional contribution to the water crisis arises from the effect of climate change. Emission of carbon dioxide and other greenhouse gases from human activities have trapped additional heat in the earth's lower atmosphere and warmed the environment by approximately  $0.75^{\circ}\text{C}$  over the last 100 years (WHO, 2014). The seemingly small temperature variation would cause dramatic changes in the natural environment, including the melting of glaciers, rising seawater levels, changes in precipitation patterns and hence increasingly intense, frequent and unpredictable extreme weather events. The impact of climate change on water resources is well documented (US EPA, 2015; World Bank, 2015a). Increasing frequency and scale of severe droughts and floods, higher groundwater depletion rate and extreme storms and rainfall patterns are some of the examples of the consequences of climate change. These natural events would continue to have a profound impact on the planet's water resources and ecosystems, subsequently affecting the economy, health and quality of life in both the developing and developed worlds (World Bank, 2015b).

## Introduction

---

Main freshwater sources exist in the forms of rivers, lakes and wetlands. The majority of the population rely on the supply of clean freshwater from rivers and lakes to sustain daily life and development. Ironically, human activities around the lake and river environments have in turn generated negative impact that would significantly deter the availability and quality of these freshwater ecosystems (WWF UK, 2015). Eutrophication, declining water levels and river flows, as well as threats to wildlife and aquatic species are some common drawbacks. Millions in both urban and rural communities will continue to suffer from water pollution and shortage. Further agricultural and industrial activities will be jeopardized and socio-economic growth will be hindered. The scale of water crisis is global. Pollution and maintenance of freshwater habitats are not limited to a particular country, continent or climate. Rivers and lakes around the globe are equally susceptible under the influence of climate change and urbanization. Several cases among many include Lake Naivasha in Kenya, the Great Ruaha River in Africa, the Pantanal wetland in South America and the Yangtze River, the Mekong River and the Aral Sea in Asia (WWF UK, 2018). Pollution, industrial development, climate change, poor water management and reducing flows are all major challenges faced by these natural water environments. The importance of freshwater ecosystem monitoring and management must not be overlooked.

Advancement in water management, water technology and engineering designs are potential ways to mitigate the effects of climate change and human activities on freshwater resources. Extensive monitoring and management of the quality and quantity of natural water cycles and resources are essential to the prediction of potential variations in the water environment, to reduce the detrimental effects of unforeseeable changes in water resources and to ensure a safe and consistent supply of freshwater in support of human activities. It is important to combine research fields in river hydrodynamics, computation fluid dynamics, climatology, hydrology and pollution with the aim to contribute to the research and development of water and environmental engineering, as well as offering cutting edge technology and analyzing tools for water practices. The scale and gravity of the global water problems demand urgent upgrades

## Introduction

---

on the efficiency and effectiveness of water management systems and simulation models. In the context of freshwater ecosystems such as rivers, lakes and wetlands, a tool that can help visualize and predict the hydraulic flows, fluctuation of water levels and pollutant dispersion at any given physical configuration will have its own merit. Such tool would provide scientific support and original perspectives for stakeholders and decision makers to tackle local water problems in the context of water management, pollutant control, ecological conservation and sustainability.

## 1.2 Research Question

Poyang Lake, the largest freshwater lake in China, plays a key role in regulating the hydrology, water quality and ecosystem in the middle reaches of the Yangtze River. The lake accounts for 14.5% of Yangtze River's annual flow capacity and acts as a natural buffer for the Yangtze River, providing extra volume for water storage, flood control and pollutant dilution (Huang et al., 2011). The lake also supports agriculture and tourism of the region and is the key freshwater source for around 12.4 million populations in nearby cities of Nanchang and Jingdezhen (Zhang et al., 2014).

Since the Three Gorges Dam (TGD) and its associated reservoirs came into operation in 2003, the flow characteristics of Yangtze River have recorded significant changes and created knock-on effects on its surrounding water bodies (Lai et al., 2014b). Erosion of upstream riverbeds and siltation at Poyang Lake's mouth due to the operation of TGD upstream could have disastrous consequences for flood prevention efforts in the next 30 years around the Poyang Lake region. More outflows from the lake to the river are simulated, causing the water storage capability of Poyang Lake to reduce (Guo et al., 2012a). The lake's water levels have recorded a declining trend in the 21<sup>st</sup> century. Monitoring stations around Poyang Lake all logged the lowest historic water levels over the last two decades and average water level of the lake dropped from 14.0 m to 13.3 m over the last 60 years (Guo et al., 2012b). The main reasons behind the drop in water levels include decreasing rainfall and influx from

## Introduction

---

upstream rivers, leading to prolonged dry period in Poyang Lake. As a result, the self purification ability reduces and hence the water quality of the lake deteriorates, causing a loss of ecological functions. The main pollutants in the region were TN, TP, NH<sub>3</sub>-N and COD (Luo et al., 2014), sourcing directly from the rivers network in the forms of industrial activities, municipal wastes from villages and agricultural waste from the use of fertilizers and poultry framing (Chen et al., 2016).

The decline in water quantity and quality in Poyang Lake has sparked increasing concerns of depreciating freshwater sources for the human and wildlife population in the region. The Poyang Lake barrage project was therefore proposed to maintain and control the lake's water levels from further decline under the influence of the climate change, the Yangtze River and urbanization in the Poyang Lake basin (Huang et al., 2011). The proposed project will involve a series of sluice gates being installed along the narrowest section of the channel at the northern mouth of the lake. The main goal of the project is to manage the water levels in Poyang Lake by closing the sluice gates during the dry seasons, while imposing no control on the water levels by opening the sluice gates in full during the wet seasons and allowing free exchanges of water, energy and biology between the lake and river (Hu and Ruan, 2011; Lai et al., 2016). In support of the proposed barrage to be built, local government bodies and hydrological authorities have designed different regulation schemes for the project with various conditions and standards over the control of water levels (Zhang et al., 2011). These schemes may alter the natural processes in the hydrological, hydrodynamic, sediment transport, water quality and ecological aspects. Serious degradation of water quality and outburst of nutrients may result in eutrophication, deterioration of wetlands, and damage to wildlife habitat for endangered birds and fishes. Therefore, it is crucial that quantitative analysis is carried out to evaluate the impacts of these schemes.

In this research, a hybrid multi-dimensional hydrodynamic and water quality model will be developed to simulate the hydraulic flows and bio-chemical properties of fluctuating water bodies under certain natural topography and bathymetry of Poyang

## Introduction

---

Lake. The study will couple an in-house 1-D river network hydrodynamic and mass transport model together with MIKE, a 2-D hydrodynamic and water quality model. The model will be validated using field-measured data from the local water authorities. The proposed barrage operational schemes can then be implemented into the model and their impact on the lake's hydraulic and water quality characteristics will be investigated and evaluated. The results can help understand further the potential consequences of the proposed barrage, contributing towards future water quality management policies and decisions and the protection of the natural environment and sustainability of Poyang Lake and its neighboring regions. In order to set up an integrated water management framework for the protection of Poyang Lake's ecosystem and surrounding communities, an accurate and representative evaluation of the lake's hydrodynamics, water quality and proposed barrage control is vital. Therefore, this research will focus on the following research question:

**Given Poyang Lake's recent challenges with the decline of water flow and deterioration in water quality, could a coupled numerical model that integrates hydrodynamic and water quality simulations be used as a tool to analyze the hydraulic changes of the region and to predict pollutant concentration under those changes? What recommendation would the model offer to stakeholders towards the proposal to construct a barrage structure at the outflow of the lake?**

The novelties of this research lie in the application of the hybrid multi-dimensional hydrodynamic and water quality models to the challenging hydro-environment of Poyang Lake. Being the largest freshwater lake in China, Poyang Lake experiences complex interaction with the Yangtze River and exhibits large water level variation with numerous pollutant inputs. Considering the size of problem spreading out across large region of river networks and catchments, the modeling domain is classified as large scale. An attempt to combine multi-dimensional models in studying the hydrodynamics and water quality of a complex hydro-environment of this scale is novel and challenging.

The complexity of the problem is then aggregated by the application of the hybrid model in evaluating the impact of the potential barrage control in Poyang Lake. This research is among the first that systematically studies the influence of a potential barrage on the lake's hydro-environment. This study focuses on a very important and timely topic of hydro-environmental modelling of engineering interventions in the natural environment and their potential impacts. The development and endeavour of this study will contribute to the learning of the field.

### 1.3 Report Structure

A general introduction regarding the background and conditions of the freshwater bodies was given, together with the aims and research directions of this project (Chapter 1). This is followed by a review of the hydrodynamic and water quality models on river and lake environments, as well as a detailed description regarding Poyang Lake on its characteristics, importance and problems (Chapter 2). This section investigates in detail the hydrology and pollution conditions of the lake habitats, the main challenges faced by the regions and existing efforts that have been done so far. The methodology to integrate the principles of hydrodynamics and water quality properties in the proposed computational model is then documented (Chapter 3). Selection of methods and tools is also explained, followed by the implementation of these models based on the conditions of Poyang Lake and the uses of parameters and variables. Validation processes are also performed with the models against field-measured data (Chapter 4). In the next section, the impact of the barrage on the lake's hydraulic behaviour and water quality variables is investigated using the numerical model developed (Chapter 5). Interpretation and discussion of the findings are summarized, with a particular focus on the sustainability and conservation of the lake's ecosystem. Suggestions on further improvement of the model and future works are included. Recommendation in terms of the lake's future water management direction and policies are presented prior to the final concluding remarks (Chapter 6).

# Chapter 2

## Literature Review

In this section, existing literature is critically assessed, summarized and analyzed in order to form the theoretical base for this study. Due to the breadth of topics involved in this research, it is essential to identify the background and key concepts across all sub-areas, as well as the underlying connections and major issues within existing research. First, a brief background on the numerical studies of lake and river environments is given to provide an outline of the development, current status and significance of previous studies. Modeling methods on both hydrodynamic and water quality and their advancement are examined and evaluated. Next, the background and current conditions of the core subject of this research, Poyang Lake, are detailed. Areas that are closely related to this research, including Poyang Lake's hydrodynamic and water quality characteristics, its relationship with nearby river networks and the Three Gorges Dam, the proposed Poyang Lake Barrage and challenges faced by the lake's ecosystem and surrounding communities. The section will conclude by looking at existing research efforts on Poyang Lake and their findings thus far. Research gaps and conflicting evidence are identified to support this study in tackling its core research questions. At the end of this section, a critical review is provided to establish the general directions and scales for this study.

## 2.1 Studies of Lakes and Rivers

The studies of rivers and lakes have been part of a continuous endeavor and exploration ever since the dawn of human civilization around freshwater bodies. Over millennia of learning and advancement across hundreds of civilizations in different continents, the studies of freshwater bodies have evolved into a network of disciplines, each specializing in a particular element within the biological, chemical, physical and geological aspects of the freshwater system. In the last century, limnology (study of inland waters), hydrometeorology (study of hydrological cycle) and potamology (study of rivers), each of which contains numerous sub-disciplines with specific classifications and focuses, emerged as some of the main disciplines in the field of water and environmental science (Wetzel, 2001). The scope of this research spreads across many of these disciplines.

The computational advancement and capabilities in recent decades have complimented and accelerated the study of rivers and lakes through numerical simulation and methods. The use of computers and numerical simulation in determining hydrodynamic behavior are mandatory towards the future development of the field, given the increasing complexity and scale of the hydrodynamic problems (e.g. multidimensional and/or in greater sizes) and hence the demand for more powerful, quicker and more efficient computing.

It is important to first explore and understand the existing technology that has been developed to investigate fluid behavior in rivers and lakes. Advancement in the modelling and principal methods used in the hydrodynamic simulation, as well as the primary purposes of those research on freshwater bodies will be investigated. Similar overview will be performed on the simulation of solute transport, water quality monitoring and pollutants modelling among rivers and lakes thus far to provide a holistic view on the numerical simulation development, contribution and its latest state in the field of hydrodynamic and water quality in water environment.

### 2.1.1 Hydraulic Modeling

In the field of fluid flows, numerous mathematical characterizations have been derived with the aim to accurately describe the behavior of fluids in natural environments. In open channel flows (i.e. river and lake environment), three main theories: the Saint Venant equations, the diffusive wave approximation and the kinematic wave approximation are commonly used in the form of partial differential equations (PDE) to define fluid dynamics (Novak et al., 2010). However, solving these PDE for real-world problems with arbitrary channel geometries and initial and boundary conditions is analytically demanding and time intensive. In light of searching for an approximation of the exact solution for the governing PDE, numerical techniques are used with the assistance of software packages and computational powers. Numerical modeling has become an integral part of hydraulic modeling and engineering.

In the numerical solution process, discretization techniques are used to simplify the governing PDE with approximate derivations. This allows the original solution, which is a function of continuous time and space variables, to be replaced by a much simpler problem, where the solution is sought only at predefined points and times. The new systems of algebraic equations are then solved by using standard numerical techniques such as root finding, integration and matrix inversion. The obtained numerical solution is eventually interpolated onto the computational grid and translated into flow variables that can easily be interpreted by the model's use.

In short, the overall procedure of hydrodynamic modeling involves the application of a theory that describes the behavior of a fluid, commonly in the form of PDE. It is followed by discretizing and simplifying the PDE into ordinary differential equations (ODE) which can then be solved using numerical techniques. Specific solution arise for different problems based on the variations in initial conditions, meshing, bathymetry and boundary conditions of the water environment. The accuracy of these input data with respect to the real life water environment determines the accuracy and reliability

## Literature Review

---

of the numerical simulation. The more comprehensive and detailed the model settings are, the more fitting and reciprocal the model is to the actual water problems. The hydrodynamic models can be divided into various types based on the characteristics of the grid system (structured and unstructured), the method used by the solver (finite differences, finite elements and hybrid approaches with finite volume) and numerical analysis approach (implicit method, explicit method and semi-implicit method).

The grid or mesh system sets up the domain and shape for the simulation. Typical cell types are triangular and quadrilateral. Structured grid is constructed with repeated pattern where every node in the domain is defined according to a specific algorithm. In an unstructured mesh, no regular pattern is followed and all the nodes are arbitrarily defined. Although structured grids offer better convergence and require less computational memory for storing elements and linkage information between nodes, unstructured meshes are becoming increasingly popular among numerical modeling due to its speed of grid generation, ability to construct complex geometry as well as flexibility of resolution in important areas within a large scale domain.

In solving the complex PDE that describe fluid behavior, finite difference method (FDM) divides the formula into small time steps and calculate the properties of the next time step based on existing information using finite difference formulation. For finite element method (FEM), the domain is discretized into finite elements and properties are calculated in every node. Shape functions are used to interpolate inside the finite element. In finite volume method (FVM), calculations are performed for every cell instead of node. FVM is based on the integral form of conservation laws and can therefore handle discontinuities in solution better than FDM, which is based on the differential form of the governing equations. FDM can be a more efficient method than FVM and FEM under a uniform structured grid. However mass is loosely conserved in FDM and improved accuracy often needs to be compromised by having small time step and grid size and higher order of approximation, which in turn increases computation demands and time. Meanwhile, FVM has the disadvantage of increasing

## Literature Review

---

the difficulty with the order of the solution functions. FEM, in contrast, can allow higher order elements to be implemented with relative ease, while maintaining the same capacity as FVM to handle irregular geometries and varying boundary conditions. Nonetheless, FEM requires higher standards on programming and understanding of numerical integration during implementation and the result is only an approximation at best. Each solving method has its advantages and drawbacks. They are widely applied across engineering and science fields, including structural analysis, electromagnetics, astrophysics, heat transfer and computational fluid dynamics. The type of solver used often depends on the conditions and purposes of each problem.

After discretizing the PDE spatially, numerical methods are used for solving the time variables in the ODE. Explicit method solves for the state of a system using information from the current state of the system, while implicit method calculates the state of a system based on information from both the current state and a later one. Although the explicit method is easier to implement and requires less computational expenses than the implicit method, it is prone to errors associated with the splitting of the internal and external modes. They also suffer from the Courant-Friedrichs-Lewy (CFL) conditions, which cause numerical instability and restricts the maximum allowable time step and thus the size of the problem (Courant et al., 1967). In light of these problems, a series of semi-implicit unstructured grid models have been developed (UnTRIM, SUNTANS, ELCIRC). These models treat only implicitly the terms (barotropic-pressure gradient, vertical viscosity in the momentum equations and divergence term in the continuity equation) that place the most severe constraints on numerical stability (i.e. CFL condition), meanwhile treating the rest of the terms explicitly. This approach avoids splitting of the mode into external and internal modes. Moreover, this allows the resulting matrix to be positive definite, symmetric and sparse. As a result, efficient solvers that guarantee fast convergence such as the Jacobian Conjugate Gradient can be used to ensure greater numerical efficiency. However, the semi-implicit method is not without flaws. Piecewise constant shape functions are used

## Literature Review

---

to represent the elevation, which means that over dissipation may occur (Baptista et al., 2005).

A fundamentally important consideration when developing a mathematical model for hydrodynamic problem is the choice of an appropriate kinematic description of the continuum. The algorithms of continuum mechanics usually make use of two classical descriptions of motion: the Lagrangian description and the Eulerian description. The Lagrangian method investigates fluid motion by considering particles as a discrete phase and tracks the pathway of each individual particle. The Eulerian method focuses on a specific continuum in space through which the fluid flows as time passes. The Lagrangian description allows an easy tracking of free surfaces and interfaces between different fluids. Its weakness is its inability to follow large distortions of the computational domain without recourse to frequent re-meshing operations. In the Eulerian method the computational mesh is fixed and the continuum moves with respect to the grid. This allows large distortions in the continuum motion to be handled with relative ease, but generally at the expense of precise interface definition and the resolution of flow details (Donea et al., 2004). Because of these shortcomings, a technique has been developed to combine the best features of both the Lagrangian and the Eulerian approaches (Chung, 2010). The choice determines the relationship between the deforming continuum and the finite mesh of computing zones, thus allowing the numerical method to deal with large distortions and provides an accurate resolution of interfaces and mobile boundaries.

The field of numerical modeling of hydrodynamic simulation is developing and maturing rapidly. Various methods and perspectives have been explored to provide more efficient and more accurate solutions. The theories are put into practice through the implementation of codes and modeling. Open source codes are widely available in solving for the 3-D Navier-Stokes equations, in conjunction with conservation equations for water volume, salt and heat (Zhang and Baptista, 2008). Table 2.1 illustrates several open source models for numerical modeling on coastal, lake and river studies

## Literature Review

---

thus far. Each of the model is classified based on their natures, with red color and green colour indicating implicit method and semi-implicit method respectively for numerical analysis in the solver.

Table 2.1 Examples of open-source hydrodynamic models

	Structured	Unstructured
<b>Finite Element</b>		TELEMAC SUNTANS ADCIRC
<b>Finite Difference</b>	POM ELCOM Delft3D TRIM	
<b>Finite Volume</b>		UnTRIM SELFE Delft3D FM MIKE21/3

The models above are prime examples of how various solving methods and different meshing mechanism can be used to solve hydro-environmental problems. For example, Samaras et al. (2016) used the open source TELEMAC and the commercial software MIKE21 to study representative wave conditions in the coastal areas of South Italy. ADCIRC, as an unstructured grid hydrodynamic model, has been used to simulate hurricane storm surge, tides and river flow in a complex river network of Southern Louisiana in USA (Westerink et al., 2008). A variant of the structured finite difference model of POM was utilized to investigate the mitigation of storm tides by coastal wetlands (Marsooli et al., 2016). ELCOM, developed by the Centre for Water Research at the University of Western Australia, is a 3-D hydrodynamic code using finite difference method with implicit solution for the numerical simulation of the hydrodynamics and the thermodynamics of inland and coastal waters (Laval and Hodges, 2000). Such model has been used to simulate the transport and interactions of flow physics in the reservoir of Lake Mead in Las Vegas, USA (Hannoun et al., 2006). A cross-scale ocean modeling in SELFE was developed by Zhang and Baptista (2008) in simulating 3-D

## Literature Review

---

estuaries and coastal circulation in a tightly coupled estuary-plume-shelf system in the Columbia River system. These examples give a glimpse of the many open source numerical models and their applications on the hydro-environment.

Of the many open source hydraulic models, Delft3D is the most popular, due to its extensive modules in modeling a variety of environmental scenarios. The Delft3D suite has option to use the finite volume method with unstructured approach in Delft3D FM module versus the finite difference method as a structured approach in Delft3D (Symonds et al., 2016). Numerous implicit and semi-implicit schemes are available in solving the complex equations under different circumstances (Deltares, 2014; Kernkamp et al., 2011). As an example, the Delft3D FM was used to unveil the main dynamic and physical properties of Kuwait Bay (Alosairi et al., 2018).

In addition to the many open source models available, researchers also use commercial software such as the MIKE suite to simulate hydro-environmental conditions. Similar to Delft3D, the MIKE model environment has a variety of modules that allow numerical simulation for flows in coastal, estuary and floodplain environments. The model utilizes the finite volume method with semi-implicit approaches in solving various equations. The MIKE model has been widely covered in literature. It was used as a numerical tool in the work of Siegle et al. (2007) and Ranasinghe et al. (2010) on coupled wave hydrodynamic-sediment-transport modelling, Babu et al. (2005) and Gurumoorthi and Venkatachalapathy (2017) on the modeling of free surface tide-driven currents, Mahanty et al. (2016) on coastal-lagoon circulation modeling and Hakim et al. (2015) on structure-induced impact on coastal and estuaries environments.

For the purpose of this project, the MIKE model will be used as the modeling platform over Delft3D due to the availability of the MIKE model software and its license from a collaborator in China. The expertise and experience from such collaborator will also benefit the project by allowing more efficient learning of the model and shortening the time needed for the model setup.

The field of hydro-environment numerical modeling faces numerous challenges in its expansion and development. Although current hydrodynamic models are well established for single phase flow, simulation for multi-phase flow and complex geometries remain a challenge for many models (Chiesa et al., 2005). Multi-phase flows between gas-fluid and fluid-solid states are important areas in the coastal-river-lake environment, in which interactions between the free water surface and wind, as well as that between the sediments and water at the riverbed are of great interest. Advancement in multi-phase flow simulation will enhance the development and provide additional depth to the field of hydro-environment. Moreover, the development of multi-model ensembles are becoming increasingly important. Application of multiple models with varying spatial and temporal resolution as well as ecological and biogeochemical complexity will provide a more comprehensive and realistic response to real-world problems than basing on isolated and deterministic predictions (Ganju et al., 2016). Combining cross-scale numerical models, whilst harvesting the power of individual model and their functions, represents the outlook for future model development.

### 2.1.2 Water Quality Modeling

For centuries, human civilizations flourished around freshwater sources. Agricultural societies thrived near rivers and lakes, where the natural cycle of flooding brought new soils and nutrients to the land. While early civilizations enjoyed a continuous source of fresh and drinkable water through the work of natural hydrological cycle, they failed to realize the effects of water quality deterioration have on soil salinization, agricultural productivity and public health. It was not until the 19<sup>th</sup> century that a better understanding of the hydrological cycle was achieved (Orlob, 1983). The consciousness of water quality was then developed after the connections between water pollution, hygiene and sanitation and enteric diseases were made. The identification of disease-causing organisms in the water bodies and the recognition of water as a form of transporting these organisms from their source to receptor have triggered rapid development in the technology of water treatment. Meanwhile, management

## Literature Review

---

of natural water resources and monitoring of water pollution became a vital part of disease prevention, public safety and urban development. Advancement of analytical techniques for the measurement of constituents and elements in the water bodies have stimulated researchers to explore more deeply into the behavior and specifics of natural freshwater sources such as rivers and lakes. Subsequently, the development of water quality modelling has begun.

Water quality models are effective tools in simulating the basic physical, chemical and biological processes of aquatic ecosystems and predicting pollutant transport in water environment. The models are capable of examining quantitatively the response of water bodies under the presence of pollutants. Predicted water quality patterns are used by decision makers to instigate effective water resource protection and management. The results generated by the water quality models would otherwise be challenging to obtain, as the hydro-environments in discussion are often difficult to access and are in such large scale that labour and material costs would be tremendous. In addition, detailed experiments and analysis are impractical and expensive to be carried out on-site for a substantial period of time under the harsh natural conditions. The numerical models also allow the simulation, prediction and assessment of the effects of any potential construction projects on the hydro-environment (Wang et al., 2013). These projects that are petrochemical, hydrological and ecological related could have significant impacts on the aquatic environment after enforcement. The water quality models offer the stakeholders a convenient yet reliable tool for environmental impact assessment, as well as the opportunities to look at multiple scenarios and possible consequences of the construction projects and to determine the optimal operational and control measures for maximum positive externalities.

The journey of numerical water quality modeling began less than a century ago. The first mathematical model to study water quality in freshwater bodies described numerically the balance of dissolved oxygen in a stream with the aim to control river pollution in Ohio state of the US (Streeter and Phelps, 1925). Building on the first

## Literature Review

---

model, the simple 1-D BOD-DO bilinear system model was developed and applied in rivers and estuaries (Burn and McBean, 1985). More BOD parameters were considered in the modified BOD-DO models (Camp, 1963; Dobbins, 1964; O'Connor, 1967). Since the late 1960s, two-dimensional models were built and applied to water quality simulation of lakes and gulfs (Gough, 1969; Welander, 1968). The development of non-linear system models then followed with consideration of the nitrogen and phosphorus cycles, as well as the phytoplankton and zooplankton systems. Additional parameters such as biological growing rates, sunlight, nutrients and temperature were included in the models. Due to the non-linear relationships, the FDM and FEM were applied as solving methods (Yih and Davidson, 1975). At this point much of the research effort was focused on the development of deterministic models applicable to steady conditions. Researchers began to recognize the stochastic nature of water quality and the random characteristic of pollutant transport in water bodies (Mehta et al., 1975; Padgett and Rao, 1979; Thayer and Krutchkoff, 1967). Their works on addressing the issue of probabilistic considerations in water quality estimation have brought about the realization that water quality cannot be precisely predicted at any given point in time and space. The inherent uncertainty in water quality arises in part due to the variability of the components involved in the many physical-chemical-biological processes and in part due to the ambiguous measurements of water quality variables (Constable and McBean, 1979). However, such realization did not deter the advancement of water quality models.

In the last few decades, the field of water quality model development has matured rapidly under the expansion of model scale and complexity. Distinct advancements include the introduction of three-dimensional water quality models (Li et al., 2011; Zheleznyak et al., 1992), the inclusion of non-point source pollution as a variable input (Tim and Jolly, 1994) and the increasing number of state variables integrated in the water quality models (Wolanski et al., 1992). The influence of sediment and its roles in affecting nutrient processes in freshwater environments have also received increasing interests (Chao et al., 2010; Liang et al., 2013). Relations between water

## Literature Review

---

quality patterns and topographical conditions are also the subjects of investigation (Lindim et al., 2011; Zheng et al., 2004). The effect of lake size on phytoplankton nutrient status were studied in Guildford et al. (1994). The influence of different type of hydraulic structures on hydrodynamic process and pollutants transport was investigated in Tang et al. (2014). Meanwhile, the significance of thermal behavior and related heat exchange processes on rivers was studied in Caissie (2006). Advanced hydrological and water temperature modeling framework that tackle basin environment at large spatial and temporal scale river was also developed (van Vliet et al., 2012).

Research attention on the numerical simulation of scalar transport in natural water bodies was facilitated by the incorporation of hydrodynamic models with water quality models. Along with the mathematical models of the physical-chemical-biological processes in natural waters, numerical solute transport simulations are helpful in assessing water pollution and designing measures for water quality remedies (Kong et al., 2013). Numerical schemes for scalar transport problems were widely studied for more efficient and accurate simulations (Falconer, 1991; Gross et al., 1999; Liang et al., 2010; Lin and Falconer, 1997). Meanwhile, alternative methods for the numerical modeling of solute transport are being explored. The Lagrangian approaches were considered in contrast to the conventional Eulerian solute transport schemes. Mathematical models that use the Lagrangian random walk particle tracking method were applied to predict and track solute transports, dispersion and vertical mixing in a variety of environments that include tidal wetlands, submerged vegetations and estuaries and coastal regions (Arega and Sanders, 2004; Barber and Volakos, 2005; Liang and Wu, 2014). Other methods such as the thermal imaging study (Liang et al., 2012) and the stochastic solute transport equations (Yoshioka and Unami, 2013) were also explored in the regime of solute transport modeling.

The integration of hydrodynamic and solute transport models, along with the advent of modern computational capability and techniques, has fueled the development of water quality models tremendously and led to the emergence of modern-day hydro-

## Literature Review

---

environmental models (Wang et al., 2004). Widely accepted modelling tools include Delft3D (van Vossen, 2000; Xu et al., 2017), WASP (Ambrose et al., 1993; Tufford and McKellar, 1999), CE-QUAL-W2 (Cole and Well, 2006; Zhang et al., 2012b), MIKE (DHI, 2017d; Liang et al., 2015; Sokolova et al., 2013) and EFDC (Hamrick, 1992; Liu et al., 2016; Wang et al., 2014c). They are commonly used in research studies and industrial analysis worldwide. The many water quality models are consistently being reviewed and compared for a selection of data requirements, modeling capability and desired purposes (Cao and Zhang, 2006; Kannel et al., 2011). The choice of an appropriate model and the required input data always depends on the purpose of the specific study. The number of water quality models being developed, both for industrial and research uses, is vast. The models that are mentioned in this section and the areas in which they are investigated in the field of hydro-environment only represent the tip of an iceberg. Such phenomenon illustrates the challenges for the development of water quality modeling, which are the accumulation of scattered efforts and the lack of systematic measurement and analysis.

The broad spectrum and many components of water quality modeling in hydro-environment creates challenges for development by its own nature. Research on current water quality modeling are constituent focused, case based and model specific. In most of the studies, a method is chosen in the form of either laboratory experiments, on-site measurements or numerical simulation to investigate a certain constituent of the water environment, such as nutrients and sediments, from a particular freshwater area using a specific water quality model that is either commonly available or developed in-house. The great degree of variability and purposes have led to a mixture of studies that are massive in number but dispersed in focus. Individual studies on a distinct problem at a certain location are feeble on their own. The same water quality model could be used for studying different constituents at locations with different topographical and nature characteristics. However, the same constituent within an area of interest is rarely studied by different models, which means there is little model comparison on a particular problem. In light of the above, the direction of this research will set

on building a standalone study that holistically covers the scale, integrates the major constituents and addresses the issues the subjected hydro-environment, while also providing supporting materials and results to other existing studies of similar regions and allowing comparison to be made between various literature covering the issues of such hydro-environment.

## 2.2 Poyang Lake: Background and Challenges

Poyang Lake (28°25'-29°45' N, 115°50'-116°44' E), located in Jiangxi province in southeastern China, is the country's largest freshwater lake (Figure 2.1). Poyang Lake connects with the the middle and lower reaches of Yangtze River through a channel in the north, accounting for 15.5% of the river's annual flow capacity (Guo et al., 2012b). Poyang lake is fed by a complex river system composed of five major rivers; Ganjiang, Fuhe, Xiushui, Xinjiang and Raohe. The lake region acts as a natural buffer for the Yangtze River, providing extra volume for water storage, flood control and pollutant dilution. The lake has a total surface area ranging from less than 1,000 km<sup>2</sup> to more than 3,000 km<sup>2</sup> depending on the seasons, with a maximum dimension of 173 km in length and 74 km in width (Wu and Liu, 2015). The Poyang Lake basin covers an area of  $16.2 \times 10^4$  km<sup>2</sup>, which accounts for nearly 97% of Jiangxi province's catchment areas (Zhao et al., 2010). Average water depth is 8.4 m with a generally flat riverbed (Cheng and Ru, 2003). Poyang Lake is situated in a humid subtropical climate in which the annual average temperature is 17°C and a frost free period of 240-330 days per year (Hui et al., 2008).

Natural resources in Poyang Lake are rich and extensive given its size and scale. In addition to direct resources in the form of water and land, the lake also has wetlands that serve as natural habitats for numerous migratory birds and aquatic species, including endangered species such as the finless porpoise and migratory waterfowls (Tan et al., 2014). Poyang Lake also poses great social and economic values as demonstrated in Figure 2.2. The lake district forms the foundation for agriculture, renewable energy

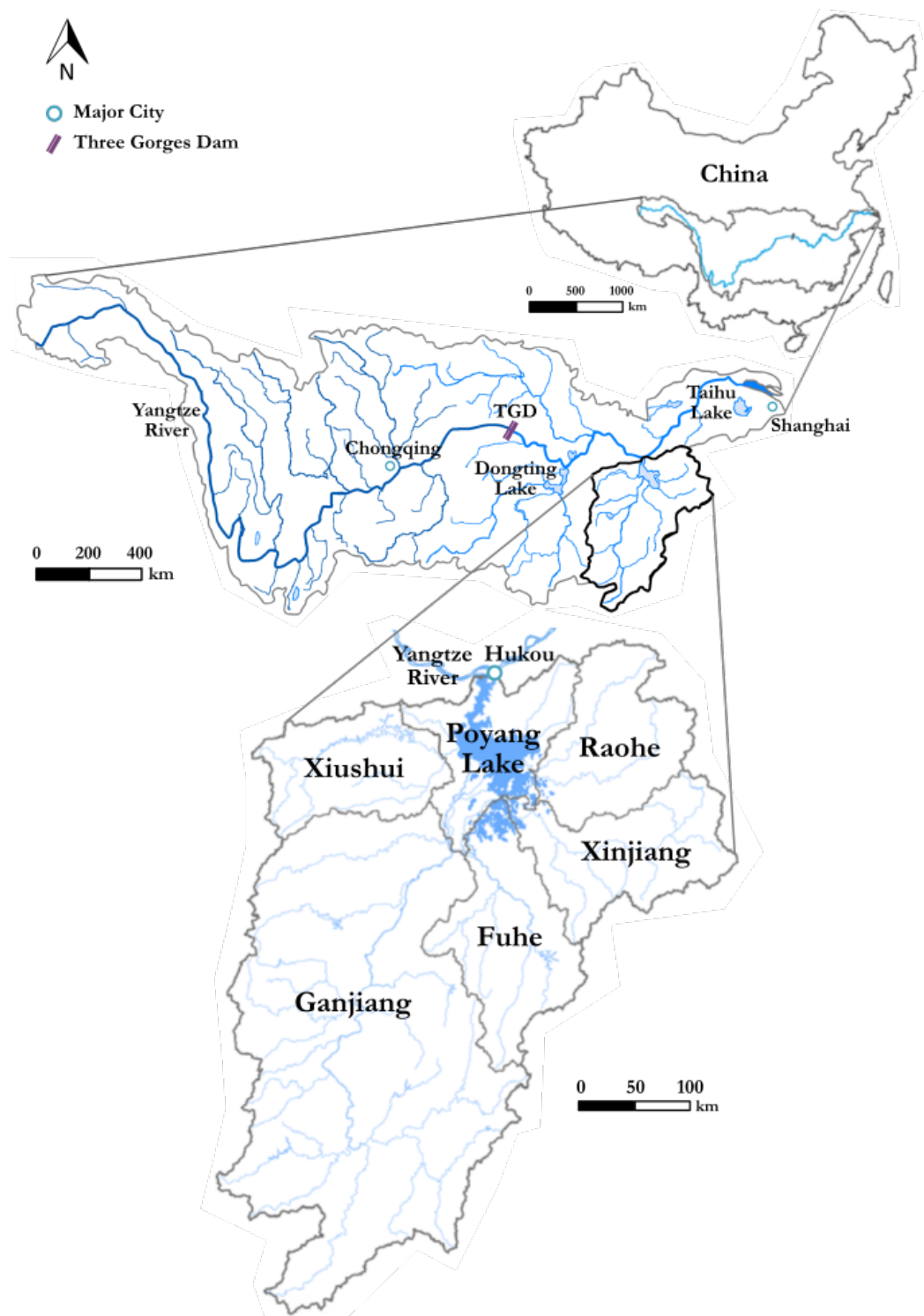


Fig. 2.1 Location of Poyang Lake in China



(a) Historical structure at Hukou



(b) Poyang Lake and Yangtze River interface



(c) Sand dredging on Poyang Lake



(d) Poyang Lake Research Headquarter at Gongqing

Fig. 2.2 Poyang Lake natural and historical environments

generation and tourism in the region. A total GDP of 548 billion Yuan (~GBP 60 billion) was recorded within the Poyang Lake region in 2010, accounting for 57.97% of the Jiangxi province total (Lv and Wu, 2013). The lake district is the main freshwater source of several nearby cities, such as Nanchang, Jingdezhen and Jiujiang, that have a combined population of over 14.5 millions (Huang et al., 2011).

### 2.2.1 Hydrodynamics and Hydrology

The hydraulic characteristics of Poyang Lake are complex and volatile in nature due to the lake being the center of an immensely dynamic river-lake system. Poyang Lake is regulated both by the five main rivers from the south and the Yangtze River in the north. Runoff from the five main river basins and their tributaries contributes to an average inflow rate of 4,700 m<sup>3</sup>/s (Tan et al., 2014). Situated within a subtropical humid monsoon zone, the lake has an annual precipitation of 1,632 mm with high seasonal and regional variations (Gao et al., 2014). 74.4% of the rainfall concentrates between the periods from March to August (Wang et al., 2014a). Prior to June every year, flow velocity ranges from 1.48–2.85 m/s in the northern lower region and 0.3–1.54 m/s in the southern higher regions. During July to October, flow velocity would be limited to 0.1 m/s. Average wind speed of Poyang Lake is at 1.8–2.7 m/s. The lake has a total number of 1,080 reservoirs of various sizes, summing up to a total capacity of  $12.6 \times 10^8$  m<sup>3</sup> to accommodate the amount of rainfall and runoff in the region (Guo et al., 2012b).

Poyang Lake is characterized by its high contrast and fluctuation in water levels and surface area between wet and dry seasons. At the highest recorded water depth of 22.59 m at Hukou station, the lake has a surface area of 4,500 km<sup>2</sup> and volume of  $340 \times 10^8$  km<sup>3</sup>. At the lowest depth of 5.90 m, the lake area and volume shrink to 146 km<sup>2</sup> and  $4.5 \times 10^8$  km<sup>3</sup> respectively (Zhang et al., 2015b). This results in great variation of the lake's bathymetry throughout the year. In wet summer seasons, high water level gives the region the bathymetry of a lake; whilst in dry winter seasons, low

## Literature Review

---

water level results in that similar to rivers and streams. The great fluctuation in water level of Poyang Lake and the difference in the lake environment between seasons can be illustrated by Figures 2.3 and 2.4, which shows the water surface area of Poyang Lake in July during the wet season and in January during the dry season respectively.

Under normal conditions, the water level in the south is greater than that in the north of the lake, and hence this gradient governs the flow of water from the south towards the north and reaches the outflow at the Yangtze River through a narrow channel at Hukou (Cai and Ji, 2009). In the beginning of the summer season from April to June, flooding along the Yangtze River basin and five rivers tributaries, coupled with an increasing rainfall, gradually raises the water levels in both the Yangtze River and Poyang Lake. In the period between July and September, although inflow from the five rivers reduces, the elevated water level of Yangtze River may drive a potential back flow in which water flows from the Yangtze River into Poyang Lake, maintaining the high water levels in Poyang Lake. There is a general 14 days inverse direction flow into Poyang Lake, approximately 2.2 times a year. The typical south-north water flow is impeded and the water levels become similar across the lake's extent (Li et al., 2015a; Shankman et al., 2006). The high water levels at Poyang Lake persist for a substantial period of time between April and September. Only from October onward the dry season arrives and water levels drop steadily due to a drop in Yangtze River's water levels, triggering an increase in the outflow of the lake.

The close interconnection between Poyang Lake with Yangtze River and the five rivers also has a direct effect on the flooding and drought status of the lake. Studies by Hu et al. (2007) showed that the surface flows from the five river basins are the primary source of the major floods in the Poyang Lake basin, with the Yangtze River inflow and its blocking effect being a complimentary role. Previous occurrence of flooding and droughts in the five river regions cohered with the significant water level changes in Poyang Lake. Such changes would be magnified should the Yangtze River region nearby experience similar trends across the same period. The peak flooding periods

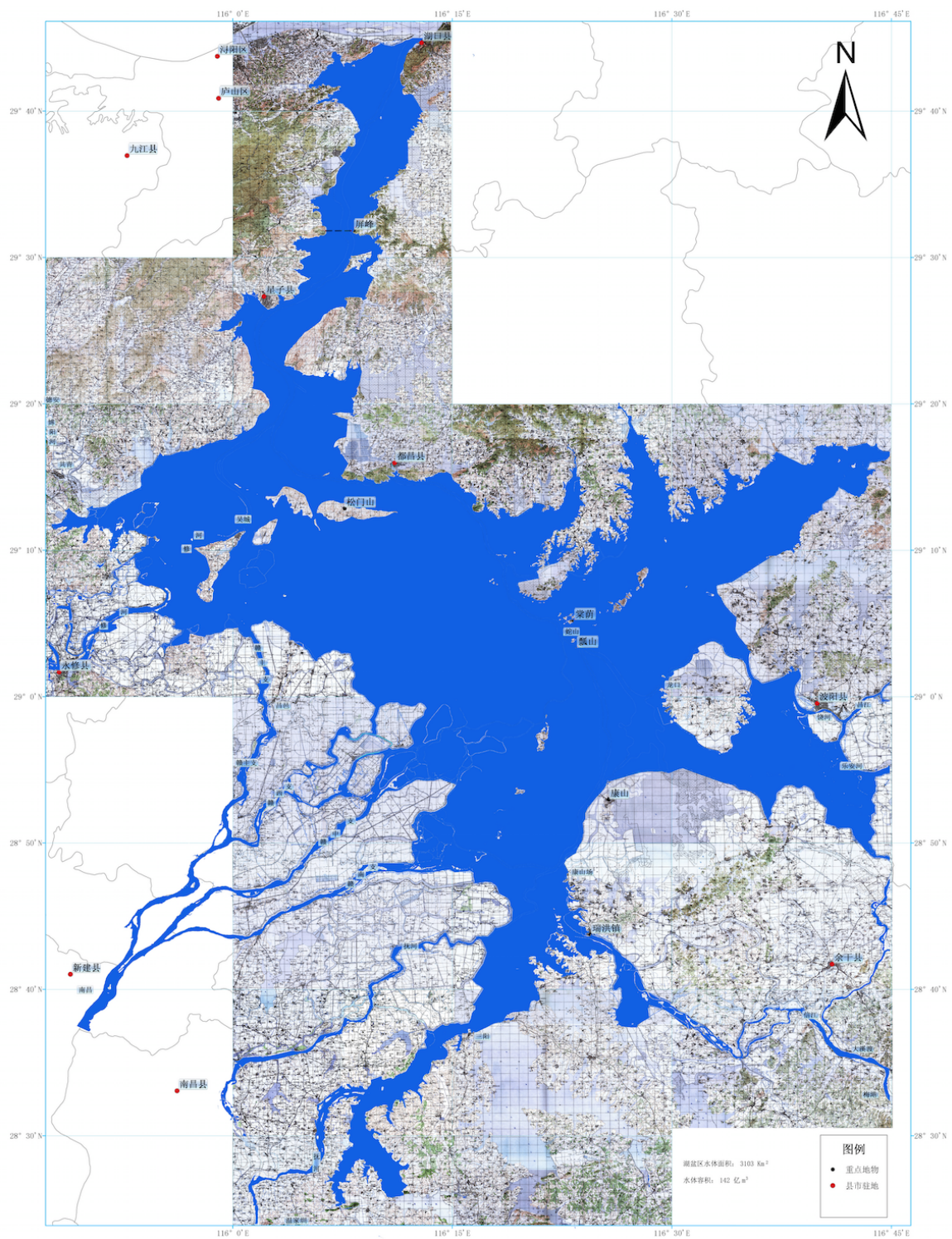


Fig. 2.3 Poyang Lake water surface environment in July during wet season

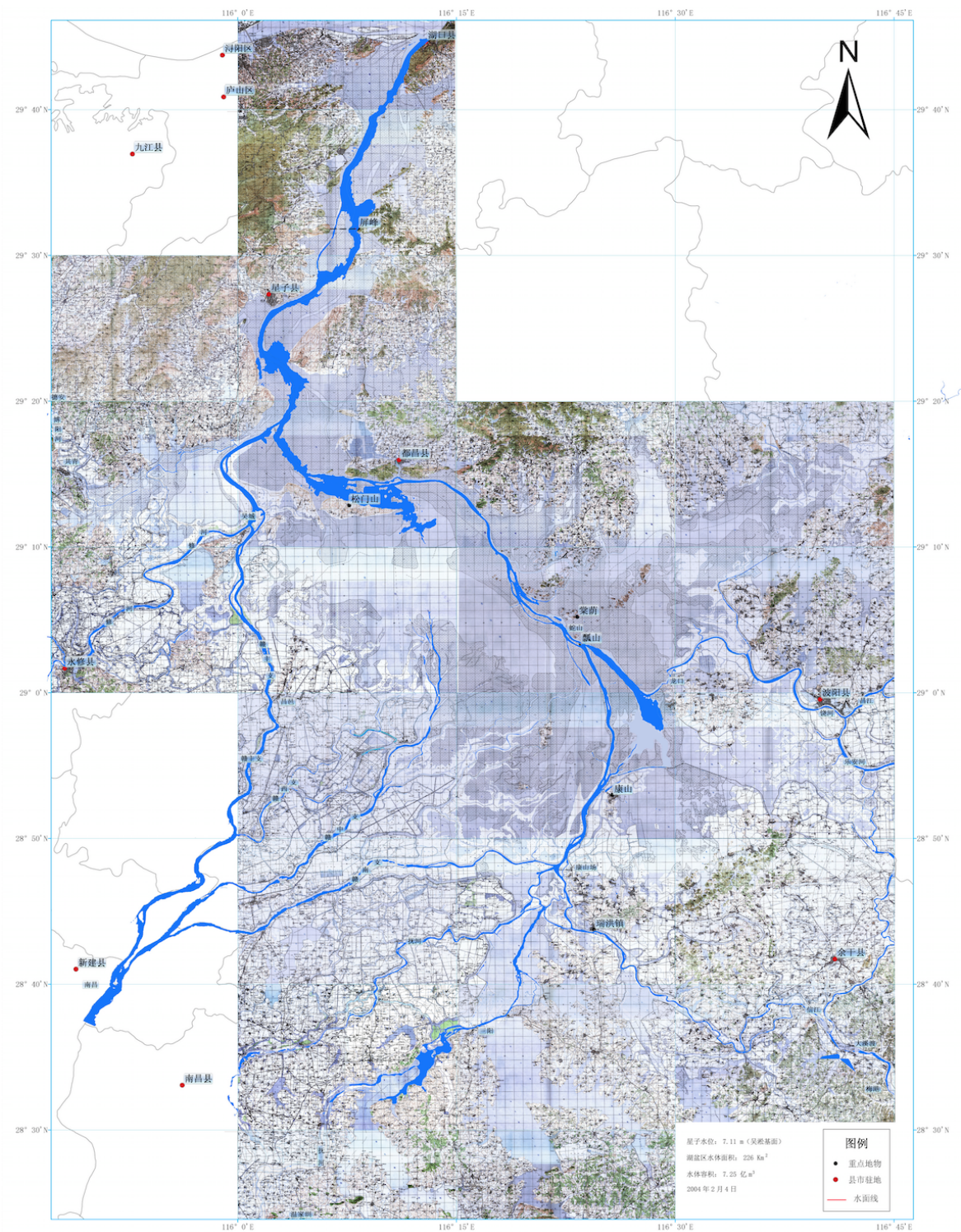


Fig. 2.4 Poyang Lake water surface environment in January during dry season

## Literature Review

---

of Poyang Lake and Yangtze River are generally 20 days apart. From 1950 to 2010, Poyang Lake experienced severe flooding in 1973, 1983, 1995, 1996, 1998 and 1999, and extreme drought in 1969, 1971, 1972, 1978, 2006 and 2007, mainly triggered by unusually high and low rainfall precipitation respectively (Li et al., 2015a; Tan et al., 2008).

Poyang Lake is facing pressing issues with its water quantity and hydraulic behavior. The lake's water levels have recorded a declining trend in the 21<sup>st</sup> century. Monitoring stations around Poyang Lake all logged the lowest historic water levels over the last two decades and average water level of the lake dropped from 14.0 m to 13.3 m over the last 60 years (Guo et al., 2012b). The main reasons behind the drop in water levels include decreasing rainfall and influx from upstream rivers.

Over the period 2000–2011, annual rainfall dropped 7.3 mm on average. The annual rainfall average of that period (1,546.8 mm) was 50.3 mm lower than that of the previous 50 years. The difference in seasonal rainfall had become increasingly pronounced, with winters recording greater rainfall than average and summers having an obvious dip compared to previous years. The drop in rainfall was coupled with the reduction in lake inflow. In the 20<sup>th</sup> century, there was a general trend of increasing inflow throughout. However in 2000–2011 there was a gradual decline in inflow by about 11.0% below that of the previous five decades. The drop in influx has a direct impact on the lake's water levels, especially during the dry seasons. The period with the lowest water levels began earlier and extended in length. Precedent dry seasons started in about mid-November, whereas over the period 2000–2011 dry seasons began in late October that was 24 days earlier in average. The end date of dry seasons however did not change, which means that along with a forward shift of the low water level period, the lake was also experiencing an extended period of dry season.

In addition, climate change and human activities such as rampant sand dredging and construction of 29 dams in upstream Yangtze River further contributed to the

issue and caused the size of Poyang Lake to shrink further (WantChinaTimes, 2012). The construction and operation of the Three Gorges Dam (TGD) also played a role in Poyang Lake's shrinkage problem. Further details of the effect of TGD on Poyang Lake will be discussed in subsequent paragraphs in this chapter. The decline in water quantity in Poyang Lake has sparked increasing concerns of depreciating freshwater sources for the human and wildlife population in the region.

### 2.2.2 Impact of Three Gorges Project

Apart from factors such as natural environmental and climate changes, artificial circumstances and human interventions are also greatly influencing the hydro-environment of Poyang Lake. The effects of the Three Gorges Dam (TGD) on Yangtze River and its associated river basins and water environments, including the Dongting Lake and the Poyang Lake, have been widely debated prior to, during and after the construction of the structure. TGD is located on the Yangtze River at the west of the city of Yichang in Hubei province, China. It is a straight-crested concrete gravity dam structure 2,335m in length with a maximum height of 185 m. The construction of the dam began in 1994 and at the time of its completion in 2006, it was the largest dam structure in the world. TGD acts as a mega hydroelectric power production unit with 32 turbine generator units in total that could generate 22,500MW of electricity. The dam also was intended to protect millions of people from the periodic flooding that plagues the Yangtze basin (Encyclopaedia Britannica, 2018).

Increasing numbers of researches investigating the relationship between Yangtze River and its nearby water bodies and the impact of TGD on the water environment including the Poyang Lake basin have surged in recent decades. Li (2008) pointed out that reducing water levels along the Yangtze River would trigger an increase in water flowing out of Poyang Lake. In addition, erosion of upstream riverbeds and siltation at Poyang Lake's mouth due to the operation of TGD upstream could have disastrous consequences for flood prevention efforts in the next 30 years around the Poyang Lake

## Literature Review

---

region. Further research emphasized on the effect of TGD on altering the lake-river interaction and weakening the river forcing on the lake, simulating more outflows from the lake to the river. As a result, the water storage capability of Poyang Lake is further reduced (Guo et al., 2012a). Hu et al. (2007) studied the impact the Poyang Lake basin effect and Yangtze River blocking effect have on the variations of Poyang Lake water level and floods at annual to decadal scales. Results show that the blocking of Yangtze River on the outflows from Poyang Lake plays a complementary role to the basin effect in influencing the lake's water level and development of floods. This finding was further reinforced by Gao et al. (2014), who stated that climate variation for the Yangtze catchment and Poyang Lake watershed was the main factor in determining the changes of water exchanges between Yangtze River and Poyang Lake. Nonetheless, they pointed out that the emplacement of TGD accelerated this rate of change.

The impact of TGD on Poyang Lake's hydrodynamics was further studied in Wang et al. (2015a). The annual average water level in Poyang Lake recorded an overall reduction in the period of 2003-2013 as compared to the period 1953-2002 (Figure 2.5). This reinforced the concept that the decline of water level in Poyang Lake is attributed to the operation of TGD. An investigation on the variation of seasonal water level fluctuations of Poyang Lake was conducted by Dai et al. (2015). The water levels during the four distinct seasons (dry season, rising season, flood season and retreating season) before and after the operation of TGD were compared. Results showed that the magnitude of water level fluctuation had changed considerably under the influence of the TGD. The water levels of Poyang Lake rose and retreated earlier in the season and the overall water levels were lowered in general. It was suggested that working strategies are necessary to balance the TGD impacts on flood control and water resources, as well as their social and ecological consequences in the Poyang Lake basin (Zhang et al., 2012a). In 2012, Poyang Lake's shrinking and drying situation was further worsened due to the reduction of Yangtze River's water levels to their lowest in five decades. In October 2012, TGD began holding back water for electricity generation, causing the water level to drop further. Poyang Lake as a result had an

extremely dry season that lasted until late March in 2013, which grew to 175 days from the usual 113-148 days period in previous years (WantChinaTimes, 2012).

The influence of TGD on the hydro-environment of Poyang Lake is prominent. The operation of TGD has altered the natural hydraulic and hydrological behavior in the Poyang Lake region. Reduction in Yangtze River's water levels diminishes its blocking effect and triggers increasing outflows from Poyang Lake, which in turn further reduces the lake's water levels and extends the length of the dry seasons. Researchers ought to be aware of the operation of TGD and the potential changes in Yangtze River when studying the hydro-environment of Poyang Lake.

### 2.2.3 Existing Research on Hydrodynamics of Poyang Lake

The extension and shift of dry seasons, coupled with a series of frequent flooding and droughts over the last few decades in the Poyang Lake region, have triggered questions on the relationship of climate change and anthropogenic activities with the lake environment. Researchers began putting their attention on the impact of climate change and land-use on the lake's hydrology and regional catchment behavior. Zhao et al. (2010) attempted to analyze the relationships between stream flow and climate variables in order to clarify the links of climatic changes with Poyang Lake's water

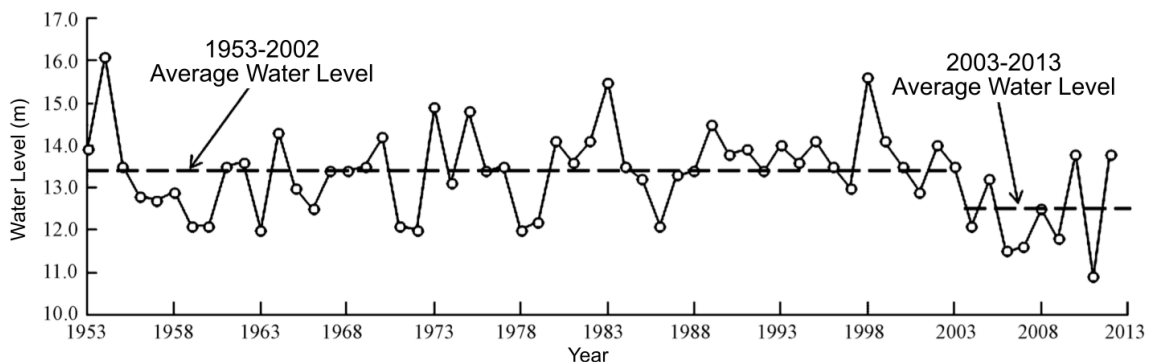


Fig. 2.5 Annual average water level at Xingzi of Poyang Lake for 1953-2013 (Source: Wang et al., 2015)

## Literature Review

---

resources. However the results were not significant, with the correlation of discharge variation more strongly related to precipitation changes than to evapotranspiration changes as the main takeaway. Ye et al. (2011) evaluated the possible impacts of climate change on both inflow generation and changes in lake water level of Poyang Lake, using a large-scale distributed hydrological model under different climate change scenarios. In that it is suggested that a more rigorous mathematical representation of the dynamics of the lake water level and the influence of the Yangtze River are needed. Ye et al. (2013) then analyzed the characteristics of hydro-climatic changes of Poyang Lake catchment based on observed data from 1960 to 2007. The major finding is that the relative effects of climate change and human activities varied among sub-catchments as well as the whole catchment under different decades. Some sub-catchments were primarily affected by human activities at certain period, while the others could be under the influence of climate change. The study also indicated a long term increase trend of precipitation and a decrease trend of potential evapotranspiration based on statistical analysis. Climate change is the dominant factor in causing the increase of annual streamflow of the Poyang Lake catchment, while human activities may be responsible for the decrease of runoff in relatively small proportion. Similar study was found in Sun et al. (2013) with the suggestion that increasing precipitation due to climate change is the major driving factor for the increase in annual streamflow in the catchment region of Poyang Lake.

There has been an obvious increase in efforts in building hydrodynamic models for Poyang Lake. Li et al. (2012, 2014) developed an integrated model that consists of a hydrological model WATLAC and a commercial 2-D hydrodynamic model MIKE21 as a first attempt to simulate the response and characteristics of Poyang Lake's large scale and highly dynamic catchment system. Their hydrodynamic model was able to respond well to the spatial lake water-level variations, the complex flow exchanges with the Yangtze River and lake flow patterns in the Poyang Lake catchment and to simulate the variation of water levels in Poyang Lake to great accuracy (Figure 2.6). The group then conducted simulations based on the 2-D hydrodynamic model MIKE21 to investigate

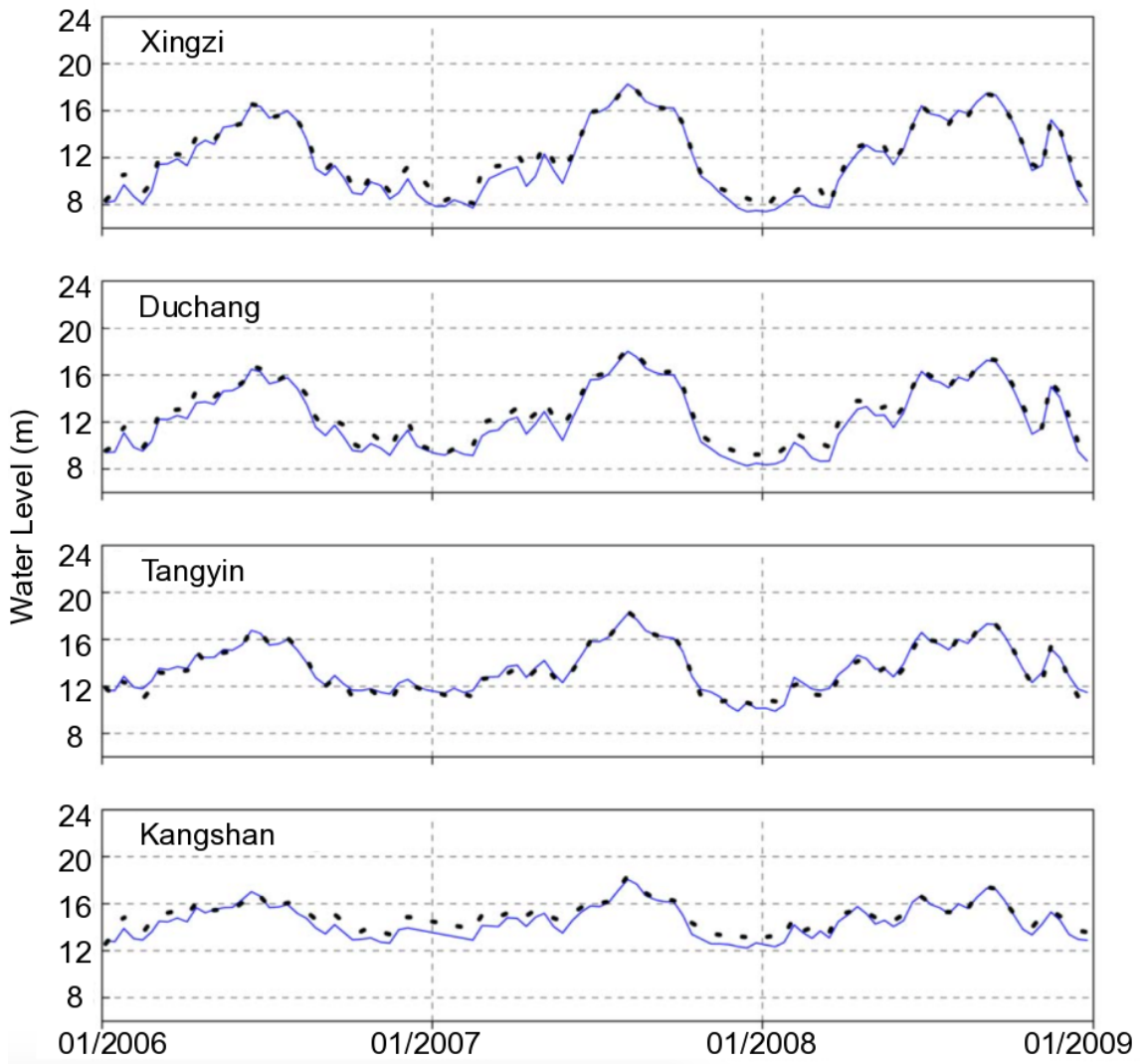


Fig. 2.6 Comparison of observed (solid line) and simulated (dotted line) lake water levels for 2006–2008 by Li et al., (2014)

## Literature Review

---

the hysteretic relationship in the lake's inundation dynamics with Yangtze River (Zhang and Werner, 2015) and to model the hydraulic characteristics and transport behavior in Poyang Lake with the aid of particle tracking sub-model or dye tracer simulations (Li and Yao, 2015; Li et al., 2015b). These models calculated the transport trajectory and residence time in large and complex lake-river system, with Poyang Lake and Yangtze River's interaction as their subject. Key statements were made on the highly spatial varying residence times that differed in hydrographically sub-regions within Poyang Lake, as well as the seasonally changing travel times from the potential pollution sources to the lake outlet ranging from less than 8 days to up to 32 days. These findings further illustrate the dynamic characteristics of Poyang Lake and the challenges in modeling its lake environment and behaviours.

The well-established Environmental Fluid Dynamics Model (EFDC) model was used to study the water levels and inundation areas of Poyang Lake from 2009 to 2011 (Lu et al., 2015). Preliminary results showed that the water surface height and inundation areas measured by Radar altimeter ENVISAT RA-2 and MODIS images correlated well with the model predictions (Figure 2.7). The 3-D layered model was then used to investigate the water age and water mass transport ability of Poyang Lake (Qi et al., 2016). Lagrangian particle tracking method was incorporated with the model to study the water age and chlorophyll *a* concentrations within the lake. The proposed Poyang barrage project was also taken into consideration. Figure 2.8 demonstrates the results of the study showing an increase in water age, especially during the winter months, under the use of barrage project. For parts of the east lake, the establishment of the barrage would raise the water age most remarkably by more than 50 days. It was suggested that the weaker water exchange ability in these specific regions will increase risks for water quality deterioration. This study is among the more comprehensive one in attempting to model Poyang Lake's hydrodynamics and to give insights on the effect of the potential barrage project. In Zhang et al. (2015a), similar practice of developing a hydrodynamic and inundation model for Poyang Lake with remote sensing data as a mean of validation can be seen. Despite successfully modeling the

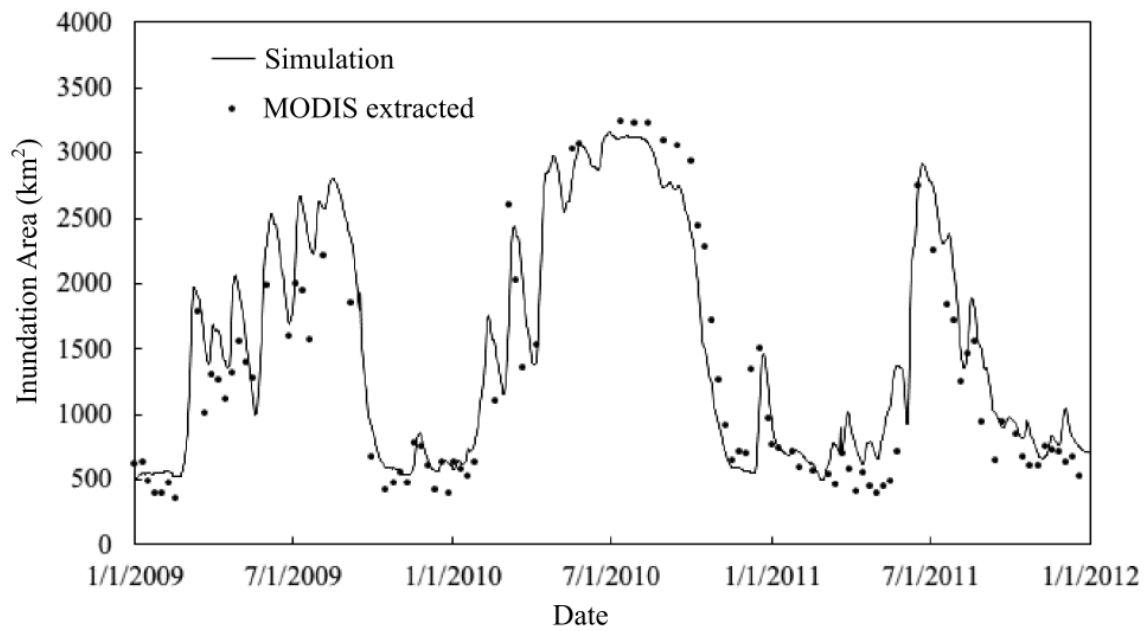


Fig. 2.7 Time series validation of inundation area between MODIS images extracted and simulation by Lu et al. (2015)

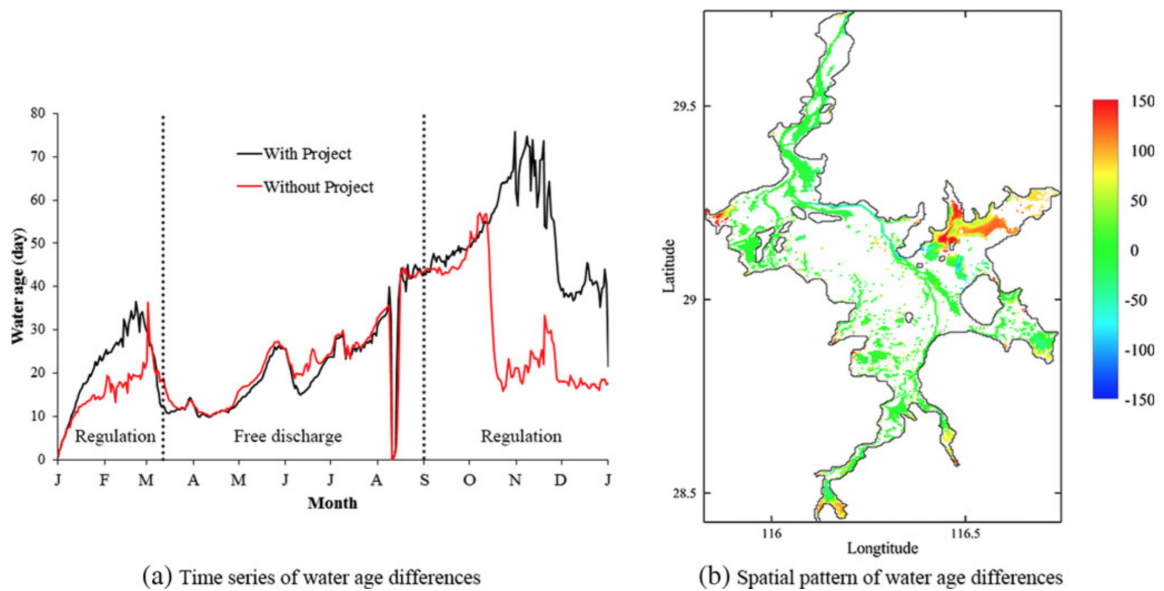


Fig. 2.8 Time series of water age differences at Hukou station and spatial pattern of water age differences on Dec 2 2009 between the barrage project case and the non-project case by Qi et al. (2016)

## Literature Review

---

hydraulic behaviours of the lake, the study did not incorporate the sediment transport and biochemical aspects of the lake nor investigate the potential barrage impact on the lake environment.

Meanwhile, other researchers adopted a different approach in building their own numerical models. In an attempt to investigate the impact of intensive human activities and ongoing climate change on large-scale water system in the middle Yangtze River basin including Poyang Lake, Lai et al. (2013) built a new model called the CHAM that dynamically couples a 1-D unsteady flow model and a 2-D hydrodynamic model. The model, particularly suitable for large-scale water systems model, was used to compare the significance of lake inflows and Yangtze River on Poyang Lake level (Lai et al., 2014a); and to investigate the impact of TGD impoundment in Poyang Lake (Lai et al., 2012, 2014b), proving that the TGD impoundment does cause significant changes to the flow regimes and hydrology of Poyang Lake. The same research group attempted to build a 2-D numerical simulation of hydrodynamic and pollutant transport for Poyang Lake (Lai et al., 2011b). However, validation and subsequent analysis of the developed model are limited. To address high water level fluctuation that causes moving boundary and varying inflow conditions, Lai et al. (2011a) tried to utilize existing dry-wet grid method on computational fluid dynamics and boundary fitted orthogonal curvilinear grid in order to build a hydrodynamic modeling system for Poyang Lake. However the verification results only covered a short period of time (9 days) and the data used is relatively old from the year 1999.

Research on the development of hydrodynamic models for Poyang Lake has been maturing rapidly. Studies using established or in-house numerical models have demonstrated the ability to simulate the hydraulic characteristics of Poyang Lake to high accuracy. This facilitates the recent effort in advancing the numerical models to incorporate additional aspects of the lake environment, such as in depth simulation of the water quality variables and more importantly, the potential presence of the Poyang Lake barrage project.

### 2.2.4 Poyang Lake Barrage

The proposal to construct the Poyang Lake Barrage was first put forward in 2008. Its aim is to maintain and control Poyang Lake's water levels from continuous and prolonged decline, especially during the period when the Yangtze River is running low and extra outflows from the lake. The barrage project proposed the construction of a series of sluice gates along the narrowest section of the channel, which is 2.8 km wide, at the north of Poyang Lake (Li, 2014), close to its intersection with the Yangtze River (Figures 2.9 and 2.10). The gates would be open during the wet season and allow the water levels in the lake to rise. The gate would then be closed during the winter period and water slowly released in a controlled manner (Finlayson et al., 2010). The project was believed by many to be the solution to the lingering drought in the Central and East China's provinces, which has had devastating impact on the environment around Poyang Lake. The project was designed to also create economic gains from electricity generation, fishery, navigation, irrigation and water supply (WantChinaTimes, 2012).

This water conservation project, however, has sparked numerous concerns regarding its impact on the environment and its effectiveness on water management. Many feared that the benefits the barrage will bring might not justify its huge budgets of 12 billion Yuan (~GBP 1.4 billion) and the potential damages it might cause to the surrounding water environment by disrupting the natural water flow between Poyang Lake and Yangtze River (Li, 2014). Local governing authorities and officials, green parties, the press and local residents all raised their views as different stakeholders with conflicting agendas. On the supportive side, officials from the local sustainable development office suggested that the project will benefit Jiangxi province through increasing control of water sources, creating job opportunities for building work and reducing flooding and drought risks (Davison, 2014). The project will promote further economic, urban housing and tourism growth, leading to a higher GDP progression in the province (Xu, 2012). Controversially, the barrage could aggravate the drought situation in other Yangtze River basins. If the water level is too low when it reaches



Fig. 2.9 Location of potential barrage in Poyang Lake (Source: CCTV China)



Fig. 2.10 Proposed barrage design in Poyang Lake (Source: WWF China)

## Literature Review

---

the estuary in Shanghai, seawater backflow could occur as a serious environmental problem. Subsequent mitigation plans and projects would only further complicate the problems and damage the ecosystem (Davison, 2014). Prioritizing the ecological diversity of the Yangtze basin and the sustainable utilization of wetlands, WWF China (2014) suggested that the project will irreversibly and unpredictably impact the water quality, fish diversity, the living habitat of the lake's porpoise and migratory birds and the silt quantity in the lower reaches of Yangtze River.

The amount of research carried out with regards to the potential impact of Poyang Lake barrage project is limited. Using extensive hydrological data and generalized linear statistical models, Zhang et al. (2012a) attempted to evaluate the impact of the barrage project on Poyang Lake wetlands. However conclusive results were lacking and further assessment based on a wide ranges of parameters such as hydrological and hydraulic characteristics of the lake, water quality, geomorphological characteristics, aquatic biota and their habitat and wetland vegetation were suggested. Focusing on the protection of wintering migratory birds habitats, Qi and Liao (2013) studied the scheme of water level regulation of the barrage project using historical hydrological data, distribution data of wintering migratory birds and basic geographical data. It was suggested that certain farmland areas should be returned to lake use in order to facilitate the execution of the proposed project. The impact of the barrage on the hydrology and bird habitats using the EFDC model (Wang et al., 2014b, 2015b) and the finless porpoise behavior using a 2-D diffusion model (Fang et al., 2016) were also examined. The general remarks from these research were that the project would have little impact on the wildlife habitats yet further research must be conducted with in depth considerations on various parameter and factors. Under the circumstances that the current level of research and demonstrations were insufficient to support the approval and construction of the barrage project, the local government postponed the development of the project and called for more scientific research and evidence of the environmental importance of the barrage project on Poyang Lake.

### 2.2.5 Water Quality

Freshwater resources in Poyang Lake consist of mainly of two forms: surface water and groundwater. Surface water resource associated with land is reported at 17.1 billion m<sup>3</sup> whilst that of the lake is 1.28 billion m<sup>3</sup>. Groundwater sources account for 3.22 billion m<sup>3</sup> in volume (Guo et al., 2012b). Population, wetlands, wildlife and forests in the Poyang Lake region strongly rely on the presence of these clean water resources to sustain and grow.

A series of water testing and monitoring have been performed by Poyang Lake's local water bureau, under the guidelines provided in "Environmental Quality Standards for Surface Water" of Ministry of Environmental Protection in China. In evaluating water quality in Poyang Lake, the standard focuses on a set of parameters, which include water temperature, pH, dissolved oxygen (DO), permanganate index (PI), biochemical oxygen demand (BOD), ammoniacal nitrogen (NH<sub>3</sub>-N), nitrate (NO<sub>3</sub>), total phosphorous (TP), total nitrogen (TN), volatile phenols, chlorophyll and several heavy metals. For each parameter, five different categories (Class I to V, with I being the cleanest and suitable for freshwater source and V being the least clean and suitable only for industrial and agricultural uses) are allocated with preset values associated to the parameter for classification. For example for ammoniacal nitrogen concentration, value below 0.15 mg/L is classified as Class I, below 0.50 mg/L for Class II, 1.00 mg/L for Class III and so on until 2.00 mg/L for Class V (Ministry of Environmental Protection, 2002). These standards are in line with the ammonium limit of 0.50 mg/L listed in the Drinking Water Directive issued by the European Commission (1998). With each parameter having a corresponding classification system, water quality testing on Poyang Lake can be clearly labeled for further indication and management.

Of the total amount of water entering Poyang Lake, Class I to III water accounted for 74.5–92.5% between 2007 and 2011. Inflows from the five rivers consisted of 87–100% of Class I to III water with main pollutants being NH<sub>3</sub>-N and TP. Although an

## Literature Review

---

exceptionally polluted inflow in Lean River with 13% Class I-III water is also entering Poyang Lake with high  $\text{NH}_3\text{-N}$  and TP concentrations (Guo et al., 2012b), the lake has been able to dilute the pollution and match a generally satisfactory water quality standard. This is also the reason why water quality in the wet seasons are generally better than that in the dry seasons.

The prolonged dry period and declining water levels in Poyang Lake lead to a drop in Poyang Lake's water capacity, which in turn reduces the self purification ability of the lake and results in the deterioration of water quality and the loss of ecological functions. Within the period of 2000-2007, the river length with water quality of Class III or worse increased from 170 km to 221 km, while the number of polluted river sections increased from 6 to 22 in the same period (Gao et al., 2010). In the 1980s, Class I and II water accounted for 85% with Class III occupied the remaining 15%. In 1990s, the proportion of Class I and II water dropped to 70% and that of Class III increased to 30%. In the years since 2003, Class I and II water only formed 50% of all waters in Poyang Lake, with Class III and IV taking up 32% and 18% respectively. In 2011, the deterioration of water quality became alarming with Class I-III water only accounted for 37.9% and Class IV-V water increased to 62.1% (Guo et al., 2012b; Tan et al., 2014). The main pollutants in the region were TN, TP,  $\text{NH}_3\text{-N}$  and COD (Luo et al., 2014). The inflow contribution of the five rivers in tonnes and percentages on each pollutant is summarized in Table 2.2. It is clear that the main contributor of pollutants to Poyang Lake are Gangjiang, Xinjiang and Raohe. Pollutants sources are diverse and spread out in the Poyang Lake region. The five rivers account for more than 80% and 60% of the lake's TN and TP inflow respectively (Chen et al., 2016). Through various natural or anthropogenic means, they enter the streams of the five rivers and are transferred into Poyang Lake.

Main sources of pollutants in the Poyang Lake region include industrial activities, municipal wastes from villages and agricultural waste from the use of fertilizers and poultry framing. Pollutant sources commonly exist as non-point source, point source,

## Literature Review

---

Table 2.2 Inflow pollutant contribution from rivers into Poyang Lake in 2013

River	NH <sub>3</sub> -N (t)	TN (t)	TP (t)	COD (t)
Xiuhe	2,831 (5.1%)	7,511 (5.3%)	448 (5.1%)	115,825 (9.6%)
Xinjiang	9,260 (16.8%)	22,938 (16.2%)	1,915 (22.0%)	197,323 (16.3%)
Raohe	9,106 (16.5%)	19,702 (13.9%)	1,191 (13.7%)	130,731 (10.8%)
Gangjiang	29,614 (53.7%)	76,944 (54.3%)	4,304 (49.4%)	634,672 (52.5%)
Fuhe	4,279 (7.8%)	14,498 (10.2%)	827 (9.5%)	127,856 (10.6%)

inner source and influx from associated rivers upstream into the lake. In 2008, discharge from industrial and municipal activities accounted for 1.389 billion tonnes. COD discharged by industrial and municipal activities were 100,300 tonnes and 345,000 tonnes respectively, meanwhile N releases for those areas were 6,260 tonnes and 28,100 tonnes apiece. Agricultural waste produces TN at 100-120 thousand tonnes per year and TP at 50-60 thousand tonnes per year. The high concentrations of pollutants are also partially generated from the mines close to a few of the rivers entering Poyang Lake as point pollutant sources (Guo et al., 2012b). Gao et al. (2016) quantified human influence on nutrient inputs of Poyang Lake basin in the past decades, showing that net anthropogenic nitrogen input and phosphorus input increased by 6 and 15 times respectively over the period. The increase of degree in human interference is triggered by agricultural production and population growth, with the intensity of nutrient influx and the average water level of the lake being the main controlling factors. In 2010, the lake recorded a TP reading at 0.010–0.230 mg/L with an average reading of 0.055 mg/L, which is under Class IV. TN reading was at 0.34–2.57 mg/L with an average at 1.28 mg/L, again under Class IV (Tan et al., 2014).

The actual efficiency of common fertilizer in boosting agricultural yields is about 30-40%. This means that in general about 60-70% of the fertilizer enters the natural environment and water bodies as a non-point source. The problem is exacerbated by excessive inputs of nitrogen fertilizer and pesticides, the annual applications of which

## Literature Review

---

increased by 50.7% and 119.7% respectively within the period 1991-2008 (Sun et al., 2012). Mistakenly believing that the amount of fertilizer used is proportional to crop yield, farmers have been known to freely apply excessive amounts and neglect the actual recommended quantity for optimal growth. Annually there is a leak of 128,000 tonnes of N and 23,000 tonnes of P (Tan et al., 2014).

On top of increasing overall discharge, the low proportion of wastewater being treated also created additional pollution problem for the regions. Many poultry and livestock farms have limited capital, resulting in the lack of measures in sewage treatment. In Jiangxi province, the amount of municipal sewage being treated was as low as 2.5% in 2007. Most of the wastewater is directly dumped into the nearby rivers and lakes. In 2010 this number had increased to 46.8%. Meanwhile, 90.1% of industrial sewage was being treated in 2000, but only 68.5% of which reached acceptable standards. The portion was raised to 92.1% in 2005. On the other hand, only 49.6% of industrial solid wastes were treated in 2009 (Guo et al., 2012b). The degree and quality of municipal and industrial sewage and waste treatment in the region are beyond unsatisfactory. In addition, policy controls on waste discharge from industrial plants and animal farms are not strictly implemented. Rules on pollution discharge are often breached.

Additionally, sand dredging and the over-planting of trees are damaging the ecology of the region. Sand dredging in the long term modifies the bathymetry of the lake and river environment, subsequently affecting the hydrodynamics of the lake. Moreover, disturbance in the riverbed triggers the release of pollutants settled and adsorbed by the sediment and contributes additional pollutant concentrations as inner pollutant sources, which account to about 1.52% of TN and 2.74% of TP annually out of the overall nutrients input (Guo et al., 2012b). Large scale planting of poplar trees, although creating income for both planters and the local government, threatens the survival of the lake's wetlands by drying up the soil and dominating water intakes from other plants. Large single-species forests are also more susceptible to pests and

## Literature Review

---

diseases. The rash of poplar planting on the shores of the lake raised great concerns from experts (Li, 2008).

Acid rain as a result of industrial activities also contribute to the declining of water quality in the region. Precipitation in the Poyang Lake region has pH values ranging from 4.38 to 5.30, lower than the 5.6 threshold to qualify as acid rain. The coverage of acid rain is estimated to be around 55.9-76.9% (Tan et al., 2008). Acid rain is hazardous to agricultural production, forest health and wetland wildlife. Moreover, acid rain contains sulfur dioxide and nitrogen oxides and reacts with aluminum in the atmosphere to further pollute the lake's water bodies (US EPA, 2018). Atmospheric deposition accounts for 2.6% and 2.3% of TN and TP respectively towards the overall nutrient contribution to Poyang Lake (Chen et al., 2016).

At the same time, heavy metals enter the lake environment as another pollutant. Toxic metal chromium (Cr) was detected in the waters close to a refuse incineration power plant near Poyang Lake (Yao et al., 2012). Laboratory sediment sample testings on heavy metals in Poyang Lake were carried out, suggesting that the lead (Pb) and cadmium (Cd) content in the lake were a cause for great concern and need to be managed meticulously (Luo et al., 2008). Heavy metals concentrations in fish species from Poyang Lake were also investigated (Wei et al., 2014). Although the metal accumulation in fish is generally low and safe for consumption, regular and long-term monitoring of the lake and its fish species is essential. The general heavy metal concentrations in Poyang Lake are within standard limits, however the management of heavy metals in Poyang Lake is not to be treated lightly as they are poisonous to aquatic wildlife and could potentially be hazardous to human via consumption.

The water quality of Poyang Lake is evidently deteriorating with potentially immense consequence regarding the ecology, wildlife and communities around the region. Under natural circumstances, the high water levels and large water volume in Poyang Lake help to dilute incoming pollutants and ensuring the water quality in

the lake. The rapid increase in industrial and farming activities of the region and the profound influence from climate change and Yangtze River have led to an increased amount of inflow pollutants and a drop in the water volume in Poyang Lake respectively. As a result, the dilution effect is weakened and water pollution worsens (Wu et al., 2014). The rising trend in nutrient levels from the conventional middle level to rich nutrients level has also caused concerns on the potential occurrence of eutrophication. Although Poyang lake is the only remaining large lake in China with no history of eutrophication, the growing nutrient levels in recent years are approaching the level of eutrophication (Tan et al., 2008). Eutrophication is catastrophic to water environments as it leads to oxygen depletion and water pollution that severely affect a wide range of wildlife species and the nearby human communities. In order to preserve the water quality standard and to prevent eutrophication in the Poyang Lake, researchers have conducted studies focusing on the nutrients and their interaction with sediment within the Poyang Lake basin.

### 2.2.6 Existing Research on Water Quality of Poyang Lake

In studying the nutrients concentration, distribution and influence on the Poyang Lake region, researchers use methods mainly consisting of sample collection and numerical modeling. The former aims to understand changes in the field by using experimental work and measurements, while the latter builds computational models using numerical methods and field data to simulate and predict water quality behavior in the lake.

Field measurement and sample analysis allow researchers to obtain concentrations of water quality indices at high resolution across different points in the lake. Among the Chinese research communities a lot of groundwork has been laid on Poyang Lake. Wang et al. (2008a,b) performed an in-site measurement of nitrogen and phosphorus concentrations of different regions in Poyang Lake and in the lake's agricultural drainage, groundwater and urban sewage during the wet season of 2005. Results reinforced the

## Literature Review

---

status of increasing nutrients inflow in Poyang Lake. However little analysis was shown from these studies. In a similar practice, Hu et al. (2012c) performed sampling of nutrients concentrations focusing on Raohe river, one of the five rivers, and discussed the pollutant sources such as fertilizers and sewage treatment. Hu et al. (2012a) monitored the concentration of nitrogen and phosphorus by sampling inflow from the five rivers during the wet and dry seasons of 2010 and 2011 with the aim of analyzing the retention capacity of Poyang Lake. It is found that the retention capacity of the lake to nutrients is high and main factors influencing such include surface runoff, non-point source pollution, rainfall and sediment release.

More specific fieldwork was also carried out to pinpoint a certain component or characteristic in the water environment. Xiang and Zhou (2011) examined the forms and distribution of phosphorus in the sediments of Poyang Lake using chemical extraction methods. Sediment samples were collected in early 2009 from six sampling sites in Poyang Lake. Results showed that phosphorus in the sediments mainly consisted of inorganic phosphorous species and decreased toward the bottom of the core (Figure 2.11). In the figure, total phosphorus, organic phosphorus and dissolved phosphorus all share similar trends. In all the six testing sites in this study, TP concentration in sediments reached above 500 mg/kg, which indicated that Poyang Lake sediments had become moderately polluted. Liu et al. (2015) studied the phosphorus contents of Poyang Lake surface sediments to reveal the influence of water level changes have on the potential phosphorus-release risk of the sediment. It is shown that the spatial distribution of various forms of phosphorus in Poyang Lake surface sediment was relatively uniform and rising water levels triggered increased phosphorus release.

Sampling and laboratory analysis were also carried out in different scales or on other water quality components. In a larger sampling scale, Zhu et al. (2004) conducted sampling on phosphorus concentration and many other water quality indices (e.g. dissolved organic carbon and transparency) around the Yangtze River region in 2003, with only one sampling point located in Poyang Lake. A national scale sampling was

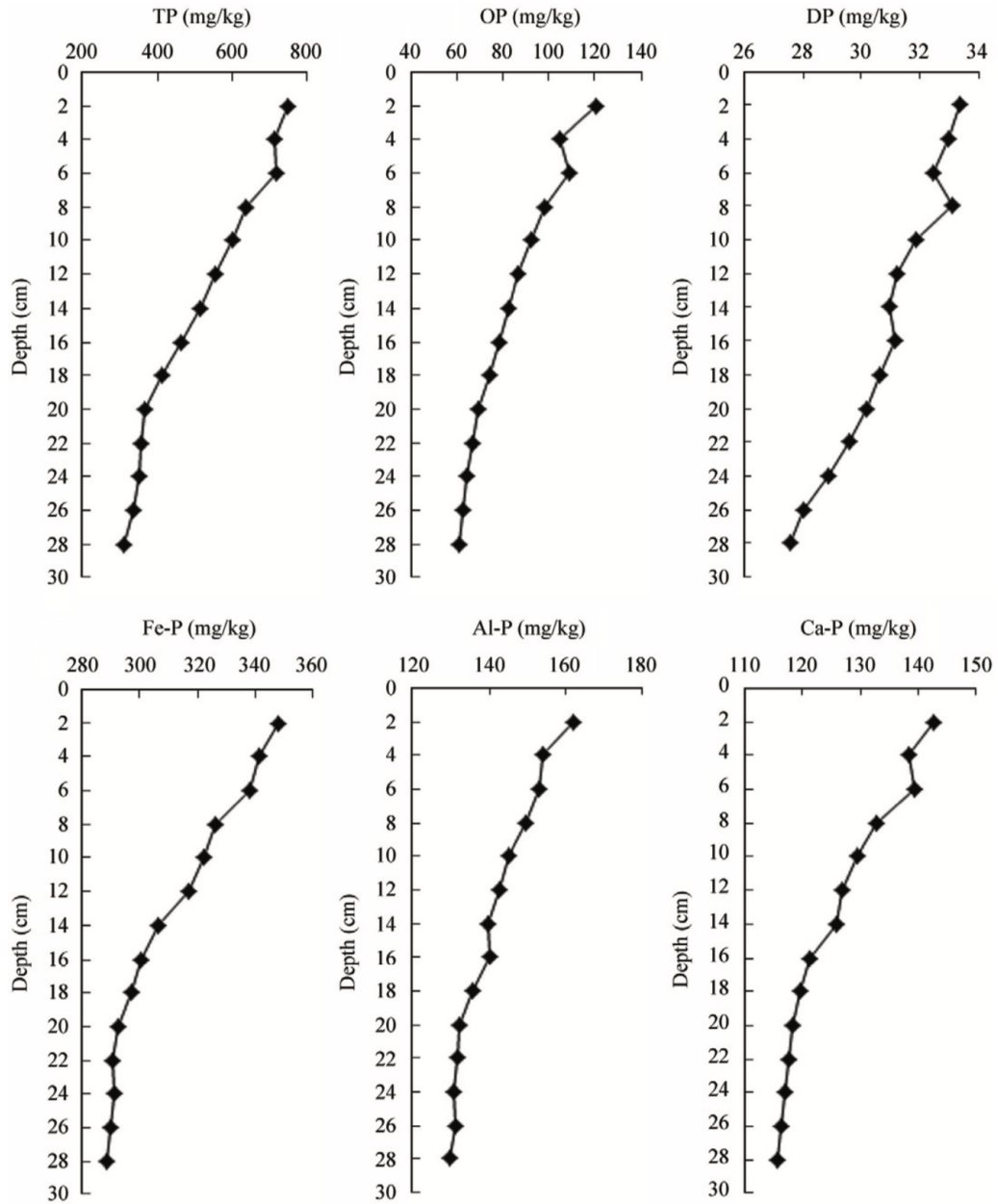


Fig. 2.11 Vertical profiles of the average content of phosphorus in Poyang Lake sediments (Source: Xiang and Zhou, 2011)

## Literature Review

Years	Sampling sites	No.	Mean
1990	Middle and lower reaches (Taihu Lake)	NG	1.090
1991	Middle and lower reaches (Taihu Lake)	NG	1.200
1992	Middle and lower reaches (Taihu Lake)	NG	1.140
1993	Middle and lower reaches (Taihu Lake)	NG	1.580
1998	Middle and lower reaches (Poyang Lake)	8	1.486
2000	Middle and lower reaches (Taihu Lake)	13	2.640
2003	Middle and lower reaches	18	1.743
2004	Whole basin	148	0.984
2007	Middle and lower reaches	27	1.200
2008	Middle and lower reaches (Poyang Lake)	33	1.216
2009a	Lower reaches (Chao Lake)	85	1.670
2009b	Middle reaches (Dongting Lake)	20	0.547
2009c	Middle and lower reaches (Taihu Lake)	40	0.860
2010a	Middle and lower reaches (Taihu Lake)	29	1.789
2010b	Middle and lower reaches (Taihu Lake)	28	0.959
2010c	Upper reaches (Dian Lake)	28	4.850
2011a	Middle and lower reaches (Poyang Lake)	15	0.873
2011b	Middle and lower reaches (Poyang Lake)	39	0.544
2012	Middle reaches (Dongting Lake)	15	1.372
2013a	Upper reaches to lower reaches	23	0.679
2013b	Middle reaches (Dongting Lake)	18	1.340
2013c	Upper reaches (Dian Lake)	36	3.307

Fig. 2.12 Concentration data of total nitrogen (TN) in the sediments of the Yangtze River basin from studies conducted from 1990 to 2013 (Source: Yang et al., 2017)

conducted by Yang et al. (2017) on TN, TP, organic carbon and pH in river basin sediments of China. The study summarized the reported mean values of TN and TP in the Yangtze River basin from other research from 1990 to 2013. Figure 2.12 listed the concentration data of total nitrogen (TN) in the sediments of the Yangtze River basin in the literature from 1990 to 2013. The sampling year, area and size of the studies were documented in the table with the mean concentration of TN calculated. This set of data demonstrated strong discrepancies in the consistency and frequency of field measurement studies over the years. Field measurements at Poyang Lake for example were taken irregularly in the year 1998, 2008 and twice in 2011 with the number of sampling ranging from 8 to 39 and the resulting TN mean recorded between 0.544 mg/l to 1.486 mg/l. Similar trends for the field measurement can be seen for TP in the Poyang Lake region.

In another study, the variation of phytoplankton chlorophyll *a* and other environmental parameters (e.g. salinity, pH, temperature, DO and turbidity) were sampled in Poyang Lake and also its main tributaries between the period 2009-2013. The study

## Literature Review

---

showed that chlorophyll *a* concentrations were significantly higher in the wet seasons than in the dry seasons, while the effect of nutrients on the phytoplankton was not obvious (Wu et al., 2014). Phytoplankton's relationship with water level fluctuation in Poyang Lake was also explored in Qian et al. (2016), indicating that Poyang Lake has a tendency to enter eutrophication. It is also suggested that the water level fluctuation habits should not be disturbed as they directly influence the ecology of Poyang Lake. Ou et al. (2012) studied the spatial distribution of chlorophyll *a* in relation to TP and TN in Poyang Lake using field measurement from 2009, showing a strong correlation between the components. This however, conflicts with the results in Wu et al. (2014).

There are a number of other studies that investigate the variation of nutrients and other water quality components through historical trend analysis and sample measurement (Huang et al., 2015b; Li and Xu, 2007; Soldatova et al., 2017; Wang et al., 2017; Zhang et al., 2016). Under the extent of this study they will not be listed out in details herein. It is clear that many studies have been conducted regarding the many aspects of Poyang Lake hydro-environment. However, contradicting results occur and many studies are without significant conclusions. Given by the scale of Poyang Lake and its dynamic characteristics, existing ground work is rather scattered and unsystematic. Discontinuity in time, space and measurement focus can be seen from existing works. Collective efforts are needed to compile a database of the lake environment with specific recording and measurement for a series of standard water quality variables at regular intervals in testing stations across the lake for a substantial period of time (e.g. 10-30 years).

Building on the backbone of field measurement and the advancement of hydrodynamic models, researchers began to develop physically based water quality models for Poyang Lake in recent years. (Ma et al., 2015) attempted to simulate the temporal and spatial distribution of nitrogen and phosphorus in Poyang Lake using the Soil and Water Assessment Tool (SWAT). The model was built using meteorological and soil data, DEM, agricultural management data and field-measured data. Calibration

## Literature Review

---

of the model was performed using data from 2003 to 2007 and validated using data from 2008 to 2012. The model demonstrated the proportion of various pollutants influx from the five rivers and over the course of the year. The results of Gangjiang being the dominant pollutant contributor and wet season having the most pollutant influx are both coherent with the findings in previous literature that analyzed inflow contributions and trends.

Li et al. (2015b) combined a 2-D hydrodynamic model in MIKE with dye tracer simulations to investigate the transport time scale in Poyang Lake for various water level variation periods. The transport time scale of a lake describes the lake's ability to renew its water content through hydrodynamics. Residence time is often used to represent the time scales of the physical transport processes and of pollutant residues in the lake environment. The shorter the residence time, the quicker the lake clears up its pollutants and associated water quality problems. The study showed that the travel times from the pollutant sources to the outlet of the lake during the wet seasons ( $\sim 32$  days) are about 4 times greater than those during the dry seasons ( $\sim 8$  days). Residence times also vary significantly from less than 10 days along the main lake channel to 365 days in some bays adjacent to the lake shorelines. Li and Yao (2015) expanded the topic by adapting a similar approach using a hydrodynamic model in conjunction with transport and particle tracking sub-models. Results showed that the mean residence time of Poyang Lake is 89 days during wet seasons and the effect of Yangtze River on the residence time is larger than that of the catchment river inflows. Both studies provided an insight on the management of chemical and ecological processes in Poyang Lake and demonstrated early attempts in modeling the transport behaviors in such a large river-lake system.

The potential effects of the barrage project in Poyang Lake are rarely explored via numerical modeling. Hu et al. (2012b) built a 2-D model based on EFDC and Delft3D to investigate the impact of the Poyang Lake barrage on the nutrient concentrations in the lake region. Simulation results illustrated that the operation of the barrage

## Literature Review

---

will lead to an increase of total inorganic nitrogen and total phosphorus concentration of 20.42% and 20.55% respectively. Huang et al. (2015a) used a coupled Artificial Neural Network with cluster technique to predict the impact of the barrage control on phytoplankton biomass in Poyang Lake, indicating that the barrage will significantly increase chlorophyll *a* concentration and adequate measures should be in place to avoid algal blooms in the lake. Some of the modelling results from the study however were not able to adequately predict the field measurement, as seen in Figure 2.13. The measurement data from 2005 to 2009 was scattered and limited in number. Although the number of measurements in 2009-2012 increased, their trends and values were not be able to capture by the simulation.

The scarcity of modeling studies on Poyang Lake's water quality is due to the large scale characteristics of the lake environment and the disconnection between existing models. Poyang Lake, being the largest freshwater lake in China, requires massive data and numerous parameters to be considered in the models. In addition, most

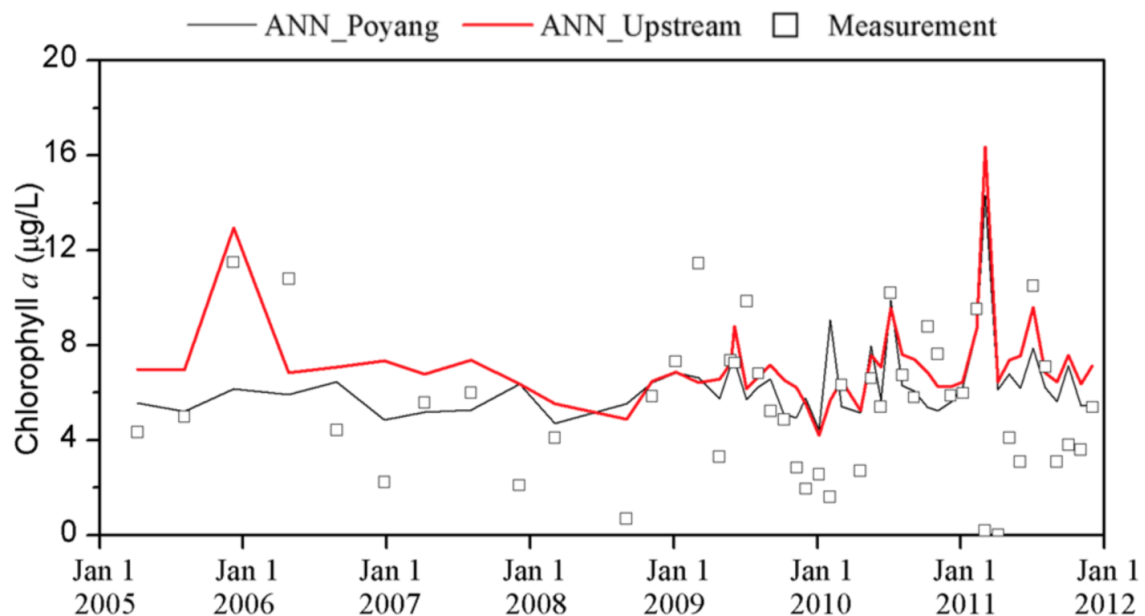


Fig. 2.13 Measured and simulation of chlorophyll *a* using Artificial Neural Network at Kangshan of Poyang Lake (Source: Huang et al., 2015a)

existing water quality models were not created to accommodate vigorous hydrodynamic conditions and predominantly agricultural circumstances in China. In many of the cases, these areas have no developed infrastructure for watershed management, limited municipal waste and sewage treatment, non-existent wastewater treatment system, but dominating livestock farming and waste pollution (Wang et al., 2011). Researchers are in the process of adapting to the challenges of modeling the complex hydro-environment of Poyang Lake. In-depth modeling of bio-chemical processes in the water environment of Poyang Lake is also lacking. Few attempts have been made to model the hydro-environment of Poyang Lake with consideration of the various processes involved in the nitrogen and phosphorus cycles. In fact, Chen et al. (2016) pointed out that the field needs further research, both practically and numerically, on the many geo-biochemical processes such as nitrogen fixation, nitrification and denitrification, biomass decomposition, inorganic phosphorus assimilation and so on. The knowledge and data related to these processes in the Poyang Lake environment will more efficiently and rigidly support the modeling of Poyang Lake's hydro-environment and their outcomes.

### 2.2.7 Improvement of Data Collection

Accurate and extensive data about Poyang Lake is one of the keys to better modeling. Chen et al. (2012) documented an attempt to compile a Geographic Information System (GIS) with functions of hydrodynamic simulation, water quality monitoring, water management and flooding dynamic modeling. However, the document is rather vague and no application has been seen from the database created thus far. Statistical regression model coupled with a GIS model was built to model water quality and estimate pollutant concentrations (Guo et al., 2012b). Four variables (DO, PI,  $\text{NH}_3\text{-N}$  and TP) are used as indicators in this model based on their data availability and frequency of exceeding standards in precedent testing. Results have shown a substantial difference between the estimation and actual data obtained, due to the lack of sufficient variables in consideration. Further studies on the relationship of pollutant

and water quality are needed. A larger database with more extensive pollutants and water quality values of Poyang Lake is also required.

Besides localized sampling of water information using controlling stations around the lake regions, researchers also adopted alternative methods for data collection and complementing the measurement of gauge stations (Cai et al., 2005). Remote sensing in the forms of satellite altimetry and Moderate Resolution Imaging Spectroradiometer (MODIS) were used to estimate the spatial-temporal extent and the change of water clarity influenced by sediment in the northern part of Poyang Lake (Cai and Ji, 2009; Cui et al., 2009) and to investigate the inundation area in Poyang Lake at both seasonal and inter-annual scales (Feng et al., 2012). Attempts to use remote sensing methods to monitor the total suspended sediment concentration and to examine the wetland vegetation and biomass distribution in Poyang Lake were also made (Cui et al., 2013; Li and Liu, 2002; Yu et al., 2012). Advancement in remote sensing technology allows more efficient data collection, but the data is often exclusive and scattered. Progression in the utilization of the data collected is not significantly linked to the development of numerical modeling and management strategy of Poyang Lake.

### 2.2.8 Extension of Monitoring Network

Given the pressing challenges described above, a series of monitoring works and management strategies had been initiated since the late 1970s with the aim to remedy and maintain the environmental and ecological values of Poyang Lake. Nineteen water quality control stations were set up in 1979 to monitor water quality and quantity at core streams and rivers entering and leaving the lake. The locations of these control stations were determined using the Grid Method on the lake areas. The stations collect monthly data that includes water temperature, atmospheric temperature, turbidity, pH value, DO, BOD, PI, nitrogen, phosphorus and ions content such as  $\text{Mg}^{2+}$ ,  $\text{K}^+$ ,  $\text{Na}^+$ ,  $\text{SO}_4^{2-}$  and  $\text{Cl}^-$ .

The uneven distribution of the control stations however, has led to doubts on the accuracy and representation of the collected water samples. Control stations in the southern regions are fewer in number than those in the northern regions without justification. Meanwhile several sampling stations in the southern regions are unjustly close within 5 km in distance. Data collected at those incoming southern rivers should not be used to characterize the water quality for the entire lake area. In addition, there is no sampling point at the central region of the lake. There is no possible and reliable mean to represent water quality conditions of the central lake region.

In 2012, a study was conducted to improve the sampling networks of the lake (Tan et al., 2014). The goal was to collect the most representative data and to present the environmental conditions and changes using minimal sampling points. This would reduce capital investments and resources requirement, stimulate the undertaking of more scientific analysis and hence provide more accurate information for management decision to be made. Mathematical models based on FVM were built and statistical methods were used to relocate and optimize the locations of control stations. It was recommended to install three additional control stations and remove one existing station in the new proposal. However no actions have been taken as of 2018.

### **2.2.9 Economic and Social Impact**

The interlinks between the social, economic and environmental aspects of Poyang Lake should also be taken into account when considering the lake's development and conservation. Xie et al. (2013) established an assessment model of land use eco-risk to reflect the risk status of regional land use in Poyang Lake, based on the principles of risk assessment and combined with the theory of landscape ecology and ecological risk. It is found that urbanization and agricultural land exploitation in the Poyang Lake region have caused the loss of ecological land and the fragmentation of land pattern, which increase the regional eco-risks. Strengthening land use management, avoiding unreasonable land use and reducing the degree of fragmentation and separation are

## Literature Review

---

needed to ensure sustainable development of the region. Zhen et al. (2011) conducted a household survey and group discussions with selected villages around Poyang Lake to determine their perceptions of and willingness to pay for the environmental conservation of the region. Most households were willing to pay for the conservation of the lake through the reduced use of agricultural chemicals and conversion of rice fields into natural wetlands. There is a strong correlation between households' dependence on wetland and water resources and their concerns to the lake's conservation. Meanwhile, Deng et al. (2011) examined the balance between economic growth and the nutrient emission in the region. It was found that restricting nutrient emissions from sections with the highest emission via taxation might be effective.

The use of land and water resources, nutrient emissions from human activities and urban and economic development in the Poyang Lake region remain key considerations in determining the balance between economic and social benefits and conservation of the natural environment. Although not being expanded upon further in this study, the scope of social-environmental relationship in Poyang Lake has great potentials for ongoing research and is pivotal in providing stakeholders the information for making decisions on engineering projects.

## 2.3 Chapter Summary

In this chapter, the literature related to hydro-environment modeling and Poyang Lake has been reviewed. The study of rivers and lakes using numerical modeling is summarized with details of the various methods and models used in current practice. The background, challenges and research efforts on Poyang Lake have been examined. Under accelerating industrialization and urbanization, the water demand for the Poyang Lake water source is expected to increase rapidly. Combined with the influence of Yangtze River and TGD, as well as the effect of climate change, the results are the decline of water quantity and the deterioration of water quality in the Poyang Lake region. These pressing challenges will directly affect wildlife habitats and wetlands

## Literature Review

---

environment in the ecosystem and threaten the human population and economic development in the Jiangxi province. Being the largest freshwater lake in the country, Poyang Lake is also a representative of water problems faced by China and rest of the other developing countries. A barrage project was proposed as an attempt to control the water quantity and improve water quality in Poyang Lake. However, such proposal is currently postponed due to the lack of scientific support.

The threats of water crisis and ecological deterioration in the Poyang Lake region drive an increasing number of studies on the many aspects of Poyang Lake over the last decade. The majority of research focuses on analyzing the hydrodynamics, hydrology and water quality of the Poyang Lake, as well as evaluating the lake's behavior under the influence of the Yangtze River, nearby rivers and estuaries, TGD and human activities. Studies are mainly conducted through samples collection and numerical modeling. Despite wide spread endeavour in the research of Poyang Lake, water quality data in the region is fragmented in time and space. Availability of data is often a problem for numerical analysis and model building. Numerical modeling looking at the many aspects of the lake environment with different methods lacks coherence and focus. Modeling results are often produced without the support of field data and lack the verification of other models to enforce credibility. Moreover, demand on variables requirement is high for current models such as SWAT and EFDC. Improving the accuracy of the numerical models by sharing and compiling data available regarding the lake would be critical for tackling environmental problems such as assessing the effects of the barrage control and protecting the wetlands and wildlife in the region.

The trend in hydro-environment modeling has been towards increasing complexity and resolution. Researchers have been expanding the scopes and details of the numerical models and integrating advanced computing powers to accommodate more complex simulations of the hydro-environment. However, attention should also be given on developing simpler, reduced and intermediate complexity models that offer more direct, appropriate and efficient solutions to address the research question at hand. A more

## Literature Review

---

user-accessible and decision-supporting tool that could tailor to the necessary problems and suggest alternative options for decision makers and stakeholders would be as valuable as a fully comprehensive and state of the art numerical model.

Based on the status of the current literature and research, this study will focus on tackling the immediate problem with the impact assessment of the barrage control on Poyang Lake's hydro-environment, using a representative and efficient numerical model. A coupled hydrodynamic and water quality model will be built with existing technique and modeling standards to simulate the lake environment based on data availability. The model will be set up as an intermediate complex tool with the aim to explore potential impacts on Poyang Lake hydrodynamics and water quality under different barrage control schemes. Variation of parameters such as water levels and ammoniacal nitrogen concentration as a result of barrage control will act as scientific evidence that allow further engineering judgment to be made on the operation of the barrage project and support the search for potential measures to tackle Poyang Lake's hydro-environmental issues. In the long term, it is hoped that the model will set an example for future engineering control evaluation in other countries and cases.

# Chapter 3

## Methodology

The basis of this research is built upon computational simulation models. The coupled models will be used as a tool to generate and analyze Poyang Lake's water environment and its surroundings. The numerical model structure consists of two major components, the hydrodynamics phase and the water quality phase. The hydrodynamics phase focuses on modeling the water flows and water fluctuation levels according to the bathymetry of Poyang Lake. The water quality phase concentrates on tracking the pollutant concentrations and variations under Poyang Lake's unique hydraulic flows. The foundation of these components are formed using theoretical principles, governing equations and numerical methods in each of their respective fields, which will be elaborated in this chapter. The two parts are then coupled together in the context of multi-dimension models, based on a collective list of dynamic components and formulas that connect the hydrodynamics and water quality elements.

Two different numerical models are used to computationally execute the theories and calculations in this research. The first one is a 1-D hydrodynamic model developed in-house by Huang et al. (2011), in which he attempted to develop a numerical tool in simulating the hydrodynamics and solute transport within the Yangtze River basin and Poyang Lake. The model also incorporated the Water Quality Analysis Simulation Program (WASP) model for water quality simulation. Huang's 1-D river network model, written in the programming language FORTRAN, is applied to a large part of Yangtze

## Methodology

---

River and its associated lakes and streams. The second model MIKE, a commercial simulation package that is widely used in the field of hydrodynamic and environmental engineering, is then applied to the main Poyang Lake region for multi-dimensional simulation. MIKE offers a user friendly working interface for researchers and engineers to model complex water environments and water-based applications. The versatility to model various scenarios, ranging from coastal and sea, water resources management, water quality, to groundwater and porous media, makes the model a well suited option to provide credible results and to help tackling the technical challenges presented in this research. Both the in-house model and MIKE model adopt similar principles and numerical methods in simulating the hydrodynamic and water quality characteristics of the water environments. Carrying out the numerical simulation part of this study with the two different models provides a more holistic and accurate judgment towards Poyang Lake's water problems.

In this chapter, the basic theories and principles involved in the numerical models will be condensed and explained in two parts; one for hydrodynamic modeling and one for water quality modeling. The first part documents the governing equations of hydrodynamic and solute transport modeling in 3-D, 2-D and 1-D scenarios. The core formulas and principle equations involved will be demonstrated along with the respective numerical methods that solve them. In the second part, the basis of the water quality model will be discussed. Brief backgrounds of certain biochemical processes involved including the dissolved oxygen process, the nitrogen cycle and the phosphorus cycle will be illustrated to allow comprehensive understanding of the water environment and hence the scope of this study. The chapter will be completed with the treatment and representation of the various water quality components and their solving method within the regime of the water quality models.

### 3.1 Part 1 - Hydrodynamics

To model hydraulic behaviors under the influence of external factors such as variation in inflows and bathymetry, the basic theory and principles of fluid mechanics in shallow water conditions which rivers and lakes generally possess must be understood. This set of rules that govern the water movement and determine the methods in solving them, under the boundary conditions specified by the domain environment, are the core drivers of the hydrodynamic models. In river and lake environment, general water flow and behavior can be categorized into 3-D, 2-D and 1-D problem depending on needs and complexity. The comprehensive case of a 3-D problem in open channel flow, which covers all aspects and elements of the principles and conditions, will first be illustrated and be used as anchor for lower dimensions in subsequent sections.

#### 3.1.1 3-D Hydrodynamic Governing Equations

Saint-Venant equations, also known as the shallow water equations (SWE), are used to describe the open-channel flow in rivers (Barré de Saint-Venant, 1871). The general form of the 3-D Saint-Venant equations includes the principles of mass conservation and momentum conservation based on the assumption of Boussinesq and static pressure hypothesis under free surface conditions (DHI, 2017c). The Boussinesq approximation assumes that all fluid properties such as density, viscosity and thermal diffusivity can be considered as constant (Boussinesq, 1897; Guo et al., 2002). In addition, hydrostatic pressure assumption states that pressure in a continuously distributed uniform static fluid varies only with vertical distance. The pressure is the same at all points on a given horizontal plane in the fluid and increases with depth in the fluid (White, 2008). The approximation arises naturally when studying flows at water environments with small depth compared to its horizontal dimensions. In such scenario, the vertical accelerations are small compared to the gravitational acceleration and the assumption is valid (Renardy, 2009).

## Methodology

---

The hydrodynamic model is based on the numerical solution of the incompressible Reynolds averaged Navier-Stokes equations. The equations illustrated hereafter are based on the formulation used in the MIKE model developed by the Danish Hydraulic Institute (DHI). The model considers the continuity of the momentum, temperature, salinity and density equations (DHI, 2017d). The governing equations of the 3-D hydrodynamic model, which comprise one local continuity equation (Equation 3.1) and two horizontal momentum equations (Equations 3.2 and 3.3), are as below:

$$\frac{\partial u}{\partial x} + \frac{\partial v}{\partial y} + \frac{\partial w}{\partial z} = S \quad (3.1)$$

$$\begin{aligned} \frac{\partial u}{\partial t} + \frac{\partial u^2}{\partial x} + \frac{\partial vu}{\partial y} + \frac{\partial wu}{\partial z} = f v - g \frac{\partial \eta}{\partial x} - \frac{1}{\rho_0} \frac{\partial p_a}{\partial x} - \frac{g}{\rho_0} \int_z^\eta \frac{\partial \rho}{\partial x} dz - \\ \frac{1}{\rho_0 h} \left( \frac{\partial s_{xx}}{\partial x} + \frac{\partial s_{xy}}{\partial y} \right) + F_u + \frac{\partial}{\partial z} \left( \nu_t \frac{\partial u}{\partial z} \right) + u_s S \end{aligned} \quad (3.2)$$

$$\begin{aligned} \frac{\partial v}{\partial t} + \frac{\partial v^2}{\partial y} + \frac{\partial uv}{\partial x} + \frac{\partial wv}{\partial z} = -f u - g \frac{\partial \eta}{\partial y} - \frac{1}{\rho_0} \frac{\partial p_a}{\partial y} - \frac{g}{\rho_0} \int_z^\eta \frac{\partial \rho}{\partial y} dz - \\ \frac{1}{\rho_0 h} \left( \frac{\partial s_{yx}}{\partial x} + \frac{\partial s_{yy}}{\partial y} \right) + F_v + \frac{\partial}{\partial z} \left( \nu_t \frac{\partial v}{\partial z} \right) + v_s S \end{aligned} \quad (3.3)$$

where  $(x, y, z)$  represent the Cartesian coordinates and  $(u, v, w)$  are their velocity components respectively,  $t$  is time,  $g$  is the gravitational acceleration,  $S$  is the discharge magnitude at point source,  $f = 2\omega \sin\phi$  is the Coriolis parameter (in which  $\omega$  is the angular rate of revolution and  $\phi$  is the geographic latitude),  $\rho$  is the water density,  $\rho_0$  is the reference density of water,  $\eta$  is the free surface elevation,  $(s_{xx}, s_{xy}, s_{yx}, s_{yy})$  are components of the radiation stress tensor,  $p_a$  is the atmospheric pressure,  $(\tau_{sx}, \tau_{sy})$  and  $(\tau_{bx}, \tau_{by})$  are the  $x$  and  $y$  components of the surface wind and bottom stresses respectively and  $(u_s, v_s)$  are the discharge velocities of inflow water,  $\nu_t$  is the vertical turbulent viscosity.

The total water depth,  $h$ , can be obtained from the kinematic boundary condition at the surface once the velocity field is known from the momentum and continuity equations. The fluid is assumed to be incompressible, hence the water density ( $\rho$ )

## Methodology

---

does not depend on the pressure, but only on the temperature and the salinity via the equation of states documented in UNESCO (1981).

$$\rho = \rho(T, s) \quad (3.4)$$

The horizontal stress terms ( $F_u$ ,  $F_v$ ) are described using gradient-stress relation:

$$F_u = \frac{\partial}{\partial x} \left( 2\nu_h \frac{\partial u}{\partial x} \right) + \frac{\partial}{\partial y} \left( \nu_h \left( \frac{\partial u}{\partial y} + \frac{\partial v}{\partial x} \right) \right) \quad (3.5)$$

$$F_v = \frac{\partial}{\partial x} \left( \nu_h \left( \frac{\partial u}{\partial y} + \frac{\partial v}{\partial x} \right) \right) + \frac{\partial}{\partial y} \left( 2\nu_h \frac{\partial v}{\partial y} \right) \quad (3.6)$$

The surface and bottom boundary condition for  $u$ ,  $v$  and  $w$ :

At  $z = \eta$ :

$$\frac{\partial \eta}{\partial t} + u \frac{\partial \eta}{\partial x} + v \frac{\partial \eta}{\partial y} - w = 0, \quad \left( \frac{\partial u}{\partial z}, \frac{\partial v}{\partial z} \right) = \frac{1}{\rho_0 \nu_t} (\tau_{sx}, \tau_{sy}) \quad (3.7)$$

At  $z = -d$ :

$$u \frac{\partial d}{\partial x} + v \frac{\partial d}{\partial y} + w = 0, \quad \left( \frac{\partial u}{\partial z}, \frac{\partial v}{\partial z} \right) = \frac{1}{\rho_0 \nu_t} (\tau_{bx}, \tau_{by}) \quad (3.8)$$

### 3.1.2 3-D Solute Transport Governing Equations

The 3-D governing equations for the transports of heat ( $T$ ) and salinity ( $s$ ) are based on the general transport-diffusion equations (DHI, 2017d):

$$\frac{\partial T}{\partial t} + \frac{\partial uT}{\partial x} + \frac{\partial vT}{\partial y} + \frac{\partial wT}{\partial z} = F_T + \frac{\partial}{\partial z} \left( D_v \frac{\partial T}{\partial z} \right) + \hat{H} + T_s S \quad (3.9)$$

$$\frac{\partial s}{\partial t} + \frac{\partial us}{\partial x} + \frac{\partial vs}{\partial y} + \frac{\partial ws}{\partial z} = F_s + \frac{\partial}{\partial z} \left( D_v \frac{\partial s}{\partial z} \right) + s_s S \quad (3.10)$$

## Methodology

---

where  $T$  is temperature,  $s$  is the salinity,  $D_v$  is the vertical turbulent diffusion coefficient that can be approximated as  $D_v = \nu_t/\sigma_T$ ,  $\hat{H}$  is a source term due to atmospheric heat exchange,  $(T_s, s_s)$  are the temperature and the salinity of the source respectively and  $(F_T, F_s)$  are the horizontal diffusion terms as defined by:

$$(F_T, F_s) = \left[ \frac{\partial}{\partial x} \left( D_h \frac{\partial}{\partial x} \right) + \frac{\partial}{\partial y} \left( D_h \frac{\partial}{\partial y} \right) \right] (T, s) \quad (3.11)$$

The surface ( $z = \eta$ ) and bottom ( $z = -d$ ) boundary conditions for the temperature and salinity are given by Equation 3.12 and Equation 3.13 respectively.

$$D_h \frac{\partial T}{\partial z} = \frac{Q_n}{\rho_0 c_p} + T_p \hat{P} - T_e \hat{E} \quad ; \quad \frac{\partial s}{\partial z} = 0 \quad (3.12)$$

$$\frac{\partial T}{\partial z} = 0; \quad \frac{\partial s}{\partial z} = 0 \quad (3.13)$$

where  $D_h$  is the horizontal turbulent diffusion coefficient. The diffusion coefficient can be related to the eddy viscosity where  $D_h = \nu_H/\sigma_T$ , in which  $\sigma_T$  is the Prandtl number (Rodi, 1984).  $Q_n$  is the surface net heat flux,  $c_p = 4217$  J/kg·K is the specific heat of water,  $T_p$  is the precipitation temperature,  $T_e$  is the evaporation temperature,  $\hat{P}$  is the precipitation rate and  $\hat{E}$  is the evaporation rate. As for scalar quantity of concentration ( $c$ ), the conservation equation for transport is given as:

$$\frac{\partial c}{\partial t} + \frac{\partial uc}{\partial x} + \frac{\partial vc}{\partial y} + \frac{\partial wc}{\partial z} = F_c + \frac{\partial}{\partial z} \left( D_v \frac{\partial c}{\partial z} \right) - k_p c + c_s S \quad (3.14)$$

where  $c_s$  is the concentration of the scalar quantity at the source and  $k_p$  is the linear decay rate of the scalar quantity.  $F_c$  is the horizontal diffusion term defined by:

$$F_c = \left[ \frac{\partial}{\partial x} \left( D_h \frac{\partial}{\partial x} \right) + \frac{\partial}{\partial y} \left( D_h \frac{\partial}{\partial y} \right) \right] c \quad (3.15)$$

### 3.1.3 2-D Hydrodynamic Governing Equations

The 2-D shallow water equations considers the horizontal plane under the principles of mass conservation and momentum conservation. The equations can be derived from the 3-D Saint-Venant equations by integrating the horizontal momentum equations and continuity equation over the total depth  $h = \eta + d$  (DHI, 2017c):

$$\frac{\partial h\bar{u}}{\partial x} + \frac{\partial h\bar{v}}{\partial y} + \frac{\partial h}{\partial t} = hS \quad (3.16)$$

$$\begin{aligned} \frac{\partial h\bar{u}}{\partial t} + \frac{\partial h\bar{u}^2}{\partial x} + \frac{\partial h\bar{v}\bar{u}}{\partial y} = f\bar{v}h - gh\frac{\partial\eta}{\partial x} - \frac{h}{\rho_0}\frac{\partial p_a}{\partial x} - \frac{gh^2}{2\rho_0}\frac{\partial\rho}{\partial x} + \frac{\tau_{sx}}{\rho_0} - \frac{\tau_{bx}}{\rho_0} \\ - \frac{1}{\rho_0}\left(\frac{\partial s_{xx}}{\partial x} + \frac{\partial s_{xy}}{\partial y}\right) + \frac{\partial}{\partial x}(hT_{xx}) + \frac{\partial}{\partial y}(hT_{xy}) + hu_sS \end{aligned} \quad (3.17)$$

$$\begin{aligned} \frac{\partial h\bar{v}}{\partial t} + \frac{\partial h\bar{u}\bar{v}}{\partial x} + \frac{\partial h\bar{v}^2}{\partial y} = -f\bar{u}h - gh\frac{\partial\eta}{\partial y} - \frac{h}{\rho_0}\frac{\partial p_a}{\partial y} - \frac{gh^2}{2\rho_0}\frac{\partial\rho}{\partial y} + \frac{\tau_{sy}}{\rho_0} - \frac{\tau_{by}}{\rho_0} \\ - \frac{1}{\rho_0}\left(\frac{\partial s_{yx}}{\partial x} + \frac{\partial s_{yy}}{\partial y}\right) + \frac{\partial}{\partial x}(hT_{xy}) + \frac{\partial}{\partial y}(hT_{yy}) + hv_sS \end{aligned} \quad (3.18)$$

where  $(x, y)$  represent the Cartesian coordinates with  $(u, v)$  as their velocity components respectively,  $d$  is the still water depth,  $h = \eta + d$  is the total water depth and  $\bar{u}$  and  $\bar{v}$  are the depth-averaged velocities as defined by:

$$h\bar{u} = \int_{-d}^{\eta} u dz, \quad h\bar{v} = \int_{-d}^{\eta} v dz \quad (3.19)$$

The lateral stresses,  $T_{ij}$ , consist of viscous friction, turbulent friction and differential advection. They are estimated using an eddy viscosity formulation based on the depth average velocity gradients with  $\nu_h$  being the horizontal eddy viscosity.

$$T_{xx} = 2\nu_h\frac{\partial\bar{u}}{\partial x}, \quad T_{xy} = \nu_h\left(\frac{\partial\bar{u}}{\partial y} + \frac{\partial\bar{v}}{\partial x}\right), \quad T_{yy} = 2\nu_h\frac{\partial\bar{v}}{\partial y} \quad (3.20)$$

### 3.1.4 2-D Solute Transport Governing Equations

The governing equations for solute transport consist of the transport of salinity, temperature and scalar quantity such as pollutants. The 2-D transport equations can be obtained by integrating the 3-D transport equations over depth:

$$\frac{\partial h\bar{T}}{\partial t} + \frac{\partial h\bar{u}\bar{T}}{\partial x} + \frac{\partial h\bar{v}\bar{T}}{\partial y} = hF_T + h\hat{H} + hT_s S \quad (3.21)$$

$$\frac{\partial h\bar{s}}{\partial t} + \frac{\partial h\bar{u}\bar{s}}{\partial x} + \frac{\partial h\bar{v}\bar{s}}{\partial y} = hF_s + hS_s S \quad (3.22)$$

and  $(\bar{T}, \bar{s})$  are the depth averaged temperature and salinity respectively. Similar principle of integration over depth is used to obtain the 2-D transport equations for solute concentration:

$$\frac{\partial h\bar{c}}{\partial t} + \frac{\partial h\bar{u}\bar{c}}{\partial x} + \frac{\partial h\bar{v}\bar{c}}{\partial y} = hF_c - hk_p\bar{c} + hc_s S \quad (3.23)$$

where  $\bar{c}$  is the depth averaged scalar quantity

### 3.1.5 2-D and 3-D Numerical Methods

Given the presence of time variables ordinary differential equations (ODE) and partial differential equations (PDE) in the Saint-Venant equations, it is impossible to solve the equations analytically. Numerical solution is therefore sought. Within the discretization of numerical scheme, there exist two main groups: explicit and implicit schemes. The explicit methods transform the Saint-Venant equations into a set of algebraic equations, which can be solved in sequence at discretization points set out at a certain length interval and time step (Hartanto et al., 2011). The explicit methods calculate the state of a system at a later time  $Y(t+\Delta t)$  from the state of the system at the current time  $Y(t)$ :

$$Y(t + \Delta t) = F(Y(t)) \quad (3.24)$$

## Methodology

---

As for implicit methods, the Saint-Venant equations are solved simultaneously at all computational points at a given time. In its formulation, all derivative terms and parameters are approximated by using the unknowns at the following time line  $t+\Delta t$ . The method advances the solution from one time line to the next simultaneously for all discretization points along the same time line. In short, implicit methods operate by solving the equation that contains both the current state of the system and the later one to find  $Y(t+\Delta t)$ :

$$F(Y(t), Y(t + \Delta t)) = 0 \quad (3.25)$$

If due to boundary conditions and assumptions that the set of SWE become non-linear, iteration is needed to find the solution (Richtmyer, 1957).

Implicit methods are more complex than explicit methods due to the extra treatment with the resolution of an algebraic system of equations, as shown in Equation 3.25. As a result, implicit methods are computationally more expensive and demanding than explicit methods. However, implicit schemes offer unconditional stability as its time step is not restricted by the Courant-Friedriches-Lewy (CFL) condition (Courant et al., 1967; Morales-Hernández et al., 2017). The CFL condition, which relates the time step to the spatial discretization and the wave speed, is imposed to prevent error propagation. Users choose between the implicit and explicit methods based on the considerations on numerical stability, computational efficiency and convergence issues.

A brief description of the spatial domains used in the multi-dimensional scenarios is provided in this session. The general formulation of the hydrodynamic and solute transport equations are shown, followed by the methods used for time integration. Subsequent considerations in the simulation such as boundary conditions, flooding and drying treatment of domain and the theories of the turbulence and bottom stress will also be discussed.

### Spatial Discretization

Finite volume method is used to perform discretization in solution domain. The spatial domain is discretized by subdivision of the continuum into non-overlapping cell blocks and elements. Although the elements in 2-D case can be arbitrarily shaped polygons, only triangles and quadrilateral elements are considered herein. In the 3-D case, a layered mesh is used: an unstructured mesh for the horizontal domain and a structured mesh for the vertical domain (Figure 3.1). The vertical mesh is based on either sigma coordinates or combined sigma/z-level coordinates (DHI, 2017c).

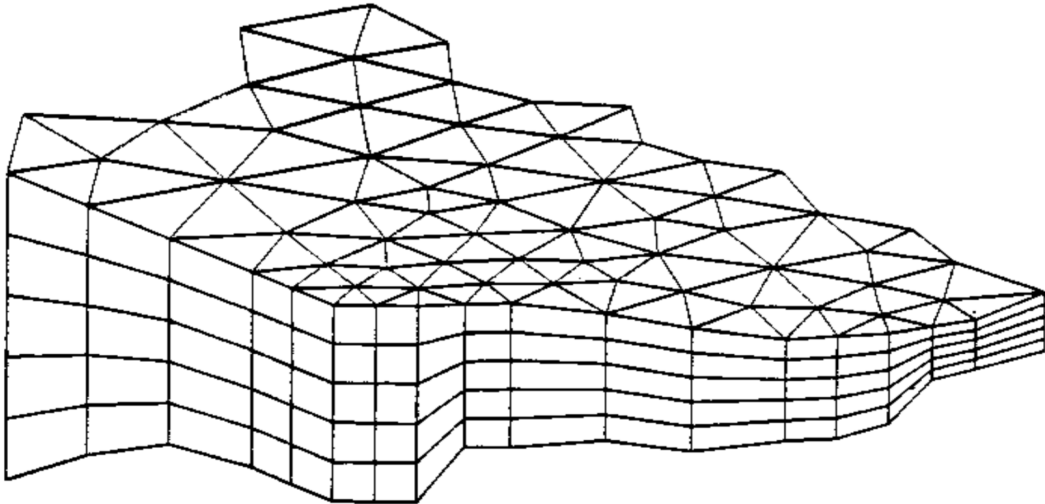


Fig. 3.1 Principle of meshing for the 3-D case (Source: DHI)

In the hybrid sigma/z-level coordinates, sigma coordinates are used from the free-surface to a specified depth ( $z_0$ ) and z-level coordinates are then used below such depth (Figure 3.2). The red line indicates the interface ( $z_0$ ) between the sigma-level and the z-level domain. The elements in both domains can be prisms with either a 3-sided or 4-sided polygonal base. Therefore the horizontal faces are either triangles or quadrilateral element. The elements are perfectly vertical and all layers have identical topology. The use of z-level coordinates allows a simple calculation of the horizontal pressure gradients, advection and mixing terms. However, such a coordinate system

## Methodology

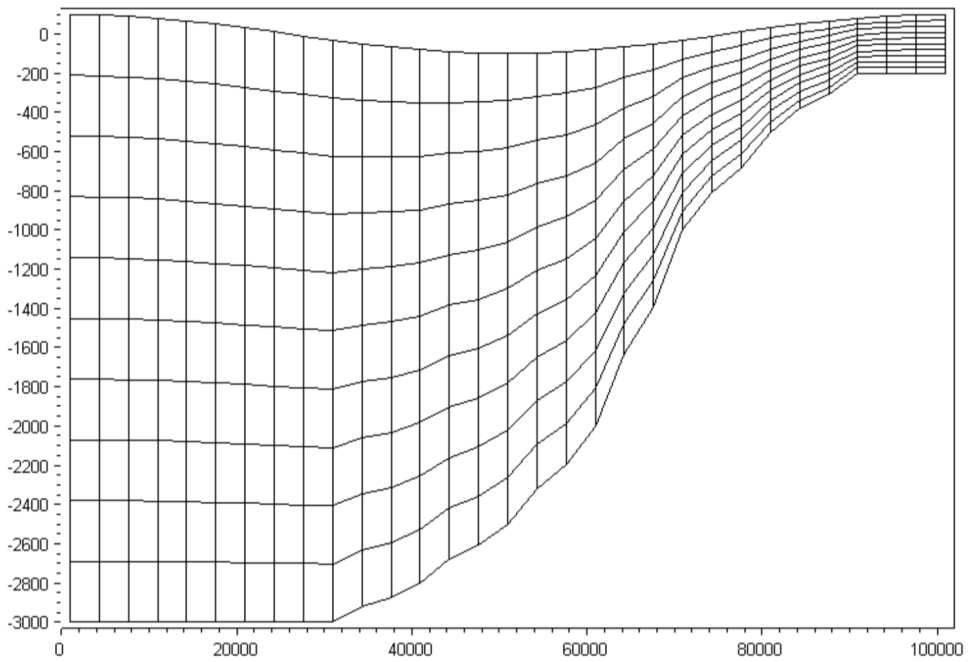
---

has high inaccuracy in representing the bathymetry that can result in unrealistic flow velocities near the bottom. In contrast, sigma coordinates have the advantages of accurately representing the bathymetry and provide consistent resolution near the bed. Nonetheless, sigma coordinates suffer from significant errors in calculating horizontal pressure gradients, advection and mixing terms in areas with sharp topographic changes and steep slopes, resulting in unrealistic flows.

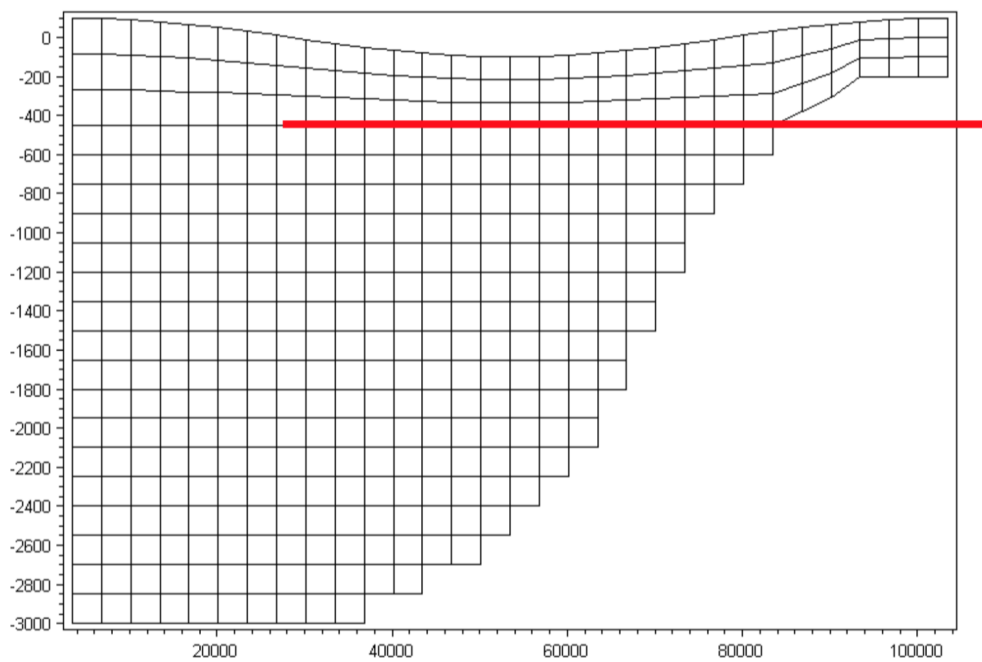
For the vertical discretization both a standard sigma mesh and a hybrid sigma/z-level mesh can be used. In this study, the lake environment of Poyang Lake is associated with steep slopes and rapid changes in bathymetry. In addition, the depth of the lake (15-30 m) is relatively small compared to the horizontal scales (60-80 km). Vertical calculations on horizontal pressure gradient, advection and mixing are less susceptible to changes. A consistent resolution near the bed is preferred and hence the sigma mesh is chosen in this study.

In the sigma domain, the vertical distribution of the layers can be specified in three different ways; equidistant, layer thickness and variable, as illustrated in Figure 3.3. For all three options the number of vertical layers must be given ( $N_\sigma$ ). The discretization of the sigma domain is labeled with the number of discrete  $\sigma$ -level ( $\sigma_i$ ), where  $i = [1, N_\sigma + 1]$ , with the bottom level of the vertical mesh,  $\sigma_1 = 0$  and at the free surface  $\sigma_{N_\sigma + 1} = 1$ . In equidistant distribution, the layers are distributed equidistant across the water depth. In layer thickness option, the fraction of each layer's thickness across the water depth must be specified. Three vertical distribution parameters; the weighting factor between the equidistant and the stretch distribution ( $\sigma_c$ ), the surface control parameter ( $\psi$ ) and the bottom control parameter ( $b$ ) are required in variable distribution. The variable  $s$ -coordinates are obtained using a discrete formulation of the general vertical coordinate system proposed by Song and Haidvogel (1994). The discrete sigma coordinates are given by Equation 3.26 with Equations 3.27 and 3.28:

$$\sigma_i = 1 + \sigma_c s_i + (1 - \sigma_c) c(s_i) \quad i = 1, (N_\sigma + 1) \quad (3.26)$$



(a) Sigma mesh



(b) Hybrid sigma/z-level mesh

Fig. 3.2 Cross section of vertical sigma mesh and hybrid sigma/z-level mesh, with interface indicated between sigma level and z-level (Source: DHI)

## Methodology

$$s_i = -\frac{N_\sigma + 1 - i}{N_\sigma} \quad i = 1, (N_\sigma + 1) \quad (3.27)$$

$$c(s) = (1 - b) \frac{\sinh \psi s}{\sinh \psi} + b \frac{\tanh(\psi(s + \frac{1}{2})) - \tanh(\frac{\psi}{2})}{2 \tanh(\frac{\psi}{2})} \quad (3.28)$$

The range of the weighting factor is  $0 \leq \sigma_c \leq 1$ , where the value of 0 corresponds to stretched distribution and the value of 1 corresponds to equidistant distribution. A small value of  $\sigma_c$  can result in linear instability. The range of the surface control parameter is  $0 < \psi \leq 20$  and that of the bottom control parameter is  $0 \leq b \leq 1$ . By increasing the value of  $\psi$ , the higher the resolution is achieved near the surface. If  $\psi > 0$  and  $b = 1$ , a high resolution is obtained both near the surface and near the bottom. If  $\psi \ll 1$  and  $b = 0$ , an equidistant vertical resolution is achieved.

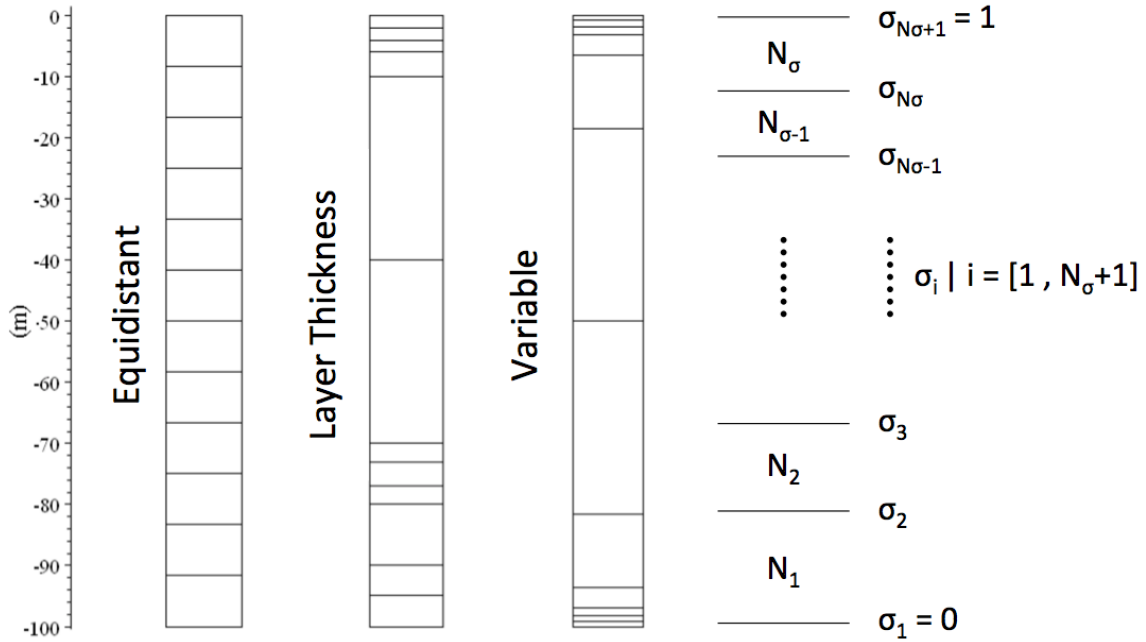


Fig. 3.3 Vertical distribution of layers for a water column in sigma mesh

## Hydrodynamic Governing Equations

The integral general form of the shallow water equations are:

$$\frac{\partial \mathbf{U}}{\partial t} + \nabla \cdot \mathbf{F}(\mathbf{U}) = \mathbf{S}(\mathbf{U}) \quad (3.29)$$

where  $\mathbf{U}$  is the vector of the conserved variables,  $\mathbf{F}$  is the flux vector function and  $\mathbf{S}$  is the vector of source terms.  $I$  and  $V$  are the inviscid and viscous fluxes respectively. The 2-D shallow water equations and the vectors in details are:

$$\frac{\partial \mathbf{U}}{\partial t} + \frac{\partial(\mathbf{F}_x^I - \mathbf{F}_x^V)}{\partial x} + \frac{\partial(\mathbf{F}_y^I - \mathbf{F}_y^V)}{\partial y} = \mathbf{S} \quad (3.30)$$

$$\mathbf{U} = \begin{bmatrix} h \\ h\bar{u} \\ h\bar{v} \end{bmatrix}$$

$$\mathbf{F}_x^I = \begin{bmatrix} h\bar{u} \\ h\bar{u}^2 + \frac{1}{2}g(h^2 - d^2) \\ h\bar{u}\bar{v} \end{bmatrix}, \quad \mathbf{F}_x^V = \begin{bmatrix} 0 \\ h\nu_H \left( 2\frac{\partial \bar{u}}{\partial x} \right) \\ h\nu_H \left( \frac{\partial \bar{u}}{\partial y} + \frac{\partial \bar{v}}{\partial x} \right) \end{bmatrix}$$

$$\mathbf{F}_y^I = \begin{bmatrix} h\bar{v} \\ h\bar{v}\bar{u} \\ h\bar{v}^2 + \frac{1}{2}g(h^2 - d^2) \end{bmatrix}, \quad \mathbf{F}_y^V = \begin{bmatrix} 0 \\ h\nu_H \left( \frac{\partial \bar{u}}{\partial y} + \frac{\partial \bar{v}}{\partial x} \right) \\ h\nu_H \left( 2\frac{\partial \bar{v}}{\partial x} \right) \end{bmatrix}$$

$$\mathbf{S} = \begin{bmatrix} 0 \\ g\eta \frac{\partial d}{\partial x} + f\bar{v}h - \frac{h}{\rho_0} \frac{\partial p_a}{\partial x} - \frac{gh^2}{2\rho_0} \frac{\partial \rho}{\partial x} - \frac{1}{\rho_0} \left( \frac{\partial s_{xx}}{\partial x} + \frac{\partial s_{xy}}{\partial y} \right) + \frac{\tau_{sx}}{\rho_0} - \frac{\tau_{bx}}{\rho_0} + hu_s \\ g\eta \frac{\partial d}{\partial y} - f\bar{u}h - \frac{h}{\rho_0} \frac{\partial p_a}{\partial y} - \frac{gh^2}{2\rho_0} \frac{\partial \rho}{\partial y} - \frac{1}{\rho_0} \left( \frac{\partial s_{yx}}{\partial x} + \frac{\partial s_{yy}}{\partial y} \right) + \frac{\tau_{sy}}{\rho_0} - \frac{\tau_{by}}{\rho_0} + hv_s \end{bmatrix}$$

## Methodology

---

The system of 3-D shallow water equations and the respective vectors can be expressed as:

$$\frac{\partial \mathbf{U}}{\partial t} + \frac{\partial \mathbf{F}_x^I}{\partial x'} + \frac{\partial \mathbf{F}_y^I}{\partial y'} + \frac{\partial \mathbf{F}_\sigma^I}{\partial \sigma} + \frac{\partial \mathbf{F}_x^V}{\partial x} + \frac{\partial \mathbf{F}_y^V}{\partial y} + \frac{\partial \mathbf{F}_\sigma^V}{\partial \sigma} = \mathbf{S} \quad (3.31)$$

$$\mathbf{U} = \begin{bmatrix} h \\ hu \\ hv \end{bmatrix}$$

$$\mathbf{F}_x^I = \begin{bmatrix} hu \\ hu^2 + \frac{1}{2}g(h^2 - d^2) \\ huv \end{bmatrix}, \quad \mathbf{F}_x^V = \begin{bmatrix} 0 \\ h\nu_H \left(2\frac{\partial u}{\partial x}\right) \\ h\nu_H \left(\frac{\partial u}{\partial y} + \frac{\partial v}{\partial x}\right) \end{bmatrix}$$

$$\mathbf{F}_y^I = \begin{bmatrix} hv \\ hvu \\ hv^2 + \frac{1}{2}g(h^2 - d^2) \end{bmatrix}, \quad \mathbf{F}_y^V = \begin{bmatrix} 0 \\ h\nu_H \left(\frac{\partial u}{\partial y} + \frac{\partial v}{\partial x}\right) \\ h\nu_H \left(2\frac{\partial v}{\partial x}\right) \end{bmatrix}$$

$$\mathbf{F}_\sigma^I = \begin{bmatrix} hw \\ hwu \\ hwv \end{bmatrix}, \quad \mathbf{F}_\sigma^V = \begin{bmatrix} 0 \\ \frac{v_t}{h} \frac{\partial u}{\partial \sigma} \\ \frac{v_t}{h} \frac{\partial v}{\partial \sigma} \end{bmatrix}$$

$$\mathbf{S} = \begin{bmatrix} 0 \\ g\eta \frac{\partial d}{\partial x} + fvh - \frac{h}{\rho_0} \frac{\partial p_a}{\partial x'} - \frac{gh}{\rho_0} \int_z^\eta \frac{\partial \rho}{\partial x} dz - \frac{1}{\rho_0} \left( \frac{\partial s_{xx}}{\partial x} + \frac{\partial s_{xy}}{\partial y} \right) + hu_s \\ g\eta \frac{\partial d}{\partial y} - fuh - \frac{h}{\rho_0} \frac{\partial p_a}{\partial y'} - \frac{gh}{\rho_0} \int_z^\eta \frac{\partial \rho}{\partial y} dz - \frac{1}{\rho_0} \left( \frac{\partial s_{yx}}{\partial x} + \frac{\partial s_{yy}}{\partial y} \right) + hv_s \end{bmatrix}$$

## Methodology

---

Integrating Equation 3.29 over the  $i^{th}$  cell and using Gauss's Theorem to rewrite the flux integral gives:

$$\int_{A_i} \frac{\partial \mathbf{U}}{\partial t} d\lambda + \int_{\Gamma_i} (\mathbf{F} \cdot \mathbf{n}) ds = \int_{A_i} \mathbf{S}(\mathbf{U}) d\lambda \quad (3.32)$$

where  $A_i$  is the area or volume of the cell,  $\lambda$  is the integration variable with respects to  $A_i$ ,  $\Gamma_i$  is the boundary of the  $i^{th}$  cell and  $ds$  is the integration variable along the boundary.  $\mathbf{n}$  is the unit outward normal vector along the boundary. Using the one-point quadrature rule and the mid-point quadrature rule to evaluate the area/volume integrals and the boundary integral, Equation 3.32 can be written as:

$$\frac{\partial U_i}{\partial t} + \frac{1}{A_i} \sum_j^{NS} \mathbf{F} \cdot \mathbf{n}_j \Delta\Gamma_j = S_i \quad (3.33)$$

where  $U_i$  and  $S_i$  are the average values of  $\mathbf{U}$  and  $\mathbf{S}$  over the  $i^{th}$  cell stored at the cell centre, NS is the number of sides of the cell,  $\mathbf{n}_j$  is the unit outward normal vector at the  $j^{th}$  side and  $\Delta\Gamma_j$  is the length/area of the  $j^{th}$  interface.

In solving the spatial discretization, both first-order and second-order schemes can be applied. An approximate Riemann solver called the Roe's scheme (Roe, 1981) is used to calculate the convective fluxes at the interface of the cells in the 2-D case and at the vertical interface of the cells in the 3-D case. In the Roe's scheme the dependent variables both sides of an interface have to be estimated. Second-order spatial accuracy is achieved by employing a linear gradient-reconstruction technique. The average gradients are estimated using the approach by Jawahar and Kamath (2000). A second-order TVD slope limiter (Van Leer limiter) is also used to avoid numerical oscillations (Darwish and Moukalled, 2003; Hirsch, 1990). As for finding the convective fluxes at the 3-D horizontal interfaces, the first-order upwinding scheme is used as the low order option. For the higher order scheme the fluxes are approximated by the mean flux value based on the cell values above and below the interface.

### Solute Transport Governing Equations

The transport equations are applicable in the salt and temperature model, the turbulence model and the scalar quantity transport model. They all follow the general form of Equation 3.9. For the 2-D case the integral form of the transport equation can be represented by Equation 3.29, in which:

$$\mathbf{U} = h\bar{c} \quad (3.34)$$

$$\mathbf{F}^I = [h\bar{u}\bar{c}, h\bar{v}\bar{c}] \quad (3.35)$$

$$\mathbf{F}^V = \left[ hD_h \frac{\partial \bar{c}}{\partial x}, hD_h \frac{\partial \bar{c}}{\partial y} \right] \quad (3.36)$$

$$\mathbf{S} = -hk_p\bar{c} + hc_s S \quad (3.37)$$

For the 3-D transport equation follows the same form given in Equation 3.29 where:

$$\mathbf{U} = hc \quad (3.38)$$

$$\mathbf{F}^I = [huc, hvc, hwc] \quad (3.39)$$

$$\mathbf{F}^V = \left[ hD_h \partial \frac{\partial c}{\partial x}, hD_h \partial \frac{\partial c}{\partial y}, h \frac{D_h}{h} \partial \frac{\partial c}{\partial \sigma} \right] \quad (3.40)$$

$$\mathbf{S} = -hk_p c + hc_s S \quad (3.41)$$

The discrete finite volume form of the transport equation is given by Equation 3.33. Similar to the shallow water equations, both first-order and second-order scheme can be applied for solving the spatial discretization. The lower order option in both 2-D and 3-D cases is the first-order upwinding scheme, in which element average values in the upwinding direction are used as values at the boundaries. For the higher order option, horizontal gradients are approximated using the values in the upwinding direction to obtain accurate second-order values at the boundaries.

### Time Integration

Consider the general form of the equations:

$$\frac{\partial \mathbf{U}}{\partial t} = \mathbf{G}(\mathbf{U}) \quad (3.42)$$

For 2-D simulations, there are two methods of time integration for both the shallow water equations and the transport equation: a lower order method and a higher order method. The lower order method is a first-order explicit Euler method:

$$\mathbf{U}_{n+1} = \mathbf{U}_n + \Delta t \mathbf{G}(\mathbf{U}_n) \quad (3.43)$$

where  $\Delta t$  is the time step interval. The higher order method is the second-order Runge Kutta method:

$$\mathbf{U}_{n+\frac{1}{2}} = \mathbf{U}_n + \frac{1}{2} \Delta t \mathbf{G}(\mathbf{U}_n) \quad (3.44)$$

$$\mathbf{U}_{n+1} = \mathbf{U}_n + \Delta t \mathbf{G}(\mathbf{U}_{n+\frac{1}{2}}) \quad (3.45)$$

For 3-D simulation the time integration uses semi-implicit method, in which the horizontal terms are treated implicitly and the vertical terms are treated either implicitly or partly explicitly and partly implicitly. The equations in the general semi-implicit form can be represented as:

$$\frac{\partial \mathbf{U}}{\partial t} = \mathbf{G}_h(\mathbf{U}) + \mathbf{G}_v(B\mathbf{U}) = \mathbf{G}_h(\mathbf{U}) + \mathbf{G}_v^I(\mathbf{U}) + \mathbf{G}_v^V(\mathbf{U}) \quad (3.46)$$

where the  $h$  and  $v$  subscripts refer to horizontal and vertical terms respectively and  $I$  and  $V$  superscripts are the inviscid and viscous terms as stated previously. For 3-D simulations, there is a lower order and a higher order time integration method similar to

## Methodology

---

the 2-D simulations. The lower order method used for the 3-D shallow water equations is written as:

$$\mathbf{U}_{n+1} - \frac{1}{2}\Delta t (\mathbf{G}_v(\mathbf{U}_{n+1}) + \mathbf{G}_v(\mathbf{U}_n)) = \mathbf{U}_n + \Delta t \mathbf{G}_h(\mathbf{U}_n) \quad (3.47)$$

The horizontal terms are integrated using a first-order explicit Euler method and the vertical term using a second-order implicit trapezoidal rule. The higher order can be written as:

$$\mathbf{U}_{n+1/2} - \frac{1}{4}\Delta t (\mathbf{G}_v(\mathbf{U}_{n+1/2}) + \mathbf{G}_v(\mathbf{U}_n)) = \mathbf{U}_n + \frac{1}{2}\Delta t \mathbf{G}_h(\mathbf{U}_n) \quad (3.48)$$

$$\mathbf{U}_{n+1} - \frac{1}{2}\Delta t (\mathbf{G}_v(\mathbf{U}_{n+1}) + \mathbf{G}_v(\mathbf{U}_n)) = \mathbf{U}_n + \Delta t \mathbf{G}_h(\mathbf{U}_{n+\frac{1}{2}}) \quad (3.49)$$

where the horizontal terms are integrated using a second-order Runge Kutta method and the vertical terms using a second-order implicit trapezoidal rule. The low order method used for the 3-D transport equations can be written as:

$$\mathbf{U}_{n+1} - \frac{1}{2}\Delta t (\mathbf{G}_v^V(\mathbf{U}_{n+1}) + \mathbf{G}_v^V(\mathbf{U}_n)) = \mathbf{U}_n + \Delta t \mathbf{G}_h(\mathbf{U}_n) + \Delta t \mathbf{G}_v^I(\mathbf{U}_n) \quad (3.50)$$

The horizontal and the vertical convective terms are integrated using the first-order explicit Euler method and the vertical viscous terms are integrated using a second-order implicit trapezoidal rule. As for the higher order, the horizontal and the vertical convective terms are integrated using a second-order Runge Kutta method and the vertical terms are integrated using a second-order implicit trapezoidal rule:

$$\mathbf{U}_{n+1/2} - \frac{1}{4}\Delta t (\mathbf{G}_v^V(\mathbf{U}_{n+1/2}) + \mathbf{G}_v^V(\mathbf{U}_n)) = \mathbf{U}_n + \frac{1}{2}\Delta t \mathbf{G}_h(\mathbf{U}_n) + \frac{1}{2}\Delta t \mathbf{G}_v^I(\mathbf{U}_n) \quad (3.51)$$

$$\mathbf{U}_{n+1} - \frac{1}{2}\Delta t (\mathbf{G}_v^V(\mathbf{U}_{n+1}) + \mathbf{G}_v^V(\mathbf{U}_n)) = \mathbf{U}_n + \Delta t \mathbf{G}_h(\mathbf{U}_{n+1/2}) + \Delta t \mathbf{G}_v^I(\mathbf{U}_{n+1/2}) \quad (3.52)$$

### Boundary Conditions

The boundaries of the simulation can be categorized into two types: closed boundaries and open boundaries. Along close boundaries, which are commonly used to represent land boundaries, normal fluxes are forced to zero for all variables. For the momentum equations, land boundaries are associated with full-slip conditions, meaning that the boundary has no effect on the flow velocity parallel in plane and close to it. For the shallow water equations, the no-slip condition can also be applied where both the normal and tangential velocity components are zero. For the open boundaries it is slightly more complex, as there are a number of different scenarios based on the different flow conditions and input data. For the flux and velocity boundary, a weak approach is used in which a ghost cell technique is applied. The primitive variables in the ghost cell are specified. The water level is evaluated based on the value of the adjacent interior cell and the velocities are evaluated based on the boundary information. For a discharge boundary, the transverse velocity is set to zero for inflow and passively advected for outflow. The boundary flux is then calculated using an approximate Riemann solver. The discharge boundary also includes a strong approach based on the characteristic theory (Sleigh et al., 1998), which the level boundary also adopts for its imposition. For the transport equations, either a specified value or a zero gradient can be given at the boundaries. For specified values, the boundary conditions are imposed by applying the specified concentrations for calculation of the boundary flux. For a zero gradient condition, the concentration at the boundary is assumed to be identical to the concentration at the adjacent interior cell.

### Flooding and Drying

The variations in different hydrodynamic behaviours result in changes in the water levels and hence changes in the area submerged in water. Part of the simulation area goes from under water (flooding condition) to being exposed to the atmosphere (drying condition) and vice versa, depending on the rise and fall of water levels. The boundary

## Methodology

---

of the water bodies in turn becomes a moving boundary according to the flooding and drying fronts. The approach for treatment of the moving boundaries problem is based on the work by Sleigh et al. (1998) and Zhao et al. (1994). When the depths are small the problem is reformulated and only when the depths are very small the elements are removed from the calculation. The reformulation is made by setting the momentum fluxes to zero and only taking the mass fluxes into consideration.

In this flooding and drying process, the depth in each element is monitored and the elements are classified as (1) flooded, (2) dry, (3) partially dry, or (4) wet. In addition, the element faces are monitored to identify flooded boundaries. An element face is defined as flooded when the following two criteria are satisfied. The first one is that the water depth at one side of face must be less than a tolerance dry depth ( $h_{dry}$ ) and the water depth on the other side of the face must be larger than a tolerance flood depth ( $h_{flood}$ ). The second criteria is that the sum of the still water depth at the side for which the water depth is less than  $h_{dry}$  and the surface elevation at the other side must be larger than zero.

An element is dry if the water depth is less than the tolerance dry depth ( $h_{dry}$ ) and none of the element faces are flooded boundaries. The element is then removed from the calculation. An element is partially dry if the water depth is larger than  $h_{dry}$  and less than a tolerance wet depth,  $h_{wet}$ , or when the depth is less than  $h_{dry}$  and one of the element faces is a flooded boundary. The momentum fluxes are set to zero in this case and only the mass fluxes are calculated. An element is wet if the water depth is greater than  $h_{wet}$ . Both the mass fluxes and the momentum fluxes are calculated in this circumstance.

The wetting depth ( $h_{wet}$ ) must be larger than the drying depth ( $h_{dry}$ ) and flooding depth ( $h_{flood}$ ). In short, the following condition must be satisfied:  $h_{wet} > h_{flood} > h_{dry}$ . The default values generally are  $h_{wet} = 0.1\text{m}$ ,  $h_{flood} = 0.05\text{m}$  and  $h_{dry} = 0.005\text{m}$ .

### Turbulence

The turbulence is simulated through an eddy viscosity concept. The eddy viscosity is often described separately for the vertical and horizontal transport. Several turbulence models are available: (1) a constant viscosity, (2) a vertically parabolic viscosity and (3) a standard k- $\epsilon$  model (Rodi, 1984). Given the relatively small vertical scale in our lake environment, the vertical eddy viscosity will be set at constant. The horizontal eddy viscosity is determined using the method proposed by Smagorinsky (1963), in which a sub-grid scale transport by an effective eddy viscosity related to a characteristic length scale is proposed:

$$\nu_H = c_s^2 l^2 \sqrt{2S_{ij}S_{ij}} \quad (3.53)$$

where  $c_s$  is an empirical constant,  $l$  is a characteristic length and the deformation rate of the eddy viscosity is given by:

$$S_{ij} = \frac{1}{2} \left( \frac{\partial u_i}{\partial x_j} + \frac{\partial u_j}{\partial x_i} \right) \quad (i, j = 1, 2) \quad (3.54)$$

### Bottom Stress

The bottom stress,  $\vec{\tau}_b = (\tau_{bx}, \tau_{by})$ , is determined by a quadratic friction law:

$$\frac{\vec{\tau}_b}{\rho_0} = c_f \vec{u}_b |\vec{u}_b| \quad (3.55)$$

where  $c_f$  is the drag coefficient and  $\vec{u}_b = (u_b, v_b)$  is the flow velocity above the bottom layer. The friction velocity associated with the bottom stress is given by:

$$U_{\tau_b} = \sqrt{c_f |u_b|^2} \quad (3.56)$$

## Methodology

---

For 2-D calculations  $\vec{u}_b$  is the depth-average velocity and the drag coefficient can be determined from the Chezy number,  $C$ , or the Manning roughness coefficient,  $n$ :

$$c_f = \frac{g}{C^2} = \frac{g}{(nh^{1/6})^2} \quad (3.57)$$

For 3-D calculations  $\vec{u}_b$  is the velocity at a distance  $\Delta z_b$  above the seabed or riverbed and the drag coefficient is determined by assuming a logarithmic profile between the bottom bed and a point  $\Delta z_b$  above the bottom bed:

$$c_f = \frac{1}{\left(\frac{1}{\kappa} \ln \left(\frac{\Delta z_b}{b_0}\right)\right)^2} \quad (3.58)$$

where  $\kappa = 0.4$  is the von Kármán constant and  $b_0$  is the bed roughness length scale. When the boundary surface is rough,  $b_0 = mk_s$ , depends on the roughness height,  $k_s$  and  $m$  is approximately 1/30. The Manning roughness coefficient can be estimated from the roughness height and the wave induced bed resistance can be determined respectively by:

$$n = \frac{25.4}{k_s^{1/6}} \quad c_f = \left(\frac{u_{fc}}{u_b}\right)^2 \quad (3.59)$$

where  $U_{fc}$  is the friction velocity calculated by considering the conditions in the wave boundary layer. Detailed description of the wave induced bed resistance can be referred to Fredsøe (1984) and Jones et al. (2014).

### 3.1.6 1-D Hydrodynamic Governing Equations

For natural open channel flow and surface runoff environments, the water depth (e.g. 5-10 m) is relatively small compared to the horizontal scale (e.g. 0.1-50 km). Hence the flow's vertical motion is negligible and horizontal flow predominates. These features allow the flow to be investigated through a depth-integrated approach, which simplifies the original 3-D Navier-Stokes equations into the 2-D SWE. In an open

## Methodology

---

channel flow environment, the governing equations are further simplified into a 1-D equation in which velocity components in the  $y$  and  $z$  directions are assumed to be insignificant. 1-D Saint-Venant equations assume that (a) hydrostatic pressure under which the streamline curvature is small, (b) the average channel bed slope is small and (c) vertical accelerations are negligible and hence homogeneous vertical planes are assumed throughout. Neglecting dynamic water pressure, Coriolis force, wind forces and viscous forces, the 1-D Saint-Venant equation can be written as:

$$\frac{\partial A}{\partial t} + \frac{\partial Q}{\partial x} = q \quad (3.60)$$

$$\frac{\partial Q}{\partial t} + \frac{\partial (Q^2/A)}{\partial x} + gA \left( \frac{\partial Z}{\partial x} + s_f + s_e \right) + L = 0 \quad (3.61)$$

where  $A$  is the wetted cross sectional area of river channel,  $t$  is time,  $Q$  is the flow discharge,  $x$  is the distance of river channel,  $q$  is the lateral discharge per unit channel length,  $g$  is the gravitational acceleration,  $Z$  is the water surface elevation above datum,  $s_e$  is the slope due to local head loss and  $s_f$  is the friction slope, which can be approximated by:

$$s_f = \frac{n^2 Q |Q|}{[A/(A/B)^{4/3}]} \quad (3.62)$$

where  $n$  is the Manning roughness coefficient and  $B$  is the wetted perimeter of river channel. The momentum of lateral discharge,  $L$  is dependent on the lateral discharge:

$$L = \begin{cases} q(u_b - Q/A) & \text{if } q \geq 0 \\ -qQ/A & \text{if } q < 0 \end{cases} \quad (3.63)$$

where  $u_b$  is the magnitude of lateral flow velocity along main streamline in river channel.

### 3.1.7 1-D Numerical Methods for Hydrodynamics

The Preissmann method, as an implicit finite difference technique, is one of the most common due to its unconditional stability, extreme robustness and ability to allow variable time and spatial steps. It is a space-centered bidiagonal method which has gradually developed to be the standard method for 1-D numerical modeling in the field of hydraulic engineering (Meselhe and Holly Jr., 1997). In this scheme, four grid points sitting on two time lines and two distance steps are used to approximate the terms in the differential equations. Two algebraic equations are obtained as a result of the approximation, representing the PDE of continuity and momentum equations. The discretization of the Preissmann scheme can be represented as follows (Huang et al., 2011; Preissmann, 1961):

$$f(x, t) = \frac{\theta(f_{j+1}^{n+1} + f_j^{n+1}) + (1 - \theta)(f_{j+1}^n + f_j^n)}{2} \quad (3.64)$$

$$\frac{\partial f}{\partial x} = \frac{\theta(f_{j+1}^{n+1} - f_j^{n+1}) + (1 - \theta)(f_{j+1}^n - f_j^n)}{\Delta x} \quad (3.65)$$

$$\frac{\partial f}{\partial t} = \frac{f_{j+1}^{n+1} - f_{j+1}^n + f_j^{n+1} - f_j^n}{2\Delta t} \quad (3.66)$$

where  $\theta$  is the temporal weighting coefficient,  $f$  is any function,  $\partial f/\partial x$  and  $\partial f/\partial t$  are the space and time derivatives of function  $f$  respectively.  $\theta$  is used in the approximation of all terms of the equation except for the time derivatives in order to adjust the influence of the points  $j$  and  $j+1$ . If  $\theta = 0.5$ , the corresponding scheme is called the ‘box-scheme’, which is a centered finite difference scheme. If  $\theta = 1$ , the scheme is known as the ‘fully-implicit scheme’ in space (Gündüz, 2004). The Preissmann scheme is second-order accurate in both time and space if  $\theta = 0.5$ , but then it is at the boundary of being marginally stable. For any  $\theta$  value between 0.5 and 1.0, the scheme is unconditionally stable for any time step, leading to an accuracy of the first-order in time and second-order in space (Sart et al, 2010). In addition, accuracy

## Methodology

---

of computations decreases as  $\theta$  shifts from 0.5 to 1.0, in which the effect magnifies as the magnitude of the computational time step increases. A conventional range for  $\theta$  is recommended between 0.55 and 0.60 to provide the optimal balance between unconditional stability and reliable accuracy. Figure 3.4 illustrates the discretization of the space derivative of the Preissmann scheme (Novak et al., 2010).

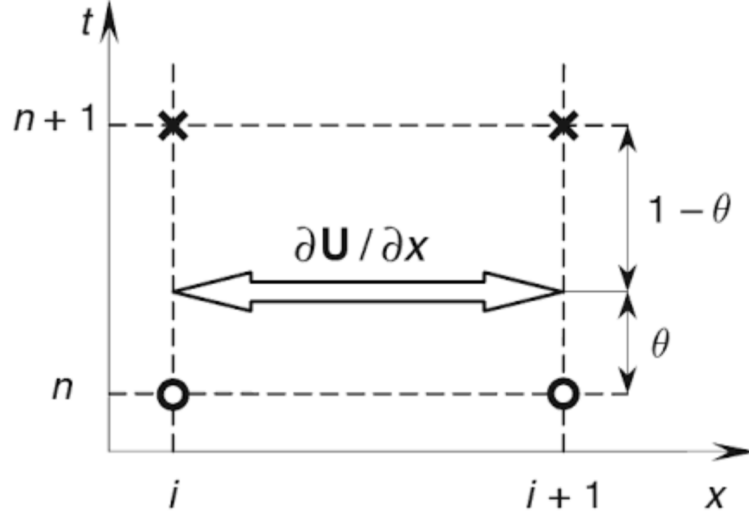


Fig. 3.4 Discretization of spatial derivative in Preissmann scheme

By substituting the approximations in Equation (3.65) and Equation (3.66) back into the governing equations and linearizing the resulting discretized equations using Taylor series expansion, two scalar algebraic equations are formed:

$$A_{1j}\Delta Q_j + B_{1j}\Delta Z_j + C_{1j}\Delta Q_{j+1} + D_{1j}\Delta Z_{j+1} = E_{1j} \quad (3.67)$$

$$A_{2j}\Delta Q_j + B_{2j}\Delta Z_j + C_{2j}\Delta Q_{j+1} + D_{2j}\Delta Z_{j+1} = E_{2j} \quad (3.68)$$

where the variables  $A$ ,  $B$ ,  $C$ ,  $D$  and  $E$  are coefficients resulting from the linearization.  $Z_j$  and  $Q_j$  are water surface elevation and discharge at the  $j^{\text{th}}$  cross-section. They are calculated for each iteration and each node, depending on variables calculated from the previous iterations or time steps. As a result, for a domain of  $N$  computational points with  $N-1$  computational segments, there are  $2N-2$  discretized equations. As there are two unknowns at each node, there are  $2N$  unknowns. Therefore two boundary

## Methodology

---

equations are needed to complete the system. The locations of the boundary conditions are dependent on the types of flow (e.g. subcritical, supercritical, or transcritical). For condition  $Fr < 1$  (subcritical flow), boundary conditions should be given at the upstream and downstream location. When  $Fr > 1$  (supercritical flow), two boundary conditions are needed from the upstream location. Boundary conditions at upstream can be given in three different ways. The first one is providing the change in water levels with respect to time,  $Z = Z(t)$ . The second is setting the flow function,  $Q = Q(t)$ . The third is giving the relationship between the flow and water levels,  $Q = Q(Z)$ . Similarly, three boundary conditions can be determined at the downstream in order to determine  $\Delta Z_N$ . They are  $Z_n = Z(t)$ ,  $Q_N = Q(t)$  and  $Q_N = Q(Z_N)$ .

At river junctions, the hydraulic conditions are governed by the mass and energy conservation equations. Mass conservation can be maintained via the adjustment of water flow at the junctions' respective to inflow and outflow streams. Assuming energy loss at river stream junctions is negligible, momentum conservation can be fulfilled between the water levels at junctions and adjacent cross sections. The continuity equation is written as:

$$\sum_{r=1}^m \Delta Q_r = A_N \frac{\Delta Z_N}{\Delta t} \quad (3.69)$$

in which  $r$  is the respective number of channel linked to junction  $N$ ,  $m$  is the total number of sub-channels linked to junction  $N$  and  $A_N$  is the storage area of  $N$ . Figure 3.5 provides a graphical representation of the continuity concept illustrated.

The discretization of the continuity and momentum equations, together with the treatment of junctions and boundary conditions, form a closed river network system of equations, in which direct solutions can be reached via the use of algorithms. A three level solution method is used to solve Equation 3.67-3.69. Linear correlation between the discharge and water level at the first ( $N = 1$ ) and last ( $N = P$ ) cross-section of a sub-channel is assumed.

$$\Delta Q_1 = G_1 \Delta Z_1 + H_1 + R_1 \Delta Z_P \quad (3.70)$$

$$\Delta Q_P = G_2 \Delta Z_1 + H_2 + R_2 \Delta Z_P \quad (3.71)$$

where  $G_1$ ,  $H_1$ ,  $R_1$  and  $G_2$ ,  $H_2$ ,  $R_2$  are the coefficients at the start and end of a sub-channel. These algebraic equations can be used to derive:

$$[\mathbf{A}] \{\Delta Z\} = [\mathbf{B}] \quad (3.72)$$

where  $\mathbf{A}$  is a coefficient matrix and  $\mathbf{B}$  is a vector that consists of explicit variables at the  $n^{th}$  time step. The Gauss-Jordan elimination method, one of the many common algorithms used to solve matrices of linear equations, is adopted in this case. The principle behind such method is to gather the unknown variables at the junctions of river streams, at which the relationship between the change in water levels and the change in water flow can be found.

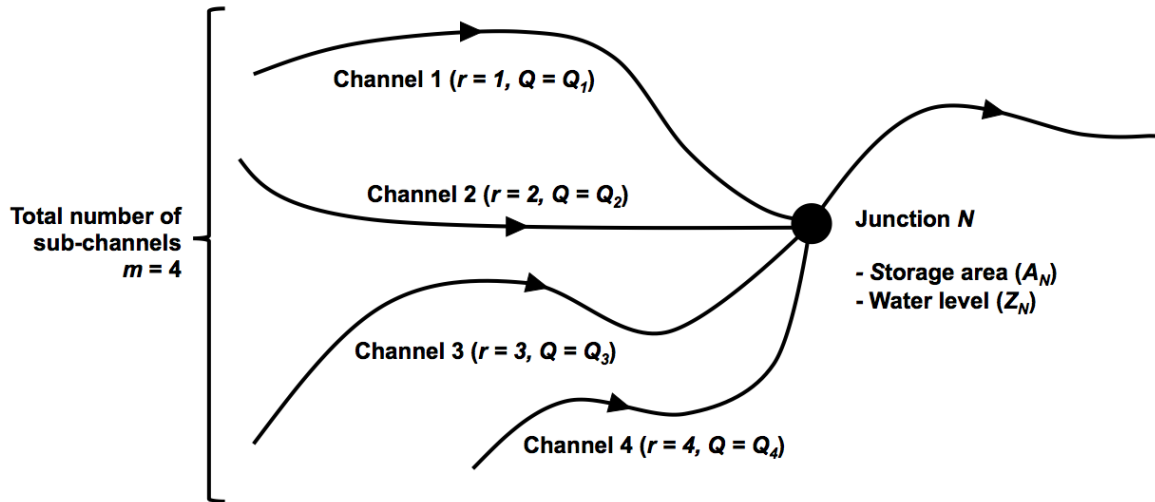


Fig. 3.5 Mass and energy conservation of channels at junction  $N$

### 3.1.8 1-D Solute Transport Governing Equations

Mass transport and solute concentrations through the water bodies are mostly unsteady and unevenly distributed. This is due to the natural and random characteristics of the lake environment and in the river networks. This study adapts the method used in Zhu and Xu (1992) to represent mass transport behaviours in rivers networks with reliable accuracy, straightforward control and efficient computational usage (i.e. low computational requirement with high computational speed). The equation below represents the solute transport equation in open channels:

$$\frac{\partial Ac}{\partial t} + \frac{\partial Qc}{\partial x} = \frac{\partial}{\partial x} \left( AD_x \frac{\partial c}{\partial x} \right) - S_c + S_k \quad (3.73)$$

where  $A$  is the wetted cross sectional area,  $c$  is the concentration of a water quality state variable,  $t$  is time,  $Q$  is the flow discharge,  $x$  is the distance of river channel,  $D_x$  is the longitudinal dispersion coefficient,  $S_c$  is the external bacterial decay term that equals to  $cK_dA$ , with  $K_d$  being the decay factor, and  $S_k$  is the kinetic source term due to chemical reaction. The conditions at junctions between river streams can be represented by:

$$\sum_{r=1}^m (Qc)_{r,l} = \left( \Omega c \frac{dZ}{dt} \right)_l + S_l \quad (3.74)$$

in which  $m$  is the number of connecting streams,  $r$  is the respective number of connecting streams,  $l$  is the intersection node number,  $\Omega$  is the water surface area of the streams' intersection,  $Z$  is the water surface elevation above datum and  $S_l$  is the external source term at intersection node  $l$ . The left hand side of the equation will give the sum of the mass of variable going into the intersection at location  $l$ , which under the principle of mass continuity will equate to the right hand side of the equation that represents the mass at junction  $l$  as a product of surface area times water depth and concentration. Any additional source at the location is also considered as an extra term.

## Methodology

---

Finite volume method is used to maintain the mass conservation of Equation 3.73. Nonetheless, additional errors introduced by the linearization in deriving Equation 3.67 and Equation 3.68 might disrupt the consistency between these equations with Equation 3.73. As a result, inner iteration is used to reduce the errors in the solution of the hydrodynamic equations. In this approach, a small time step from  $t_{n-1}$  to  $t_n$  is replaced by  $R$  half-time steps of the implicit scheme. Inner iteration is first performed for the sub-step from  $t_{n-1}$  to  $t_{n-(R-1)/R}$ , equating to  $t_{n-1} + \Delta t/R$  and yielding an approximation of the hydrodynamic variables at  $t_{n-(R-1)/R}$ . The same procedure is then carried out for  $R$  times until the sub-step from  $t_{n-1/R}$  to  $t_n$  is reached. When the time stepping and iteration procedure are completed, the original approximation for the variable at  $t = n-1$  is replaced on the grid by the new value at  $t = n$  and so on (Huang et al., 2018). This improves the mass conservation level in the solution of Equation 3.73. The staggered grids method, which positions the hydrodynamic and water quality variables at the cross sections and the centre of a control volume respectively, are also used to further improve the mass conservation accuracy.

### 3.1.9 1-D Numerical Methods for Solute Transport

The mass transport governing equation (Equation 3.73) is discretized using the implicit upwind scheme to maintain consistency between the hydrodynamic and mass transport equations. Each term in the equation are written as follows:

$$\left\{ \begin{array}{l} \frac{\partial(AC)}{\partial t} = \frac{(AC)_i^{k+1} - (AC)_i^k}{\Delta t} \\ \frac{\partial(QC)}{\partial x} = \frac{(QC)_i^{k+1} - (QC)_{i-1}^{k+1}}{\Delta x_{i-1}} \\ \frac{\partial}{\partial x} \left( AD_x \frac{\partial C}{\partial x} \right) = \frac{1}{\Delta x_{i-1}} \left[ \frac{(AD_x)_i^{k+1} C_{i+1}^{k+1} - (AD_x)_{i-1}^{k+1} C_i^{k+1}}{\Delta x_i} \right. \\ \left. - \frac{(AD_x)_{i-1}^{k+1} C_i^{k+1} - (AD_x)_{i-1}^{k+1} C_{i-1}^{k+1}}{\Delta x_{i-1}} \right] \\ S_c = \overline{K}_{d_{i-1}}^{k+1} (AC)_i^{k+1} \\ S_k = \overline{S}_{k_{i-1}}^{k+1} \end{array} \right. \quad (3.75)$$

## Methodology

---

where  $\overline{K_d}$  and  $\overline{S}$  are the mean values of the decay factor and source term respectively over the studied river section,  $k$  is the initial time step,  $k+1$  is the end time step. Forward difference method is used to discretize the equations into:

$$a_i C_{i-1} + b_i C_i + c_i C_{i+1} = z_i \quad (i = 1, 2, \dots, n) \quad (3.76)$$

where  $a_i$ ,  $b_i$ ,  $c_i$  are variables calculated for each iteration based on other variables at previous iteration or time-step,  $z_i$  is the explicit term,  $C_i$  is the concentration of solute at the end of each section, while  $n$  is the number of sections in the domain. The generalized equations can then be reduced into a set of simultaneous equations based on the location of the cross-sections in the domain. The tridiagonal matrix algorithm (TDMA), which is also called the Thomas algorithm (Thomas, 1949), is used to solve the 1-D solute transport equations. The method involves a forward elimination phase followed by a backward substitution phase.

For any river stream within the river network, there are four potential flow patterns based on the flow direction at their respective starting and ending cross sections (Figure 3.6). These patterns dictate the formulae used to predict the solute concentration in the river streams. The consideration of these four different scenarios are essential to accurately simulate the solute transport behaviour across the flow networks. The concentration at each cross section and the solution procedure for each scenario are documented in (Huang et al., 2011) and will not be further explained herein.

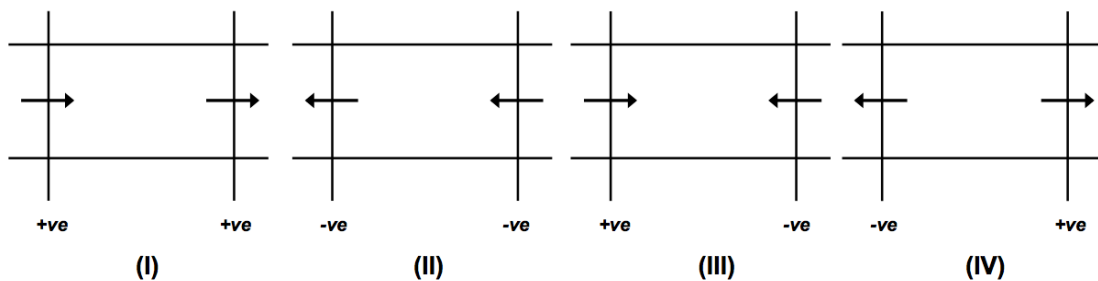


Fig. 3.6 Four potential flow directions in one river section

### 3.2 Part 2 - Water Quality

In water environment, the transportation and interaction between key variables such as nutrients and biomass are closely influenced by a series of complex physio-chemical processes. Major fundamental processes include the dissolved oxygen process, the biological oxygen demand process, the nitrogen cycle, the phosphorus cycle and the phytoplankton kinetics. These key processes are all interconnected and often contribute to the outcome of other processes. The water quality in lake and river environments is largely determined by these processes. Prior to showing the formulation of these processes in the water quality models, each of the processes will be explained.

#### 3.2.1 Dissolved Oxygen Process

Dissolved oxygen (DO) is the measure of gaseous oxygen dissolved in water bodies. The concentration of DO directly affects the living habitats of aquatic wildlife and alters a healthy ecological balance. DO in the aquatic environment is produced by photosynthesis of algae and plants, by direct absorption from the atmosphere via diffusion and by rapid movement through aeration. DO is consumed by respiration of plants, animals and bacteria and is involved in many other processes including BOD degradation, sediment oxygen demand and oxidation of nitrogen compounds. The interlinking role of DO in many of these processes thus positions it to be a key indicator of water quality modeling. It is important to maintain DO concentration at levels acceptable for the sustainability of the lake environment. The methodology for dissolved oxygen dynamics analysis in streams, rivers and estuaries is well developed (O'Connor and Thomann, 1972). The variations in DO concentration are described as a function of the naturally occurring aerobic respiratory processes (photosynthesis, respiration and re-aeration) and degradation of organic matter. The complexity is increased by adding the anaerobic interaction with the underlying sediments and by considering nutrients processes such as nitrification of ammonia to nitrate.

## Methodology

---

**Reaeration** is the process describing the interchange of oxygen between the water and the atmosphere. The majority of the oxygen content in water bodies comes from atmospheric reaeration. The reaeration process expresses the reaeration related to the saturation concentration of oxygen. At concentration lower than the saturation level, oxygen is transferred from the air to the water phase at a specific rate, called the reaeration constant. If the concentration becomes higher than the saturation level, oxygen will be transferred to the atmosphere in a similar manner. The change of DO concentration with regards to reaeration can be expressed in the formula (DHI, 2017e):

$$\frac{dDO}{dt} = K_2(C_s - DO) \quad (3.77)$$

where  $K_2$  is the reaeration rate at 20°C (1/d), which is dependent on the flow velocity  $V$ , water depth  $h$  and wind speed  $W_v$ . The expression includes a saturation level for oxygen in water  $C_s$  in which  $T$  is the temperature (°C) and  $S$  is the salinity (ppt):

$$K_2 = 3.93 \cdot V^{0.5}/h^{1.5} + (0.728 \cdot W_v^{0.5} - 0.371 \cdot W_v + 0.0372 \cdot W_v^2)/h \quad (3.78)$$

$$C_s = T \{0.00256 \cdot S - 0.41022 + T(0.007991 - 0.0000374 \cdot S - 0.000077774 \cdot T)\} \\ + 14.652 - 0.0841 \cdot S \quad (3.79)$$

In the 1-D river network model, the reaeration rate ( $K_2$ ) is expressed using the O'Connor-Dobbins formula (Gualtieri et al., 2002; O'Connor and Dobbins, 1956):

$$k_{qj} = 3.93 v_j^{0.5} D_j^{-1.5} \quad (3.80)$$

where  $k_{qj}$  is the flow-induced reaeration rate constant (1/d),  $v_j$  is the average water velocity in segment  $j$  (m/s) and  $D_j$  is the average segment depth (m).

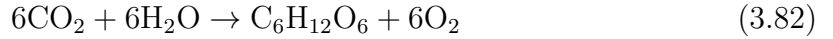
## Methodology

---

**Respiration** from autotroph and heterotrophs consumes oxygen and can be described as dependent of the temperature. Respiration equation is represented as:

$$R = R_1 \cdot F_1(h) \cdot \Theta_1^{T-20} + R_2 \cdot \Theta_2^{T-20} \quad (3.81)$$

where  $R_1$  is the photosynthetic (autotroph) respiration at 20°C,  $R_2$  is the respiration rate of bacteria (heterotrophic) at 20°C,  $F_1(h)$  is the light dampening function,  $\Theta_1$  is the temperature coefficient for photosynthetic respiration/production,  $\Theta_2$  is the temperature coefficient for heterotrophic respiration/production and  $T$  is the temperature (°C). On the other hand, **photosynthesis** is an oxygen producing process from the conversion of carbon dioxide and water into glucose and oxygen. The overall equation of the process and the model formulation are given respectively as (DHI, 2017e):



$$\begin{cases} P = P_{max} \cdot F_1(h) \cdot \cos 2\pi(\tau/a) \cdot \Theta_1^{T-20} & \text{if } \tau \in [t_{up}, t_{down}] \\ P = 0 & \text{if } \tau \notin [t_{up}, t_{down}] \end{cases} \quad (3.83)$$

where  $P$  is the actual oxygen production (gO<sub>2</sub>/m<sup>2</sup>/d),  $P_{max}$  is the maximum production at noon (gO<sub>2</sub>/m<sup>2</sup>/d),  $\tau$  is the actual time of the day related to noon,  $a$  is the actual relative day length and  $[t_{up}, t_{down}]$  is the time of sunrise and sunset respectively. The photosynthetic oxygen production and the autotrophic respiration vary with the water depth due to the light dependency of the autotrophs. The depth variation is modelled using the Beer-Lambert Law with light dampening function,  $F_1(h) = e^{-k \cdot h}$  in which  $k$  is the light extinction coefficient (Swinehart, 1962). The oxygen producing process of photosynthesis by algae and plants is time varying over the course of a day. In addition, there is a diurnal variation, which is at its maximum at noon and follows the sinusoidal variation of daily light intensity. Photosynthesis takes place during the day-time only. The actual day length is automatically calculated in the model depending on the time of the year and the latitude. Concurrent with the oxygen producing photosynthesis is

## Methodology

---

the oxygen consuming respiration by plants and algae. Whereas oxygen production only occurs in daytime, respiration processes continue throughout the day and night.

The **degradation of BOD** is another oxygen consuming process. The carbonaceous biological oxygen demand is an expression of the quantity of organic matter in the water environment. Degradation of the organic matter gives rise to an equivalent amount of oxygen consumption. The BOD degradation will therefore be part of the oxygen balance. It is worth noting that the process is also a source of nutrients as the nitrogen and phosphorus are part of the organic matter. The inorganic nutrients (e.g. ammonia) being products of BOD degradation can be oxidized and give rise to an additional oxygen consumption. The degradation of organic matter can be described by first-order kinetics. The process is dependent on the temperature, the oxygen concentration and the concentration of the organic materials. The overall equation and the model formulation are represented respectively as below:



$$\frac{dBOD}{dt} = K_3 \cdot BOD \cdot \Theta_3^{T-20} \cdot \frac{DO}{DO + HS_{BOD}} \quad (3.85)$$

where  $K_3$  is the degradation constant for organic matter at 20°C,  $HS_{BOD}$  is the half saturation oxygen concentration for BOD (mgO<sub>2</sub>/l) and  $\Theta_3$  is the Arrhenius temperature coefficient. The modeling of BOD is an interrelated part of the DO modelling and the BOD degradation stops under anaerobic condition (DO = 0). The differential equations describing both process are coupled and solved simultaneously.

**Nitrification** describes the process in which ammonia is transformed into nitrite (NO<sub>2</sub><sup>-</sup>) and then nitrate (NO<sub>3</sub><sup>-</sup>). For the purpose of simpler expression in subsequent formulation in this study, nitrite and nitrate will be expressed as NO<sub>2</sub> and NO<sub>3</sub> respectively without the ion notation. Meanwhile, ammonia in aqueous solution consists of two principal forms; unionized ammonia (NH<sub>3</sub>) or ammonium ion (NH<sub>4</sub><sup>+</sup>).

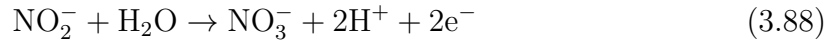
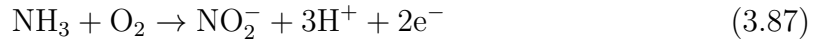
## Methodology

---

Their relative concentrations are pH and temperature dependent (Körner et al., 2001) and their chemical equilibrium can be expressed as:



For this study, the ammoniacal nitrogen ( $\text{NH}_3\text{-N}$ ) is used to represent the nitrogen mass in the water contributed by ammonia and ammonium (Jafari and Khayamian, 2008). The nitrification process consists of the following two stage transformations that convert ammonia into nitrate (American Water Works Association, 2013):



The stoichiometric conditions and the molar weights determine the amount of oxygen consumed by nitrification. From the equation for every mg of ammoniacal nitrogen oxidized,  $2 \times (32/14) = 4.57$  mg of oxygen is consumed. This gives the 'yield' factor of the process. In the model, the oxygen consumption due to nitrification process is described as a first-order process.

$$Y_i \frac{d\text{NH}_3\text{-N}}{dt} = K_4 \cdot \text{NH}_3\text{-N} \cdot \Theta_4^{T-20} \cdot \frac{\text{DO}}{\text{DO} + \text{HS}_{\text{nitr}}} \quad (3.89)$$

where  $Y_i$  is the yield factor representing the amount of oxygen consumed by nitrification, ( $\text{gO}_2/\text{gNH}_3\text{-N}$ ),  $K_4$  is the nitrification rate at  $20^\circ\text{C}$ ,  $\Theta_4$  is the temperature coefficient for nitrification,  $\text{HS}_{\text{nitr}}$  is the half saturation concentration for nitrification ( $\text{mgO}_2/\text{l}$ ).

The decomposition of organic material in benthic sediment can have profound effects on the concentrations of oxygen in the overlying waters. The decomposition of organic material includes deposited microscopic algae as well as plant material and other organisms, which results in the exertion of an oxygen demand at the sediment-water interface. This is hence termed **sediment oxygen demand (SOD)**. SOD is

## Methodology

---

assumed to depend only on the oxygen concentration and temperature, described by the common Arrhenius expression. A Michaelis-Menten expression is used to simulate the processes under low oxygen conditions (Higashino et al., 2004; Nakamura and Stefan, 1994). In the model, SOD includes the natural oxygen demand as well as the oxygen demand from deposited BOD originating from pollution sources. A value of  $0.5 \text{ gO}_2/\text{m}^2/\text{d}$  is recommended for the natural sediment oxygen demand and a value of  $1.5 \text{ gO}_2/\text{m}^2/\text{d}$  for the total oxygen demand (Jørgensen, 1979). The model formulation of the process can be expressed as:

$$\frac{d\text{SOD}}{dt} = \Theta_{\text{SOD}}^{T-20} \cdot \frac{\text{DO}}{\text{DO} + \text{HS}_{\text{SOD}}} \quad (3.90)$$

where  $\text{HS}_{\text{SOD}}$  is the half-saturation oxygen concentration for SOD ( $\text{mgO}_2/\text{l}$ ) and  $\Theta_{\text{SOD}}$  is the temperature coefficient for SOD.

### Overall Oxygen Balance

Below summarizes the balance equations contributed to the DO processes:

$$\begin{aligned} \frac{d\text{DO}}{dt} &= \text{reaeration} - \text{nitrification} - \text{BOD decay} + \text{photosynthesis} - \text{respiration} - \text{SOD} \\ &= \frac{d\text{DO}}{dt} - Y_1 \frac{d\text{NH}_3\text{-N}}{dt} - \frac{d\text{BOD}}{dt} + P - R - \frac{d\text{SOD}}{dt} \\ &= [K_2(C_s - \text{DO})] - Y_1 \left[ K_4 \cdot \text{NH}_3\text{-N} \cdot \Theta_4^{T-20} \cdot \frac{\text{DO}}{\text{DO} + \text{HS}_{\text{nitr}}} \right] \\ &\quad - \left[ K_3 \cdot \text{BOD} \cdot \Theta_3^{T-20} \cdot \frac{\text{DO}}{\text{DO} + \text{HS}_{\text{BOD}}} \right] + [P_{\text{max}} \cdot F_1(h) \cdot \cos 2\pi(\tau/a) \cdot \Theta_1^{T-20}] \\ &\quad - [R_1 \cdot F_1(h) \cdot \Theta_1^{T-20} + R_2 \cdot \Theta_2^{T-20}] - \left[ \Theta_{\text{SOD}}^{T-20} \cdot \frac{\text{DO}}{\text{DO} + \text{HS}_{\text{SOD}}} \right] \end{aligned} \quad (3.91)$$

### 3.2.2 Nitrogen Cycle

The nitrogen cycle describes the relationship between different forms of nitrogen and their associated processes in the water environment (Figure 3.7). The nitrogen cycle starts with the **fixation** of free nitrogen gas from the atmosphere by microorganisms. This process turns inert nitrogen gas into reactive nitrogen compounds such as ammonium salts that are more accessible to microorganisms for further reactions. In addition, the process of **ammonification** also contributes to ammonium in the water environment. The decomposition of dead organic matter and organic waste leads to a release of organic nitrogen which is subsequently converted into ammonium by bacteria. The **assimilation** of nitrate and ammonium by plants and algae in water represents the process in which, as phytoplankton grow, dissolved inorganic nitrogen is taken up and incorporated into biomass. The process is the formation of organic nitrogen compounds like amino acids from inorganic nitrogen compounds in the water environment. Organisms such as plants and certain bacteria that cannot fix nitrogen gas depend on the ability to assimilate nitrate or ammonium for their growth.

Ammonia and ammonium, in the presence of nitrifying bacteria and oxygen, is converted to nitrate in a process called **nitrification**. The process is carried out by aerobic autotrophs; *Nitrosomonas* and *Nitrobacter* predominate in fresh waters. It is a two-step process with *Nitrosomonas* bacteria responsible for the conversion of ammonia and ammonium to nitrite and *Nitrobacter* responsible for the conversion of nitrite to nitrate. Essential to this reaction process are aerobic conditions. The process is also depending on DO, pH and flow conditions, which in turn leads to spatially and temporally varying rates of nitrification. To properly account for this complex phenomenon in the modeling framework would be difficult and would require a database that is usually unavailable. The kinetic expression for nitrification contains three terms; a first-order rate constant, a temperature correction term and a low DO correction term, which represents the decline of the nitrification rate as DO levels approach 0.

## Methodology

**Denitrification** refers to the reduction of nitrate or nitrite to nitrogen gas and other gaseous products such as nitrous oxide ( $N_2O$ ) and nitric oxide ( $NO$ ). This process is carried out by a large number of heterotrophic and facultative anaerobes. Under normal aerobic conditions found in the water column, these organisms use oxygen to oxidize organic material. Under the anaerobic conditions found in the sediment bed, in bacteria films on plants, or during extremely low oxygen conditions in the water column, these organisms are able to use nitrate as the electron acceptor. The process of denitrification is considered a sink of nitrate. The kinetic expression for denitrification contains three terms: a first-order rate constant, a temperature correction term and a DO correction term, which represents the decline of the denitrification rate as DO levels rise above 0.

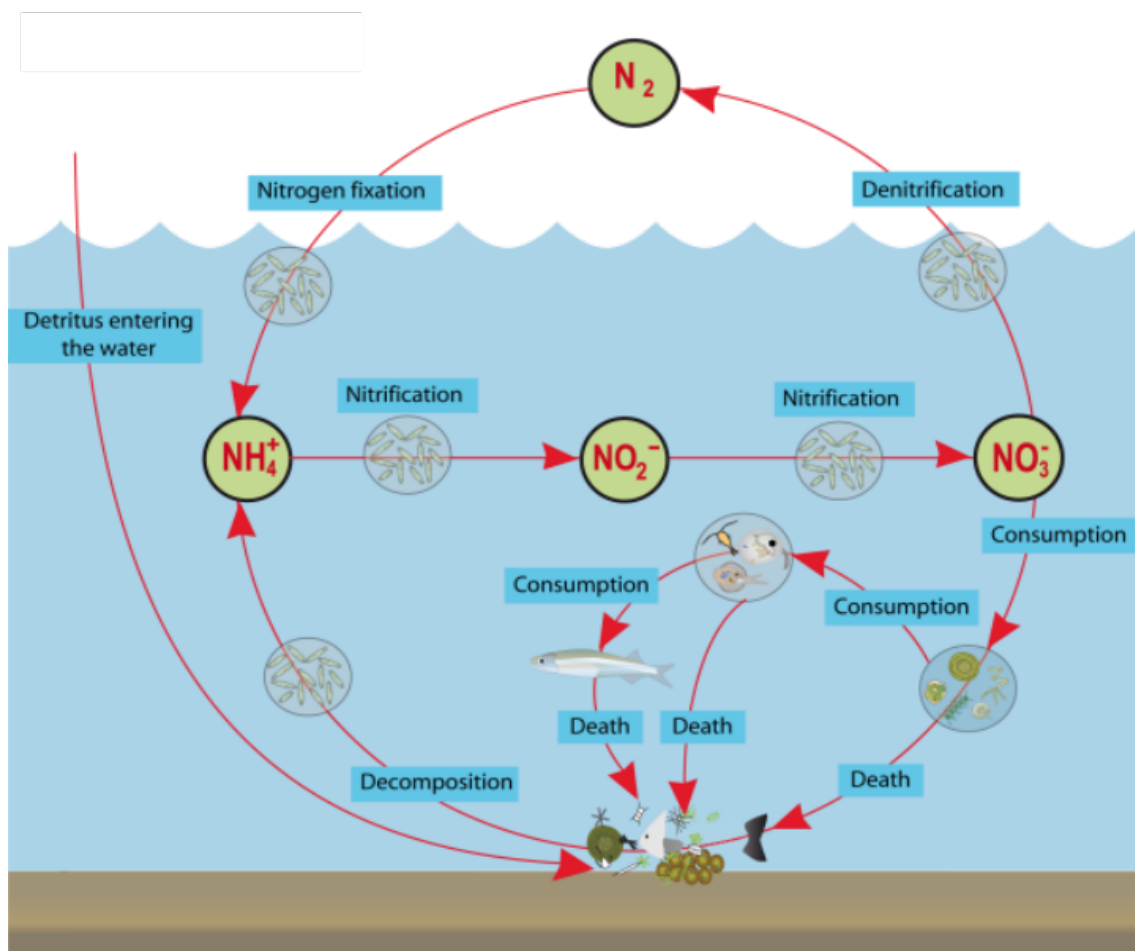


Fig. 3.7 Nitrogen cycle (modified from the Queensland Government)

## Methodology

---

The major processes mentioned above that influence the concentration of nutrients, DO and BOD in the water bodies are integrated into the numerical models through a series of formulae and variables. In the 1-D network model that uses WASP water quality model as a blueprint (Ambrose et al., 1993), four nitrogen variables are modeled: phytoplankton nitrogen, organic nitrogen, ammoniacal nitrogen and nitrate. A summary is illustrated by the equations below:

### Phytoplankton Nitrogen

$$\frac{\partial(PC\alpha_{NC})}{\partial t} = G_{P1}\alpha_{PC}PC - D_{P1}\alpha_{PC}PC - \frac{v_{s4}}{D}\alpha_{PC}PC \quad (3.92)$$

### Organic Nitrogen

$$\frac{\partial ON}{\partial t} = D_{P1}\alpha_{NC}f_{on}PC - k_{71}\Theta_{71}^{T-20} \left( \frac{PC}{k_{mPc} + PC} \right) ON - \frac{v_{s3}(1-f_{D7})}{D} ON \quad (3.93)$$

### Ammoniacal Nitrogen

$$\begin{aligned} \frac{\partial NH_3-N}{\partial t} = & D_{P1}\alpha_{NC}(1-f_{on})PC + k_{71}\Theta_{71}^{T-20} \left( \frac{PC}{k_{mPc} + PC} \right) ON \\ & - G_{P1}\alpha_{NC}P_{NH_3}PC - K_4\Theta_4^{T-20} \left( \frac{DO}{k_{NIT} + DO} \right) NH_3-N \end{aligned} \quad (3.94)$$

### Nitrate Nitrogen

$$\begin{aligned} \frac{\partial NO_3}{\partial t} = & K_4\Theta_4^{T-20} \left( \frac{DO}{k_{NIT} + DO} \right) NH_3-N - G_{P1}\alpha_{NC}(1-P_{NH_3})PC \\ & - K_6\Theta_6^{T-20} \left( \frac{K_{NO_3}}{K_{NO_3} + DO} \right) NO_3 \end{aligned} \quad (3.95)$$

in which:

$$P_{NH_3} = NH_3-N \left( \frac{NO_3}{(K_{mN} + NH_3-N)(K_{mN} + NO_3)} + \frac{K_{mN}}{(NH_3-N + NO_3)(K_{mN} + NO_3)} \right) \quad (3.96)$$

## Methodology

---

The variables are as listed:

$\text{NH}_3\text{-N}$	Ammoniacal nitrogen concentration (mg N/L)
$\text{NO}_3$	Nitrate concentration (mg N/L)
PC	Phytoplankton carbon concentration (mg C/L)
DO	Dissolved oxygen concentration (mg $\text{O}_2$ /L)
ON	Organic nitrogen concentration (mg N/mg L)
$\alpha_{NC}$	Nitrogen to carbon ratio (mg N/mg C)
$G_{P1}$	Phytoplankton growth rate (1/d)
$\alpha_{PC}$	Phosphorus to carbon ratio (mg P/mg C)
$D_{P1}$	Phytoplankton death and respiration rate (1/d)
$v_{s4}$	Net settling velocity of phytoplankton (m/d)
D	Segment depth (m)
$f_{ON}$	Fraction of dead phytoplankton recycled to the organic nitrogen food
$k_{71}, \Theta_{71}$	Organic nitrogen mineralization rate (1/d) and its temperature coefficient
$k_{mPc}$	Half saturation constant for phytoplankton limitation (mg C/L)
$f_{D7}$	Fraction of dissolved organic nitrogen
$K_4, \Theta_4$	Nitrification rate (1/d) and its temperature coefficient
$K_{NIT}$	Half saturation constant for oxygen limitation of nitrification (mg $\text{O}_2$ /L)
$K_6, \Theta_6$	Denitrification rate at 20°C (1/d) and its temperature coefficient
$K_{NO_3}$	Michaelis constant for denitrification (mg $\text{O}_2$ /L)
$P_{\text{NH}_3}$	Preference for ammonia uptake term
$K_{mN}$	Half saturation constant for nitrogen (g N/L)
$v_{s3}$	Organic matter settling velocity (m/d)

## Methodology

---

The 2-D/3-D water quality model integrates the nitrogen cycle with similar formulations and consideration with the ammoniacal nitrogen process, nitrite process and nitrate process (DHI, 2017e). Each components are associated with an individual formula with respective variables involved. The detailed formulations for each process are as below:

### Ammoniacal nitrogen process

$$\begin{aligned}\frac{d\text{NH}_3\text{-N}}{dt} &= \text{BOD decay} - \text{nitrification} - \text{plant uptake} - \text{bacteria uptake} + \text{respiration} \\ &= \left( Y_{BOD} \cdot K_3 \cdot \text{BOD} \cdot \Theta_3^{T-20} \cdot \frac{\text{DO}}{\text{DO} + \text{HS}_{\text{BOD}}} \right) - \left( K_4 \cdot \text{NH}_3\text{-N} \cdot \Theta_4^{T-20} \right) \\ &\quad - UP_p \cdot (P - R_1 \cdot \Theta_1^{T-20}) - \left( UP_b \cdot K_3 \cdot \text{BOD} \cdot \Theta_3^{T-20} \cdot \frac{\text{NH}_3\text{-N}}{\text{NH}_3\text{-N} + \text{HS}_{\text{NH}_3}} \right) \\ &\quad + UP_p \cdot R_2 \cdot \Theta_2^{T-20}\end{aligned}\tag{3.97}$$

### Nitrite process

$$\begin{aligned}\frac{d\text{NO}_2}{dt} &= \text{nitrification of NH}_3 \text{ to NO}_2 - \text{nitrification of NO}_2 \text{ to NO}_3 \\ &= \left( K_4 \cdot \text{NH}_3\text{-N} \cdot \Theta_4^{T-20} \cdot \frac{\text{DO}}{\text{DO} + \text{HS}_{\text{nit}}} \right) - \left( K_5 \cdot \text{NO}_2 \cdot \Theta_5^{T-20} \right)\end{aligned}\tag{3.98}$$

### Nitrate process

$$\begin{aligned}\frac{d\text{NO}_3}{dt} &= \text{nitrification of NO}_2 \text{ to NO}_3 - \text{denitrification} \\ &= \left( K_5 \cdot \text{NO}_2 \cdot \Theta_5^{T-20} \right) - \left( K_6 \cdot \text{NO}_3 \cdot \Theta_6^{T-20} \right)\end{aligned}\tag{3.99}$$

## Methodology

---

The variables are as listed:

$\text{NH}_3\text{-N}$	Ammoniacal nitrogen concentration (mg N/L)
$\text{NO}_2$	Nitrite concentration (mg N/L)
$\text{NO}_3$	Nitrate concentration (mg N/L)
DO	Dissolved oxygen concentration (mg $\text{O}_2$ /L)
$Y_{\text{BOD}}$	Nitrogen content in organic matter (mg $\text{NH}_3\text{-N}$ /mg BOD)
$K_3, \Theta_3$	Degradation constant for biomass (1/d) and its temperature coefficient
$K_4, \Theta_4$	Conversion rate of ammonia to nitrite (1/d) and its temperature coefficient
$K_5, \Theta_5$	Conversion rate of nitrite to nitrate (1/d) and its temperature coefficient
$K_6, \Theta_6$	Denitrification rate (1/d) and its temperature coefficient
$\text{UN}_p$	Ammonia uptake by plants (mg N/mg $\text{O}_2$ )
$\text{UN}_b$	Ammonia uptake by bacteria (mg N/mg BOD)
$\text{HS}_{\text{BOD}}$	Half saturation oxygen concentration for BOD (mg $\text{O}_2$ /L)
$\text{HS}_{\text{NH}_3}$	Half saturation concentration for ammonia uptake by bacteria (mg N/L)
$\text{HS}_{\text{nitri}}$	Half saturation concentration for nitrification (mg N/L)
P	Photosynthesis respiration production (g $\text{O}_2$ /m <sup>2</sup> /d)
$R_1, \Theta_1$	Photosynthetic rate (g $\text{O}_2$ /m <sup>2</sup> /d) and its temperature coefficient
$R_2, \Theta_2$	Respiration rate of bacteria (g $\text{O}_2$ /m <sup>2</sup> /d) and its temperature coefficient

### 3.2.3 Phosphorus Cycle

Phosphorus is a vital nutrient that supports growth in living organisms. Phosphorus is commonly located on land in rock and soil. Its artificial usage as fertilizers and detergents has in turn caused pollution in the water environments when discharged improperly. Excessive phosphate in water bodies can lead to eutrophication and subsequently massive algae blooms in fresh water environment that endanger aquatic species and wildlife. In the phosphorus cycle, inorganic phosphorus enters the water bodies via various natural and human sources such as runoff from land and sewage from industrial plants. The dissolved inorganic phosphorus is then incorporated into biomass to support phytoplankton and plants growth. Some of the phytoplankton and plants are consumed by animals and the phosphorus is either integrated into their tissues or excreted. After death, the living organisms decay and release the organic phosphorus back into the water and soil. Nonliving organic phosphorus must then undergo mineralization or bacterial decomposition into inorganic phosphorus before utilization by biomass again as the cycle resumes. There is also an adsorption-desorption interaction between dissolved inorganic phosphorus and suspended particulate matter in the water column. The subsequent settling of the suspended solids together with the sorbed inorganic phosphorus can act as a significant loss mechanism in the water column and is a source of phosphorus to the sediment.

In the 1-D river model, three phosphorus variables are considered. The variables include phytoplankton phosphorus, organic phosphorus and inorganic orthophosphate phosphorus. Both organic phosphorus and inorganic phosphorus are divided into particulate and dissolved concentrations by spatially variable dissolved fractions. The model herein uses a saturating recycle mechanism, a compromise between conventional first-order kinetics and a second-order recycle mechanism. This mechanism slows the recycle rate if the phytoplankton population is small, but does not permit the rate to increase continuously as phytoplankton increases. The phosphorus equations are summarized below:

### Phytoplankton Phosphorus

$$\frac{\partial(\text{PC} \cdot \alpha_{PC})}{\partial t} = G_{P1}\alpha_{PC}\text{PC} - D_{P1}\alpha_{PC}\text{PC} - \frac{v_{s5}}{D}\alpha_{PC}\text{PC} \quad (3.100)$$

### Organic Phosphorus

$$\frac{\partial \text{OP}}{\partial t} = D_{P1}\alpha_{PC}f_{OP}\text{PC} - k_{83}\Theta_{83}^{T-20} \left( \frac{\text{PC}}{k_{mPc} + \text{PC}} \right) \text{OP} - \frac{v_{s3}(1 - f_{D8})}{D}\text{OP} \quad (3.101)$$

### Orthophosphate Phosphorus

$$\frac{\partial \text{PO}_4\text{-P}}{\partial t} = D_{P1}\alpha_{PC}(1 - f_{op})\text{PC} - k_{83}\Theta_{83}^{T-20} \left( \frac{\text{PC}}{k_{mPc} + \text{PC}} \right) \text{OP} - G_{P1}\alpha_{PC}\text{PC} \quad (3.102)$$

in which:

PC	Phytoplankton carbon concentration (mg P/L)
OP	Organic phosphorus concentration (mg P/L)
PO <sub>4</sub> -P	Orthophosphate phosphorus concentration (mg P/L)
$\alpha_{PC}$	Phosphorus to carbon ratio (mg P/mg C)
$G_{P1}$	Specific phytoplankton growth rate (1/d)
$D_{P1}$	Phytoplankton death and respiration rate (1/d)
$v_{s3}$	Organic matter settling velocity (m/d)
$v_{s5}$	Inorganic sediment settling velocity (m/d)
D	Segment depth (m)
$f_{OP}$	Fraction of dead phytoplankton recycled to organic phosphorus pool
$k_{83}, \Theta_{83}$	Organic phosphorus mineralization (1/d) and its temperature coefficient
$k_{mPc}$	Half saturation constant for phytoplankton (mg C/L)
$f_{D8}$	Fraction dissolved organic phosphorus

## Methodology

---

In 2-D/3-D water quality models, the processes influencing the concentration of dissolved phosphorus are broken down into: (1) the degradation of BOD, in which organic bound phosphorus is released and becomes dissolved phosphate. (2) phosphorus uptake via the photosynthesis and respiration processes by vegetation and phytoplankton. (3) adsorption of dissolved phosphorus to particles that forms particulate phosphorus (PP) and release of dissolved phosphorus from the inorganic PP and (4) resuspension and sedimentation of particulate phosphorus in which a critical flow velocity along with suspension/deposition rate are included to set the threshold for the process. The adsorption, desorption and sedimentation processes are the main factors affecting the concentration of particulate inorganic phosphorus. Particulate organic phosphorus is not described explicitly, but when BOD is degraded phosphorus is released as orthophosphate phosphorus. The phosphorus processes are calculated simultaneously with the BOD-DO and the nitrogen processes. The equations for these processes are:

### Dissolved Phosphorus

$$\begin{aligned} \frac{dDP}{dt} &= \text{BOD decay} - \text{plant uptake} - \text{bacteria uptake} + \text{respiration} \\ &= \left( Y_2 \cdot K_3 \cdot \text{BOD} \cdot \theta_3^{T-20} \cdot \frac{\text{PO}_4\text{-P}}{\text{PO}_4\text{-P} + \text{HS}_{\text{PO}_4}} \right) - UN_p \cdot (P - R_1 \cdot \theta_1^{T-20}) \quad (3.103) \\ &\quad - \left( UN_b \cdot K_3 \cdot \text{BOD} \cdot \theta_3^{T-20} \cdot \frac{\text{PO}_4\text{-P}}{\text{PO}_4\text{-P} + \text{HS}_{\text{PO}_4}} \right) + UN_p \cdot R_2 \cdot \theta_2^{T-20} \end{aligned}$$

### Particulate Orthophosphate Phosphorus

$$\begin{aligned} \frac{d\text{PO}_4\text{-P}}{dt} &= \text{adsorption} - \text{desorption} - \text{suspended BOD} + \text{sedimentation} \\ &= \left( K_8 \cdot DP \cdot \theta_8^{T-20} \right) - \left( K_7 \cdot PP \cdot \theta_7^{T-20} \right) - (S_2/h) + (S_3/h \cdot PP) \quad (3.104) \end{aligned}$$

## Methodology

---

in which:

$PO_4\text{-P}$	Orthophosphate phosphorus concentration (mg P/L)
$PP$	Particulate phosphorus concentration (mg P/L)
$DP$	Dissolved phosphorus concentration (mg P/L)
$Y_2$	Phosphorus content in organic matter (mg P/mg $O_2$ )
$K_3, \Theta_3$	Degradation constant for biomass (1/d) and its temperature coefficient
$K_7, \Theta_7$	Conversion rate of PP to DP (1/d) and its temperature coefficient
$K_8, \Theta_8$	Rate of adsorption of DP (1/d) and its temperature coefficient
$HS_{PO_4}$	Half saturation concentration for P by bacteria (mg P/L)
$UP_p$	Phosphorus uptake by plants (mg P/mg $O_2$ )
$UP_b$	Phosphorus uptake by bacteria (mg P/mg BOD)
$P$	Photosynthesis respiration production (g $O_2/m^2/d$ )
$R_1, \Theta_1$	Photosynthetic rate (g $O_2/m^2/d$ ) and its temperature coefficient
$R_2, \Theta_2$	Respiration rate of bacteria (g $O_2/m^2/d$ ) and its temperature coefficient
$S_2$	Resuspension rate for inorganic particulates (m/d)
$S_3$	Sedimentation rate for inorganic particulates (m/d)
$h$	Water depth (m)

### 3.2.4 Temperature Process

Temperature is a key environmental factor that influences the reaction rate of many of the bio-chemical processes and the growth of microorganisms in water environment. Being able to model temperature change in the models allows more accurate and reliable simulations. The temperature process incorporates an exchange rate to account for the net surface heat transfer at the interface with the air:

$$\frac{dT}{dt} = -\frac{(E - (T - A_T))}{STC \cdot h} \quad (3.105)$$

where  $E$  is the surface heat exchange coefficient (Watts/m<sup>2</sup>K),  $T$  is the water temperature (°C),  $A_T$  is the ambient air temperature (°C),  $STC$  is the specific thermal capacity of sea water (MJ/m<sup>3</sup>K) and  $h$  is the water depth (m). The water depth is input from the Hydrodynamic module and the temperature is specified by the users.

### 3.2.5 Solving Methods

The description of the processes and variables is formulated as a set of ordinary coupled differential equations representing the rate of change for each state variable based on the processes in the system. During simulation the model system integrates one time step by simulating the transport of advective state variables based on hydrodynamics. Initial concentrations, coefficients, constants and forcing functions are loaded into the models and evaluated. The module then integrates one time step and returns updated concentration values to the general flow model system that advances to the next time step. If a process affects more than one state variable, or the state variables affect each other, the differential equations are said to be coupled with each other. The processes contains mathematical expressions (Equation 3.106) using arguments such as

## Methodology

---

numbers, constants, forcings and state variables. Processes always describe the rate at which the subject changes.

$$\frac{dc}{dt} = \sum_{i=1}^n \text{process}_i \quad (3.106)$$

where  $c$  is the concentration of the state variable and  $n$  is the number of processes involved for specific state variable.

There are two main kinds of processes: transformation and settling processes. Transformation is a point description of a process not dependent on neighbouring points. Settling is a process transporting state variables to neighbouring points down the water column. The calculation of a state variable with a settling process is therefore dependent on information from neighbouring points.

The water quality module in 2-D/3-D is coupled to the advection-dispersion (AD) module, which means that the water quality modeling focuses on the transforming processes of compounds in the water bodies while the AD module is used to simulate the simultaneous transport process (DHI, 2017b). The transport equations that describe the dynamics of advective water quality state variables can be written as:

$$\begin{aligned} \frac{\partial}{\partial t}(hc) + \frac{\partial}{\partial x}(uhc) + \frac{\partial}{\partial y}(vhc) + \frac{\partial}{\partial z}(whc) &= \frac{\partial}{\partial x} \left( h \cdot D_x \cdot \frac{\partial c}{\partial x} \right) \\ &+ \frac{\partial}{\partial y} \left( h \cdot D_y \cdot \frac{\partial c}{\partial y} \right) + \frac{\partial}{\partial z} \left( h \cdot D_z \cdot \frac{\partial c}{\partial z} \right) - F \cdot h \cdot c + S_c \end{aligned} \quad (3.107)$$

where  $c$  is the concentration of the state variable,  $(u, v, w)$  are the velocity components in  $x, y, z$ -direction respectively,  $(D_x, D_y, D_z)$  are the dispersion coefficients in respective direction,  $h$  is the water depth,  $F$  is the linear decay coefficient and  $S_c$  is the external source and sink term. The general advection-dispersion equation that handles the transport of scalar quantities, salinity and temperature is presented below:

$$\frac{\partial c}{\partial t} + \frac{\partial u_i c}{\partial x_i} = \frac{\partial}{\partial x_i} \left( D_i \frac{\partial c}{\partial x_i} \right) + S \quad (3.108)$$

where  $c$  is the concentration of the scalar variable,  $D_i$  is the dispersion coefficients and  $S_c$  is the source-sink term. The module utilizes an explicit scheme named QUICKEST for the advection-dispersion modelling. The numerical algorithm and solution technique applied in the model are documented in Vested et al. (1992) and Ekebjerg and Justesen (1991) and will not be discussed in details herein.

### 3.3 Chapter Summary

This chapter demonstrates the theories and principles behind the numerical models used in this study. The computational models are separated into two major sections; the hydrodynamic modeling and the water quality modeling. In the hydrodynamic section, the governing equations on the hydrodynamic and solute transport, as well as their respective numerical methods, are explained. The theories and methods are then expanded from one-dimensional into multi-dimensional scenarios. In the water quality section, fundamental bio-chemical processes are first documented to provide a basic understanding of the water environment. Focus has been given on the dissolved oxygen process, the nitrogen cycle and the phosphorus cycle due to their interlinking characteristics and their influence on key water quality components (i.e. oxygen, BOD and nutrients). The formulation of each process is then illustrated with respect to one-dimensional and multi-dimensional models. The methodology demonstrated in this chapter forms the basis of the numerical models that will be set up and put into practice in the next chapter.

# Chapter 4

## Models Development

Computational simulation of this study is conducted across multi-dimensions. First, an in-house one dimensional (1-D) hydraulic model is used to simulate the hydrodynamic and solute transport behaviour in parts of the Yangtze River reach close to the Poyang Lake region. The five main rivers in the province and their associated river networks and catchments are also included. The open source water quality model WASP is also used to model 1-D water quality in the same domain. Results generated from the 1-D models are fed into the two-dimensional (2-D) simulation. The 2-D hydraulic and water quality simulation focuses on the main Poyang Lake region, using established modeling platform in the MIKE21 and MIKE ECO Lab models. Three-dimensional (3-D) simulation then concludes the computational calculation by using the MIKE21/3 ECO Lab model on 3-D treatment. In this chapter the details of each model and the components involved in setting up the simulations will be discussed. Validation of the models' results with field-measured data will be carried out to ensure the reliability and credibility of the models and subsequent analysis.

# 4.1 1-D Simulation Setup

## 4.1.1 Study Regions and Resources

The study area in 1-D simulation covers the majority of the middle and lower reach of Yangtze River. Two major freshwater lakes, Dongting Lake and Poyang Lake, together with the river branches linking the main river stream and lakes are also integrated in the simulation. The area under consideration is shaded with grey in Figure 4.1. The river networks are simplified into a model domain with 144 sub-channels, 15 main inflow boundaries and all the lateral flow from 336 small branches and local sub-regions around the sub-channels. The total length of the channels sums up to 4,772.8 km. The major inflow boundaries are marked in the figure as red circles for reference.

Topographic data in the form of digital elevation map (DEM) and measured terrain data of the main stream, tributaries and freshwater lakes were used in this study. The large geographical area covered in this simulation and the sheer difficulties and costs in obtaining topographic data in natural environments mean that the data is often incomplete and fragmented. A linear interpolation method based on the Delaunay triangulation irregular networks (Peucker et al., 1978) was used in regions with available measured bed data. These regions include Dongting Lake, Poyang Lake and their associated river networks. In some branched river channels where measured data were only available at some cross-sections, a curvilinear grid-based method was used to improve the interpolation accuracy (Huang et al., 2011). Hydrology data including flow and discharge measured at 128 control stations from 1991 to 2011 was used to validate the model. The data was provided by Changjiang Water Resource Commission, respective hydrological bureaus in Hubei, Hunan, Jiangxi and Anhui Provinces and the National Administration of Surveying and Mapping and Geoinformation of China.

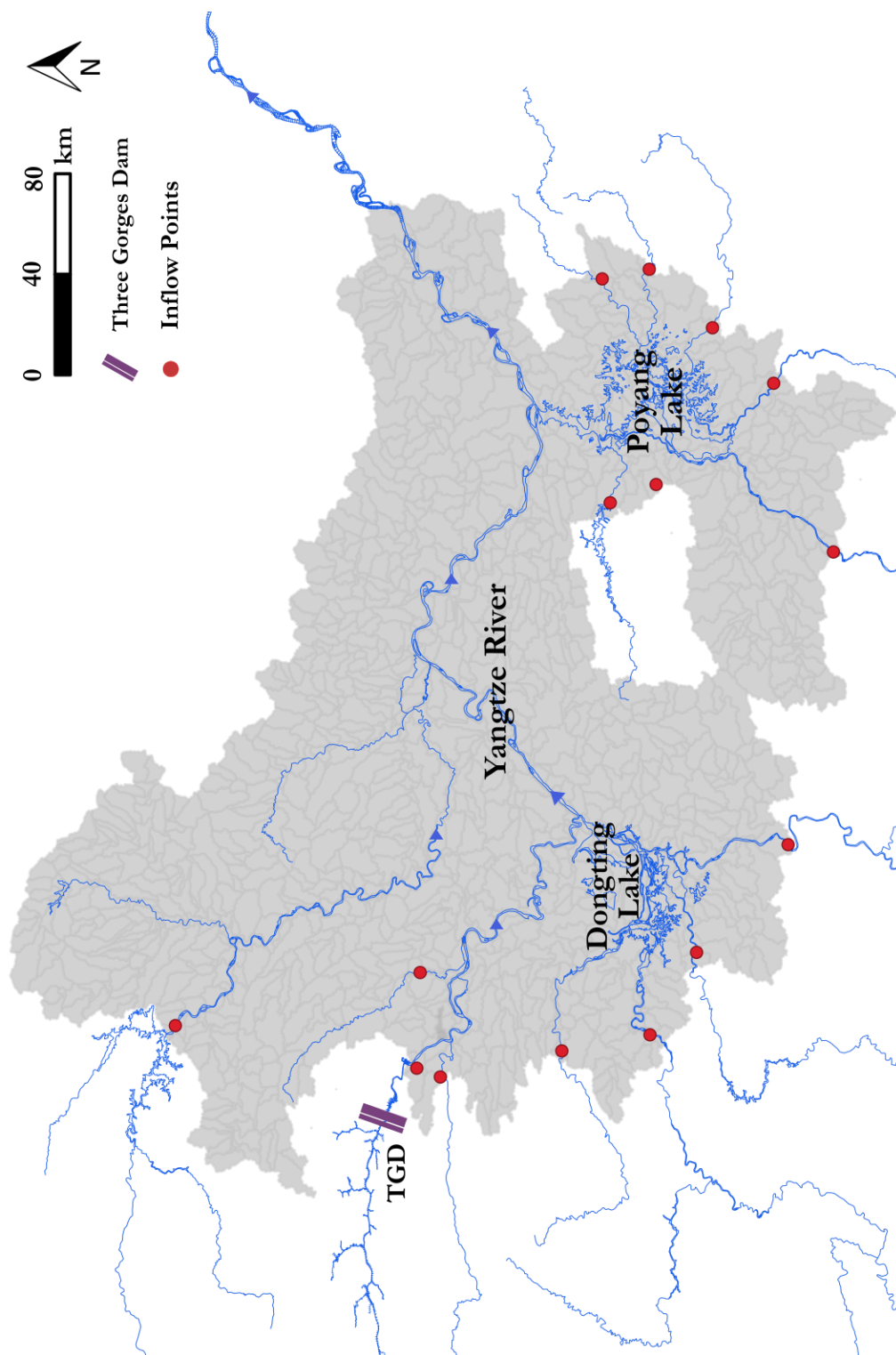


Fig. 4.1 1-D simulation area of the middle and lower reach of Yangtze River

## Models Development

---

Special attention is given to the representation of cross-sections for the lake regions due to the large variations in lake boundaries between dry and wet seasons. Poyang Lake alone has 480 cross-sections in the current model. Figure 4.2 is generated directly from GIS data of the region showing the cross sections of the lake and its associated river network in the model. The average distance between two adjacent cross-sections is 1,324 m. The sampling spacing in between the cross-sections is set at 10-20 m intervals for thalweg and 30-50 m for other areas. The density of the cross-sections has to be relatively high to allow sufficient sampling points across different bathymetric areas, ranging from narrow trenches to open waters in large lake areas, and to maintain calculation accuracy during dry seasons with low water levels.

### 4.1.2 Models Parameters

Model hydrodynamic simulation is performed for the period from 2000 to 2009 with major water-quality analysis between 2004 and 2013. Computational time step is set at 300 seconds. A roughness coefficient is assigned to every grid cell based on the water level and flow rate within the cell, ranging from 0.02 to 0.04 s/m<sup>1/3</sup>. The 1-D water quality simulation is performed using the WASP model. The model solves equations based on the key principle of mass conservation. The model is integrated under the hydrodynamic model and reacts accordingly to the hydrodynamic simulation and behaviours. Main considerations in the water quality model include the nitrogen cycle, the phosphorus cycle and the associated reaction variables for DO and BOD. These factors are represented in the model through a series of key parameters (Table 4.1). Their values are based on the WASP model (Ambrose et al., 1993) and are further modified using past experience and knowledge of the local lake environment (Huang et al., 2011). Temperature coefficients for the rate constants are within the range of 1.05-1.08 and are therefore not listed individually. The Di Toro method is used to model light formation (Di Toro et al., 1971).

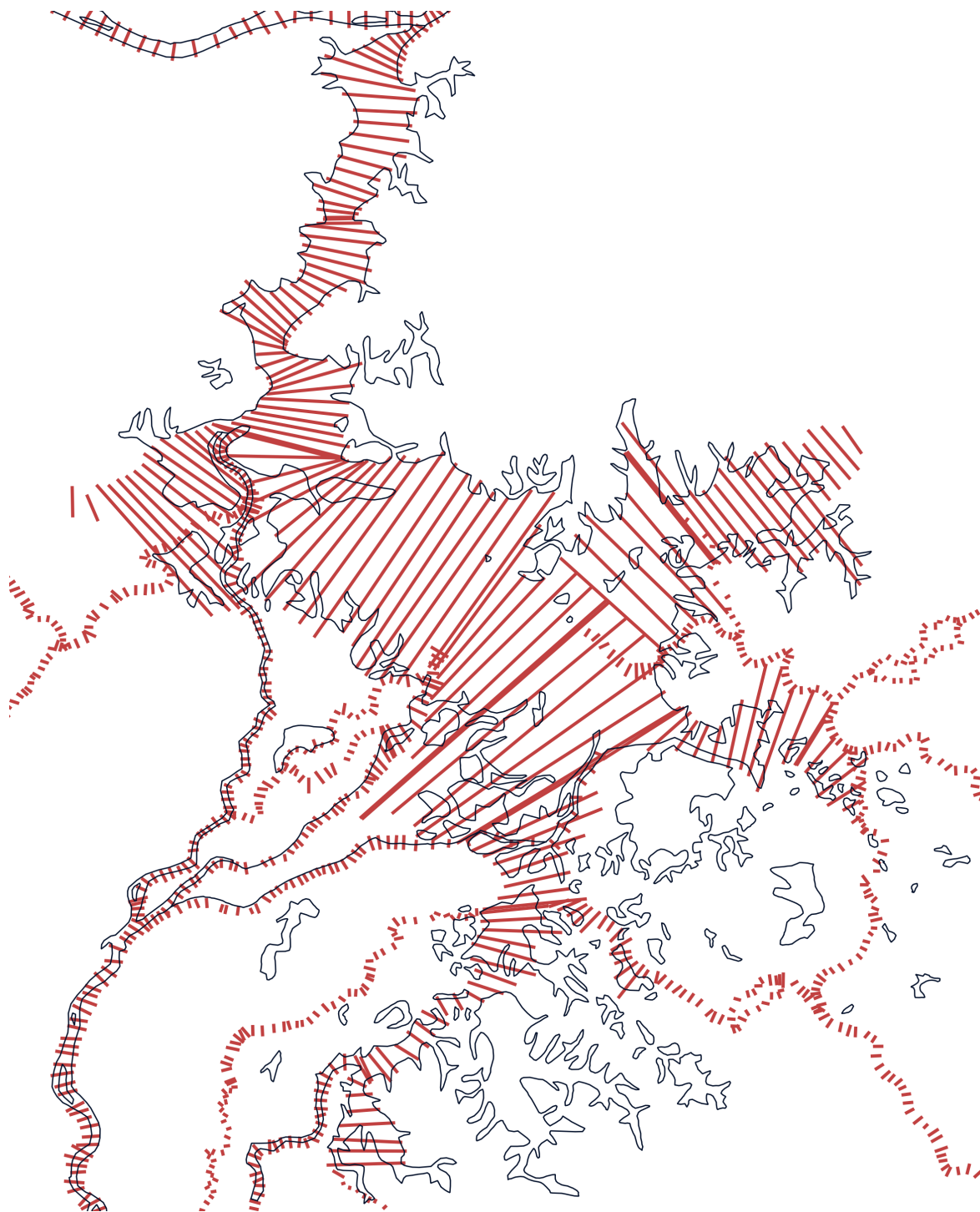


Fig. 4.2 1-D simulation area and cross-sections of Poyang Lake basins

## Models Development

---

Table 4.1 List of model parameters for 1-D water quality simulation

Parameter	Symbol	Value	Unit
Half saturation constant of N for O <sub>2</sub> limitation	$k_{NIT}$	2.0	mgN/L
Nitrification rate at 20°C	$K_4$	0.20	d <sup>-1</sup>
Phytoplankton growth rate constant	$k_{1C}$	2.0	d <sup>-1</sup>
Half-saturation constant of N for phyt. growth	$k_{MNG}$	0.025	mgN/L
Half-saturation constant of P for phyt. growth	$k_{MPG}$	0.001	mgPO <sub>4</sub> -P/L
Carbon-to-chlorophyll ratio	$\alpha_{CCHL}$	80.0	mgC/mgChl
Nitrogen-to-carbon ratio in phytoplankton	$\alpha_{NC}$	0.15	mgN/mgC
Phosphorus to carbon ratio in phytoplankton	$\alpha_{PC}$	0.042	mgP/mgC
Oxygen to carbon ratio	$\alpha_{OC}$	2.67	mgO <sub>2</sub> /mgC
Phytoplankton respiration rate	$k_{1R}$	0.10	d <sup>-1</sup>
Non-predatory phytoplankton death rate	$k_{1D}$	0.02	d <sup>-1</sup>
Decomposition rate constant for phyt. in sediment	$k_{PZD}$	0.02	d <sup>-1</sup>
Decomposition rate of CBOD in sediment at 20°C	$k_{DS}$	4.23	d <sup>-1</sup>
Half saturation constant of BOD for O <sub>2</sub> limitation	$k_{BOD}$	0.4	mgO <sub>2</sub> /L
Half saturation constant for phyt. limitation	$k_{mPc}$	0.0	mgC/L
CBOD Deoxygenation rate at 20°C	$k_d$	0.10	d <sup>-1</sup>
Grazing rate on phyt. per unit zooplankton population	$k_{1G}$	0.25	L/mgC·d
Organic nitrogen mineralization rate constant	$k_{71}$	0.22	d <sup>-1</sup>
Decomposition rate of organic N in sediment at 20°C	$k_{OND}$	0.0004	d <sup>-1</sup>
Mineralization rate of dissolved organic P	$k_{83}$	0.22	d <sup>-1</sup>
Decomposition rate of organic P in sediment at 20°C	$k_{OPD}$	0.0004	d <sup>-1</sup>
Denitrification rate at at 20°C	$k_{2D}$	0.02	d <sup>-1</sup>
Reaeration rate at at 20°C	$K_2$	1.0	d <sup>-1</sup>
Fraction of dead phyt. recycled to organic P pool	$f_{op}$	1.0	-
Saturation light intensity for phytoplankton	$I_s$	175.0	Ly/d

## 4.2 1-D Model Validation

### 4.2.1 1-D Hydrodynamic Validation

The 1-D hydrodynamic model is validated using the field-measured data in Poyang Lake over the period from 2000 to 2009. Discharge data measured during the same period at 16 input hydrological stations and water level data measured at Datong hydrological stations are used as the upper and lower boundaries respectively. The initial values of the water level and discharge are obtained automatically by iteration under the control of boundary values. Comparisons between the model results and measured field data are made and the model performance is evaluated.

The simulated water surface elevation from the 1-D river model is compared with the field-measured data at locations across Poyang Lake. These locations are distributed along the main channels of Poyang Lake (Figure 4.3) and are capable in representing the hydrodynamics of the lake throughout a yearly cycle. The presence of hydrological stations at these easily accessible locations also allow the collection of a more comprehensive set of field-measured data.

The model performance is assessed using the root mean square error (RMSE) and the Nash–Sutcliffe coefficient of efficiency (NSE) (Nash and Sutcliffe, 1970). RMSE is selected for quantifying the prediction error in terms of the units of the variable calculated by the model, whereas NSE is chosen as a dimensionless goodness-of-fit indicator to represent the degree to which the model simulations match the data from observations. These quantitative assessments given by the formula below provide an evaluation of the model’s predictive abilities (Legates and McCabe, 1999).

$$\text{RMSE} = \sqrt{\frac{1}{N} \sum_{i=1}^N (T_i - \hat{T}_i)^2} \quad (4.1)$$

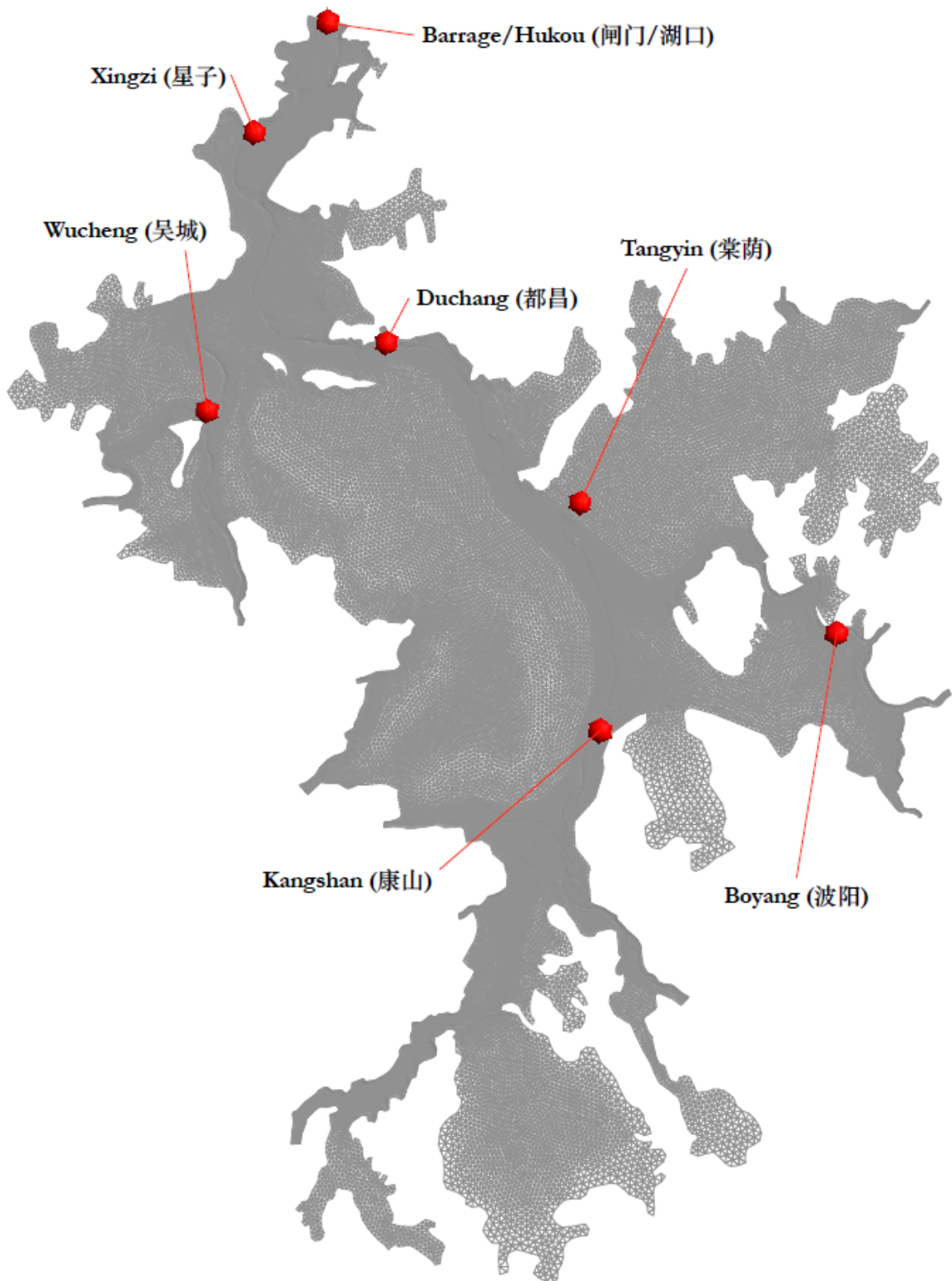


Fig. 4.3 1-D hydrodynamic model validation locations

$$\text{NSE} = 1 - \frac{\sum_{i=1}^N (T_i - \hat{T}_i)^2}{\sum_{i=1}^N (T_i - \bar{T}_i)^2} \quad (4.2)$$

in which  $N$  is the number of observations,  $\hat{T}_i$  is the model-predicted value,  $T_i$  is the observed value and  $\bar{T}_i$  is the mean value. A zero RMSE value indicates a perfect fit and the smaller the RMSE value the closer the correlation is between the simulated value and measured data. NSE represents the complement to unity of the ratio between the mean square error of observations against the predicted values and the variance of the observations. The coefficient of efficiency takes values  $-\infty < \text{NSE} < 1$  (Ritter and Muñoz-Carpena, 2013). NSE of value 1.0 represents a perfect fit. In general, a NSE value of 0.40 or above as satisfactory for daily time-steps. NSE values higher than 0.60 and 0.75 are considered good fit and very good fit respectively (Moriassi et al., 2007).

In Figures 4.4 and 4.5 are 6 subplots comparing the surface elevations of the simulated results against field-measured data. On the  $x$ -axis is the time in years from 2000 to 2009 and on the  $y$ -axis is the surface elevation in meters. The black line represents the simulated results from the 1-D river model and the red circles mark the measured elevations at that location. The RMSE and NSE of each subplot are calculated and labeled in the figure respectively.

Based on the resulting figures and the statistical indicators, the figures illustrate excellent matches between the simulated results and measured data. The resulting RMSEs are within the range of 0.330-0.631 m and NSEs are in the range of 0.926-0.977. The model-generated hydrodynamic behaviour fits exceptionally well with the measured data. Although there are occasionally slight differences at the lower surface elevations over the winter period, for example those in 2001 and 2002 at Duchang and in 2004 and 2008 at Tangyin, these discrepancies are insignificant to the overall agreement between the data. In general, the 1-D river model is able to consistently produce correct trends and accurate magnitude of the water level fluctuation for a substantial period of time across the validation locations in the Poyang Lake.

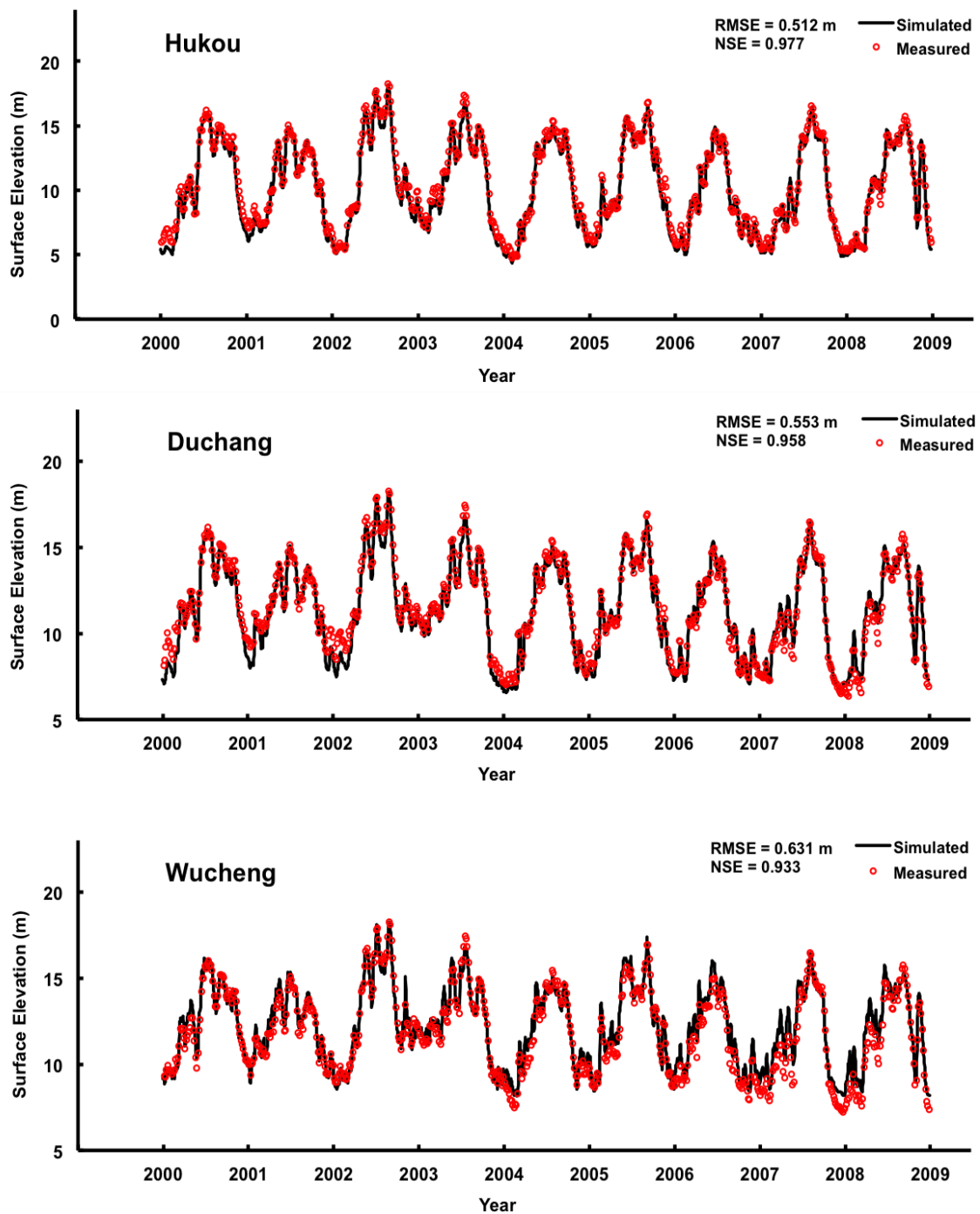


Fig. 4.4 Measured water surface elevations compared with 1-D river model predictions at Hukou, Duchang and Wucheng

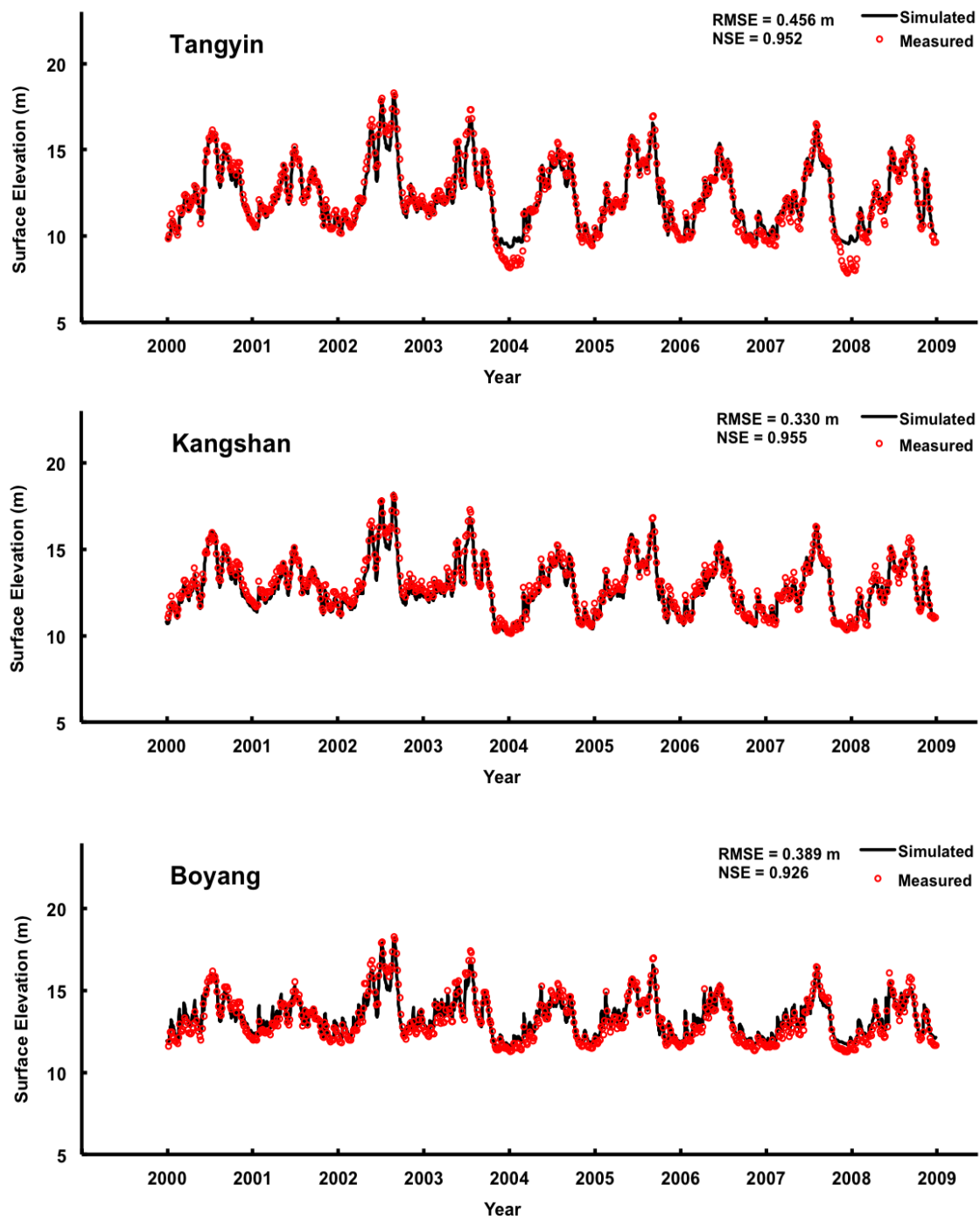


Fig. 4.5 Measured water surface elevations compared with 1-D river model predictions at Tangyin, Kangshan and Boyang

### 4.2.2 1-D Water Quality Validation

The WASP model that is responsible for the water quality simulation calculates the concentration of major water quality variables based on a series of parameters and formulas. The resulting concentrations are compared to the field-measured data to validate the water quality model.

The 1-D simulation area, as mentioned in the beginning of this chapter, covers the majority of Yangtze River regions including both the Dongting Lake and the Poyang Lake. However, because Poyang Lake is the main subject of this study and the simulated results from the 1-D model will act as the boundary conditions of the multi-dimensional model, the validation herein will target the Poyang Lake regions only, to ensure that the results at the river-lake intersections and near the boundary locations are as accurate as possible. Stations that are close to the location of the boundary conditions or influenced by nearby inflow entries into the Poyang Lake are prioritized for validation. Nonetheless, further selection of validation points is required as some stations are limited by the lack of field-measured water quality data. Difficult climate and geographical conditions as well as the high costs in time and labour in field measurements all contribute to the lack of frequent data sampling in the Poyang Lake regions, resulting in a relatively limited set of field data at many of the stations. Based on the existing set of field water quality data, 7 stations are selected for comparison with the simulated results from 1-D model, as shown in Figure 4.6.

Although the 1-D water quality model takes into consideration a number of state variables and their respective processes in the water environment, only several of the key state variables are suitable for validation due to the absence of field measurements. For example, the validations on BOD,  $\text{NO}_3$  and ON are difficult to carry out due to close to nonexistence of field-measured readings. Working with existing data at hand, the validation for 1-D water quality model will focus on the state variable;  $\text{NH}_3\text{-N}$ , TP, DO and TEMP. The results are shown from Figures 4.7 to 4.10. Each figure consists of



Fig. 4.6 1-D water quality model validation locations

## Models Development

---

subplots that compare the simulated result with the field-measured data of the same state variable at 4 different stations. On the  $x$ -axis is the time in years from 2004 to 2014 and on the  $y$ -axis is the concentration of the state variable in mg/l or temperature in degree Celsius. The black line illustrates the simulated results from the 1-D water quality model and the red circles present the field-measured readings at the certain location.

The measured ammoniacal nitrogen ( $\text{NH}_3\text{-N}$ ) concentrations in XinjiangEast, FuheMouth, XiuheMouth and ChangjiangMouth are compared against the 1-D model predictions in Figure 4.7. Although the simulated  $\text{NH}_3\text{-N}$  concentrations are in the same order with the field measured data, they fail to match the fluctuating trends in all of the locations. Peaks and troughs in the simulated predictions often miss the field measurements, which are particularly obvious in the plots of XinjiangEast and XiuheMouth. The resulting RMSEs and NSEs are in the range of 0.184-0.372 mg/l and -0.569-0.151 respectively. These represent a great discrepancy with the field measurements and an unsatisfactory prediction performance.

The measured TP concentrations in Xingzi, XiuheMouth, XinjiangWest and GangjiangSouth are compared against the 1-D model predictions (Figure 4.8). In all of the four plots, the simulated results follow the field measurements under the same order and occasionally matching at close proximity. However, it is difficult to conclude that any one of the black lines to match the field measurements in great accuracy. The effects of scattered field measurements are more prominent in these figures. The field-measured data fluctuate in high degrees and do not seem to follow any distinct trend. As a result, the model performance records RMSEs in the range of 0.028-0.129 mg/l and NSEs from -1.267 to -0.253. Additional runs with adjustment on the model parameters are carried out. Parameters such as half-saturation constant of phosphorus for phytoplankton growth and nitrification rate are modified but these adjustments are relatively small given the conventional range of the constants. Improvement in

the simulated concentrations could not been seen. Sensitivity of the model lies with elements such as the bathymetry and the inflow data from the boundary conditions.

The comparisons between simulated predictions and field-measured data are certainly more pronounced with DO and TEMP. In Figure 4.9, the measured DO concentrations in Xingzi, GanjiangSouth, XinjiangWest and ChangjiangMouth are compared against the 1-D model predictions. Similarly in Figure 4.10, the measured temperature in Xingzi, GanjiangSouth, XinjiangEast and ChangjiangMouth are compared with the 1-D model results. In both figures, the simulated results show satisfactory likelihood with the field measurements. The DO validation records RMSEs of 1.253-1.862 mg/l and NSEs of -0.706-0.499 while the TEMP validation results in RMSEs of 2.115-3.238 °C and NSEs of 0.851-0.932. Both validations on DO and TEMP are conclusively more satisfactory and indisputable than the other two state variables.

In general, the model predictions of DO and temperature agree satisfactorily with the field-measured data but not so for the predictions of NH<sub>3</sub>-N and TP. Major discrepancies are mainly caused by the insufficient and inaccurate field measurements and the change in climate and bathymetry. Issues regarding the field-measured data and potential improvement will be discussed in subsequent chapters in more details.

### 4.3 Multi-Dimensional Simulation Setup

#### 4.3.1 Study Regions and Resources

2-D and 3-D model computation is defined by the boundary incorporating the main Poyang Lake district from Junshan Lake in the south to the potential barrage location in the north; and the east covering the entries of Changjiang, Leanhe and Xinjiang rivers to the west connecting to Xiushui and Ganjiang rivers (Figure 4.11). Given the nature of high water surface area fluctuation (from 5,000 km<sup>2</sup> in wet seasons to 50 km<sup>2</sup> in dry seasons) of the Poyang Lake region, high grid resolution is required to

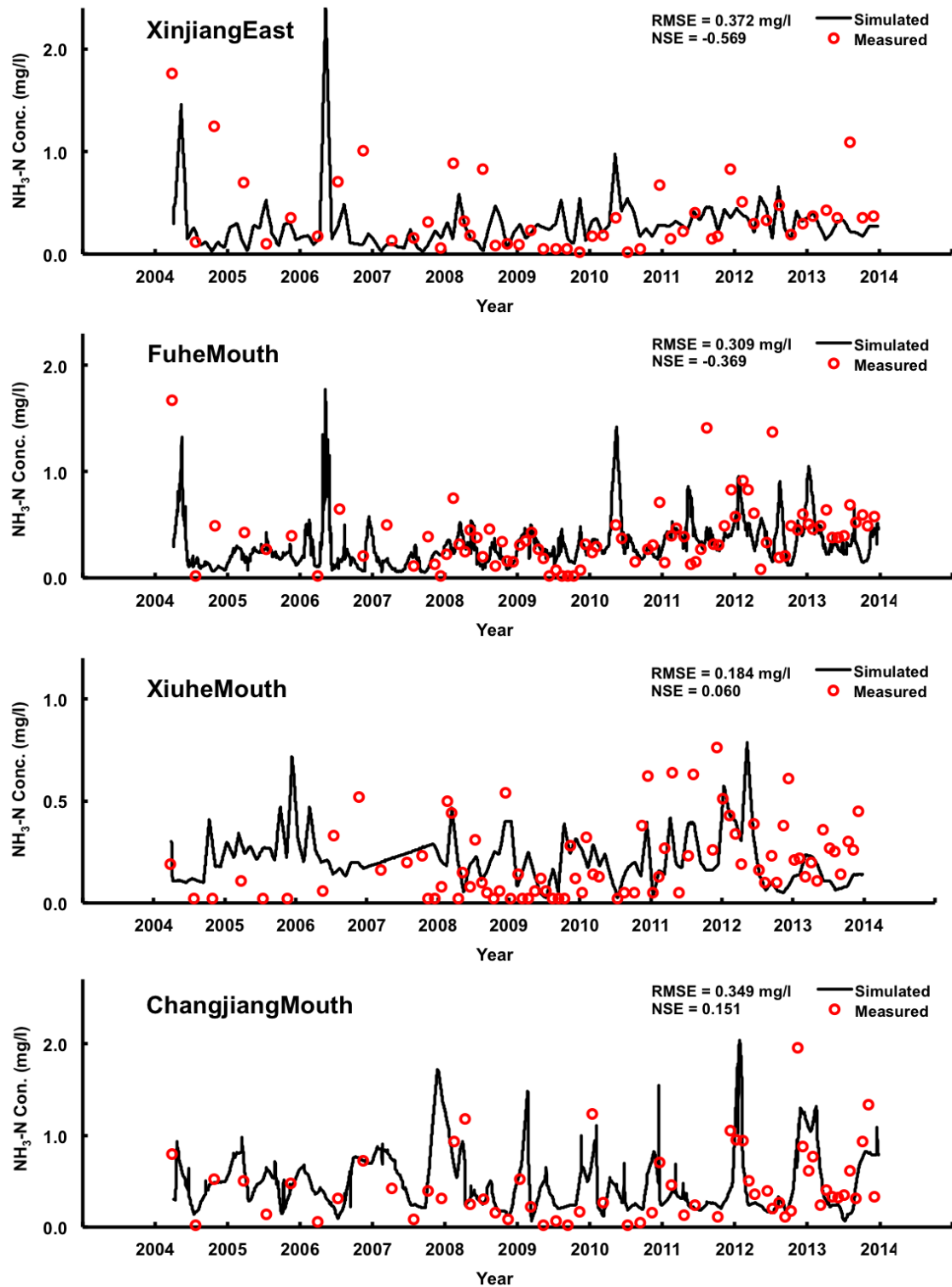


Fig. 4.7 Measured NH<sub>3</sub>-N compared with 1-D model predictions at stations across Poyang Lake

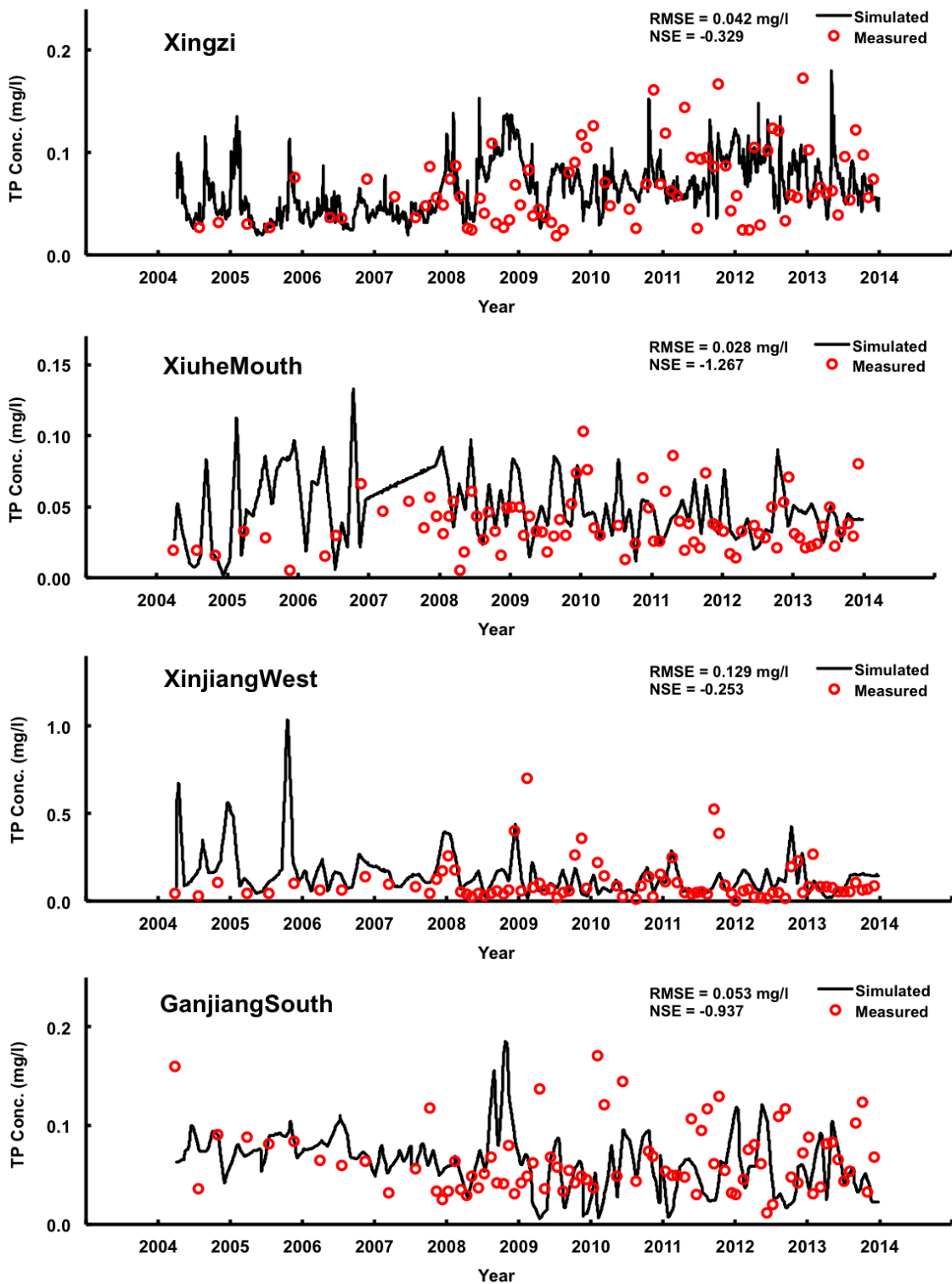


Fig. 4.8 Measured TP compared with 1-D model predictions at stations across Poyang Lake

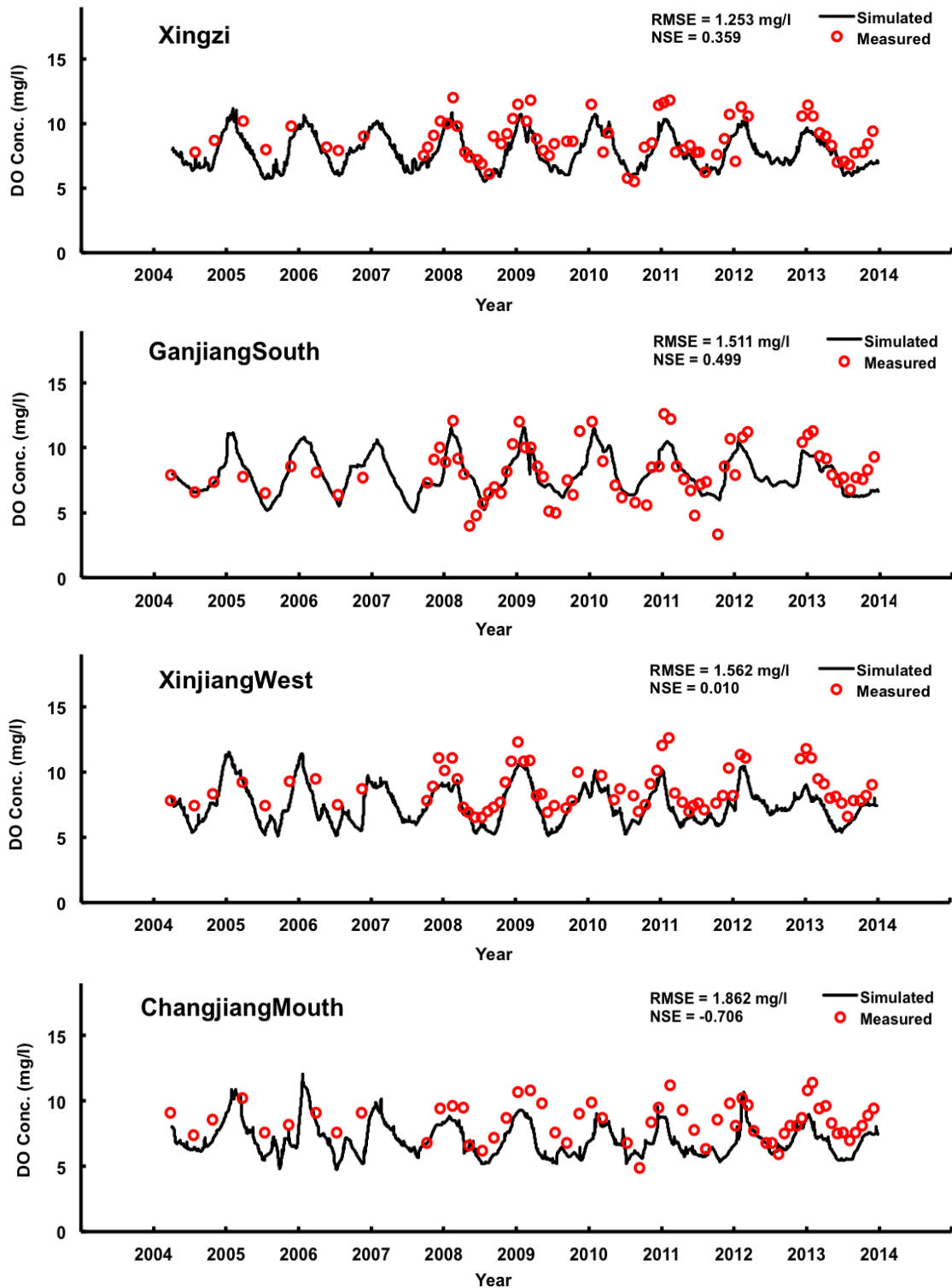


Fig. 4.9 Measured DO compared with 1-D model predictions at stations across Poyang Lake

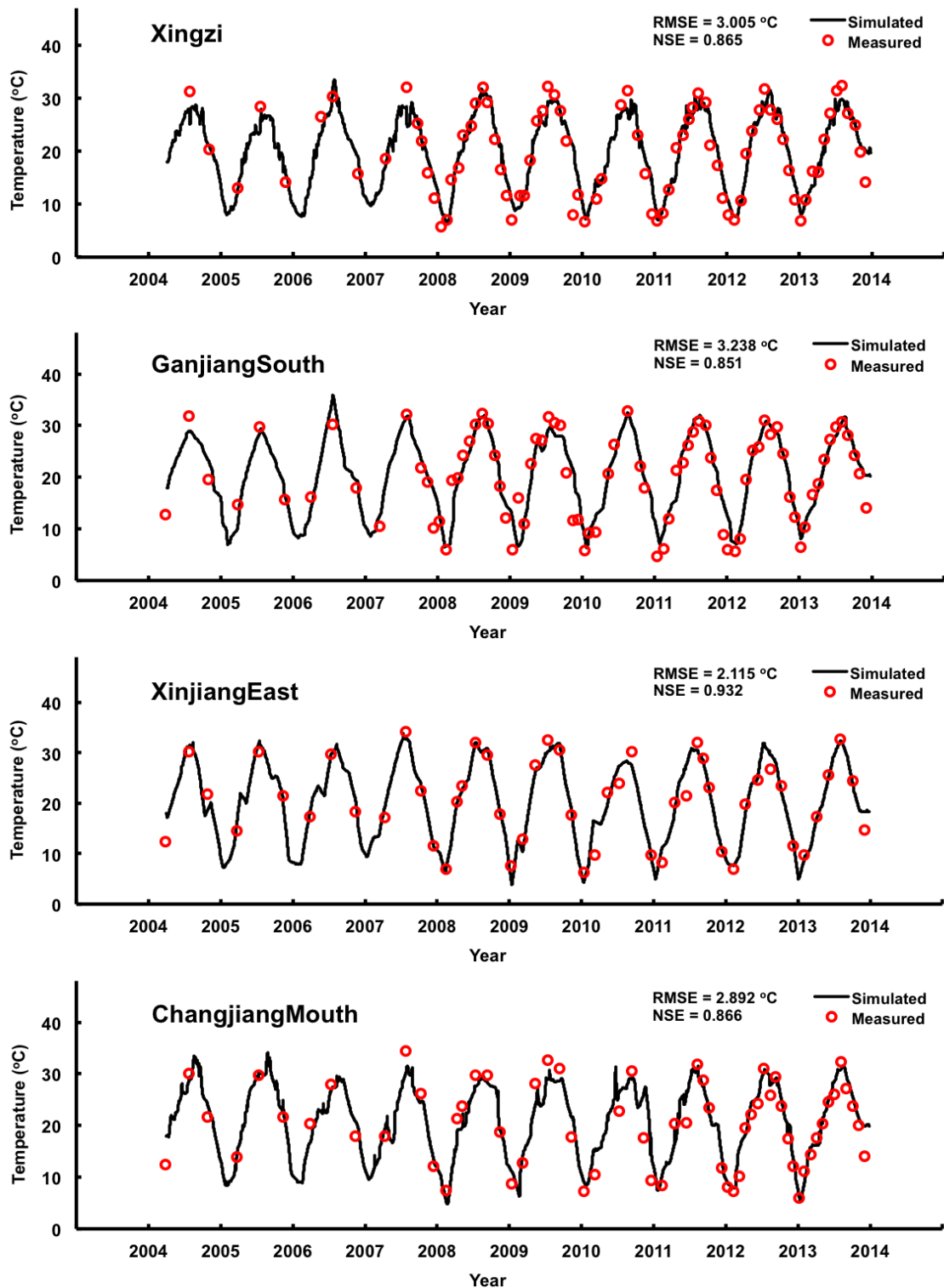


Fig. 4.10 Measured TEMP concentration compared with 1-D model predictions at stations across Poyang Lake

## Models Development

---

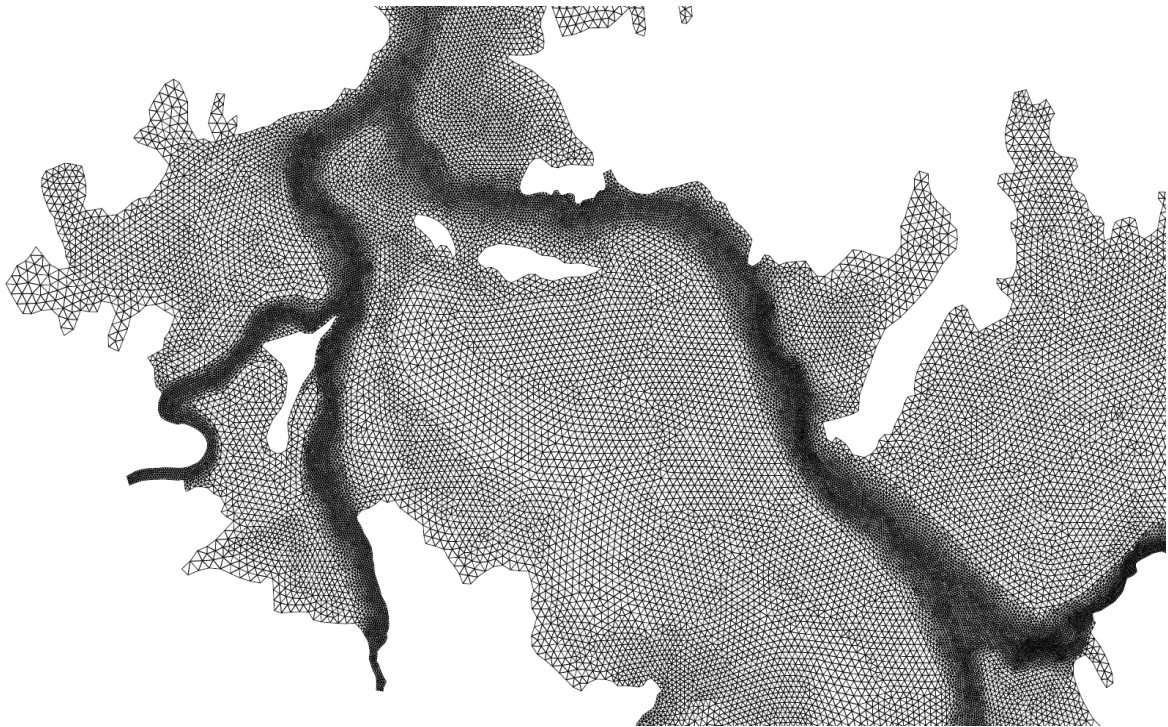
capture and respond to the changes in such complicated water environments. In general, 50–60 m grid size is needed for main flow channels. However, a grid of this size will increase computation expenses and reduce efficiency. An unstructured triangular grid system is used to reduce unnecessary calculations whilst providing accurate modeling in the boundary areas. Irregular inner and outer boundaries of the lake environment can be filled using variable grid size at different areas. Grid sizes vary from 60–150 m for main channels, 150–300 m for river channels, 300–400 m for high activity lakes, 400–500 m for medium activity lakes, 500–600 m for semi-closed dish-shape depressions and 600–800 m for closed lakes by reclamation. Variations of the element size and mesh density at different region of the lake are illustrated in Figure 4.12.

A final mesh of 56,658 points is produced with 109,494 individual units and 15,556 sides. The 2-D mesh layers are positioned at three depth levels of Poyang Lake to give a 3-D representation of the simulation. In total, the simulation consists of  $56,658 \times 3$  nodes in the setup of a vertical sigma mesh. This grid system ensures an accurate representation of the bathymetry distribution, flow field solution and mass transport balance between sub-regions of Poyang Lake. The low requirement for computation capability of this meshing method also facilitates the modeling of high water level fluctuation and solute transport conditions in Poyang Lake.

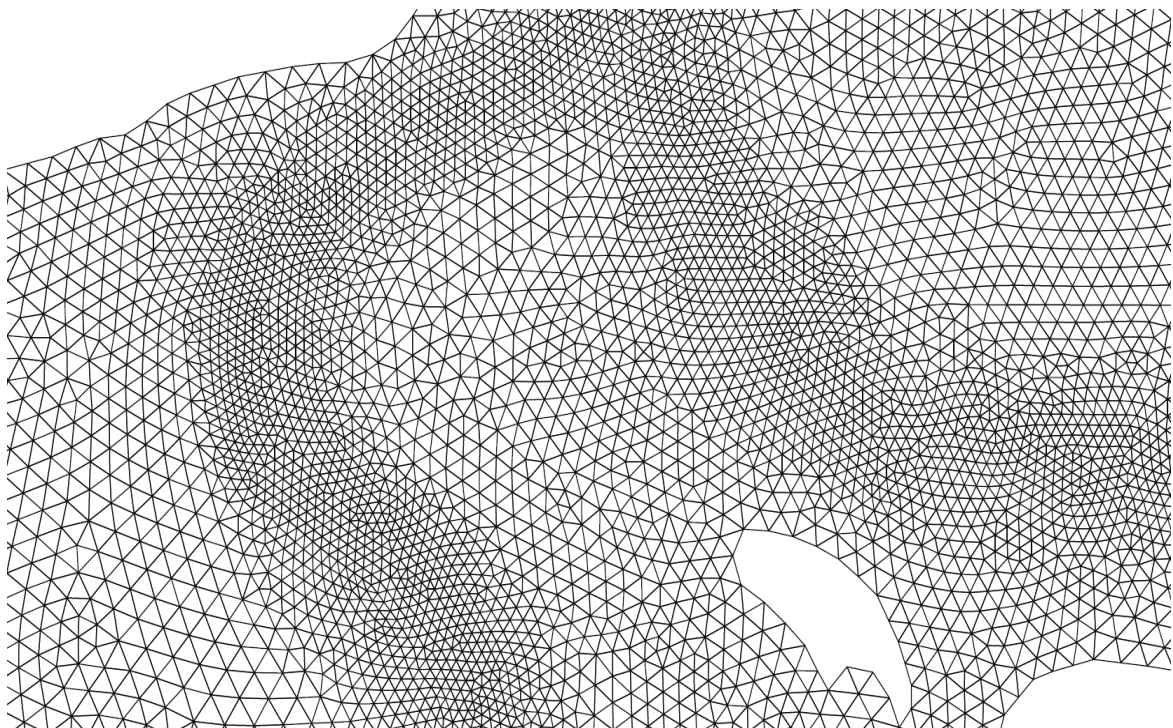
A global topographical data set for Poyang Lake is difficult to obtain given its extensive water coverage of nearly 5,000 km<sup>2</sup>. This study uses the DEM provided by Jiangxi Institute of Water Science in conjunction with 90m image resolution data to generate the basic bathymetry of the lake region. Triangular mesh is formed using discrete point data and linear interpolation is used to generate the appropriate elevations at those points. Deviation of the resulting bathymetry is possible due to continuous sand dredging and water transportation within the region in recent years, causing further decrease in bed elevation which is estimated at about 3–5 m. This would trigger diversion of water flow from the main channels to small streams and reduce the degree of wetting and drying processes in floodplain. Issues regarding the



Fig. 4.11 Poyang Lake 2-D unstructured mesh



(a) Dense element density at main channel as compared to other regions



(b) Details of variation in triangular element size

Fig. 4.12 Sections of 2-D unstructured mesh

effect of landscape changes of Poyang Lake on numerical modeling will be further discussed in later chapter.

### 4.3.2 Boundary Conditions

Poyang Lake is a large scale water environment that comprises of complex river network as inflows. In order to accurately simulate the lake's hydro-environment, the incoming rivers connecting to the lake and their characteristics need to be accounted for as boundary conditions in the model. In this study, 16 boundary conditions are set up around Poyang Lake. These boundaries are open boundaries that provide hydraulic information in the form of discharge ( $Q$ ) or water level ( $Z$ ) and water quality data (WQ) that includes DO, BOD,  $\text{NO}_3$ ,  $\text{NH}_3\text{-N}$ , ON and OP concentrations, together with temperature and salinity. The input files are based on results generated from the 1-D river network simulation, combining with field-measured data provided by the local water authorities.

The boundary data cover the period from 2004 to 2013, in which 1-D simulation provides from 2004 to 2013 and field-measured data of the same period compliment and fine-tune abnormality in the inputs. Linear interpolation by Akima method is used to segregate the data set into consistent time intervals (Akima, 1970). Some of the missing water quality data are derived from existing literature. For example, the values of  $\text{PO}_4\text{-P}$  for the input of 2-D simulation are calculated from the resulting OP values from 1-D simulation or field measured TP values based on a ratio of 15%  $\text{PO}_4\text{-P}$  to 85% OP documented in the literature (Wang et al., 2008a; Wu, 2014; Xiang and Zhou, 2011). Meanwhile some missing gaps, such as the phytoplankton and organic nitrogen concentrations are assigned with reference drawn from precedent studies of similar lake environments. The locations of the 16 boundaries within the Poyang Lake simulation mesh are illustrated in Figure 4.13. The names and input file types of the boundaries are summarized in Table 4.2.

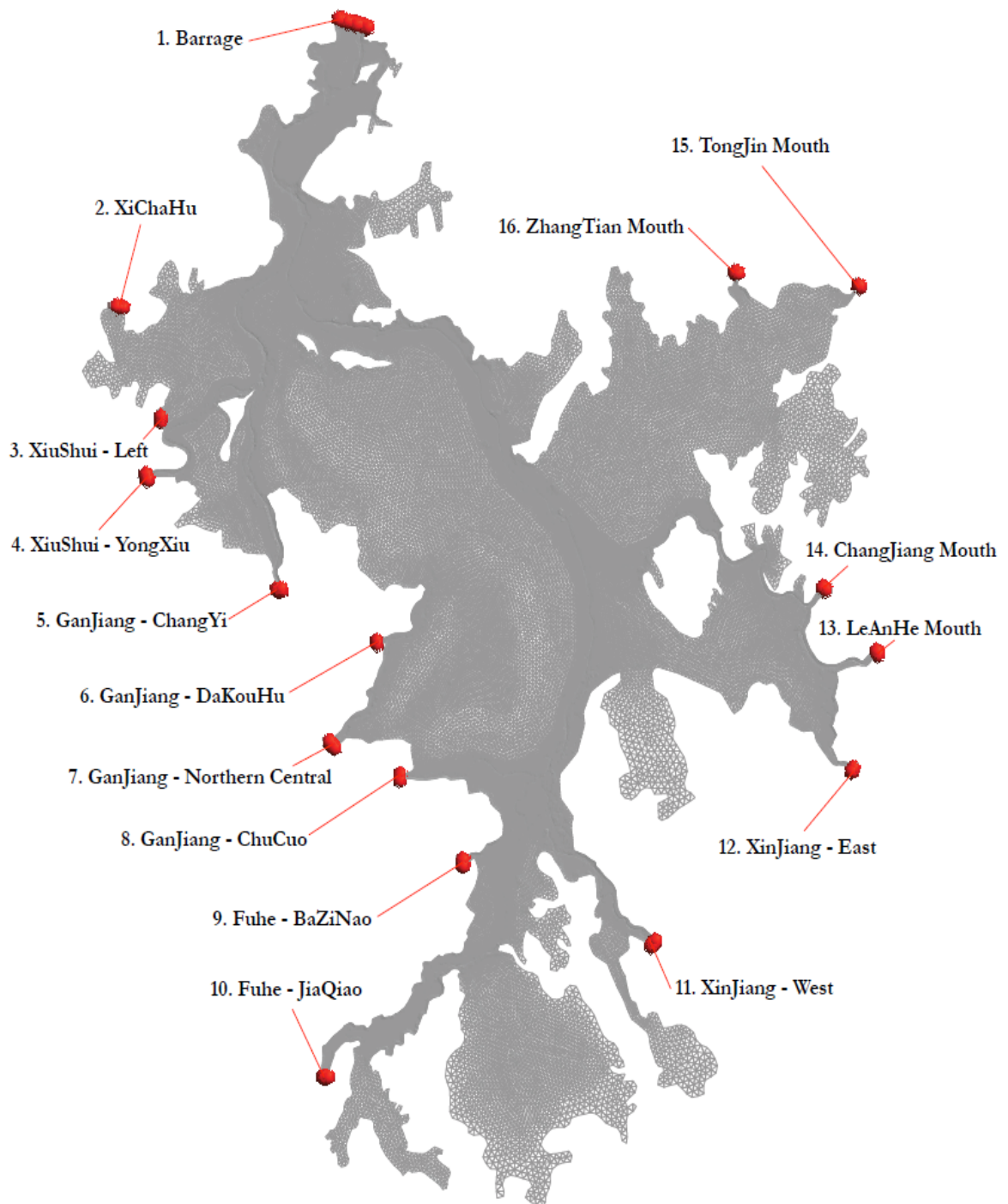


Fig. 4.13 Locations of the 16 boundary conditions in Poyang Lake

## Models Development

Table 4.2 Locations of boundary condition and their input types

ID	Locations	Chinese Name	Input Type	
			Hydrodynamic	Water Quality
1	Barrage	闸门	Z	WQ
2	XiChaHu	西汉湖	Q	WQ
3	XiuShui - Left	修水左小支	Q	WQ
4	XiuShui - YongXiu	修水永修	Q	WQ
5	GanJiang - ChangYi	赣江昌邑	Q	WQ
6	GanJiang - DaKouHu	赣江北中支	Q	WQ
7	GanJiang - Northern Central	赣江北中支	Q	WQ
8	GanJiang - ChuCuo	赣江南支滁槎	Q	WQ
9	Fuhe - BaZiNao	抚河小支八字脑	Q	WQ
10	Fuhe - JiaQiao	抚河架桥	Q	WQ
11	XinJiang - West	信江西支	Q	WQ
12	XinJiang - East	信江东支	Q	WQ
13	LeAnHe Mouth	乐安河口	Q	WQ
14	ChangJiang Mouth	昌江河口	Q	WQ
15	TongJin Mouth	童津河口	Q	WQ
16	ZhangTin Mouth	樟田河口	Q	WQ

The MIKE model is a comprehensive hydro-environmental platform that can simulate and tackle problems in different water environments, ranging from coastal modeling, urban flooding to groundwater management. MIKE21/3 Flow Model FM with a flexible mesh approach is used as the modeling system for the 2-D simulation in this study. The hydrodynamic module and ECO Lab module are employed for the hydrodynamic simulation and water quality modeling respectively. The MIKE modeling system features graphical user interface (GUI) platforms that are user-friendly and straightforward to set up and manage. The MIKE software provides an all-in-one

platform that allows input file preparation, mesh generation, parameter setting, post processing and plot outputs to be performed within one interface.

### 4.3.3 Model Parameters and Control - Hydrodynamic

The hydrodynamic aspect of the simulation is performed via the hydrodynamic module under the MIKE21 Flow Model FM. The triangular mesh mentioned in Section 4.3.1 is set up and implemented into the module via the MIKE Zero Mesh Generator. It is a tool for the generation and editing of unstructured meshes. The mesh file is an ASCII file containing the information of the geographical position and bathymetry for each node point in the mesh, as well as the information of the node-connectivity in the mesh. The definitions of open (i.e. flowing) and close (i.e. land) boundaries are determined by the allocation of codes and are also provided in the ASCII file. Datum shift and minimum depth cutoff options are available to fine-tune the mesh and bathymetry of the domain. The period to be covered by the simulation is determined via the specification of the simulation start date, the overall number of time steps and the overall time step interval. The simulation always starts with time step number 0 and the simulation start date is the historical data and time corresponding to time step 0. The time steps for the hydrodynamic calculations and the advection-dispersion calculations are dynamic and each determined to satisfy stability criteria.

### Solution Technique

The simulation time and accuracy of each run can be controlled by the order of numerical scheme used in the numerical calculations. Both the time integration and space discretization in this module have the options of a lower first order scheme or a higher order scheme. The lower order scheme gives a faster but less accurate simulation, whilst the higher order scheme gives more accurate results at the expense of a longer simulation time. Choosing a higher order scheme for the time integration and space discretization will increase the computing time by a factor of 3-4. Given the mass

## Models Development

---

scale of simulations necessary in this study, the lower order scheme is chosen to be the primary option for all simulations. When time integration of the shallow water equations is performed, the explicit scheme is used and due to stability restriction the time interval must be selected so that the CFL number is less than 1. To avoid potential stability problem, the critical CFL number in this simulation is set to 0.8.

### Flood & Dry

As illustrated in Chapter 3, the flood and dry function of the model allows the elements to react to the variation in water levels and hence the moving water boundaries. A drying water depth, a flooding water depth and a wetting depth have been specified at 0.005 m, 0.05 m and 0.1 m respectively in the model.

### Eddy Viscosity

The horizontal eddy viscosity is calculated using the Smagorinsky formulation with the Smagorinsky coefficient equals to 0.28. A general range of the Smagorinsky coefficient is between the interval of 0.25 to 1.0. The minimum and maximum eddy viscosities are set at  $1.8 \times 10^{-6} \text{ m}^2/\text{s}$  and  $1.0 \times 10^{10} \text{ m}^2/\text{s}$  respectively.

### Density

For 2-D simulation, barotropic mode is chosen that both temperature and salinity will be constant and the density will not be a function of the two variables. This is a more direct approach compared to the density being a function of both temperature and salinity, as the transport equations for the temperature and salinity must be solved. The simulation time will then be increased significantly due to the additional transport equations being solved. Moreover, the effect of density gradients in 2D shallow water equations is generally small and hence the density term can be neglected.

## Models Development

---

### Forcing, Structures & Sources

Coriolis forcing is included through a constant specified reference latitude of  $18.5^\circ$ . Wind forcing, ice coverage, tidal potential, wave radiation and hydraulic effects from structures such as weirs, piers and gates are not considered due to the low significance and rare occurrence.

Annual precipitation and evapotranspiration are documented as 1,630 mm and 1,049 mm respectively over the period 1960-2010 (Li et al., 2015a; Zhang et al., 2014). Their distributions across the lake region are uneven temporally and spatially. Taking into consideration the effect of vegetation interception and ground infiltration (Guo et al., 2008), the net contribution of these effects are not significant towards the mean water depth of Poyang Lake at 12-15 m. It is therefore considered plausible to neglect these terms in the numerical model.

The effects of rivers, intakes and outlets from power plants and nearby farmlands can be included in the simulation as point sources. However without the access to data related to power plants and farmlands in the Poyang Lake region, it is difficult to approximate the actions of the additional sources such as their magnitudes and the velocity at which the water is discharged into the ambient water. Hence no source is added in this case.

### Bed Resistance

The bed resistance of the domain is specified as a function of the Manning roughness coefficient;  $f(n) = 1/n$ . As previously stated, the Manning roughness coefficient varies with the nature of the bed and is used in the Manning's formula to calculate flow velocities in open channels (Manning, 1891). A basemap containing the ground roughness distribution of Poyang Lake is obtained from the Jiangxi Provincial Water Conservancy Planning Design and Research Institute. A data file is created by superimposing the unstructured mesh with the ground roughness data. The model then uses piecewise constant interpolation to map out the entire dataset. The input data vary spatially but are constant in time. Figure 4.14 illustrates the bed resistance across the simulation domain of Poyang Lake. The rougher the surface, the higher the Manning roughness coefficient and hence the lower the  $1/n$  value represented in the figure. The model chooses a free slip land boundary condition. Quadratic drag formulation is used for bottom drag calculation.

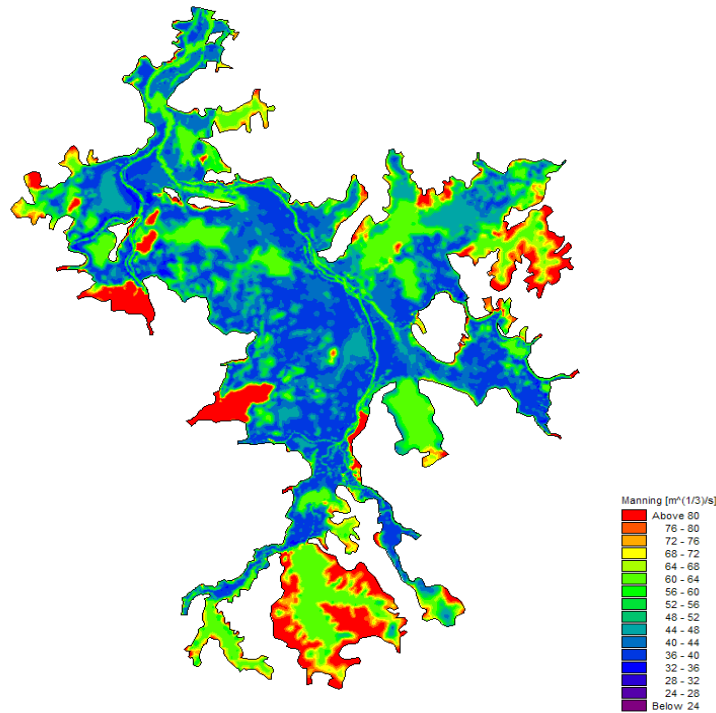


Fig. 4.14 Bed roughness across simulation domain in Poyang Lake

### Initial Conditions

The initial values for the hydrodynamic variables can be specified through the setting of constant values, spatially varying surface elevation and spatially varying water depths and velocities. However, with the rapidly changing nature and the sheer scale of Poyang Lake, the data on surface elevation, water depths and velocities of the entire lake at any one point is hardly feasible to obtain. As a result, the setting of constant values is adopted in this approach. An arbitrary surface elevation that is close to field-measured data has been set to be the initial condition for the simulation. Velocities  $u$  and  $v$  in  $x$  and  $y$  directions respectively are set at zero in this case. Extra buffer period is given at the beginning of each simulation to allow the stabilization and iteration of the calculation from the initial static state of the lake towards actual values. To avoid the generation of shock waves, the initial surface elevation should be roughly matching the boundary conditions at the start of the simulation.

### Boundary Conditions

When the mesh file is input to MIKE, the set-up editor scans the file for boundary codes and displays the recognized codes as separate boundaries. The specification of boundary information for each boundary is made subsequently. In our set-up, 16 boundary conditions are created across the Poyang Lake domain. Boundaries connecting these 16 locations are set as land boundaries with the full slip boundary condition applied. For the boundary at the Barrage (BC1), water level that is variable in time and constant along boundary is input through a time series file. It is assumed that the physical structure of the barrage does not affect the hydraulic flow throughout the simulation. For the rest of the boundaries (BC2 - BC16), a discharge boundary is deployed with a data file containing the total discharge varying in time at the location. All of these input files are created using the simulation results from the 1-D simulation.

### Outputs

Simulation of large scale lake environment creates large result files. It is often impossible to have the computed discrete data in the whole area and at all time steps saved in the result files. In practice, sub areas and subsets must be selected for subsequent analysis. For 2-D field variables, possible output formats include having the selected field data in geographical points, lines, areas, cross section or domain. Mass budget, discharge and inundation are also available as an output item. To output the field variables at certain points (e.g. a hydrological station with field-measured data), the geographical coordinates of the location are input via an ASCII file containing the  $x$ - and  $y$ -coordinates and name specification for each point. Similar practice is performed with outputting the line series by specifying the first and last point on the line and number of discrete points on the line. As for the area and domain series, the discrete field data within a polygon can be selected. The closed region is bounded by a number of line segments specified by the coordinates of the vertex points of the polygon. Domain series are specifically determined for mass budget calculation. For the cross-section series, the first and the last point between which the cross section is defined. The cross section is defined as a section of element faces. Based on the availability of the field-measured data, the output points are set at multiple locations around the lake. Area series output is also chosen to give a spatial representation of the water level across the Poyang Lake domain with respect to the change in time. The velocity flow field is integrated with the output for validation in subsequent section. In our model setup, the following field variables are recorded: surface elevation, vertical and horizontal velocity, flow directions and temperature. Global numerical output is performed at a frequency of 360, which represents an output every 0.5 hours in the simulation time frame of a year.

Table 4.3 summarizes the model parameters and their values of a general 2-D hydrodynamic simulation in this study.

Table 4.3 List of 2-D hydrodynamic model parameters

Parameter	Value
Mesh Nodes	56658
Mesh Elements	109494
Simulation Period	2008/06/01 - 2008/12/31
Time Step	5 seconds
Total Time Steps	11,100,000
Solution Technique	Time Integration - Low Order Space Discretization - Low Order
Density Type	Barotropic
Flood & Dry	Drying Depth - 0.005 m Flooding Depth - 0.05 m Wetting Depth - 0.1 m
Eddy Viscosity	Smagorinsky formulation, Constant - 0.28
Coriolis Forcing	Constant
Wind Forcing	Not Included
Ice Coverage	Not Included
Tidal Potential	Not Included
Wave Radiation	Not Included
Net Precipitation	0 mm/day
Sources & Structures	Not Included
Initial Water Level	16.1 m
Roughness	Varying, 0.023 - 0.03
Simulation Unit	2.4GHz CPU, 512MB DDR RAM
Parallel Simulation	Yes (OpenMP)
Simulation Time	25 hours

### 4.3.4 Model Parameters and Control - Water Quality

The water quality aspect of the simulation is performed by the ECO Lab module under the MIKE21/3 Flow Model FM. ECO Lab module is a numerical unit designed specifically for ecological and water quality modelling. It is used as a platform for customizing models that describe water quality, eutrophication, heavy metals and ecology in aquatic ecosystem using process oriented formulations. In numerical modeling terms, the standards for describing and tailor-making an ecosystem is high. This is due to the extensive quantity of the information needed and the great variation of the many ecological parameters, not to mention the potential scales and scopes involved in the many aspects of the ecosystem. The strength of modern numerical water quality models is to offer a simple modification and implementation of the mathematical description of the ecosystem that could be coupled into and work alongside the hydrodynamic models. The ECO Lab module can integrate state variables in the form of dissolved substances, particular matter of dead or living material and living biological organisms. The chemical and biological processes together with interactions between the state variables and their physical process with sedimentation can all be described in the model. The ability to integrate and quantify the many possible causal relations between the state variables and their effects on the ecosystem remain the top objective for most water quality models. The ECO Lab module's ability to incorporate essential biogeochemical processes, whilst remain interconnected and compatible with the hydrodynamic module, deem it suitable for our study.

In the MIKE ECO Lab module, a template file is used as a basis to manage the actual model formulation and the solution parameters (i.e. the integration method and update frequency). The MIKE model provides a number of standard templates describing common processes related to environmental problems and water pollution (DHI, 2017a). These templates provide the basic skeleton in modeling and tackling common problems in the water environment associated with excess nutrients concentrations, oxygen depletion due to release of BOD, bacterial survival and degradation

## Models Development

---

of chemical substances etc. Dependent on the nature of the water quality problem under consideration, the model can be adjusted to different levels of detail. The complexity of the model ranges from the simplest version, which includes BOD and DO only, through the introduction of sediment and water interactions and the inclusion of inorganic nitrogen to the most complex level where the BOD is divided into three forms; dissolved, suspended and deposited for detailed simulation and analysis.

The main investigation of this study is on the spreading, degradation and interaction between the inorganic nutrients related to nitrogen and phosphate. With such intention in mind, one of the templates provided by the ECO Lab module has been selected as the blueprint of the water quality template for our model and underwent further modification. The original template file describes the processes associated with the variables; BOD, oxygen, ammoniacal nitrogen, nitrate, orthophosphate, particulate phosphorus, temperature, faecal coliform and total coliform. The BOD is described by only one state variable instead of three separated identities as that extra complexity could not be supported with sufficient field data. The effects of ammoniacal nitrogen on the oxygen concentration can be studied in this template and so can the concentrations of ammoniacal nitrogen itself. Denitrification and the exchange process between the bottom sediment and the water bodies are also included which give a comprehensive coverage on the nutrient processes.

Further modifications of the template have been made to tailor for the needs of this study. The concentration of total phosphorus, by summing the concentrations of orthophosphate and particulate phosphorus, has been added as a derived output to facilitate future results comparison and analysis. Processes and parameters related to the faecal coliform and total coliform are removed from the template as they are not considered in our investigation. The re-aeration rate ( $K_2$ ) as an auxiliary variable is streamlined and reduced to three standard methods; (i) Thyssen-expression for application to small streams, (ii) O'Connor-Dubbins-expression for ordinary rivers and (iii) Churchill-expression for rivers with high flow velocities. Other user-defined

## Models Development

---

expressions that require the input of additional coefficients have been taken out for simplification and more efficient model operation. The above modifications are done by manually adding or removing any formulas associated with the subject processes, as well as performing due diligence to all the related constants to ensure that the modifications have not affected the calculation of other processes.

The triangular mesh used in the hydrodynamic simulation will be retained for the water quality simulation. The positions of the open and close boundaries, as well as the setting for simulation period and time step, are identical to that of the hydrodynamic simulation. The integration methods for solving the process equations have been detailed in Chapter 3 and will not be repeated herein. Focus will be given on the structure of the setup template and the parameters involved. The water quality template consists of a series of formulations and components, each serving different functions and purposes in the simulation.

### State Variables

State variables represent the variables that describe the state of the ecosystem and whose states are the main interest of the model simulation. State variables are usually the most important variables in a process oriented template and represent the main deliverables of the water quality model. In ECO Lab the state variables that are present in the water column could use the advection-dispersion module for calculating its transport and movement based on the hydrodynamic of the flow. State variables that are present in the sediment cannot be transported based on the advection-dispersion module. In this study, the state variables of interests are all concentration based with no fixed nature. The 7 state variables are; dissolved oxygen (DO), ammoniacal nitrogen ( $\text{NH}_3\text{-N}$ ), nitrate ( $\text{NO}_3$ ), biochemical oxygen demand (BOD), orthophosphate ( $\text{PO}_4\text{-P}$ ), particulate phosphorus (PP) and temperature (TEMP). They are selected based on their influence on water quality in lake-river environment and the availability of their data and field measurements.

### Constants

Constants are defined as any input parameter that are constant in time, but can vary in space. Examples of constant include different specific rate coefficients, half-saturation concentrations and other universal constants such as gas constant and atomic weights. The constants in ECO Lab can be divided into two groups: built in constants or user-specified constants. The former are automatically provided by the model system during execution, whereas the latter have to be specified in the setup. Built-in constants include latitude, longitude and bed level of the model area. Only some of these coefficients can be determined by calibration. Other coefficients used will be based on values found from literature or actual measurements and laboratory tests. A selection of user-specified constants used in this model are listed in Table 4.4.

### Forcings

Forcings are defined as any input parameter that are spatial and temporal varying parameters of an external nature that affect the ecosystem. Typical examples of forcings are temperature, salinity, solar radiation and water depth. Forcings are used as arguments in the mathematical expressions of processes in a template. The ECO Lab model has the ability to refer to forcings that are calculated in the hydrodynamic module of MIKE. These forcings are input into the ECO Lab module as built-in forcings, for example the water depth, flow velocity and salinity in this study.

### Processes

Processes describe the transformations that affect the state variables. That means processes are used as arguments in the differential equations that ECO Lab solves to determine the state of the state variables. In other words, processes are direct translation in ECO Lab terms of the equations describing the many biochemical processes in Chapter 3. Processes formulate equations that may consist of state

## Models Development

---

Table 4.4 List of 2-D water quality model constants

Constant	Value	Unit
Temperature: Maximum absorbed solar radiation	4992	/daylength
Temperature: Displacement of solar radiation	1	hour
Temperature: Emitted heat radiation	1608	/daylength
Oxygen processes: Reaeration temperature coefficient	1.02	-
Oxygen processes: Respiration of animals and plants	3	/day
Oxygen processes: Respiration temperature coefficient	1.05	-
Oxygen processes: Max oxygen production by photosynthesis	3.5	/day
Degradation: First order decay rate at 20°C	0.5	/day
Degradation: Decay rate temperature coefficient	1.02	-
Degradation: Half-saturation oxygen concentration	2	mg/l
Sediment processes: Sediment oxygen demand	0.5	g/m <sup>2</sup> /day
Sediment processes: SOD temperature coefficient	1.00	-
Sediment processes: Resuspension of organic matter	0.5	g/m <sup>2</sup> /day
Sediment processes: Sedimentation rate for organic matter	0.8	m/day
Sediment processes: Critical flow velocity	1	m/s
Nitrogen content: Ratio of ammonium released from BOD decay	0.29	gNH <sub>4</sub> /gBOD
Nitrogen content: Uptake of ammonia in plants	0.066	-
Nitrogen content: Uptake of ammonia in bacteria	0.109	-
Nitrification: Flag for reaction order (1: first order, 2: half order)	1	-
Nitrification: Ammonia decay rate at 20°C	1.54	/day
Nitrification: Nitrification temperature coefficient	1.13	-
Denitrification: Oxygen demand by nitrification	4.47	gO <sub>2</sub> /gNH <sub>4</sub>
Denitrification: Half-saturation constant	0.05	mg/l
Denitrification: Flag for reaction order (1: first order, 2: half order)	1	-
Denitrification: Denitrification rate (nitrate into nitrogen)	1	/day
Denitrification: Denitrification rate temperature coefficient	1.16	-
Phosphorus content: Ratio of phosphorus released at BOD decay	0.009	gP/gBOD
Phosphorus content: Uptake of P in plants	0.009	-
Phosphorus exchange with bed: Resuspension of PP	0.5	g/m <sup>2</sup> /day
Phosphorus exchange with bed: Decomposition of PP	0.8	m/day
Phosphorus exchange with bed: Critical velocity of flow	1	m/s
Phosphorus processes: Decay constant for PP	0.1	/day
Phosphorus processes: Decay temperature coefficient	1.00	-
Phosphorus processes: Formation constant for PP	0.1	/day
Phosphorus processes: Formation temperature coefficient	1.00	-

## Models Development

---

variables, auxiliary variables, other processes and constants previously stated in the template. A sequence of arguments and operators are also involved which is quite similar to a normal spreadsheet calculation: the calculation is essentially a ‘one-liner’ and must result in a single value. Valid arguments are numeric constants, previously defined variables and function calls. Valid operators are the standard mathematical operators "+", "-", "\*", and "/" and the ‘IF-THEN-ELSE’ control structure. For example, the nitrification process can be represented in the Processes section as:

IF *ReactionOrderNitrification* == 1

THEN *Nitrification* = *NitrificationRate*\**NitrificationProcess*\**Ammonia*

ELSE *Nitrification* = *NitrificationRate*\**NitrificationProcess*\*SQRT(*Ammonia*)

in which *ReactionOrderNitrification* is a constant defined as the flag for reaction order. If the flag is 1, first order is chosen. If the flag is 2, half order is chosen. *NitrificationRate* is a constant representing the ammonia decay rate at 20°C. *NitrificationProcess* is defined as an auxiliary variable with its own expression regarding the Arrhenius temperature correction formula. *Ammonia* is the state variable representing the ammoniacal nitrogen concentration. The end value *Nitrification*, as the net change in nitrate concentration, is then incorporated into the calculation of state variables. There are another 20 processes included in the template with regards to reaeration, ammonia and ammonium release, denitrification, phosphorus resuspension and sedimentation etc. They are formulated under similar principles and hence will not be listed out herein.

### Auxiliary Variables

Auxiliary variables are defined as mathematical expressions with a sequence of arguments and operators. They are commonly included in the mathematical expressions of Processes in the template, although sometimes they are used for specifying results directly. Arguments in auxiliary variable expression could be state variables, constants,

## Models Development

---

forcings or other auxiliary variables. The auxiliary variables are calculated in the order they are defined in the ECO Lab model, starting from the top to the bottom of the list. As a result, only auxiliary variables defined above the present auxiliary variable expression can be used as argument in the auxiliary variable expressions. The reason for such operation is to split long processes expressions into sub-expressions under auxiliary variables, which allows simpler and easier interpreted processes expressions. The presence of auxiliary variables also allow the calculation of intermediate results. Typical examples of auxiliary variables are dimensionless factors that are used as multipliers in the processes expressions. The auxiliary variables used in this model include expressions for the oxygen saturation concentration, reaeration rate, relative day-length, solar irradiance factor and temperature capacity factor.

## Dispersion

Dispersion describes the transport of variables due to non-resolved processes in the numerical models. Assuming horizontal dispersion in the multi-dimensional model, a dispersion coefficient is assigned individually for each state variable. The dispersion can be formulated in two ways; dispersion coefficient formulation and scaled eddy viscosity formulation. In the former, the dispersion coefficient must be specified either as constant in time and space or varying in domain, in which a data file containing the varying dispersion coefficient across the domain needs to be prepared before setting up the hydrodynamic simulation. When the latter formulation is used, the dispersion coefficient is calculated as the eddy viscosity used in solution of the flow equations multiplied by a scaling factor. The scaling factor can be specified either as constant or varying in the domain. It can be estimated by  $1/\sigma_T$ , where  $\sigma_T$  is the Prandtl number. The default value for the Prandtl number is 0.9 corresponding to a scaling factor of 1.1. When more sophisticated eddy viscosity models such as the Smagorinsky or k- $\epsilon$  models are used, it is recommended that the scaled eddy formulation should be used, which is the case chosen for this study.

## Models Development

---

It is difficult to devise generally applicable values for the dispersion coefficient. However, using Reynolds analogy, the dispersion coefficient can be written as the product of a length scale and a velocity scale. In shallow waters the length scale can often be taken as the water depth, while the velocity scale can be given as a typical current speed. Values in the order of 1 are usually recommended for the scaling factor. Peeters and Hofmann (2015) estimated dispersion coefficient in medium-sized lake to range from 0.1 to 0.7 m<sup>2</sup>/s. Given the lack of studies and information available on the dispersion coefficient in a larger lake the size of Poyang Lake, inputting a 2-D dispersion coefficient data file is not feasible. Updating the scaled eddy viscosity based on the length scale (the water depth) and velocity scale (the current speed) spontaneously during simulations, although created additional loads on the computational units, can ensure the accuracy for the value of a relatively influential parameter in the model.

### Initial Conditions

Similar to the setup in the hydrodynamic model, the initial values of each variables at the boundary conditions can be specified. The initial conditions can be specified as constant or varying in the domain. Although it will be beneficial to the simulation to have 2-D distribution of each state variable across the lake as initial concentrations, such data on all the state variables of Poyang Lake at any one time within a substantial period is difficult to obtain. In addition, directly inputting the concentration results from 1-D simulation will aggregate any potential inaccuracy due to the 1-D simulation using interpolation in calculating many of the concentrations in the central region of the lake. As a result, the setting of constant concentration values at boundaries is used in this case. Extra buffer period is again given at the beginning of the simulation to allow stabilization to develop from the initial values.

### Boundary Conditions

All the 16 boundaries set up in the mesh and used in the hydrodynamic model will be retained for the water quality model. For all the boundaries (BC1 - BC16), concentrations of each state variables are input via time-series data files. These files are created using the simulation results generated from the 1-D simulation. The specification of the individual boundary information for each section and each component is made subsequently. For example in BC11 (Xinjinag West), a time-series data file containing the DO concentration over the simulation period is required as an input for the state variable DO. Similarly one input file is required for each of the other 6 state variable (NH<sub>3</sub>-N, NO<sub>3</sub>, BOD, PO<sub>4</sub>-P, PP and TEMP). In total 7 input files are required for this boundary. The same procedure is repeated until all the 16 boundaries are set up with their respective input files for each state variable.

### Update Frequency

The time step for the update of the ECO Lab equations is the overall time step specified in the hydrodynamic module multiplied by the update frequency. For example, if the time step in the hydrodynamic module is set at 5 seconds and the update frequency is at 360, then the time step for the calculations will be at  $5 \times 360 = 1,800$  seconds (30 mins). Selection of the update frequency and hence the time step for the model, is based on considerations of the time scales of the processes involved. A balance is needed between the precision of the numerical solution against the simulation time. A small update frequency will increase the accuracy of the simulation but also increase the overall simulation time. Based on the nature of the processes involved in our study, an update frequency of 360 is deemed to be sufficient in preserving the precision of the simulation with a reasonable simulation time.

### Outputs

The format available for output files in the water quality model is identical to that of the hydrodynamic model. In a 2-D field simulation, possible output formats include point series, line series and area series, as well as mass budget and discharge for domain and cross-section. Output points are set at multiple locations around the lake at which field-measured data is available for comparison. Area series output is also chosen to give a spatial and temporal representation of the different state variable concentrations across the Poyang Lake domain. The time-varying concentration distributions will allow the visualization and tracking of the behaviour of key water quality indices. In our model setup, the following field variables are recorded: DO, NH<sub>3</sub>-N, NO<sub>3</sub>, BOD, PO<sub>4</sub>-P, PP and TEMP. Global numerical output is at a frequency of 8,640, which represents an output every 12 hours in the simulation time frame of a year.

### 4.3.5 Model Parameters and Control - 3-D Model

Most of the settings in 3-D model are similar to those in 2-D simulation. The major difference lies with the extra parameters brought in with the addition of the vertical dimension, namely the vertical mesh, the vertical eddy viscosity and the bed resistance.

#### Vertical Mesh

In 3-D simulation the vertical domain is supplied in the form of a layered mesh. In the sigma domain, three different options are available in terms of specifying the vertical distribution of the layers, which are equidistant, layer thickness and variable. In this model the three options were tested with the same set up and simulation. It is found that the difference on the vertical distribution on hydrodynamic results is negligible. The variable layers are chosen for subsequent simulations with  $\sigma_c = 0.5$ ,  $\psi = 0.2$  and  $b = 1$ .

### Vertical Eddy Viscosity

The vertical eddy viscosity is calculated using the log law formulation. The method uses a parabolic eddy coefficient, scaled with local depth and bed and surface stresses. Minimum and maximum value for the eddy viscosity need to be specified in this option, which are  $1.8 \times 10^{-6} \text{ m}^2/\text{s}$  and  $0.4 \text{ m}^2/\text{s}$  respectively in our case.

### Bed Resistance

In the case of 3-D simulation, the bed resistance is structured differently and can be specified by using the quadratic drag coefficient or roughness height ( $k_s$ ). Using the ground roughness distribution provided by the Jiangxi Provincial Water Conservancy Planning Design and Research Institute, the roughness height can be calculated and entered for the 3-D simulation.

### 4.3.6 Parallel Computing

Simulation speed plays a vital role in numerical modeling of water environment. Speed improvement and optimization give the opportunity to use more refined models and to undertake more model runs and variations within a viable time frame. MIKE model has parallelization function available in many of its modules. The process splits the simulation work onto multiple processors in the computers and allows simultaneous calculations across the domains, hence shortening the total simulation times.

The computational engines in MIKE21/3 and ECO Lab are available in two parallelized versions; OpenMP which relies on shared memory and MPI which runs on distributed memory architecture. In OpenMP, the computational tasks are divided on a number of threads. A set of compiler directives, library routines and environment variables facilitates the shared memory approach and the calculations are made through the multiprocessor and multicore computer environment. In MPI, which stands for Message Passing Interface, the computational mesh is partitioned into a number of

physical sub-domains and the work associated with each sub-domain is processed by an individual processor. The data exchange between processors is based on the halo-layer approach with overlapping elements while the distribution of work and data is based on the domain decomposition concept.

The reduction of simulation time is dependent on the number of core processors available and their individual processing power in the computing unit. With the use of a high performance computer, the simulation can be accelerated significantly. MIKE is also compatible with the Graphics Processing Unit (GPU) computing approach in which the computers graphics card is utilized to perform the model's intensive calculations. In the case when both of the above are not available (e.g. in this study), a number of computers with multiple core processors are used to increase the computing power and reduce simulation time for each run.

### 4.3.7 Management of Simulations

Simulation of such a complex water environment requires expensive computational costs and time. In order to generate representative results efficiently with minimum computational costs, many of the simulations are set with a period of a 1 year cycle which normally requires a real time simulation of 1 week. However, as with many other numerical simulations, a stabilizing period at the beginning of the simulation is often needed to allow the model to settle with the discrepancies between the initial conditions and numerical calculations. Figure 4.15 compares two simulations with identical settings; one covering the period 01/10/2007-01/01/2009 (15 months) while the other covering the period 01/01/2008-01/01/2009 (12 months). Water levels from three locations in Poyang Lake are examined from these two simulations. It is not surprising to find out that both simulations have nearly identical results, except at the very beginning of the shorter simulation period around January 2008 where the stabilization takes place. Similar comparisons have been made with the water quality simulation over the two periods. Figure 4.16 illustrates results on several water quality

indices (DO, NH<sub>3</sub>-N and PO<sub>4</sub>-P) at different locations across the lake. It is clear that for the simulation from January 2008 to January 2009 (red line), the water quality variables first start off from the initial condition and gradually stabilize with the results generated from the longer simulation (blue line), which has already stabilized given its earlier start. From the graphs, each simulation takes a certain amount of time to stabilize and convert to a common equilibrium in the system. The length of such stabilizing period varies from model to model, but for this project it is reasonable to say that such stabilizing period is normally within 1 month. To provide sufficient buffering time for each simulation, the 1 year simulation period will be run as a 14-month simulation with the results from the first two months disregarded.

### 4.3.8 2-D and 3-D Simulation Comparison

A full 3-D simulation with both the hydrodynamic and water quality component for the period 01/10/2007-01/01/2009 (15 months) takes 536.5 hours. Meanwhile, a full 2-D simulation of the same period takes 198.6 hours using identical computational units, which translates to nearly 2.7 times quicker in real simulation time. The results of both simulations are shown in Figure 4.17 regarding hydrodynamics and in Figure 4.18 regarding water quality. In the former, the water levels are compared at three locations across Poyang Lake. 2-D simulation results are drawn in blue lines and 3-D simulation results are shown in red lines. It is clear that 2-D simulation has produced hydrodynamic results that are very close to those generated from the 3-D simulation. Although the two set of results contain a difference of about 0.2m on average, it is difficult to tell such difference from the graphs. Similar comparison has been made regarding water quality indices in Figure 4.18. Three water quality indices (DO, NH<sub>3</sub>-N and PO<sub>4</sub>-P) at different locations in Poyang Lake have been selected for comparison. The results produced by the 2-D and 3-D simulations are close. In terms of likelihood the water quality results are not as similar to the hydrodynamic ones, but the water quality results generated from both 2-D and 3-D simulations have shared nearly exact trends over the three graphs and are only occasionally differed by small amount over the

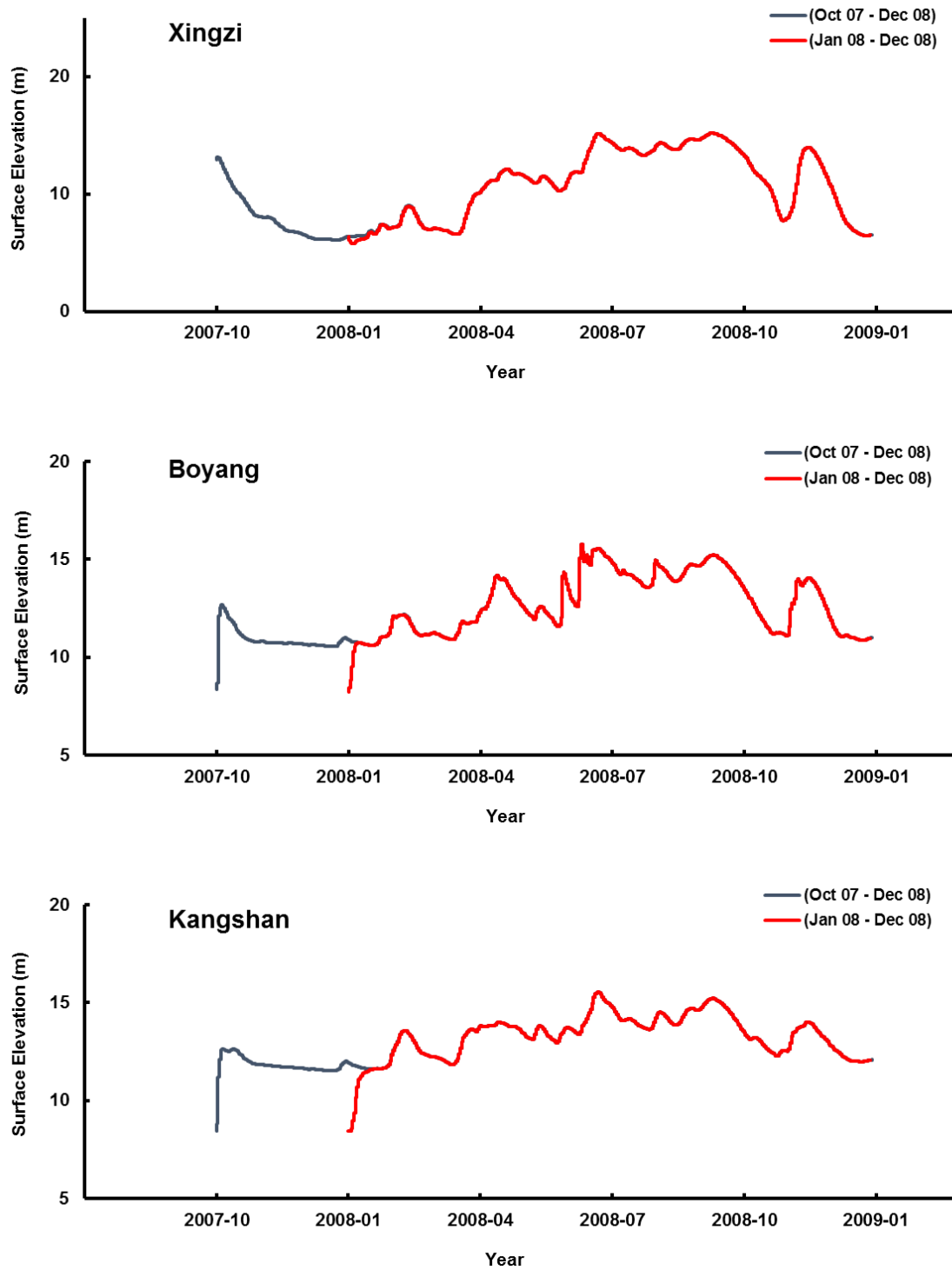


Fig. 4.15 Surface elevation comparison of two simulation periods at Xingzi, Boyang and Kangshan

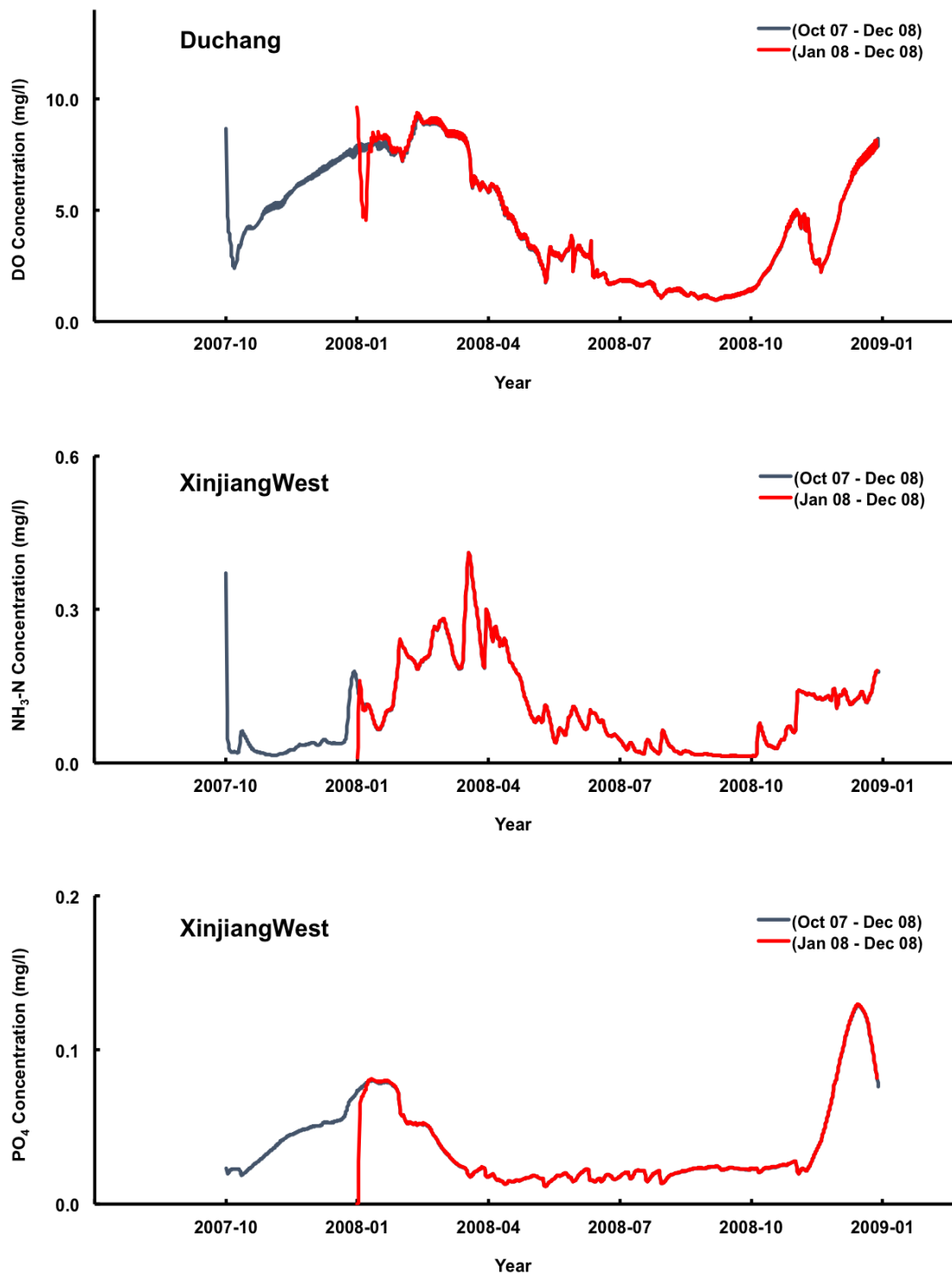


Fig. 4.16 Water quality comparison of two simulation periods of DO at Duchang, NH<sub>3</sub>-N at XinjiangWest and PO<sub>4</sub>-P at XinjiangWest

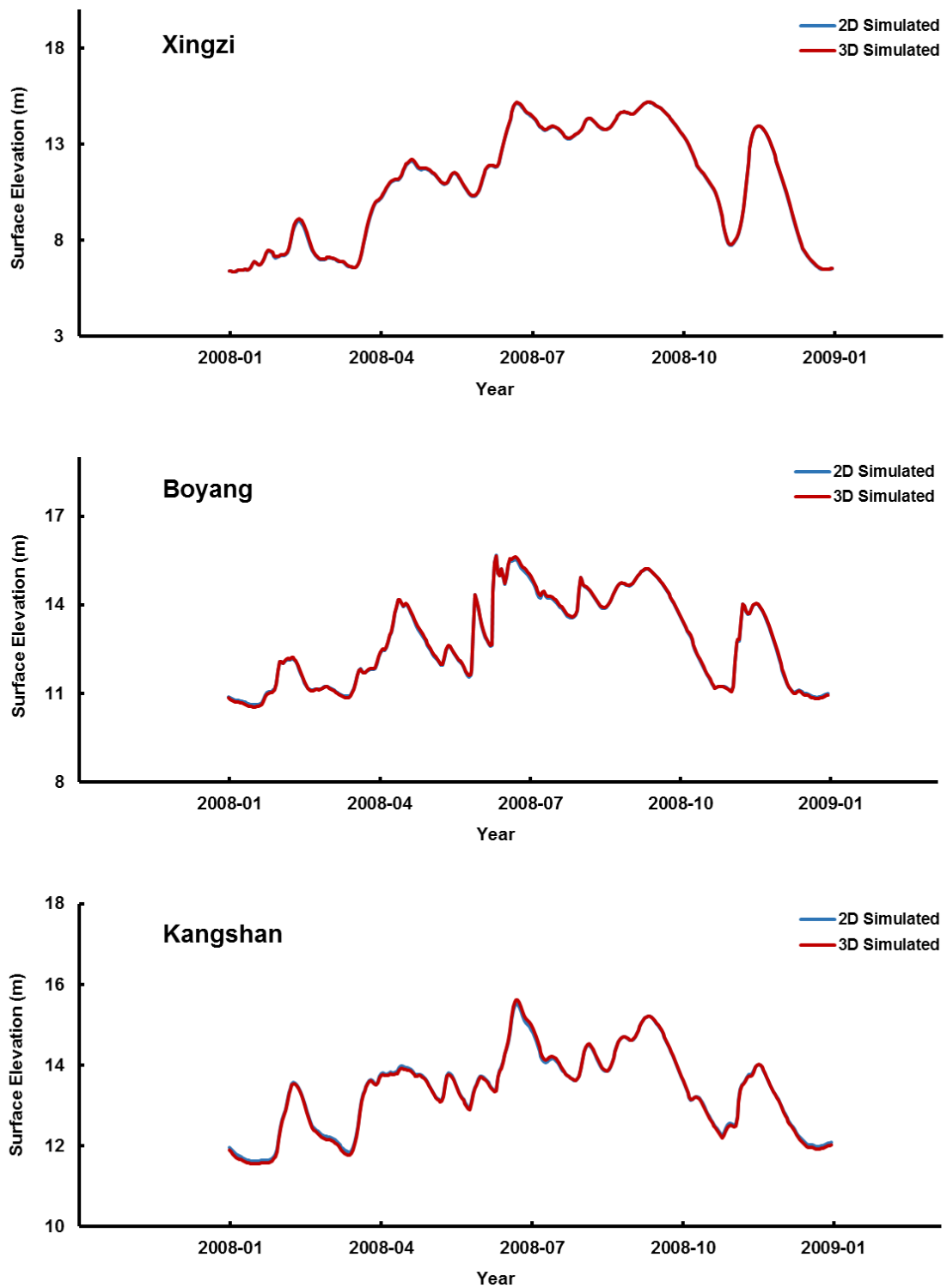


Fig. 4.17 Surface elevation comparison of 2-D and 3-D simulation at Xingzi, Boyang and Kangshan

## Models Development

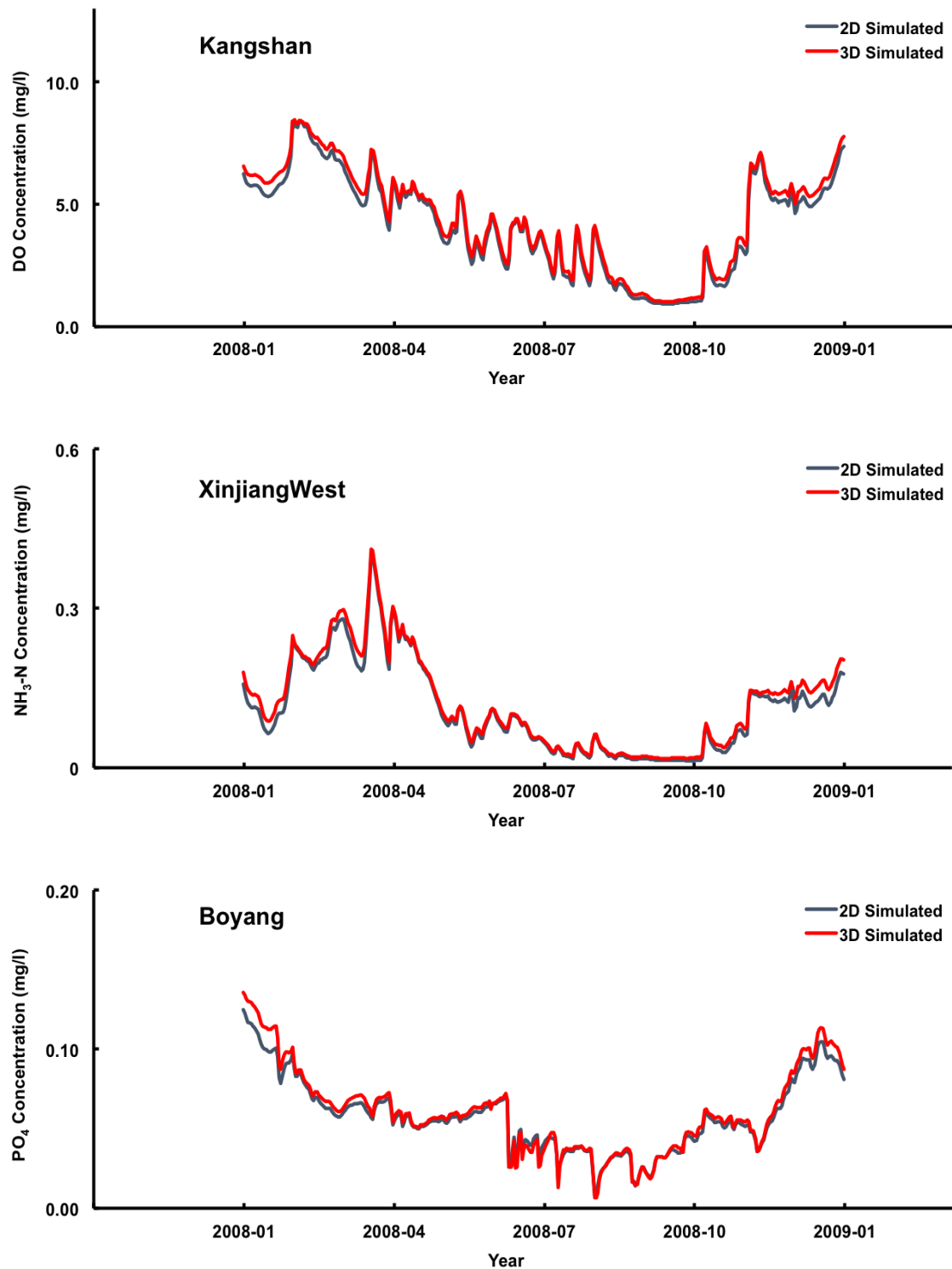


Fig. 4.18 Water quality comparison of 2-D and 3-D simulation of DO at Kangshan, NH<sub>3</sub>-N at XinjiangWest and PO<sub>4</sub>-P at Boyang

dry winter period. It is reasonable to conclude that 2-D simulations in hydrodynamic and water quality have produced comparable results with similar accuracy to those generated by 3-D simulations. The local phenomenon within different regions of the lake are not to be ignored. However for the purpose of this study, which looks at the holistic conditions of Poyang Lake, 2-D simulation has proven to be more efficient and computationally cheaper than 3-D simulation with close to identical results. Therefore 2-D simulation will be adopted to generate future results from this stage onward.

### 4.4 2-D Model Validation

The 2-D hydrodynamic and water quality models are validated using field data collected from Poyang Lake. Generating simulated results for multiple years will be difficult and inefficient due to the complexity and long simulation time of the 2-D model. The period of interest will therefore be limited to the year 2008, for which the available field data are most comprehensive.

#### 4.4.1 2-D Hydrodynamic Validation

Simulated hydrodynamic results are compared with the field-measured data collected from the same set of hydrological stations as shown in Figure 4.3. The results of the validation for the 2-D hydrodynamic model are illustrated in Figure 4.19 and 4.20. In Figure 4.19, the measured water surface elevations at Hukou, Duchang and Wucheng are compared with the results generated from the 2-D hydrodynamic model. Both the simulated predictions at Hukou and Wucheng match both the general trends and the minor peaks and troughs in the field measurements closely throughout the period. Similar results can be seen at Kangshan and Boyang in Figure 4.20. The RMSE of these four locations ranges between 0.515 m to 0.972 m, showing very small water level variance between the predicted values and field observations. In addition, the NSEs in these locations are within the range of 0.683-0.976, indicating a very good performance

## Models Development

---

rating from the 2-D hydrodynamic model in predicting the lake's hydraulic behaviours. The overall simulated results show strong correlations with the field measurements.

Despite having similar trends between the simulated results and field measurements during the summer seasons, the simulated results at Duchang and Tangyin have unusual spans of simulated flat water levels that did not match with the field measurements during the winter dry periods. Both locations have statistical indicators showing good correlation between the simulated results and the field-measured data with Duchang recording 1.299 m and 0.792 for RMSE and NSE respectively and Tangyin recording 1.126 m and 0.686 under the same indices. The RMSEs of these two locations are relatively higher than the rest of the locations, signaling a greater degree of variance between the simulation and observations.

To further investigate the issues, the surface elevations and the total water depth from the simulation have been compared at Duchang and Tangyin. In Figure 4.21, the total water depth (red line) during the winter period recorded close to zero meter in both locations. This indicates that the locations reached a dry state with no or little flow of water. This could be explained by the geography of the lake as both locations are situated close to the edge of Poyang Lake's main channel. High degree of water level fluctuations in the lake promotes drying and wetting process in large area across the lake. As a result, areas such as Duchang and Tangyin recorded little or zero total water depth during the winter seasons and these dry periods are reflected in the simulation. The discrepancy between the field measurements and simulated results in these locations could be due to the insensitivity in the model in responding to dry seasons and low water levels.

The standards of the 1-D hydrodynamic model validation can be assured with the comparison with literature. Similar validations for hydrodynamic simulation can be seen in Hu et al. (2012b); Li et al. (2014). The coherence between the field measured data and the simulation in this study matches those shown in Figure 2.6 on Page 33.

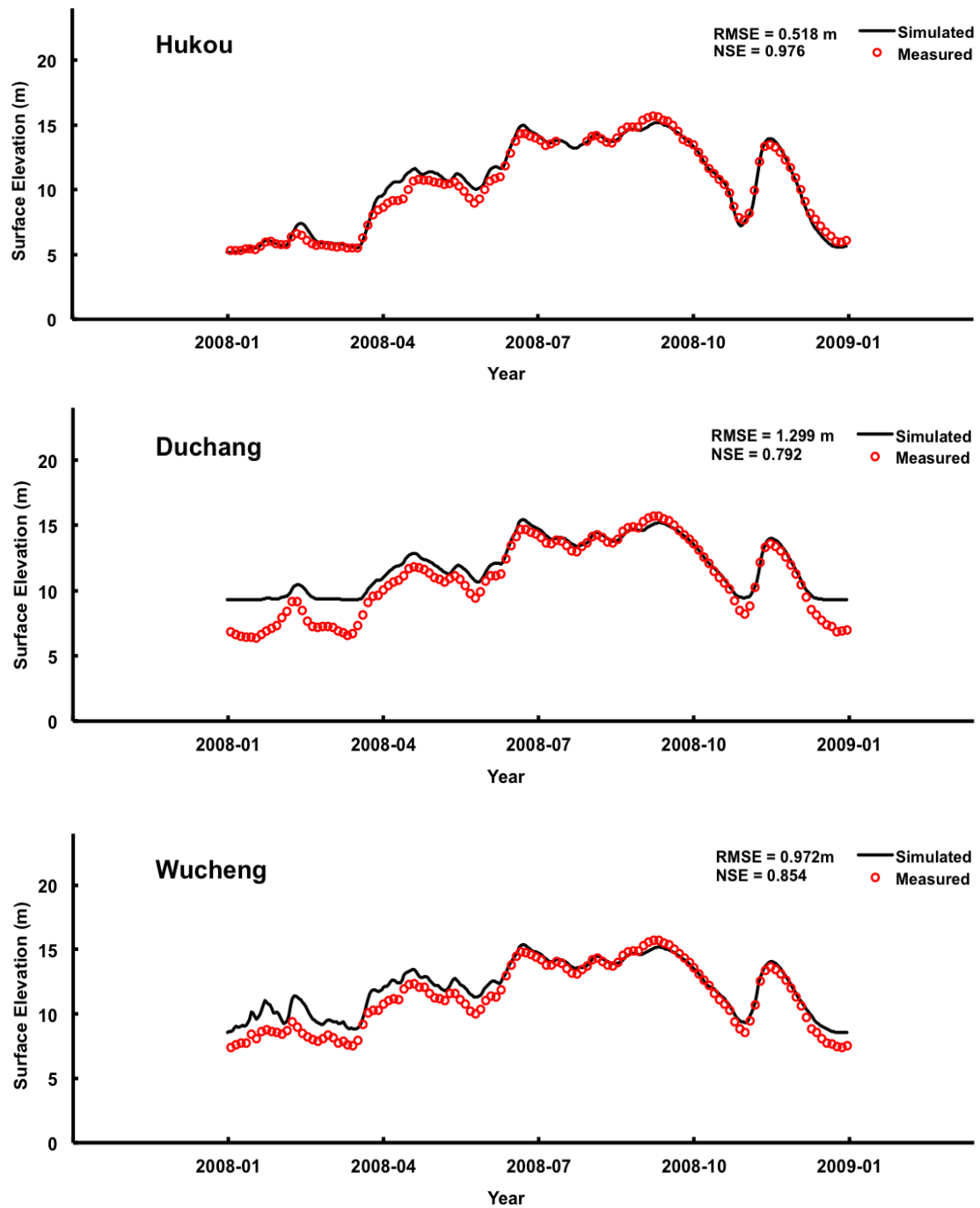


Fig. 4.19 Measured water surface elevations compared with 2-D hydrodynamic model predictions at Hukou, Duchang and Wucheng

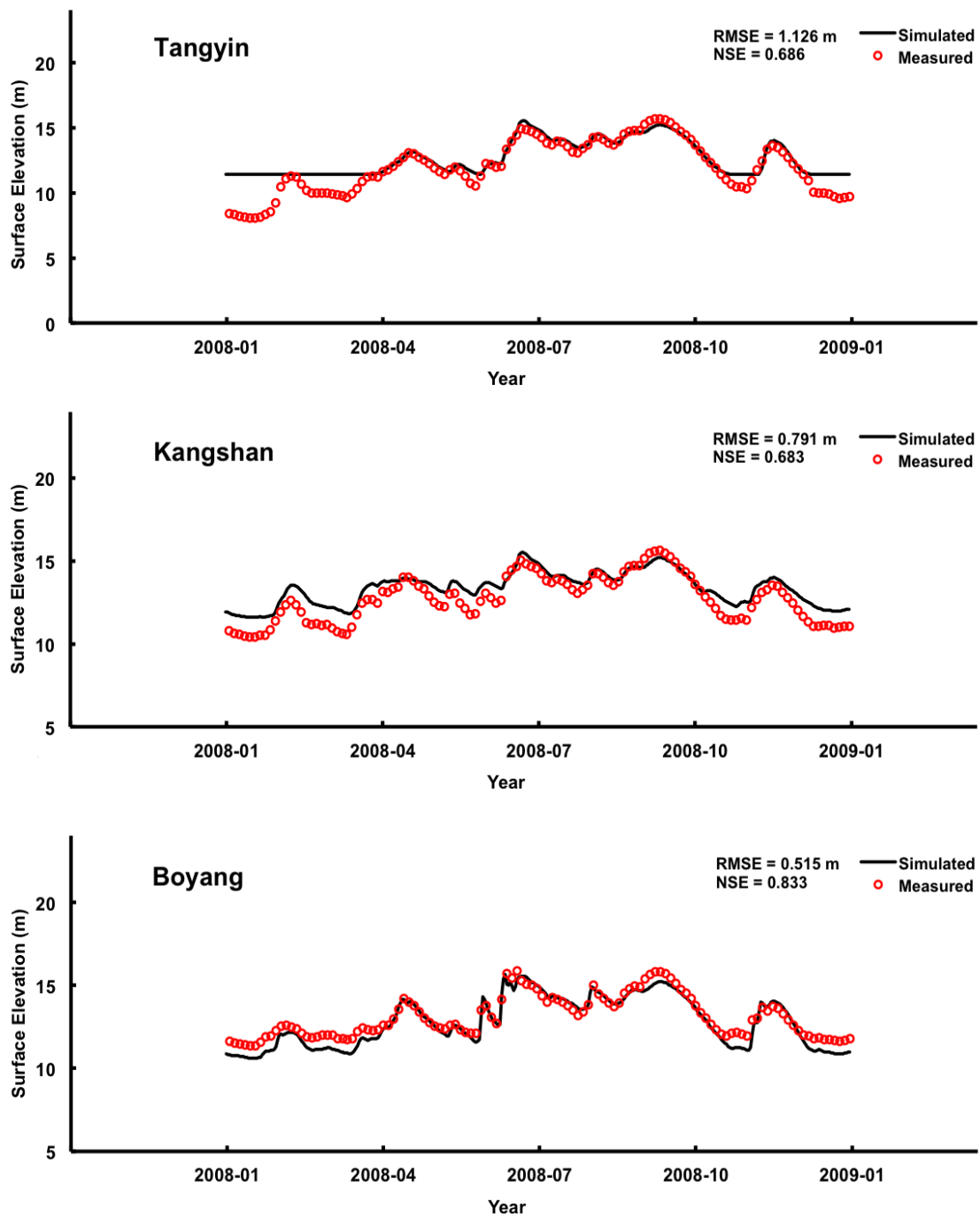


Fig. 4.20 Measured water surface elevations compared with 2-D hydrodynamic model predictions at Tangyin, Kangshan and Boyang

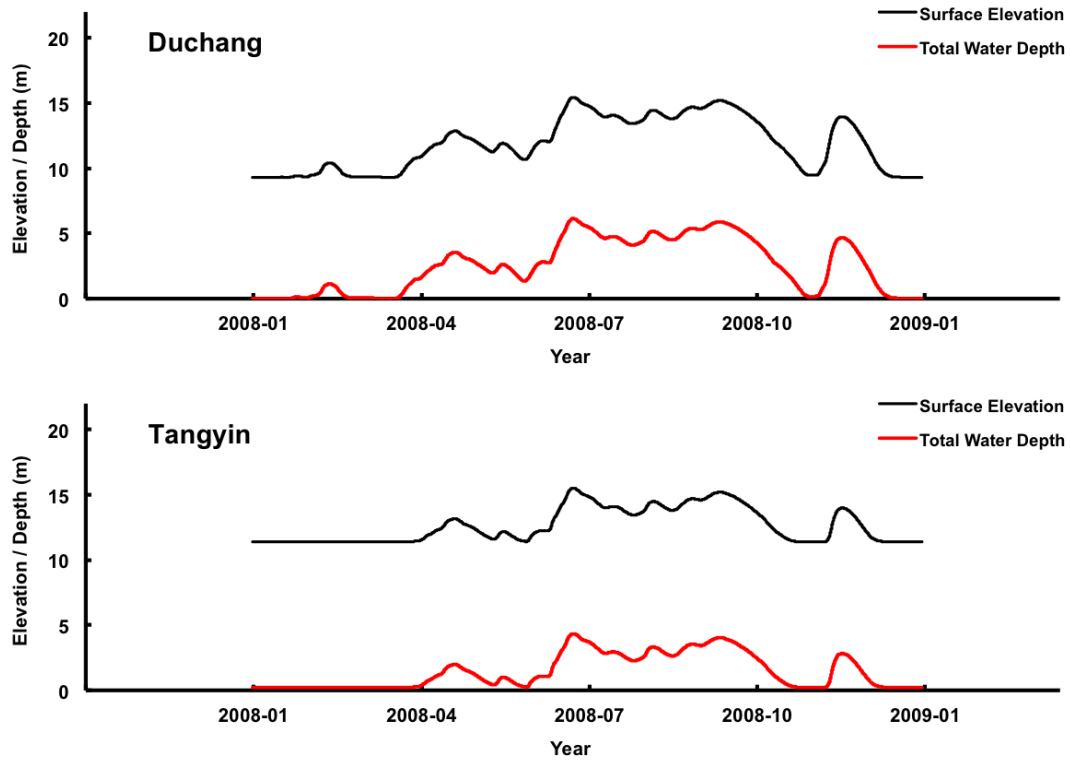


Fig. 4.21 Water surface elevations compared with total water depth from 2-D simulation at Duchang and Tangyin

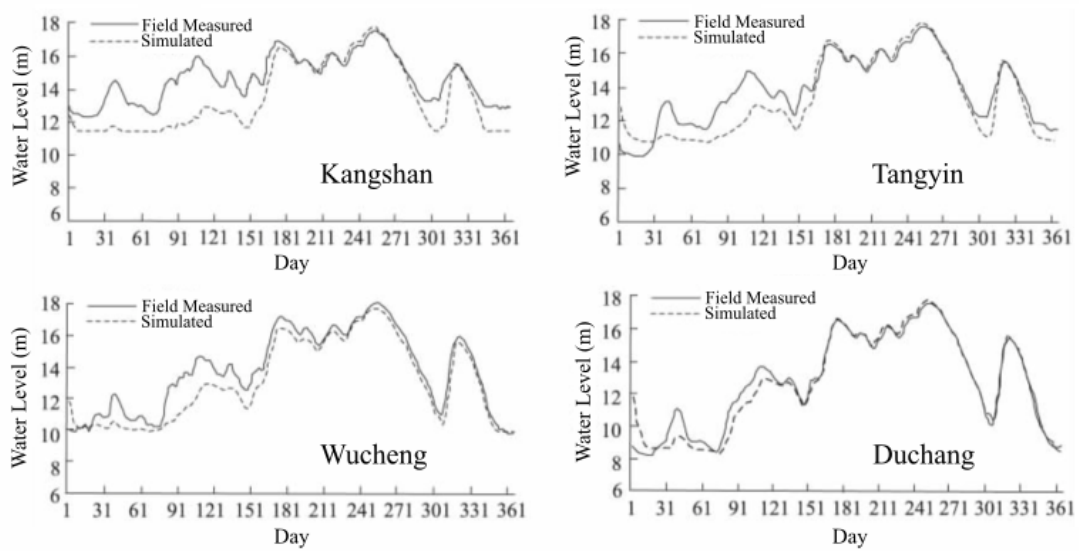


Fig. 4.22 Comparison of the simulated and field measured water level in Poyang Lake for 2008 (Source: Hu et al., 2012b)

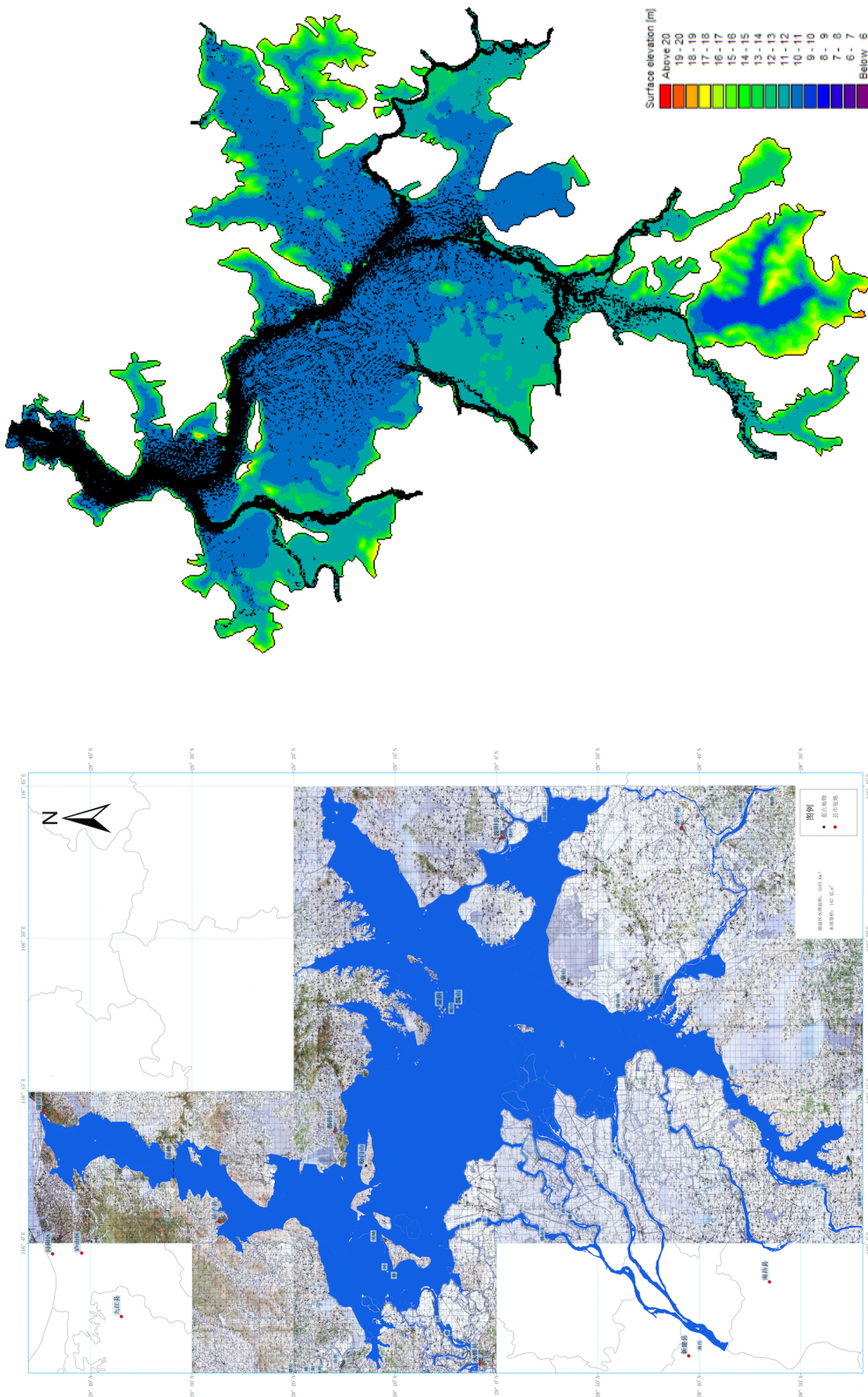
## Models Development

---

It is not uncommon for large scale numerical simulation to have small discrepancies between the field measurements and simulation due to the many factors and elements involved in the complex hydro-environment. As seen in Figure 4.22, clear gaps between the simulated values and field measurements were present for locations such as Wucheng, Kangshan and Tangyin during the dry season.

In addition to water surface elevations, the water flow field can be used as an indicator for hydrodynamic model validation. The water flow over time and space can be represented as vectors in the domain. These vectors are shown as arrows in the domain that comprise of both the direction and magnitude of the flow at any particular location of the lake. Two overall flow fields of the domain are chosen at different time from the same simulation; one showing the flow field during wet period in July and one showing the flow field during the dry period in January (Figures 4.23 and 4.24).

Both flow fields are used to compare against the satellite images of the water surface environment of Poyang Lake over the same period of the year, which have previously been shown in Chapter 2 on Page 26 and 27 as Figure 2.3 and 2.4 respectively. The flow field during the wet period in July demonstrates a large area of water surface that covers the majority of the lake domain, as indicated by the presence of black arrows/dots in those areas in Figure 4.23b. The concentrated black area along the main channel in the lake signifies higher velocity flow in those areas which align with the usual hydrodynamic behaviour of the lake during wet season. Meanwhile, the flow field during the dry period in January further reinforces the validity of the model by matching the water surface environment of Poyang Lake over the same period. As seen in Figure 4.24b, flow field with higher velocity is neatly concentrated in the narrow streams of Poyang Lake in the dry season, closely duplicating the same phenomenon shown in the satellite captured water coverage image of Poyang Lake in January (Figure 4.24a), a period when the lake exhibits the river-like environment and behaviour.

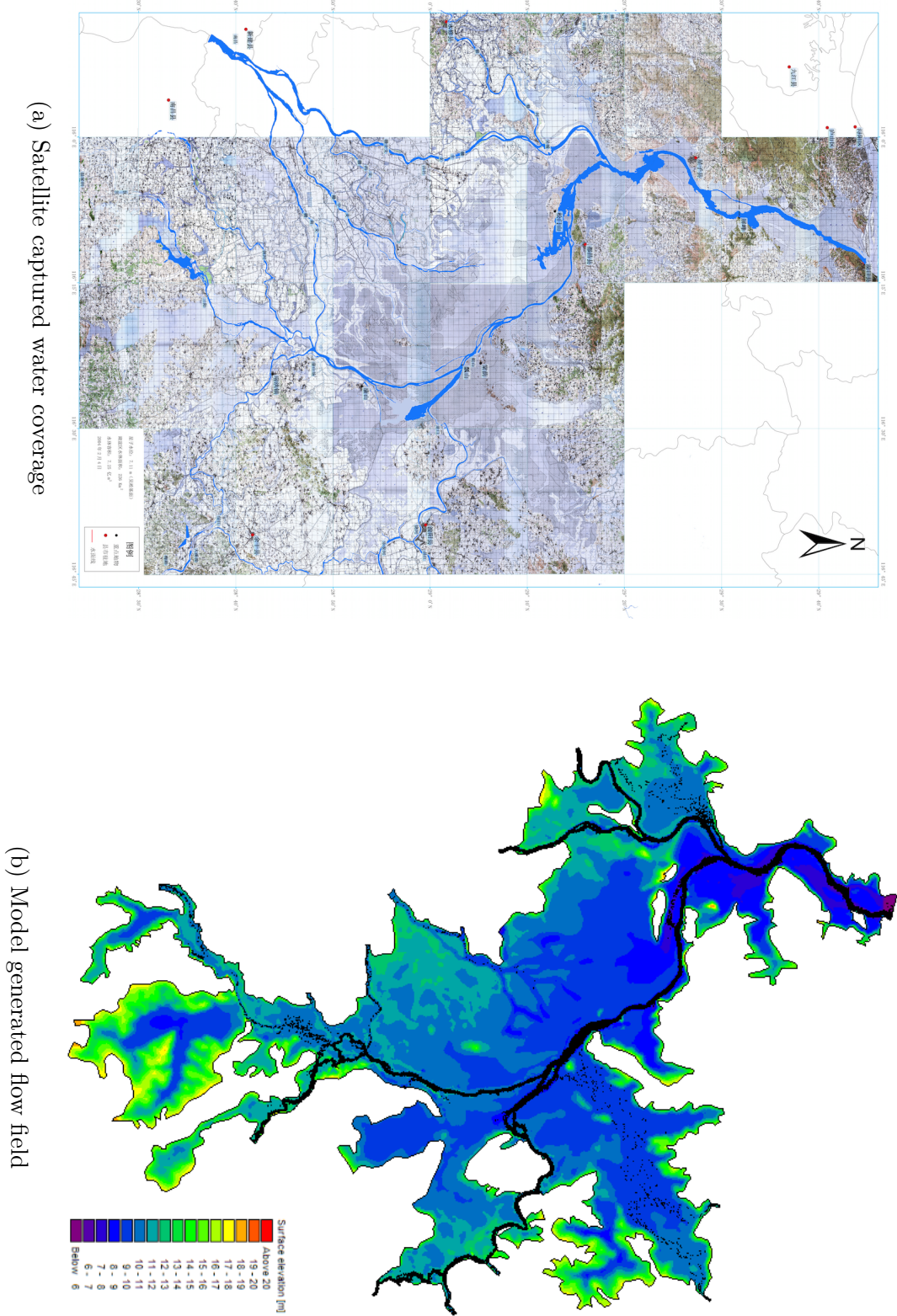


(a) Satellite captured water coverage

(b) Model generated flow field

Fig. 4.23 Comparison of satellite captured water coverage and model generated flow field of Poyang Lake during wet season

Fig. 4.24 Comparison of satellite captured water coverage and model generated flow field of Poyang Lake during dry season



Based on the close proximity of both sets of images, the simulated flow fields have further proven the ability of the model to replicate hydrodynamic behaviour in the lake in an accurate and reasonable manner. Although the flow velocity in locations around the lake can also be used to compare against simulated flow velocity from the model, data on the actual field-measured flow velocities are unavailable. Comparison using flow fields with recorded images is deemed to be sufficient in this case.

### 4.4.2 2-D Water Quality Validation

The 2-D water quality results from the simulation are compared against the field-measured data in 2008 for validation. As opposed to the 1-D validation that aims at locations near the 2-D model boundary locations, the current water quality validation focuses on the region around the main channel and the central of the lake district. The locations of the stations with field-measured data are illustrated in Figure 4.25. The validation herein will focus on four variables;  $\text{NH}_3\text{-N}$ , TP, DO and TEMP. The comparison between simulated results and field-measured data for these 4 variables is summarized in Figures 4.27-4.30. In those figures, the black lines represent the simulated results and the red circles are the field measurements. The  $x$ -axis labels the time of the year in 2008 and the  $y$ -axis marks the concentrations of the variables in mg/l or the temperature in degree Celsius.

The measured ammoniacal nitrogen ( $\text{NH}_3\text{-N}$ ) concentrations at Zhuxikou, Tangyin, GanjiangSouth and XinjiangWest are compared against the 2-D model predictions in Figure 4.27. Both Zhuxikou and Tangyin exhibited similar trend in simulation results and measured data, mainly due to their close proximity to the main channel in the northern region of the lake. Generally, there is a drop in ammoniacal nitrogen concentration during the summer wet season. This is caused by the high rate of nitrification from the microbes in the water, as well as an increased in water volume that lead to an increased dilution effect in the lake. Occasionally there are sudden peaks from the simulated results, which are due to an increase influx of high ammoniacal

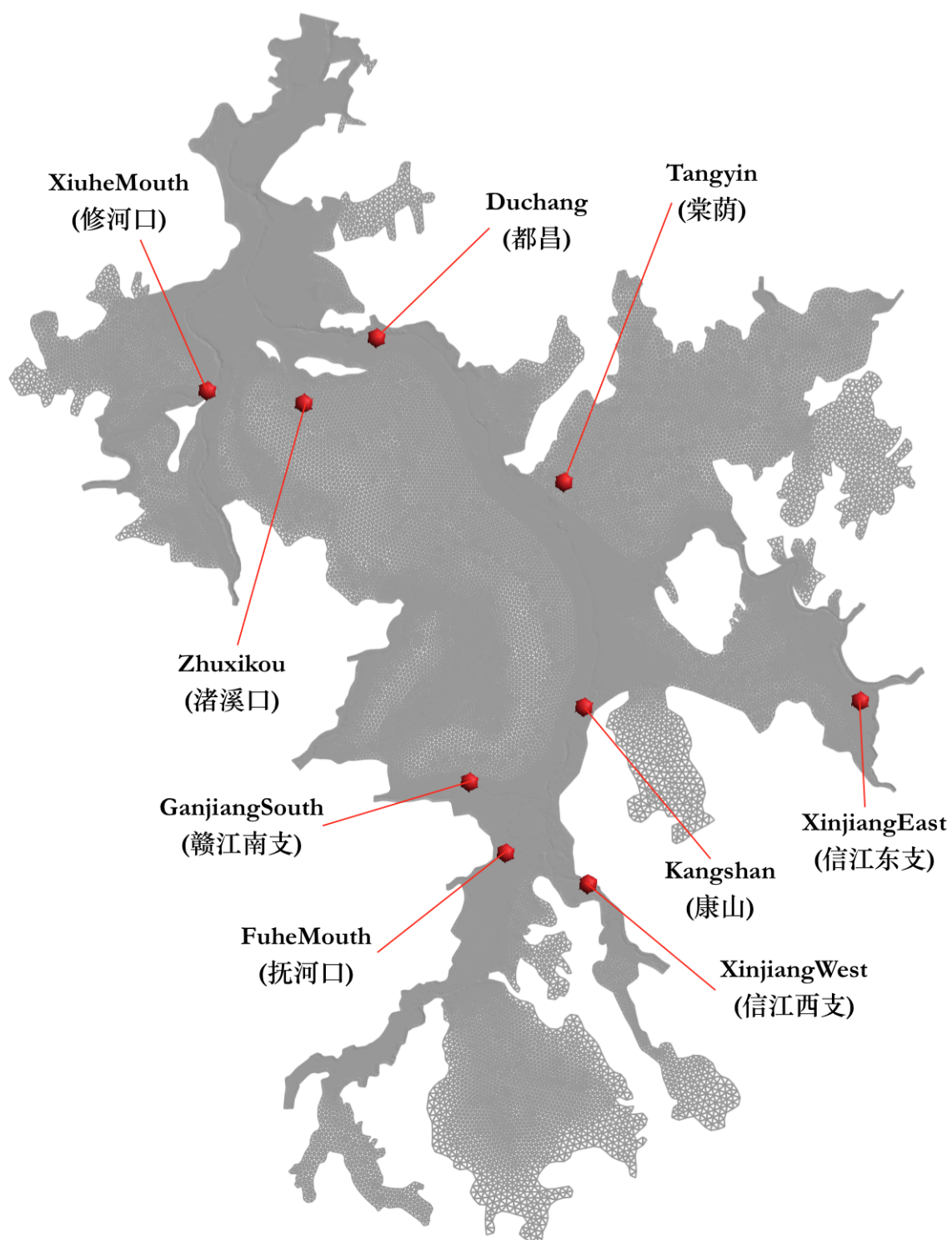


Fig. 4.25 2-D water quality model validation locations

## Models Development

---

nitrogen concentrated inflow from the five rivers during the beginning of the flooding seasons. The RMSEs and NSEs of the four locations range from 0.169 to 0.367 mg/l and from 0.052 to 0.928 respectively. GangjiangSouth illustrates an excellent model performance while Zhuxikou, Tangyin and XinjiangWest demonstrate an unsatisfactory one. The high NSE of GanjiangSouth is attributed to the model being able to successfully simulate the sudden rise in measurement value to good accuracy. The conditions in the other three locations are different with more than a several of the measurement points totally missed by the predicted results. These have significant effects on the resulting NSEs given that there are only 12 field measurements recorded within the period. For example, the NSE in XinjiangWest will drastically increase from 0.345 to 0.755 if the model prediction is closer to only two more field measured points in the figure. The limited number of field measurements magnifies the representation and impact of the variance between the model prediction and field measurements.

In Figure 4.28, the measured TP concentrations at Kangshan, GanjiangSouth, XiuheMouth and XinjiangWest are compared against the 2-D simulation. Kangshan and XiuheMouth have both showed a drop in TP concentration during the wet seasons, due to an increased biological uptake by microorganisms and algae in the summer months. GanjiangSouth and XinjiangWest did not exhibit the exact same trend due to their locations being closer to the boundary. The TP concentrations in those locations are dominated by the inflow TP concentrations instead. RMSEs and NSEs for the four locations range 0.007-0.046 mg/l and -1.932-0.830 respectively. Apart from XiuheMouth, the model performance at Kangshan (0.459), GanjiangSouth (0.795) and XinjiangWest (0.830) are close to the satisfactory to very good standards. The limited number of field measurements again plays a part in the poor performance at XiuheMouth. Three field measurements can be seen remote from the general model prediction and other field measurements. The presence of these three anomalies significantly reduces the NSE value from which could be close to 0.567 to the current value at -1.932.

## Models Development

---

Similar comparisons between the measured data and simulated results are performed for the water quality variable DO and TEMP. In the DO validation (Figure 4.29), simulated concentrations at Zhuxikou, Tangyin, Kangshan and FuheMouth all demonstrated a trend of higher values in the winter months and lower values in the summer months. Meanwhile, the simulated temperature results at Duchang, XinjiangEast, Kangshan and FuheMouth are realistic with a hot summer and a cold winter that match the climatic nature of a tropical location (Figure 4.30). Temperature, water volume and algal processes are among the major factors that contributed to DO variation. The rise in temperature and water volume during the summer season trigger DO depletion and promote dilution in the water bodies and hence resulting in the decrease of DO in the same period. In addition, temperature encourages bio-activities. Oxygen and nutrients uptake for algae growth increase during the wet season, resulting in the further decline of DO concentrations and correlating to the drop in TP concentrations as mentioned earlier. Despite being able to demonstrate the correct trends, the model performance in predicting the DO concentration is not satisfactory with RMSEs ranging 1.174-2.659 mg/l and NSEs of -2.846-0.213. In contrast, the predicted temperature records a very good performance with the field-measured data with RMSEs of 0.693-3.719 °C and NSEs between 0.780 and 0.993.

Simulation of nutrient concentrations in hydro-environment is challenging. Validation results in literature can be used as a general guidance. As mentioned in previous chapter, a coupled Artificial Neural Network with cluster technique to predict the impact of the barrage control on phytoplankton biomass in Poyang Lake was built in Huang et al. (2015a). The validation of such study in estimating the chlorophyll *a* concentration is shown in Figure 2.13 on Page 51. The simulation present a not very fitting correlation with the field measurements that mimics the circumstances seen in the validation in our study. In contrast, the validation carried out in Hu et al. (2012b) for TIN and TP concentration was satisfactory. Although no statistical indicator was provided to quantitatively support the process, the field data and simulation results

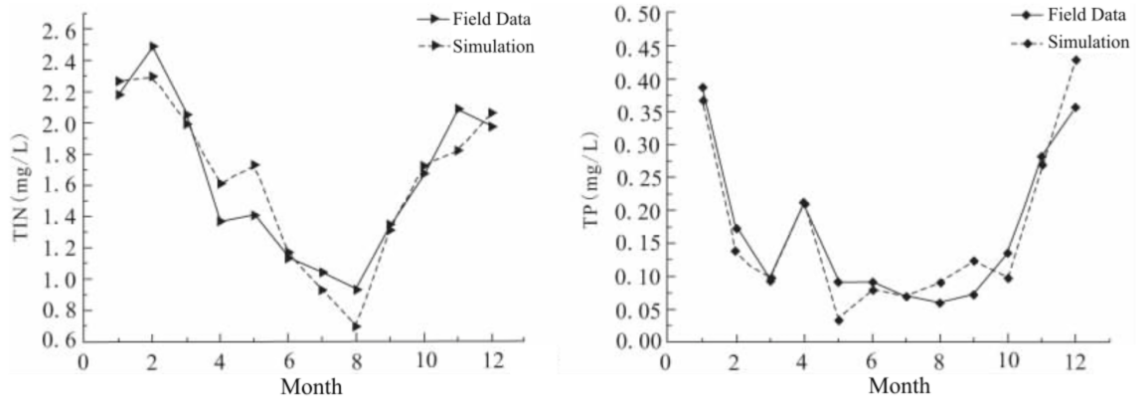


Fig. 4.26 Comparison of the simulated and field measured monthly-averaged TIN and TP in Poyang Lake for 2010 (Source: Hu et al., 2012b)

were in close proximity throughout the period in 2010 (Figure 4.26) and this study sets a standard for others to aspire to in terms of nutrients concentration simulation.

Deviation between computed results and observed measurements can be caused by many reasons in the modelling. Inaccurate specification of concentration at the model boundaries, misplacement or negligence of pollutant sources and incorrect initial concentrations and discharge loadings are potential factors triggered by external industrial, social and agricultural activities that are often difficult to locate, monitor and extract data. In terms of numerical modeling, defective hydrodynamic setup and water quality process description, as well as unstable numerical solutions are all possible causes of unsatisfactory model performance. Model simulations are generally poorer for shorter time steps than for longer time steps (Engel et al., 2007). In addition, the exclusion of sediment modeling in Poyang Lake in this model is also a factor that might contribute to the inaccuracy of the validation. The movement of sediments and its relationship with nutrients uptake and release in the lake environment are potential arguments for simulation inaccuracy and validation imprecision. Furthermore, movement of sediments changes the bathymetry of the lake environment and the unstructured mesh used in this study will not be able to project and modify the changes of landscapes and environment accordingly.

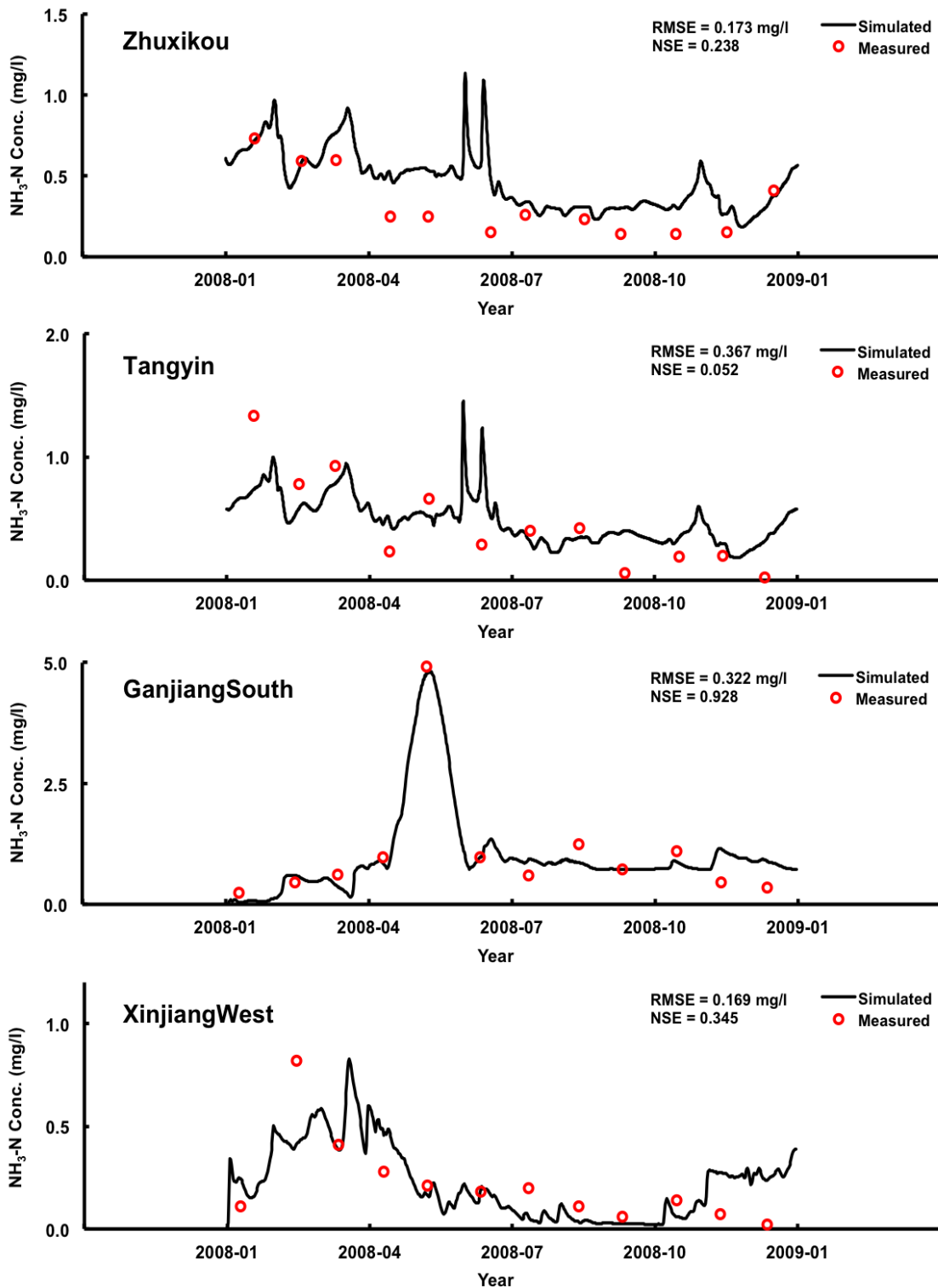


Fig. 4.27 Measured NH<sub>3</sub>-N compared with 2-D water quality model predictions at stations across Poyang Lake

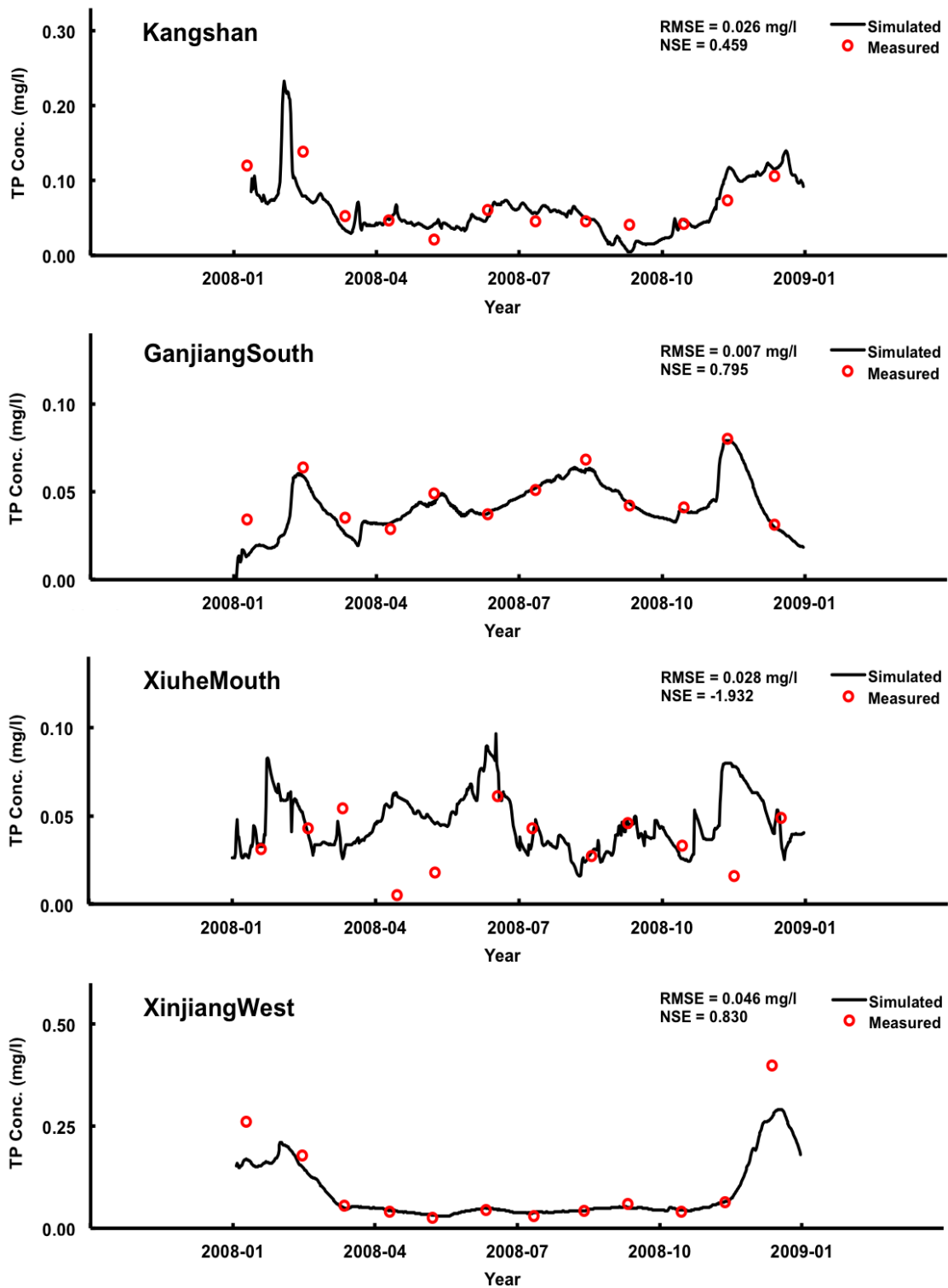


Fig. 4.28 Measured TP compared with 2-D water quality model predictions at stations across Poyang Lake

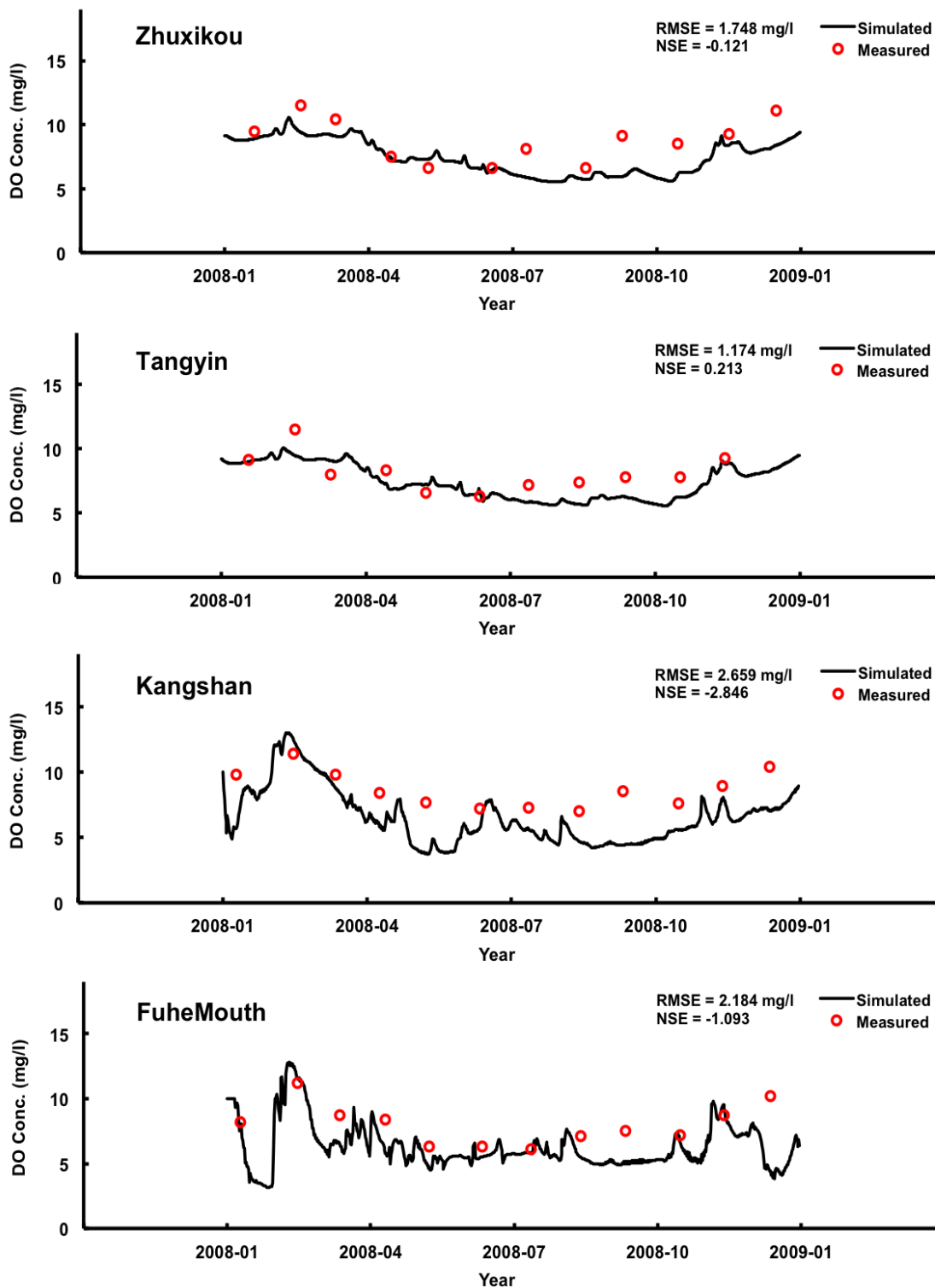


Fig. 4.29 Measured DO compared with 2-D water quality model predictions at stations across Poyang Lake

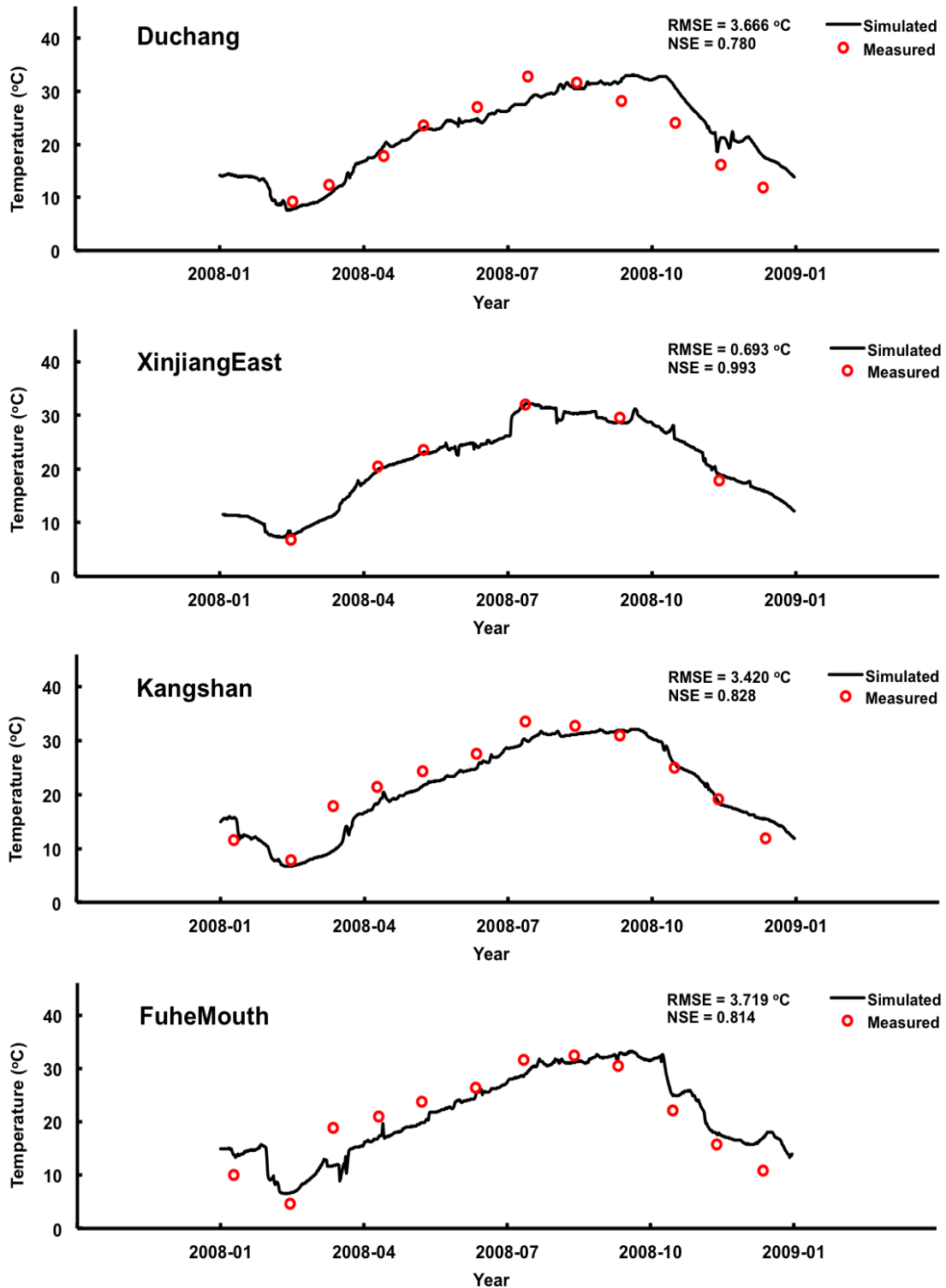


Fig. 4.30 Measured TEMP compared with 2-D water quality model predictions at stations across Poyang Lake

## Models Development

---

The numerical models are built upon layers of information that involved numerous mathematical formulation and solving methods through multi-dimensions. Errors could aggregate in the models through each stage of simulation and lead to discrepancy between measured data and simulation results during validation. Although high resolution mesh and local boundary conditions are added to the multi-dimensional models as an advancement from the simple 1-D cross-sections in the Poyang Lake basin, small and insignificant errors in the input data from the 1-D hydraulic model could alter the flow behaviour and concentration dispersion and transfer into miscalculations in the 2-D model. Sensitivity test with across the model parameters in both the 1-D and 2-D numerical models could also be performed to investigate the significance of the model variables. However due to the time constraint of this project such sensitivity test could only be done as future works.

Imprecise measured data due to inadequate and inaccurate field measurements may also cause variation. As seen from many of the figures in the validation process, some of the field-measured data are often recorded with unusual values that are not coherent with the general trends. To further study such phenomenon, the hydrology of the Poyang Lake region is further explored. Related studies on the hydrology of the Poyang Lake catchments show no abnormal hydrological events nor distinct hydrodynamic recordings in 2008 (Gao et al., 2014; Li et al., 2015a). The annual mean area of Poyang Lake basin and its annual budget with precipitation, evapotranspiration and outflow discharge for the year 2008 are all among average for the period 2006-2010, as seen in Table 4.5 (Liu et al., 2013). Majority of the literature focuses on the hydrological trends in Poyang Lake across a period of several decades. Localized research over a year-long period that demonstrates the micro variation with the hydrodynamics and water quality variables are very rare. Given the complex nature of the lake environment and relationships between the different variables, it is challenging to seek out simple coherent pattern for the explanation of particular behaviours in the field-measured data. Further work is required to explore in details the holistic interlinks and the degree of impact between different hydrological, hydraulic and water quality parameters.

## Models Development

---

Table 4.5 Annual mean area and annual budget of water balance of Poyang Lake basin for 2006-2010 (Source: Liu et al., 2013)

Year	Lake Area (km <sup>2</sup> )	Precipitation (mm)	Evapotranspiration (mm)	Outflow Discharge (mm)	Water Budget (mm)
2006	1985.7	1696.7	771.9	961.8	-37.0
2007	2075.2	1217.8	829.7	611.2	-223.1
2008	2220.9	1474.5	774.4	764.9	-64.8
2009	2092.9	1367.1	794.3	636.2	-63.3
2010	2528.8	2159.4	750.8	1325.6	83.0

## 4.5 Chapter Summary

This chapter illustrates the details of setting up the hydrodynamic and water quality model for 1-D, 2-D and 3-D simulations. Main components including the unstructured mesh, boundary conditions, control parameters and potential assumptions are documented. Model validation is performed using field-measured data from Poyang Lake. Both the hydrodynamic model produced respectable results in 1-D simulation that match the field-measured data. Since the 1-D simulation results are subsequently used as the boundary conditions for multi-dimensional simulations, focus on validation has been put on locations at the river-lake intersection and near the boundary of the lake. The validation for the 1-D water quality model is not very satisfactory in contrast. Statistical indices demonstrate a rather unsatisfactory performance for the model in predicting NH<sub>3</sub>-N and TP of the region. As for multi-dimensional simulation, several studies have been conducted to prove that 2-D simulation is as accurate as the 3-D simulation in this case, whilst providing more efficient computational usage and shorter simulation time. The validation of a 2-D simulation is also carried out with the hydrodynamic simulation showing great coherence with the field-measured data in 2008. The 2-D velocity flow field in both the wet and dry season matches well with the actual flow characteristics of Poyang Lake. For the validation with the water

## Models Development

---

quality simulation, there are variance seen in some of the locations for the variables  $\text{NH}_3\text{-N}$ , TP and DO, which are partially due to the lack of consistent field-measured data in a shorter span (1 year period) and the potential difference caused by sediment transport which is not considered in this study. Overall, the hybrid model performs fairly in simulating the hydrodynamic and water quality of Poyang Lake with room of improvement.

# Chapter 5

## Potential Barrage Water Management Schemes for Poyang Lake

### 5.1 Introduction

The Poyang Lake barrage project was proposed to maintain and control the lake's water levels from further decline under the influence of the climate change, the Yangtze River and urbanization in the Poyang Lake basin. The proposed project will involve a series of sluice gates being installed along the narrowest section of the channel at the northern mouth of the lake. The main goal of the project is to manage the water levels in Poyang Lake by closing the sluice gates during the dry seasons, while imposing no control on the water levels by opening the sluice gates in full during the wet seasons and allowing free exchanges of water, energy and biology between the lake and river (Hu and Ruan, 2011; Lai et al., 2016). By increasing the water volume and hence water surface area during the dry seasons, the project can create a positive impact through the conservation of wetlands and wildlife habitats, maintain freshwater resources for municipal and agricultural uses and generate economic gains from navigation, fishery and tourism. In support of the proposed barrage to be built, local government bodies and hydrological authorities have designed different regulation schemes for the project with various conditions and standards over the control of water levels.

### 5.2 Operational Schemes

In this study, five different proposed schemes (S1-S5) will be examined (Huang et al., 2011; Zhang et al., 2011). Scheme 1 was proposed by the Jiangxi province government based on a series of in-house hydrological studies. It will be concentrating on the overall impact of the barrage on the regions surrounding the Poyang Lake and in nearby areas within the province. Schemes 2, 3 and 4 are proposals put forward by the Yangtze River Water Conservancy Committee. These schemes focus on the overall picture of Yangtze River and the impact of the barrage on both Poyang Lake and downstream of the Yangtze River basin. Scheme 5 was designed by the China Institute of Water Resources and Hydropower Research (IWHR) to scientifically evaluate the barrage project through research and modeling and to offer objective opinions regarding the sustainability and environment of Poyang Lake. Various complex factors including environmental, political, economic and geographical reasons are behind these proposals but for the scope of this study only the technical and engineering aspects and the impact on the hydro-environment will be discussed. Although the proposed schemes are driven by their proposers with different aims and perspective, all of the schemes are for the benefits of Poyang Lake environment with the hope to tackle existing water issues. For analysis purposes, a reference scheme labelled as Scheme 0 will be used as a control with no barrage implementation and hence the hydrodynamics and water quality conditions are assumed to be at their natural state.

These proposals detail the barrage movement and water level controls in five hydrological flow periods in Poyang Lake: inflow period, storage period, recharging period, supply period and outflow period. Table 5.1 illustrates the difference between the schemes with respect to different flow periods and gate controls. All schemes follow free-flow state in their inflow period during the wet seasons. These schemes have predetermined criteria for water levels in the Lake and require different duration of operation at respective flow periods. During inflow period, the main objective of the

## Potential Barrage Water Management Schemes for Poyang Lake

---

gate is to maintain water levels of the lake and release flood pressure in the region. In storage period, the gate is controlled in such a way that the discharge rate and water levels are maintained at a certain degree for the benefits of river transports, ecosystem and sufficient water supply. During water recharging period in October, the month is split into 3 intervals of 10 days each. Gradual decrements are implemented during these intervals to reduce the water levels from approximately 14m to around 11.5m in general. Supply period aims to control the loss of water in Poyang Lake and maintain high water level. For outflow period, water levels are maintained for flood release purposes and hence are lower than previous periods.

The numerical model developed in this study is applied to examine the impact of different barrage schemes on Poyang Lake's hydro-environment. The operational patterns of the schemes in Table 5.1 are translated into variations in water levels at the location of the barrage over a period from 2005 to 2008 (Figure 5.1). These water levels will be entered into the model as the boundary condition at the barrage (BC1) for 2-D hydrodynamic simulation. Controlling the water levels at the barrage, which is at the outlet of the lake, will essentially change the flowing pattern and hence the hydrodynamics and solute behaviour of the entire lake.

In Figure 5.1,  $x$ -axis labels the time of the year in 2007 and the  $y$ -axis marks the surface elevation in meters. S0 represents the natural water level variations in the lake without any interference from the barrage control. Low water levels during the winter periods are obvious, with the lowest water levels often observed in December and January every year. The water levels gradually increase over the months of March to June, triggered by the flooding seasons in the Yangtze River and the five rivers. The high water levels are maintained in the months of July to September due to back flows into Poyang Lake triggered by the elevated water levels of Yangtze River during the wet seasons. From October onward, the water levels drop rapidly from above 15m to around 10m. The dry seasons arrive and the cycle repeats again. The same trend can be observed over the years.

## Potential Barrage Water Management Schemes for Poyang Lake

Scheme	S1	S2	S3	S4	S5
Proposed by	Jiangxi Province	Yangtze River Water Conservancy Committee	Yangtze River Water Conservancy Committee	Yangtze River Water Conservancy Committee	China IWHR
<b>Inflow Period</b>					
Date	1 May - 31 Aug	1 Apr - 31 Aug	1 Apr - 31 Aug	1 Apr - 31 Aug	1 Apr - 31 Aug
Water Level	>15.5 m	>15.5 m	>15.5 m	>15.5 m	15.5 m
<b>Storage Period</b>					
Date	1 Sept - 30 Sept	1 Sept - 30 Sept	1 Sept - 30 Sept	1 Sept - 30 Sept	1 Sept - 30 Sept
Minimum Flow ( $Q_{min}$ )	2,100 m <sup>3</sup> /s	-	-	-	-
Water Level	15.5 m	14.5 - 15.5 m	14.5 - 15.5 m	14.5 - 15.5 m	14.5 - 15.5 m
<b>Recharging Period</b>					
Date	1 Oct - 31 Oct	1 Oct - 31 Oct	1 Oct - 31 Oct	1 Oct - 31 Oct	1 Oct - 31 Oct
Water Level	>14 m	14.5 m; 14 m; 13 m; 11.5 m	14.5 m; 14 m; 13 m; 12 m	14.5 m; 13.5 m; 12.5 m; 11.5 m	>12 m
<b>Supply Period</b>					
Date	1 Nov - 29 Feb	1 Nov - 29 Feb	1 Nov - 29 Feb	1 Nov - 29 Feb	1 Nov - 29 Feb
Minimum Flow ( $Q_{min}$ )	925 m <sup>3</sup> /s	-	-	-	$Q_{out} = Q_{in}$
Water Level	-	10 - 11 m	12 m	10 m	12.5 m
<b>Outflow Period</b>					
Date	1 Mar - 30 Apr	1 Mar - 31 Mar	1 Mar - 31 Mar	1 Mar - 31 Mar	1 Mar - 31 Mar
Minimum Flow ( $Q_{min}$ )	-	-	-	-	10,000 m <sup>3</sup> /s
Water Level	12 m	10 - 11 m	12 m	10 m	11 m

Table 5.1 Proposed barrage operational schemes

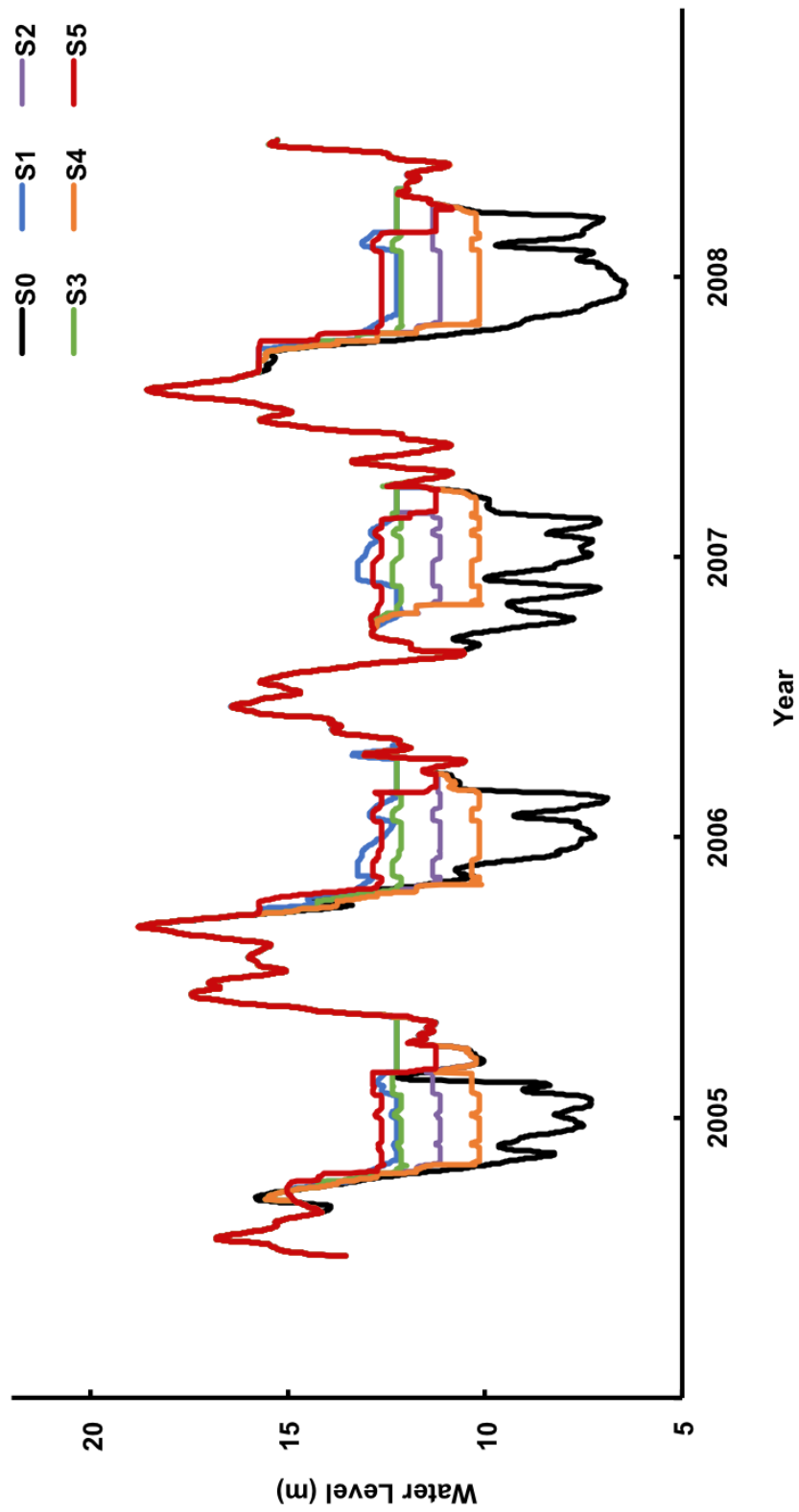


Fig. 5.1 Water levels at the proposed barrage location under different operational schemes

## Potential Barrage Water Management Schemes for Poyang Lake

---

The implementation of water level control from S1 (red line) includes dramatically rising the water levels of the lake during the dry seasons. It proposes to store water in Poyang Lake during the winter so that the normally low water levels at around 10m can be raised to nearly 15m. Once the dry period is over, S1 allows the natural environment to take control again by releasing the stored water, resulting in the drop in water levels in March and April prior to its rise again due to the flooding season from May to August. It is logical that the Jiangxi province is proposing a barrage control plan with high water levels characteristics to aggressively tackle the problem of water shortage in Poyang Lake. However, such an approach might be less favourable to other provinces downstream of Yangtze River as the problems might migrate elsewhere with such big changes in a complex and interlinking water environment.

S5 proposed by the China IWHR (orange line) exhibits similar barrage control as S1. Both schemes strive to maintain high water levels in the winter periods, although S5 has more steady and stable levels throughout as compared to S1. Meanwhile, the schemes (S2-S4) suggested by the Yangtze River Water Conservancy Committee have moderate approaches. These schemes illustrate three different degrees of engineering control with water levels spread out between 11m to 14m during the dry seasons, with S3 (green line) being the most ambitious, S2 (purple line) being the intermediate and S4 (blue line) being the mildest. S3 has the highest water level standard among the three that is only slightly lower than those levels set in S1 and S5. In contrast, S4 has the lowest water levels control and is closest to the natural flow state of the lake. These three schemes present a relatively gentle approach compared to S1 and S5, with considerations on minimizing the disturbance on the natural wildlife habitats and on hydraulics of downstream cities such as Shanghai and Nanjiang. Mass and sudden increase in water levels could potentially flood the wetlands and disrupt natural processes, as well as create water problems in downstream regions. The degree of acceptable rise in water levels will be of interest in our subsequent analysis. From Figure 5.1 it can be seen that the schemes and their water levels are most distinct in the period of 2007, with the water levels in descending order of  $S1 > S5 > S3 > S2$

> S4 > S0. Simulations using the 2-D model built in this study will be based on the variation of water levels in 2007 under the different barrage control schemes (S0-S5).

### 5.3 Barrage Effect on Lake Hydrodynamics

Simulation using the coupled 2-D model with each scheme's barrage control proposal have produced hydrodynamic results that include the temporal and spatial variation of the water levels in Poyang Lake in 2007. Four locations; Xingzi (northern), Wucheng (northwestern), Kangshan (southern) and Boyang (eastern) are chosen to represent the changes in water levels at different parts of Poyang Lake. The surface elevations at these locations under the influence of the schemes in 2007 are illustrated in Figure 5.2. In the figures, the  $x$ -axis represents the time of the year in 2007 and the  $y$ -axis marks the water levels in meters.

In all the diagrams, S0 represents the natural scenario in which no barrage control is implemented and S1 to S5 are colour coded lines as shown in the legend. The diagrams demonstrate the intention of the barrage control, which is to have no interference with the lake's flow during the wet summer seasons and only to increase and maintain its water levels in the dry winter seasons, by showing the divergence of water levels under different schemes during the winter months (January to April, October to December) and the convergence of all schemes into the same water levels fluctuation throughout the wet seasons from May to September.

The scheme comparison on the surface elevations also shows that the resulting water levels fluctuation is correlated to the degree of barrage control. Of the five schemes, S4 has the lowest water levels at the barrage during the dry period and this is reflected on other locations across the lake. In all three locations, S4 (blue line) exhibits the lowest water levels among the schemes and is the closest to the natural water levels throughout. The water levels in S2 and S3 follow the similar trend and gradually increase according to the rise of water levels at the barrage under the same schemes.

## Potential Barrage Water Management Schemes for Poyang Lake

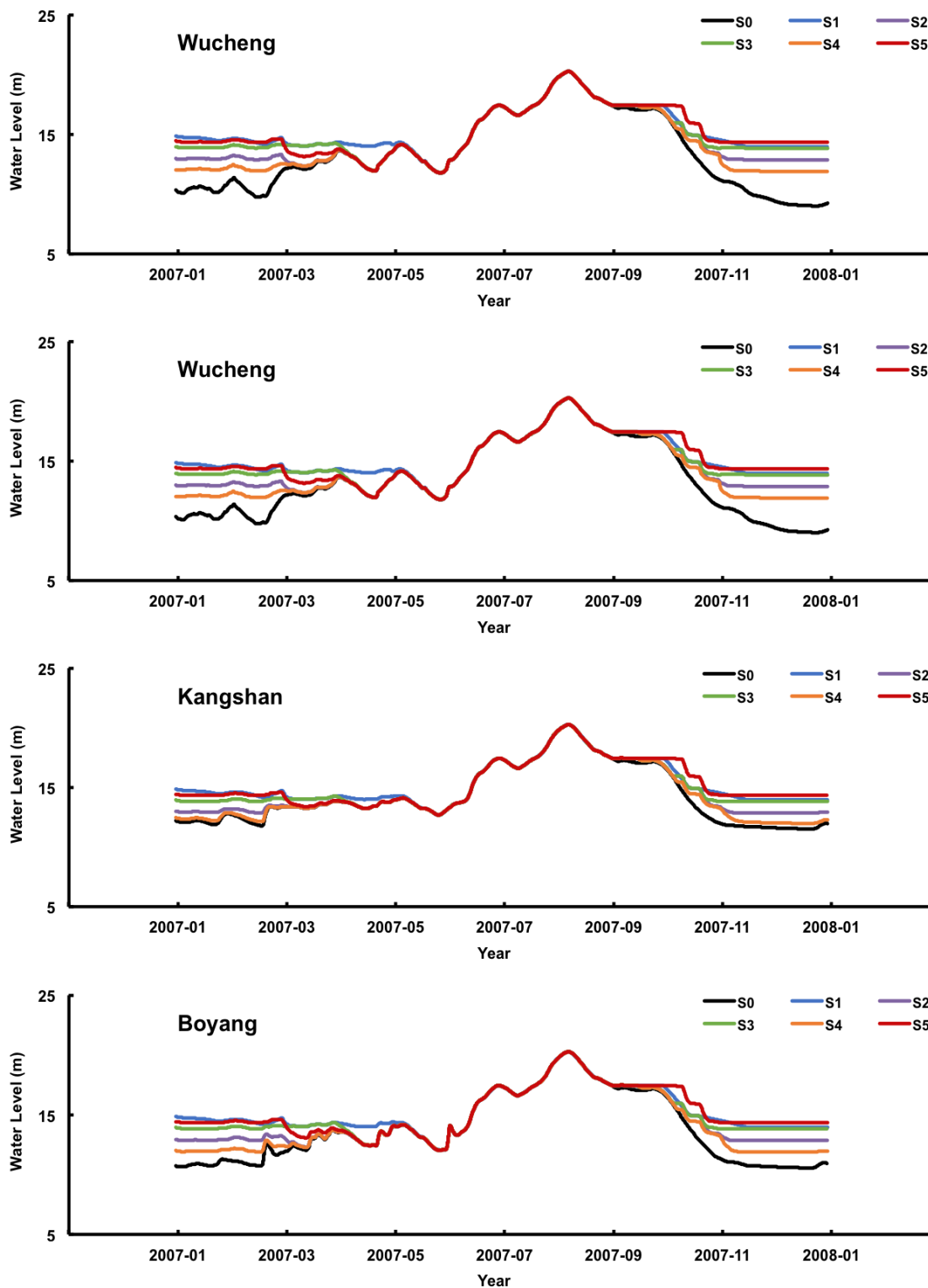


Fig. 5.2 Scheme comparison of water levels at Xingzi, Wucheng, Kangshan and Boyang

## Potential Barrage Water Management Schemes for Poyang Lake

---

Both S1 and S5 result in the highest water levels in all three locations, demonstrating that the high water levels plan at the barrage would effectively translate into high surface elevations in areas across Poyang Lake. These diagrams have shown that the hydrodynamics of Poyang Lake reacts to the barrage control according to the degree of intervention on water levels.

The gaps between the schemes however, vary between locations. The difference between water levels generated by different schemes in the winter season at Kangshan is smaller than those in Wucheng, Xingzi and Boyang. The smaller differentiation in water levels at a southern location further away from the barrage may suggest that the barrage's effect decreases according to distance and at locations with higher elevations in general. Locations in the northern and eastern regions will be influenced by the barrage in greater degree, as shown by the larger differentiation in water levels between different schemes at Xingzi, Wucheng and Boyang.

The influence of the barrage control on different regions of Poyang Lake and the global Poyang Lake domain can be investigated further by using the spatial distribution diagram. The natural variation of surface elevation in Poyang Lake is simulated and illustrated as shown in Figures 5.3, 5.4 and 5.5. These figures contain snapshots of the simulation throughout the year in 2007 with a color palette indicating the surface elevations of the lake domain.

In Figure 5.3, the natural state of the lake with no barrage implementation is shown. Image from Figure 5.3a illustrates a clear outline of the low water levels in the main river channel during the winter period. The lake is reduced to the characteristics of a river and the low surface elevations (7-9m) are obvious in blue colour towards the top half of the lake. As the flooding season begins, gradual rise in water levels can be seen in Figures 5.3b and 5.3c with the fading of blue colour and the emergence of green areas (12-14m). The increase in water levels becomes prominent through the summer months under both the flooding seasons in the five rivers and in the Yangtze River.

## Potential Barrage Water Management Schemes for Poyang Lake

---

Surface elevation peaks uniformly in the lake at 18m in Figure 5.3c. As the drying season approaches, surface elevations drop to medium levels in October (Figure 5.3g) and return to the lowest levels in around December (Figure 5.3h), similar to those in January and the cycle repeats.

Figures 5.4 and 5.5 describe the surface elevations of the domain in identical period and simulation setup, but with the implementation of the barrage operating under Scheme 1 and Scheme 4 respectively. S1 proposes the highest water levels control at the barrage among all the schemes and its effects are demonstrated distinctively by the spatial distribution of surface elevations in Figure 5.4. The barrage raises water levels in the dry season, resulting in a relatively homogeneous surface elevations across the lake district at an earlier stage in the year. The previously low surface elevations along the main channel of the lake disappear in the early months of 2007 (Figures 5.4a and 5.4b). Little difference can be seen between the winter and spring months as the surface elevations stay constant at about 11-16m from January to June. The great surge of water levels during the flood seasons can be seen in Figures 5.4e and 5.4f, with surface elevations rising to about 18m. When the barrage is not in effect in the wet seasons, the hydraulic behaviours of the lake in S1 mimics that of the natural state (S0). In the later months of 2007, the water levels drop and stabilize at around 12-13m (Figures 5.4g and 5.4h), as opposed to the significant decline observed in the same months in S0. The overall trend of surface elevations under S1 shows a less volatile water levels fluctuation over the course of the year.

Scheme 4, being the scheme with the lowest water levels setting at the barrage, shows an influence on the surface elevation by rising the water levels of the lake, albeit in a lesser degree than Scheme 1 (Figure 5.5). The surface elevations in January and March in S4 are in the range of 10-12m (Figures 5.5a - 5.5c), which is higher than those in S0 but lower than those in S1. The differences in surface elevation between the schemes are obvious with S0 showing clear outline of the main channel in blue, S4 showing patches of blue-green colour at higher surface elevation and S5 showing

## Potential Barrage Water Management Schemes for Poyang Lake

---

a larger region of light green that indicates the highest water levels among the three schemes. During the flooding period S4 exercises no barrage control similar to S0 and S5 and the surface elevations rise to 16-18 m (Figures 5.5e and 5.5f) accordingly. In the later months in 2007 the drop in water levels began with S4 having higher surface elevations than S0 but not as high as those in S1 (Figures 5.5g and 5.5h). This follows the same pattern among the schemes, as shown in the earlier winter months in the year where S4 is the median between the bolder S5 with higher water levels control at the barrage and the natural state S0 with low water levels during the dry period.

The difference between scenarios with barrage control (S1 and S4) and the natural state (S0), together with the contrast in degree and rate of surface elevation rise between S1 and S4, have further reinforced that the highest the water levels set at the barrage, the greater the rise in water levels for the lake.

The rise in water levels due to barrage control will lead to the increase of water volumes and the expansion of water surface areas in Poyang Lake during the dry seasons. Under natural conditions, the water surface areas in 2007 were recorded at 1,831 km<sup>2</sup> and the water volume in the lake at 66.9×10<sup>8</sup> m<sup>3</sup>. Results generated from the numerical model under different schemes are summarized in Table 5.2 below:

Table 5.2 Water surface area and volume of Poyang Lake under Scheme 0-5

Scheme	0	1	2	3	4	5
Water Surface Area (km <sup>2</sup> )	1,831	2,244	1,995	2,148	1,914	2,251
Water Volume (×10 <sup>8</sup> m <sup>3</sup> )	66.9	80.7	71.3	76.3	69.0	81.4

S5 provides the largest increase in both the water surface area and volume among all the schemes due to its high water level control at the barrage. S4 has relatively the lowest impact on water level changes and hence its impact on the surface areas and volume is also the smallest. In general, the influence of barrage on water volume changes is relatively small, with the biggest impact coming from S5 at 14.5×10<sup>8</sup> m<sup>3</sup> that is at ~20% of the lake capacity at most. The increase in volume in S4 is only at

## Potential Barrage Water Management Schemes for Poyang Lake

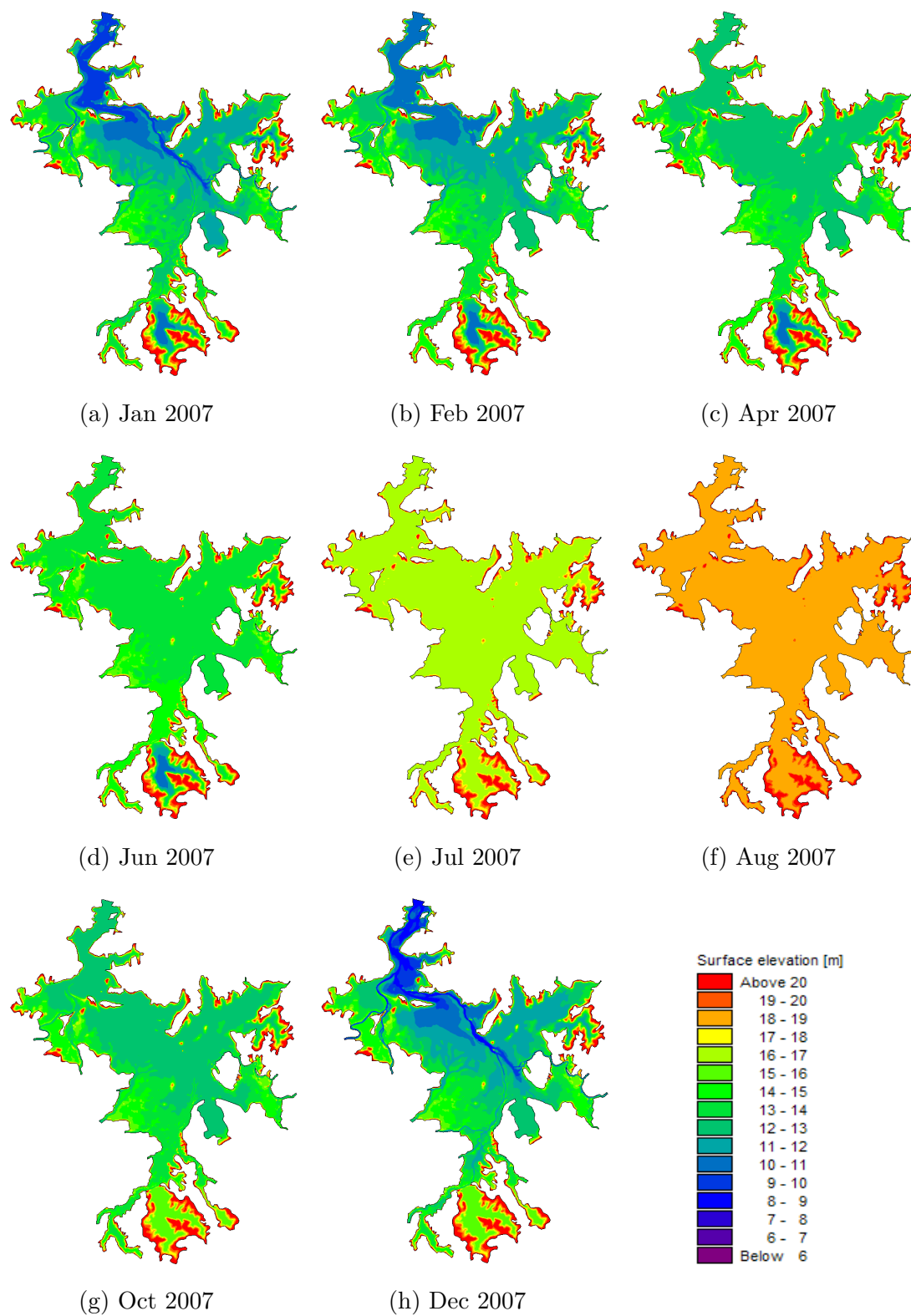


Fig. 5.3 Scheme 0 surface elevation spatial distribution in 2007

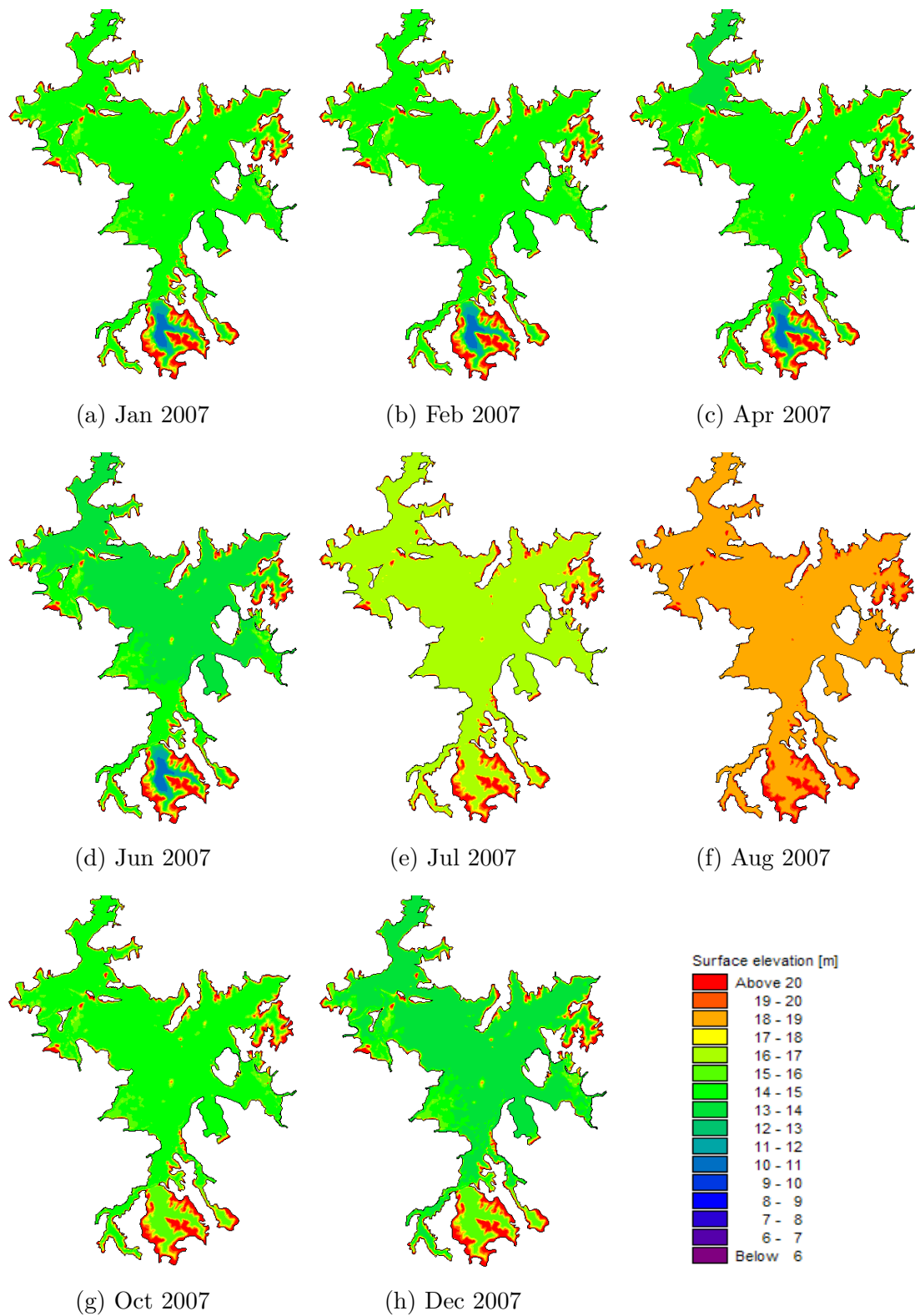


Fig. 5.4 Scheme 1 surface elevation spatial distribution in 2007

## Potential Barrage Water Management Schemes for Poyang Lake

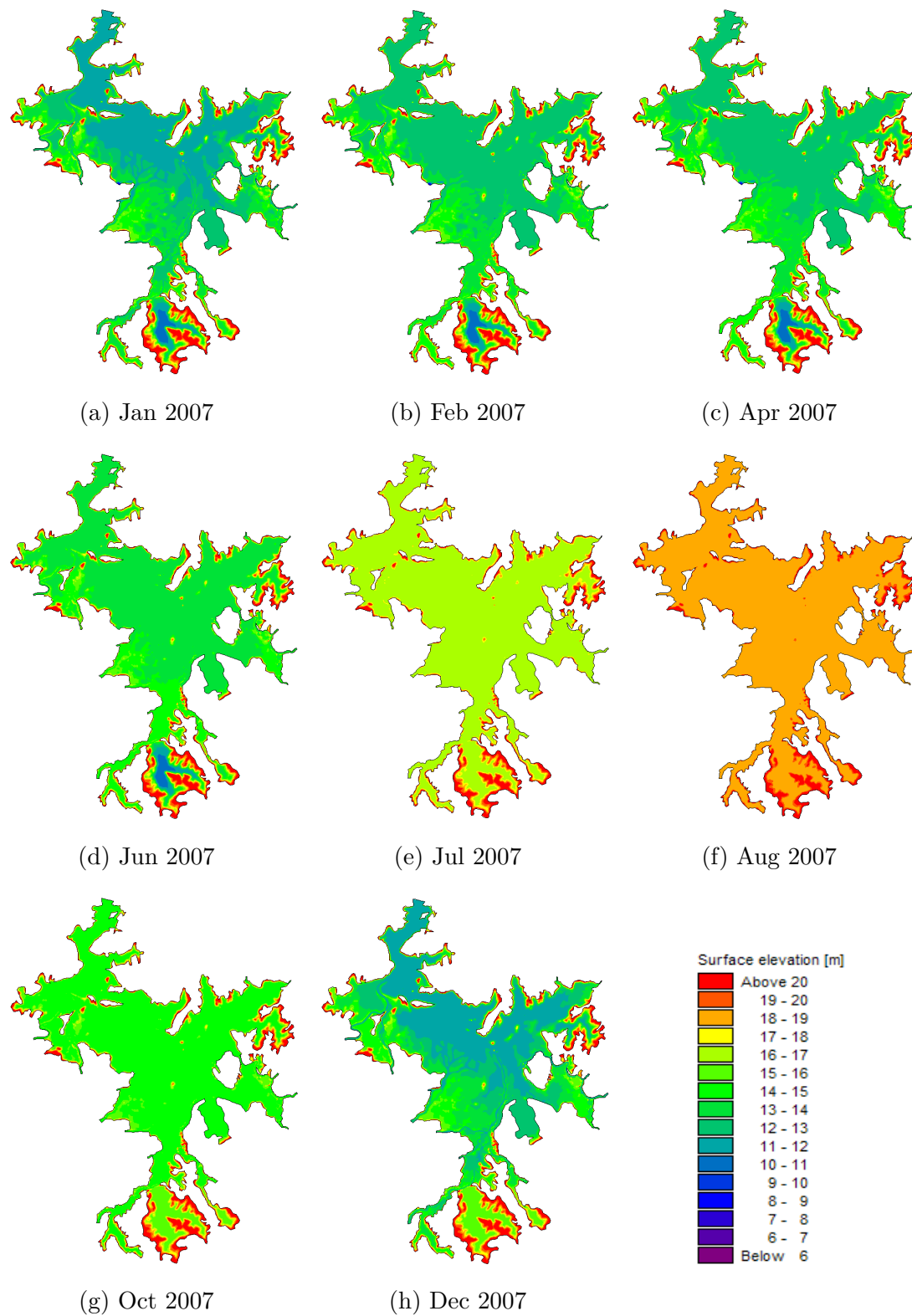


Fig. 5.5 Scheme 4 surface elevation spatial distribution in 2007

## Potential Barrage Water Management Schemes for Poyang Lake

---

$2.1 \times 10^8 \text{ m}^3$  which is a  $\sim 3\%$  change. With the Poyang Lake being a wide but shallow water body, the barrage has significant influence on increasing the surface areas through the rise of water levels, however the impact on water volume is limited.

Although successfully alleviating the problem of low water levels in the dry seasons, the rapid increase in water levels under the barrage schemes will also bring subsequent environment concerns. Reduction in water level fluctuation in the lake will diminish the flow exchange between the Yangtze River and Poyang Lake, hence decreases the water flow rate and velocities. Lower water turnover rate could result in longer retention time for pollutants and cause eutrophication. Moreover, huge rise in water level will flood extra lake regions that potentially include wetland areas and wildlife habitats, in which wet-dry conditions and sun radiation are essential. Further investigation is needed on the impact of the barrage scheme on these aspects.

### 5.4 Barrage Effect on Water Quality

The water quality of Poyang Lake under different barrage control schemes is examined. Simulations using the hydro-environment model developed in this study have produced water quality results that include the temporal and spatial variation of three water quality variables in Poyang Lake in 2007. These three variable concentrations; dissolved oxygen (DO), ammoniacal nitrogen ( $\text{NH}_3\text{-N}$ ) and orthophosphate ( $\text{PO}_4\text{-P}$ ), are chosen because of their pivotal roles in many of the bio-chemical processes in the lake environment. Three locations; Boyang, XiuheMouth and Xingzi, are chosen to represent the changes in concentrations of the water quality variables at different parts of Poyang Lake.

#### 5.4.1 Impact on DO Concentration

In Figure 5.6, the DO concentrations at Boyang, XiuheMouth and Xingzi under the effect of barrage control schemes are illustrated. In the figures, S0 represents the

## Potential Barrage Water Management Schemes for Poyang Lake

---

natural scenario in which no barrage control is implemented and S1 to S5 are colour coded lines as shown in the legend. The  $x$ -axis labels the time of the year in 2007 and the  $y$ -axis marks the DO concentration in mg/l. The DO concentration follows a similar trend in all the three locations with generally higher DO concentrations during the dry winter period and lower DO concentrations in the wet summer times. The increase in temperature, reduction in flow rate due to flooding and the growth of algae and microorganisms are potential causes of such concentration decline.

The difference in influence of the barrage scheme is not significant across the three locations. In the early months of the year, high DO fluctuation is seen in all the schemes and locations prior to the flooding season in which the different concentrations from the various schemes converge under the same hydraulic characteristics. The concentrations then diverge again in the later stage of the year as water levels drop. S1 and S5, being the two schemes with the highest water level control at the barrage, resulted in the lowest DO concentrations among all the schemes. This could be due to the elevated water levels reducing lake-river exchange and water velocities, leading to a lesser degree of current induced reaeration in the water bodies. This reason can be applied across all the schemes as nearly all the schemes in all three locations have recorded lower DO concentrations than that of the natural state (S0). The DO concentration at the end of 2007 at Xingzi in particular, shows great reduction under the use of barrage schemes from the original concentration in black line. The decrease in DO concentrations could be vital as aquatic wildlife and water vegetation in Poyang Lake requires DO for growth and survival. Large increase in water levels in the region under the barrage schemes could risk damaging and endangering the living habitats of many wildlife species in the water environment of Poyang Lake.

The effect of DO depletion might not be noticeable in Figure 5.6, given that the locations in discussion are in close proximity with the boundary and could be affected by inflow DO concentrations. In Figures 5.7-5.9, the DO concentrations under the influence of barrage schemes across the whole of Poyang Lake domain are present.

## Potential Barrage Water Management Schemes for Poyang Lake

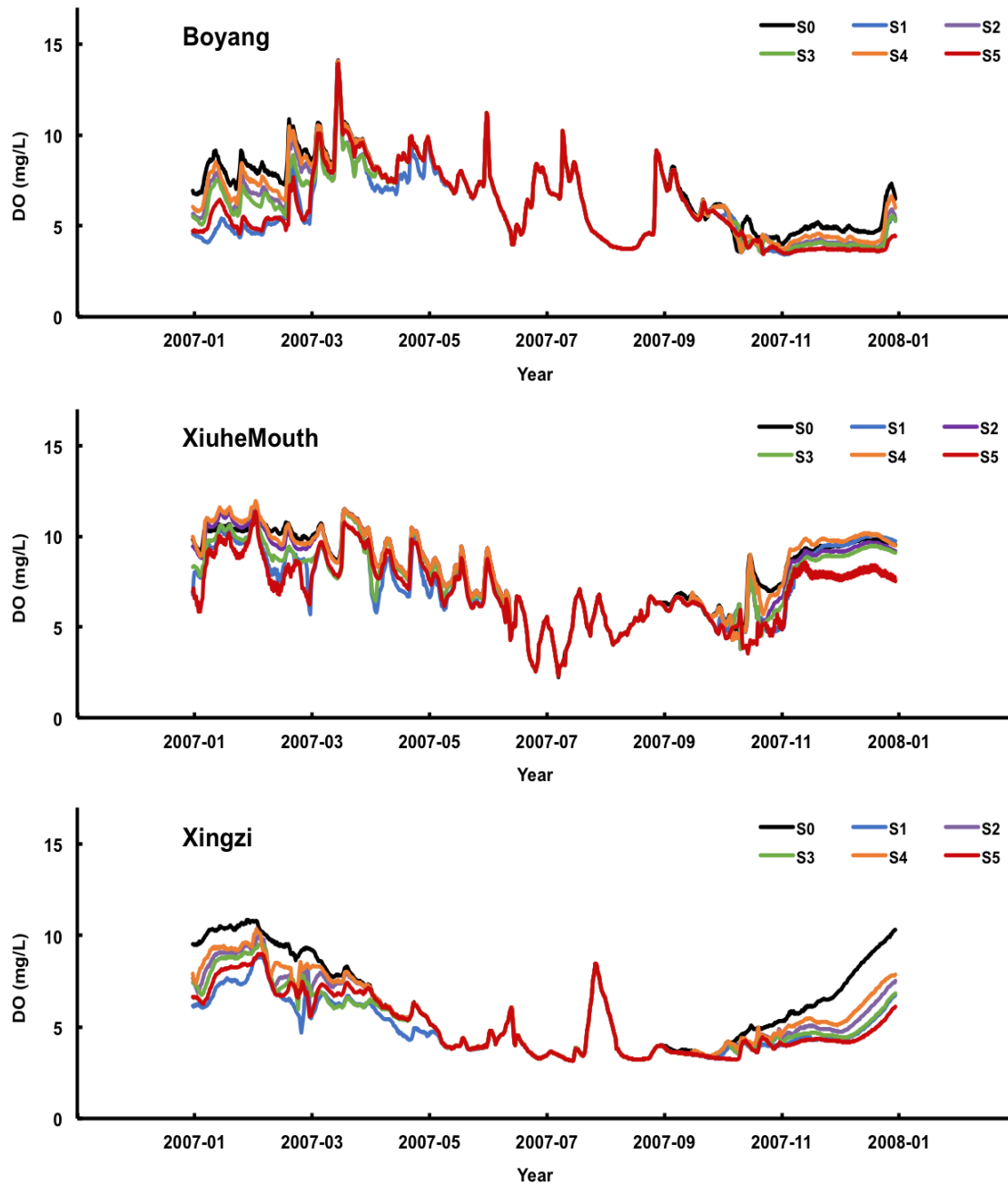


Fig. 5.6 Scheme comparison of DO at Boyang, XiuheMouth and Xingzi

## Potential Barrage Water Management Schemes for Poyang Lake

---

Figure 5.7 represents DO concentrations in its natural state in 2007. Figures 5.8 and 5.9 show the same variable under the implementation of S1 and S4 respectively. In its natural state, the DO concentrations in the early months of 2007 (Figures 5.7a and 5.7b) show great variation along the main channel ranging between 4.0-11.0 mg/l. As the water levels rise in the flooding season, the DO concentrations begin to decrease from 5.0-8.0 mg/l in April (Figure 5.7c) to below 3.0 mg/l in July (Figure 5.7e). Although there are influx of high DO concentrations from some of the boundaries in the west side of the lake, the overall DO concentration in the domain remains below 3.0 mg/l in Figure 5.7f. As the dry season returns, water levels drop and the water flow in streams increases and facilitates oxygen exchange, the narrow line of higher DO concentration is seen again in Figure 5.7h.

In Figure 5.8, high water levels induced by the barrage scheme S1 have created a vastly different spatial distribution of DO concentration than that in S0 in the early months of 2007. During the dry season, rise in water levels reduces the current induced aeration in the lake and both Figures 5.8a and 5.8b show a majority of low DO concentrations at around 3.0 mg/l with a burst of high DO concentration on the northwestern part of the lake due to DO concentrated inflows from the boundaries. As the flooding season approaches, continuous increase on water levels combining with the rise in temperature leads to a further reduction in the DO concentrations. Throughout the summer period (Figures 5.8d-5.8f), the majority of the lake's DO concentrations are below 3.0 mg/l, which are below the usual DO standard of 5.0 mg/l for aquatic wildlife. As water levels decline in the winter months, little variation can be seen in DO concentrations (Figures 5.8g and 5.8h). High DO concentrations incoming from the northwestern boundaries in the lake can not alter the general low DO concentrations across the lake domain.

Although Scheme 4 exhibits the lowest degree of water level rise among the schemes, its effect on the DO concentration is apparent. The main channel with high DO concentrations in Figures 5.9a and 5.9b exist, in contrast to its absence in S1, but

less distinct than that in S0. From April onward, S4's DO concentration distribution looks similar to that in S0 (Figure 5.9c). S4 is able to reinstate quickly because of its relatively small water level rise compared to S1. In the flooding season, the scheme exhibits similar concentration distribution as those in S0 and S5 (Figures 5.9d-5.9f). In the winter months, the drop in water levels and higher water flow return the DO concentrations in the main channel to a higher level at about 4.0-5.0 mg/l (Figure 5.9h). Overall, S4 operates in a moderate manner during the dry season that does not disturb the DO concentrations as much as S1, but the rise in water levels certainly hinders the reaeration process in the lake and the overall reduction in DO concentrations is evident from the figures.

### 5.4.2 Impact on NH<sub>3</sub>-N Concentration

The effects of barrage schemes on the lake's NH<sub>3</sub>-N concentration are present in Figure 5.10. The same three locations; Boyang, XiuheMouth and Xingzi, used in the DO concentration comparison are adopted herein. In the figures, S0 represents the natural scenario in which no barrage control is implemented and conditions under S1-S5 are lines colour coded as shown in the legend. The *x*-axis labels the time of the year in 2007 and the *y*-axis marks the NH<sub>3</sub>-N concentration in mg/l. The NH<sub>3</sub>-N concentrations from the three locations are volatile during the early months of the year and become smooth during the summer with extremely low concentrations. As the dry season arrives again, the NH<sub>3</sub>-N concentrations rise again. The vigorous fluctuations of NH<sub>3</sub>-N concentration under different schemes during the first few months of 2007 could be due to the influence of nearby inflows with unstable NH<sub>3</sub>-N concentrations. This could happen when the inflow rivers have multiple pollutant sources upstream such as industrial plants and agricultural farms in which chemicals and fertilizers are used and discharged in the water bodies. As a result, the NH<sub>3</sub>-N concentrations fluctuate in greatly with occasional spikes. During the flooding season, the increase in water quantity is able to dilute the pollutants and hence the concentrations reduce.

## Potential Barrage Water Management Schemes for Poyang Lake

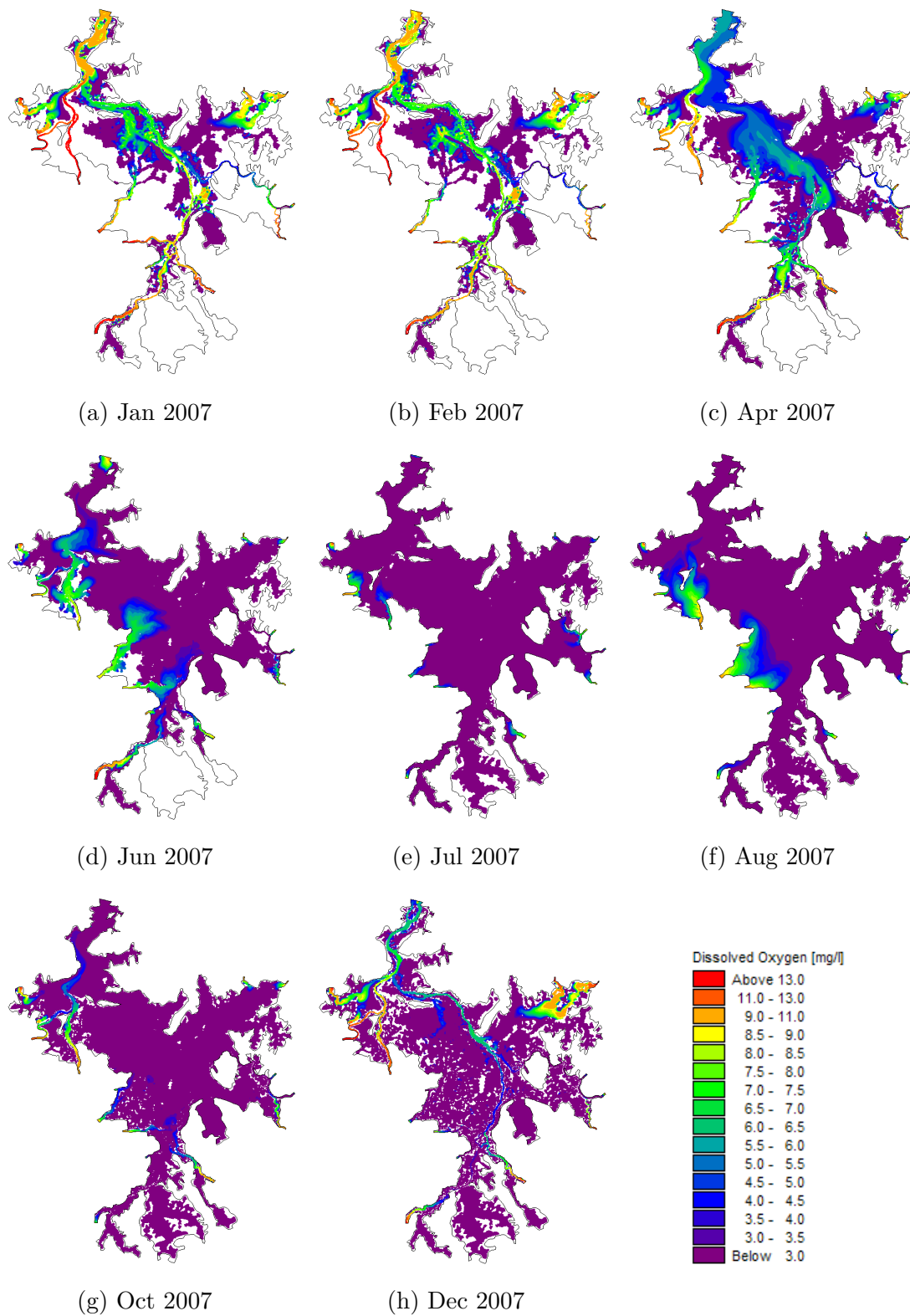


Fig. 5.7 Scheme 0 DO spatial distribution in 2007

## Potential Barrage Water Management Schemes for Poyang Lake

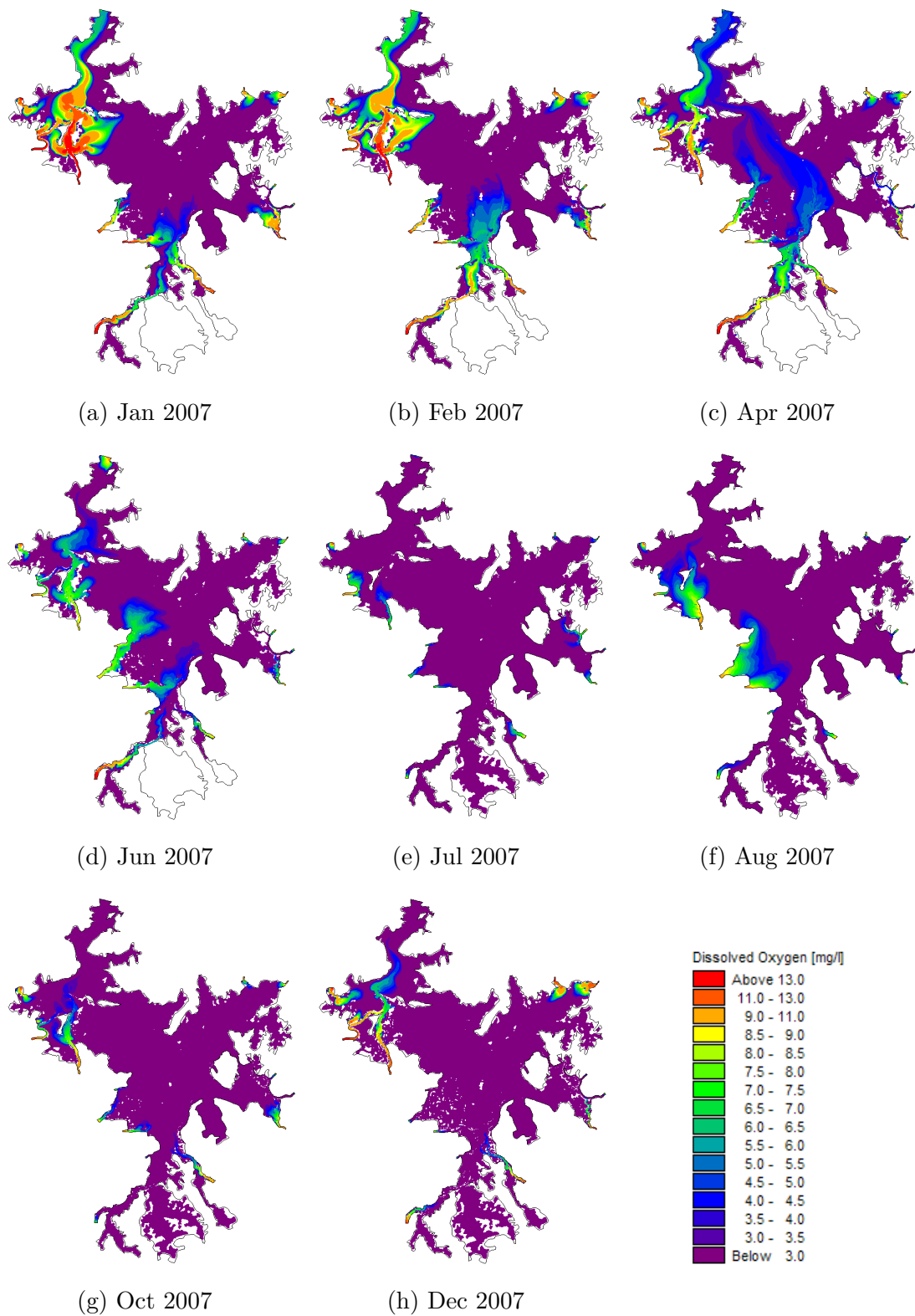


Fig. 5.8 Scheme 1 DO spatial distribution in 2007

## Potential Barrage Water Management Schemes for Poyang Lake

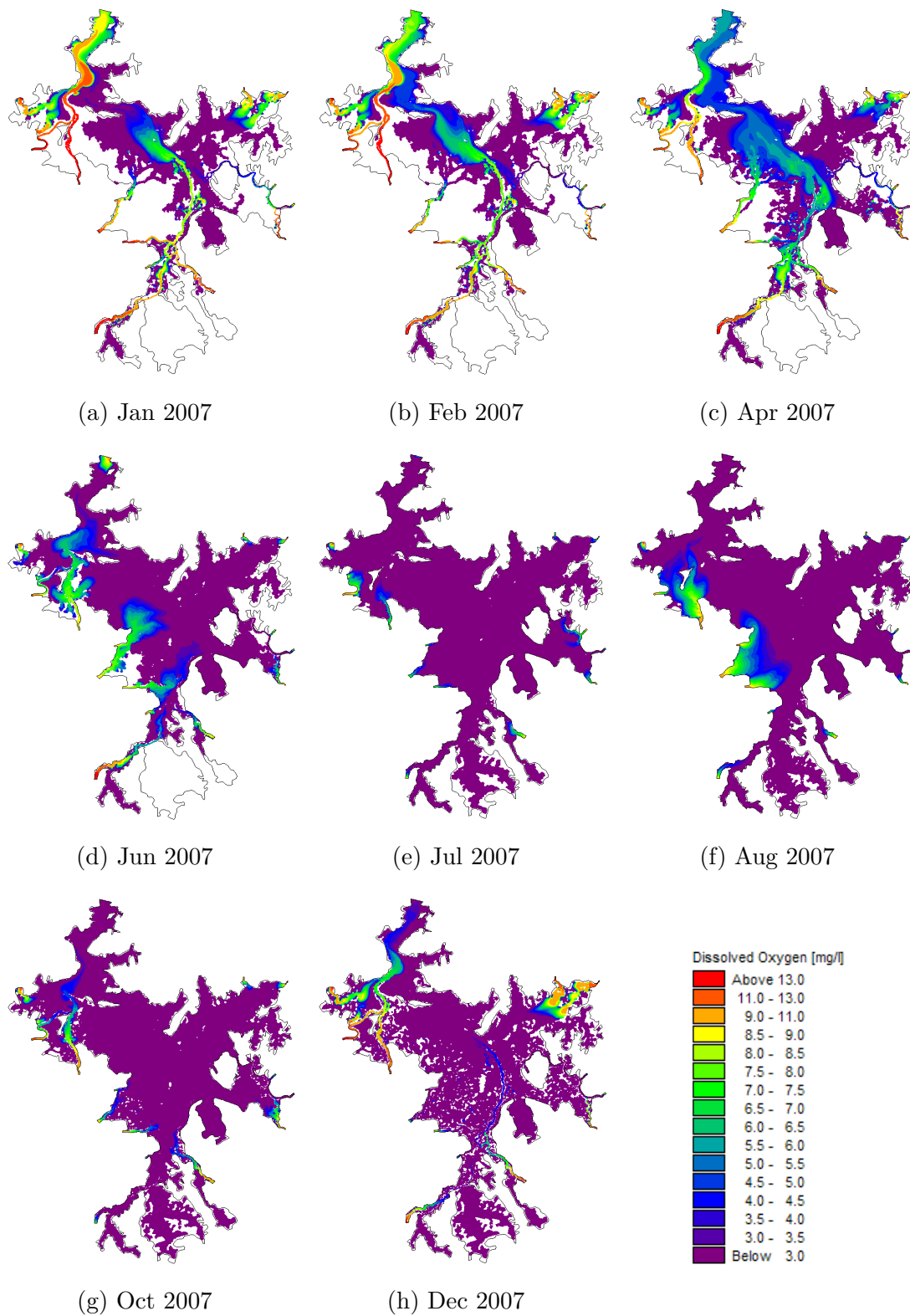


Fig. 5.9 Scheme 4 DO spatial distribution in 2007

## Potential Barrage Water Management Schemes for Poyang Lake

---

The influence of different barrage schemes on  $\text{NH}_3\text{-N}$  concentration correlates to the amount of water level rise in the schemes. The difference between the schemes is most obvious during the first half of the year, when higher water levels schemes such as S1, S3 and S5 showing the lowest  $\text{NH}_3\text{-N}$  concentration among the schemes. In the second half of the year when the  $\text{NH}_3\text{-N}$  concentration is very low, difference between the  $\text{NH}_3\text{-N}$  concentration under the schemes is minuscule. Nonetheless, all the barrage schemes have demonstrated that increasing water levels and water volume in Poyang Lake will enhance the dilution effect of  $\text{NH}_3\text{-N}$  in the water and hence resulting in a reduction in the  $\text{NH}_3\text{-N}$  concentration, as shown by the colour lines underneath the black line in all three locations in the figures.

In Figures 5.11-5.13, the spatial distribution of the  $\text{NH}_3\text{-N}$  concentrations in Poyang lake under the effect of barrage schemes are shown. The natural state of the distribution with no barrage influence is shown in Figure 5.11. During the early dry period in the lake, high  $\text{NH}_3\text{-N}$  concentrated inflows from various boundaries ranging from 0.025-1.00 mg/l enters Poyang Lake, resulting in distinct pathways of higher  $\text{NH}_3\text{-N}$  concentration across the lake domain (Figures 5.11a and 5.11b). When the flooding season begins, increase in water levels begin to dilute the  $\text{NH}_3\text{-N}$  concentration (Figures 5.11c and 5.11d). Blue regions in the figures with  $\text{NH}_3\text{-N}$  concentrations at 0.050-0.075 mg/l start to diffuse and disappear into the purple region that has concentration below 0.010 mg/l. During the wet season, the  $\text{NH}_3\text{-N}$  concentration in the domain is most diluted. The general concentration of the lake is below 0.010 mg/l (Figures 5.11d and 5.11f). Inflows with higher  $\text{NH}_3\text{-N}$  concentration in the west side of the lake are quickly neutralized and do not affect the overall concentration of the domain. In the winter time, drop in water levels results in the rise of  $\text{NH}_3\text{-N}$  concentration in narrow streams and rivers along the lake's main channel, as shown in Figure 5.11h and the yearly process repeats.

Under the barrage influence, the  $\text{NH}_3\text{-N}$  concentration in S1 is reduced in the dry season due to a rapid increase in water levels in the same period. As shown in

## Potential Barrage Water Management Schemes for Poyang Lake

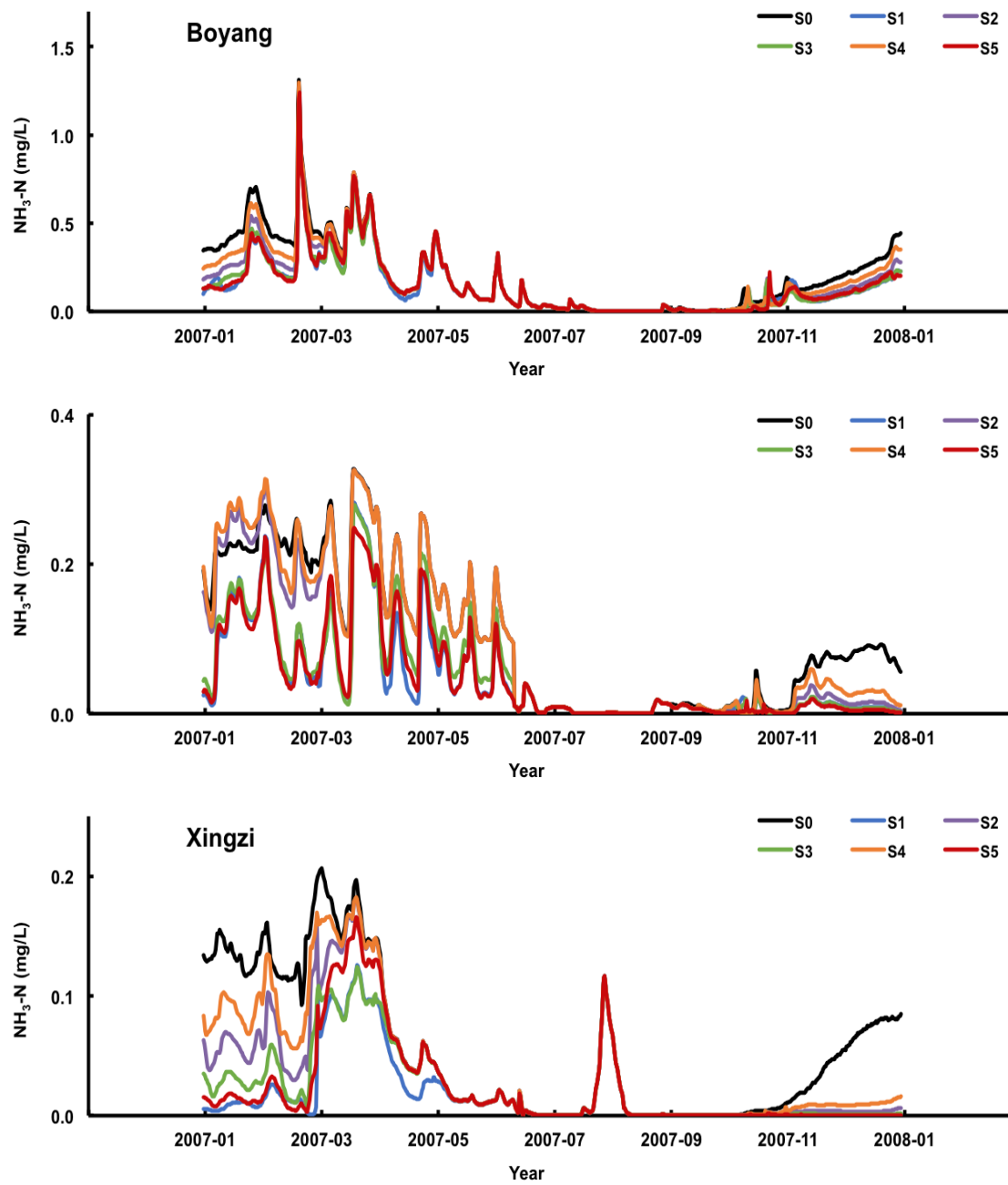


Fig. 5.10 Scheme comparison of  $\text{NH}_3\text{-N}$  at Boyang, XiuheMouth and Xingzi

Figures 5.12a and 5.12b, the main channel showing high  $\text{NH}_3\text{-N}$  concentrations in S0 has disappeared. Boundary inflows with high  $\text{NH}_3\text{-N}$  concentration can be seen in the eastern and northwest regions, then soon being diluted once they enter the lake area. With such high water levels maintained throughout most of the year, the dilution effect on  $\text{NH}_3\text{-N}$  concentration can be seen throughout the flooding period, prior the winter months when the concentration slightly rises again. The trend on  $\text{NH}_3\text{-N}$  concentration variation in S4 is similar to that in S1 (Figure 5.13), only with a higher resulting  $\text{NH}_3\text{-N}$  concentration due to weaker dilution effect. The spatial distributions of  $\text{NH}_3\text{-N}$  concentrations among the schemes have shown that the implementation of barrage has a positive effect on  $\text{NH}_3\text{-N}$  reduction using the dilution effect.

### 5.4.3 Impact on Phosphorus Concentration

The impact of the barrage on phosphorus concentration is examined in this section. With particulate phosphorus (PP) data being available in the three locations; Boyang, XiuheMouth and Xingzi, Figure 5.14 will look at the total phosphorus (TP) concentration at those locations under the influence of the various barrage schemes, while the spatial distribution of the Poyang Lake domain will focus on the orthophosphate ( $\text{PO}_4\text{-P}$ ) concentration.

In Figure 5.14, S0 represents the natural scenario in which no barrage control is implemented whilst conditions under S1-S5 are lines colour coded as shown in the legend. The  $x$ -axis labels the time of the year in 2007 and the  $y$ -axis marks the TP concentration in mg/l. The TP concentration seems to follow a particular trend. For all the three locations, the TP concentration is higher in the dry period and lower in the wet period. Although in XiuheMouth and Xingzi there is a sudden surge in TP concentration in each location around August, the overall TP concentration in all the three locations remain in close proximity throughout the year.

## Potential Barrage Water Management Schemes for Poyang Lake

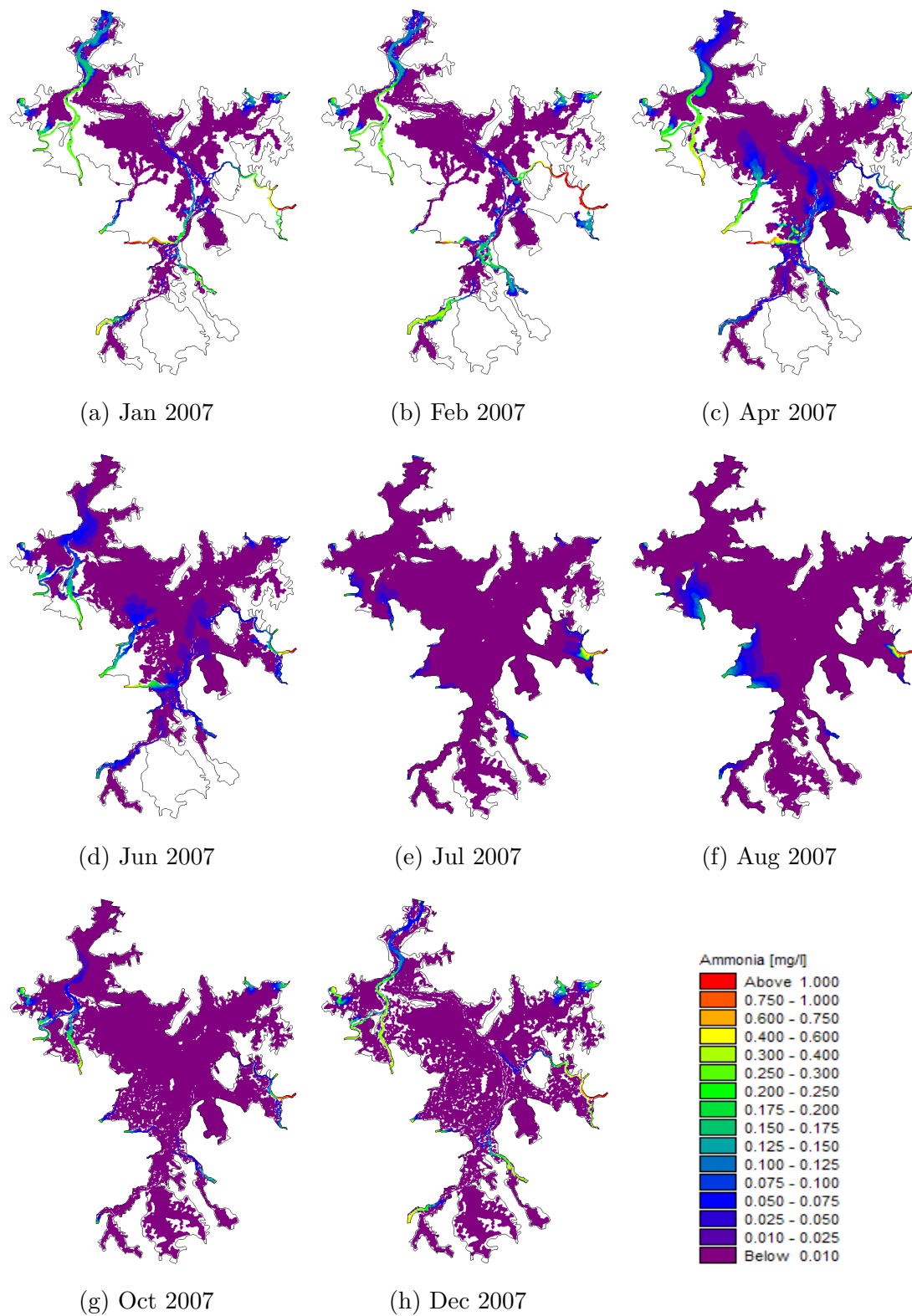


Fig. 5.11 Scheme 0  $\text{NH}_3\text{-N}$  spatial distribution in 2007

## Potential Barrage Water Management Schemes for Poyang Lake

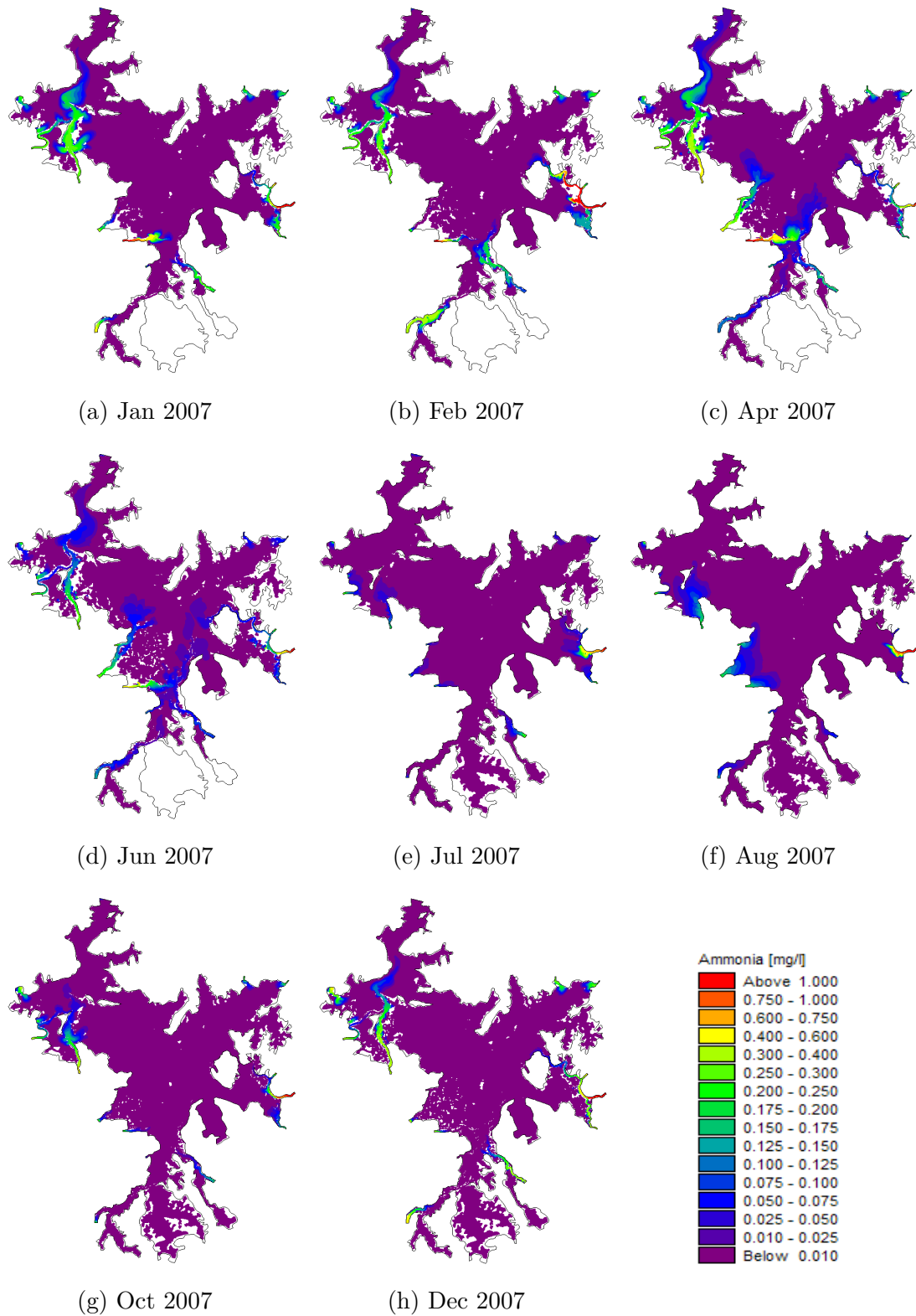


Fig. 5.12 Scheme 1  $\text{NH}_3\text{-N}$  spatial distribution in 2007

## Potential Barrage Water Management Schemes for Poyang Lake

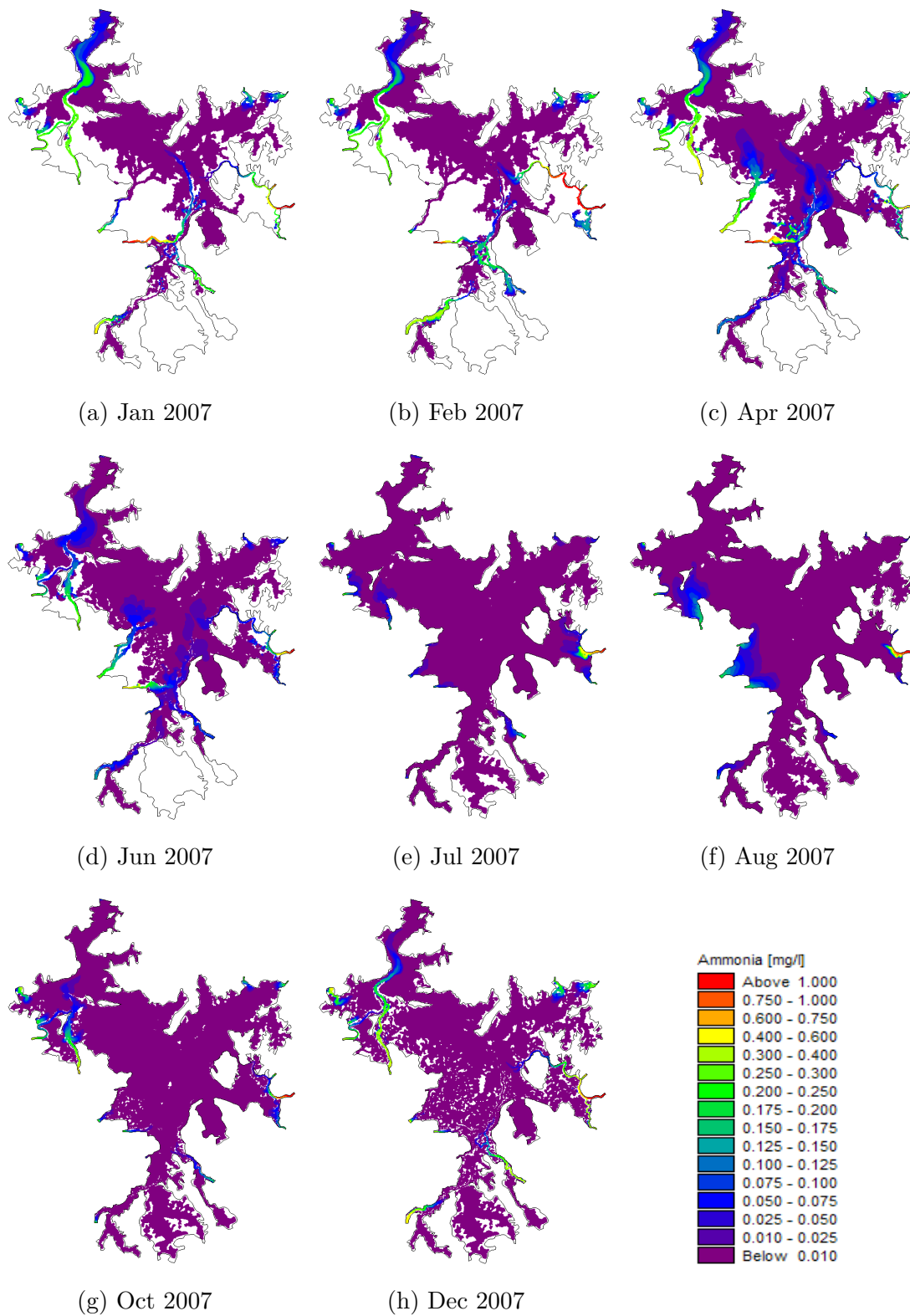


Fig. 5.13 Scheme 4  $\text{NH}_3\text{-N}$  spatial distribution in 2007

## Potential Barrage Water Management Schemes for Poyang Lake

---

The effect of barrage control schemes on the TP concentration in Poyang Lake can also be seen in Figure 5.14. Although the gaps between TP concentrations of different schemes are small, it is clear that the schemes with the highest rise in water levels (e.g. S1, S3 and S5) record the lowest TP concentration among other schemes. In the case of Xingzi, the gaps are more prominent with S1 and S5 showing the greatest impact on TP concentration reduction. The implementation of the barrage schemes has resulted in a drop in TP concentration, as shown by the colour lines beneath the black line representing the natural state at the three locations. This is due to the enhancement of dilution effect under the effect of the barrage. In addition, increase in bio-activities during the summer times will lead to an increase uptake of phosphorus for growth. This also explains the slight drop in the TP concentration prior to the beginning of July in all three locations.

The spatial distributions of the  $\text{PO}_4\text{-P}$  concentration in Poyang Lake under different barrage operational schemes are shown in Figures 5.15-5.17. In Figure 5.15, no barrage implementation has been performed and the  $\text{PO}_4\text{-P}$  distribution shown is at its natural state in the Poyang Lake environment. In the early months of 2007, the  $\text{PO}_4\text{-P}$  concentration is high along the main river streams with low water levels. Concentrations in the range of 0.015-0.075 mg/l can be observed (Figures 5.15a and 5.15b). When the water levels rise in April, the  $\text{PO}_4\text{-P}$  concentration spreads out to a larger region as shown by the increase in blue color in Figure 5.15c. The influx of  $\text{PO}_4\text{-P}$  concentration from boundaries remain high in June at 0.060-0.065 mg/L as seen in Figure 5.15d. As the flooding season develops, the increase in lake water volume dilutes the  $\text{PO}_4\text{-P}$  concentration. Although inflows with higher  $\text{PO}_4\text{-P}$  concentration can be observed in Figures 5.15e and 5.15f, the overall concentration in the majority of the lake district is below 0.005 mg/l. In the later months of the year, drop in water levels in the lake triggers the increase of  $\text{PO}_4\text{-P}$  concentration along the lake's main channel, as seen by the clear red, green and blue narrow line in Figure 5.15h.

## Potential Barrage Water Management Schemes for Poyang Lake

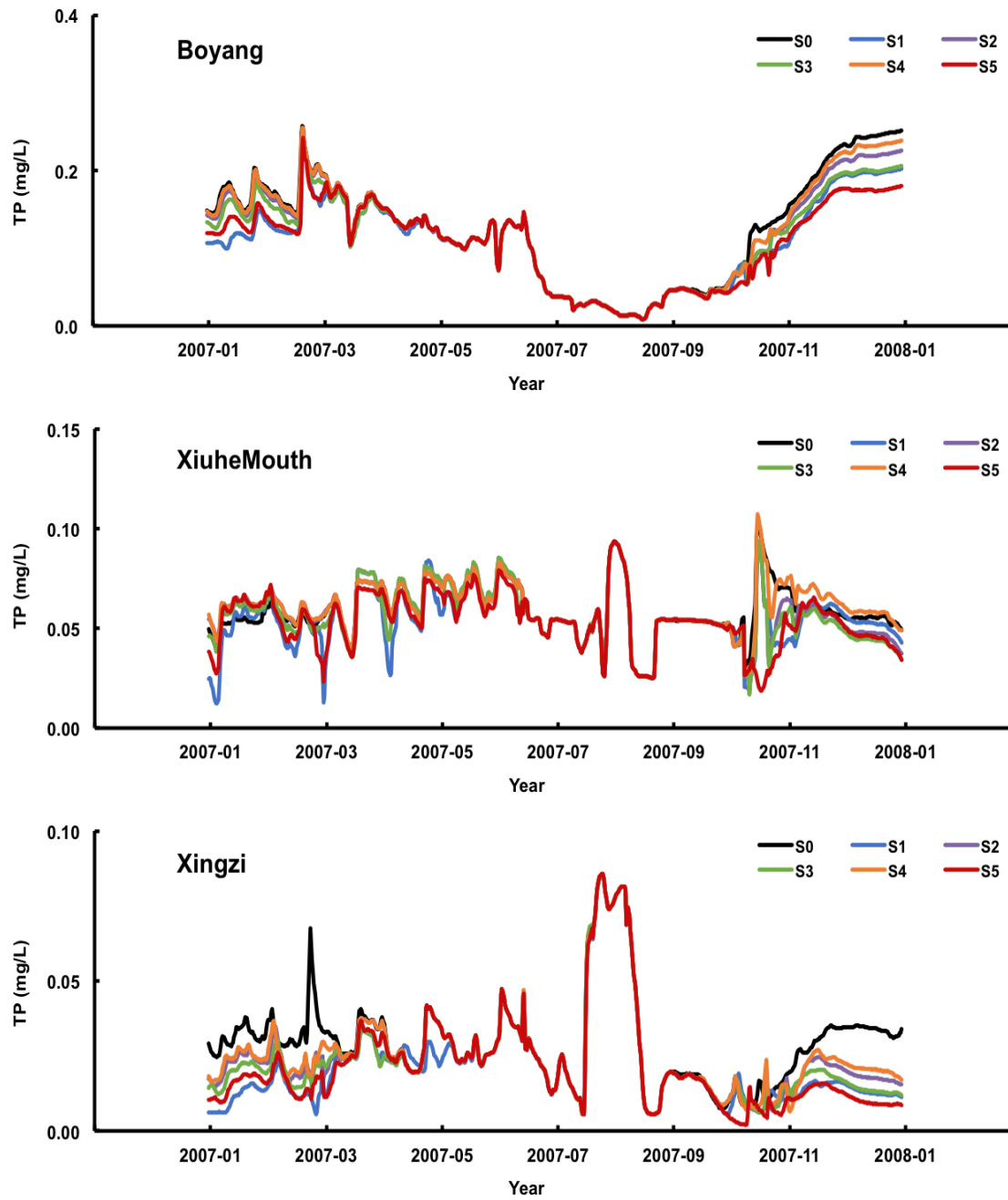


Fig. 5.14 Scheme comparison of TP at Boyang, XiuheMouth and Xingzi

## Potential Barrage Water Management Schemes for Poyang Lake

---

The  $\text{PO}_4\text{-P}$  distribution under the influence of S1 and S4 are shown in Figures 5.16 and 5.17. Using S1 as an example, the increase in water levels cause by the barrage have alleviate the  $\text{PO}_4\text{-P}$  concentrated stream in the middle of the lake domain during the dry season (Figures 5.16a and 5.16b). As the water levels rise further due to flooding, the  $\text{PO}_4\text{-P}$  distribution mimics those in S0, including the sudden outburst of  $\text{PO}_4\text{-P}$  concentration in June which coheres with the sudden bursts shown in the scheme comparison figure earlier in Figure 5.14. The dilution effect on  $\text{PO}_4\text{-P}$  concentration is observed throughout the flooding period until October (Figure 5.16f), by then the winter season begins with lowering of water levels and increasing  $\text{PO}_4\text{-P}$  concentrations (Figure 5.16h). The variation on  $\text{PO}_4\text{-P}$  concentration in S4 follows similar pattern as S1 (Figure 5.17), only at higher  $\text{PO}_4\text{-P}$  concentrations in general due to a weaker dilution effect generated by the lower rise of water levels. The spatial distributions of  $\text{PO}_4\text{-P}$  concentration among the schemes have shown that the implementation of barrage has successfully reduced  $\text{PO}_4\text{-P}$  concentration due to dilution effect.

The distribution results of the water quality variables can be used to compare with the rare Poyang Lake barrage study from the literature. As mentioned in the literature review, Hu et al. (2012b)'s study used the 2-D EFDC model to investigate the impact of the Poyang Lake barrage on the nutrient concentrations of the lake. Figure 5.18 illustrates the monthly-averaged distribution of TIN and TP in Poyang Lake. The simulation domain in the study focused mainly on the main channel of the lake. Since the figure was in black and white in the literature and the scale of the parameter is not coherent, direct changes can only be seen from a larger area of higher TIN and TP concentrations during January and a more widespread and lower concentrations for both TIN and TP during October. The study concluded that the barrage operation will increase by 20.42 % for TIN and 20.55 % for TP during dry season. The findings however are not prominent as the study used only month-averaged values and presented only two figures for each nutrient concentration. In comparison, the simulation conducted in this project covers a more comprehensive area in Poyang Lake and the holistic snapshots over a yearly cycle give a more representative view of

## Potential Barrage Water Management Schemes for Poyang Lake

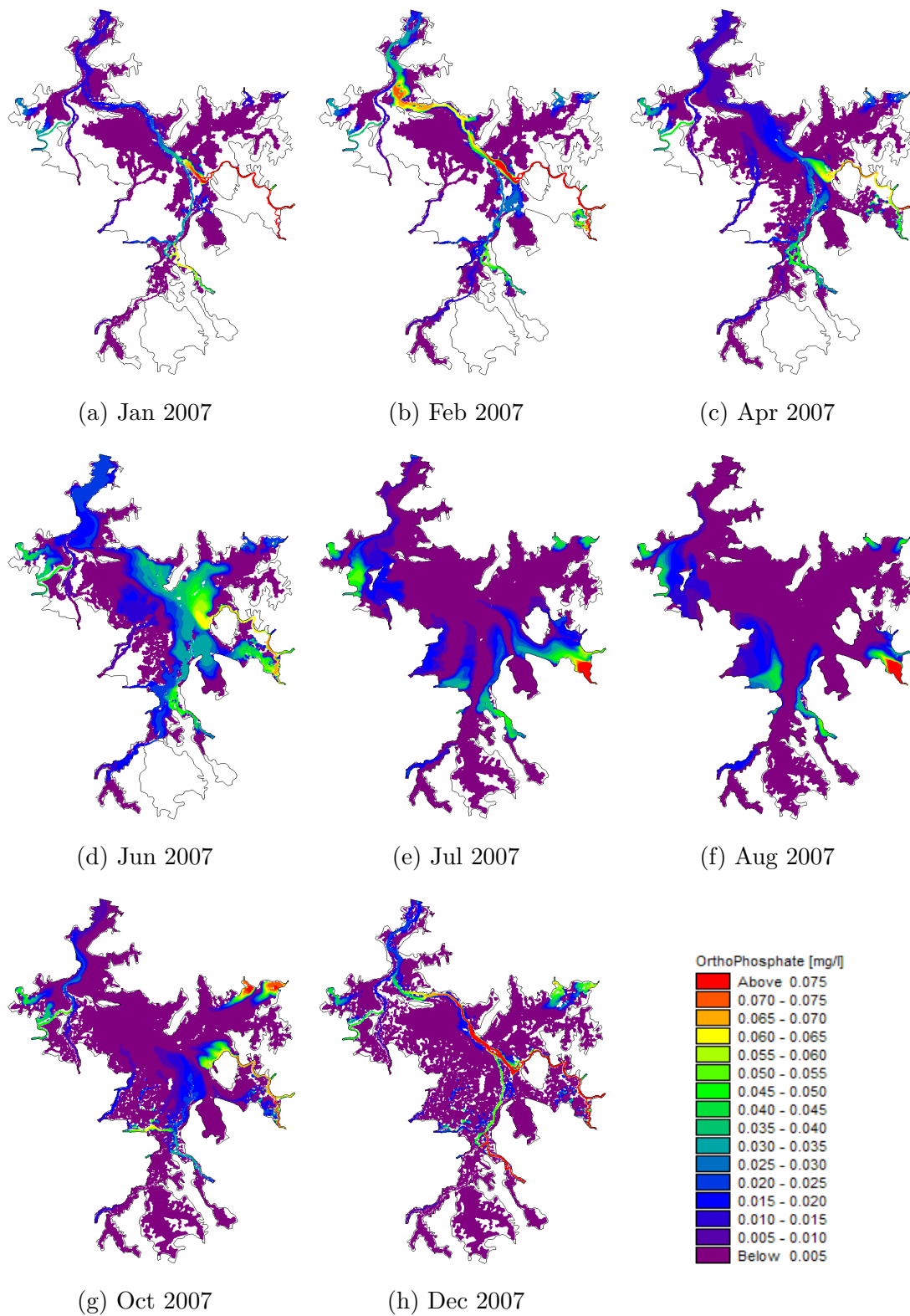


Fig. 5.15 Scheme 0  $\text{PO}_4\text{-P}$  spatial distribution in 2007

## Potential Barrage Water Management Schemes for Poyang Lake

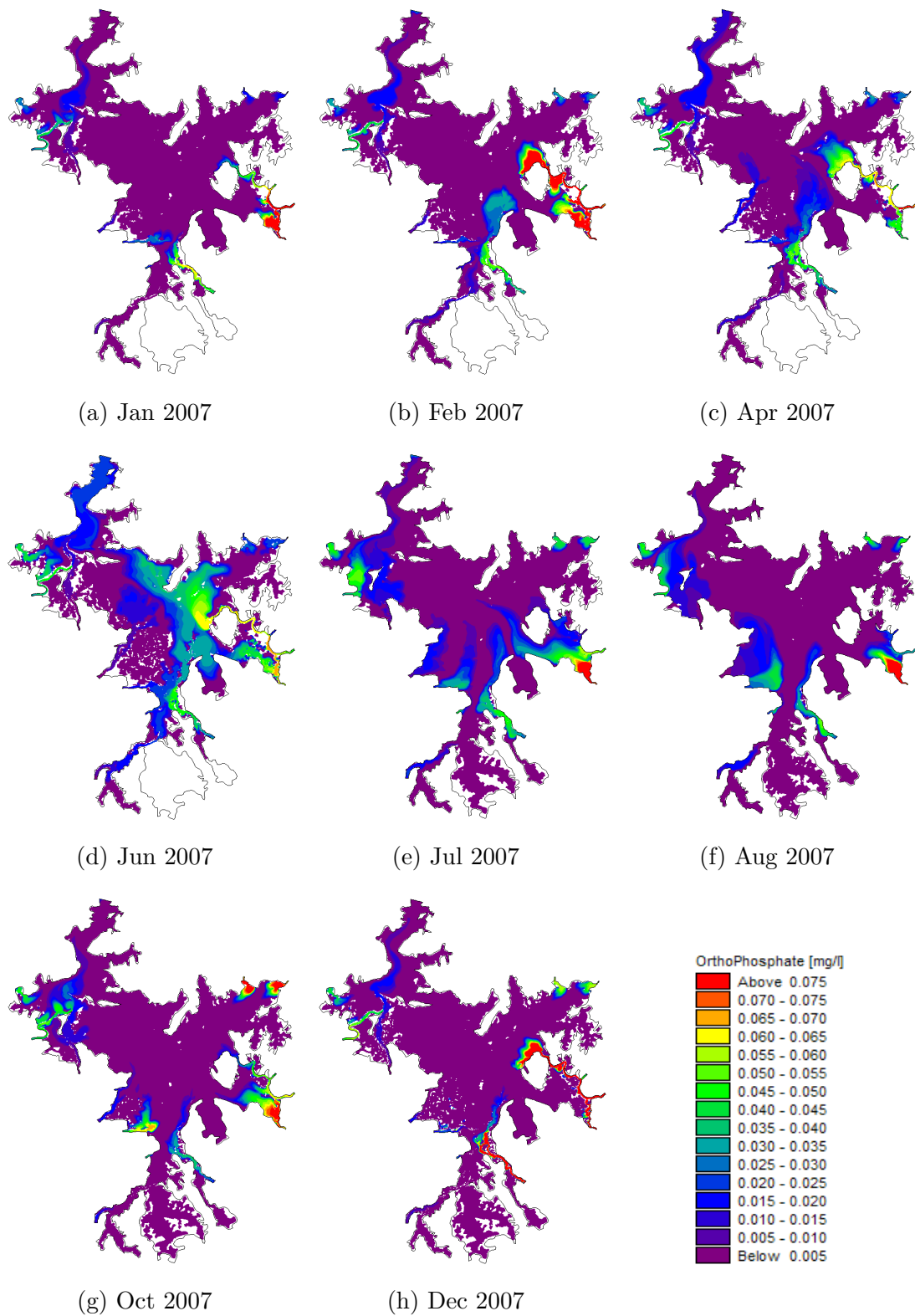


Fig. 5.16 Scheme 1  $\text{PO}_4\text{-P}$  spatial distribution in 2007

## Potential Barrage Water Management Schemes for Poyang Lake

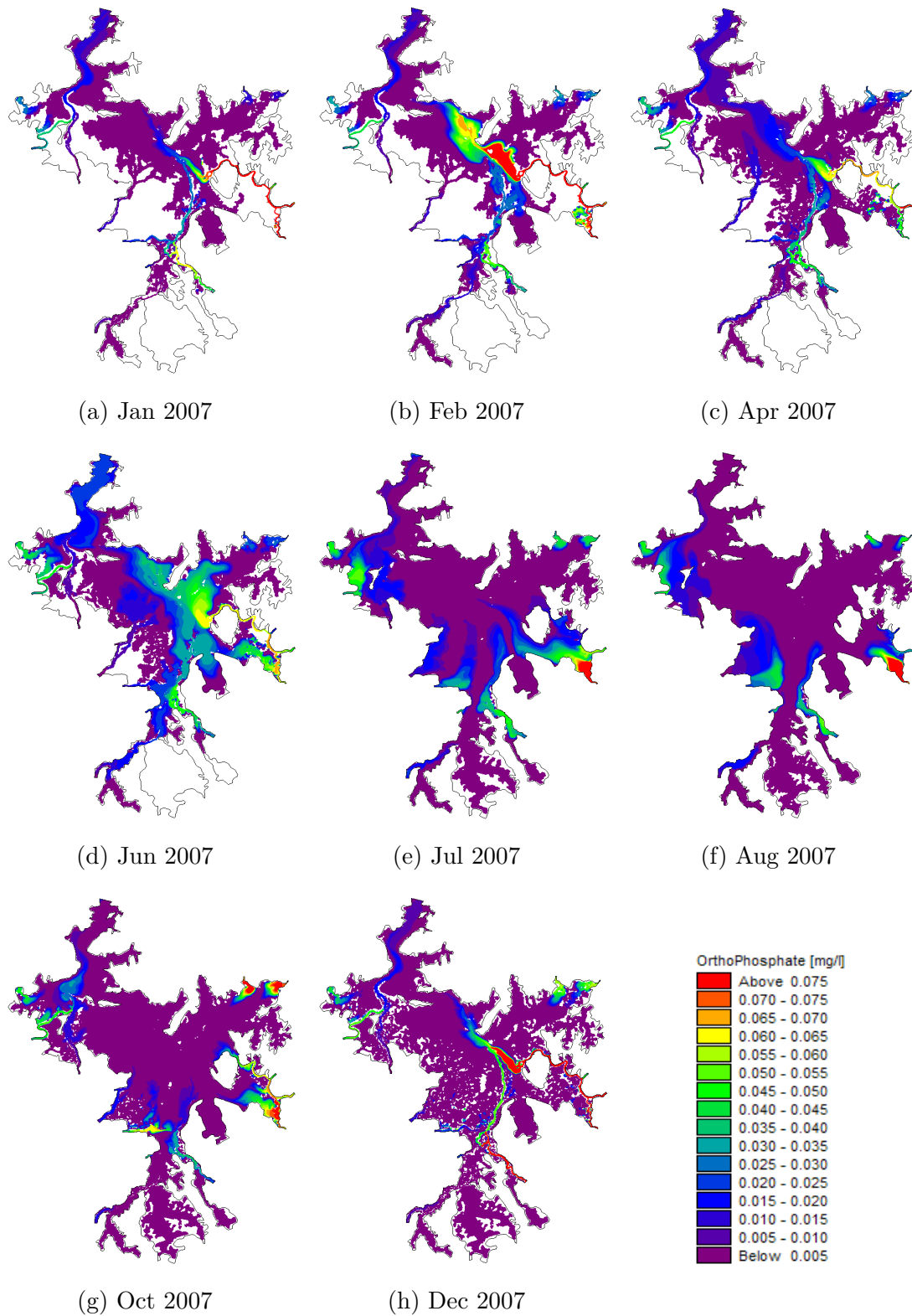


Fig. 5.17 Scheme 4 PO<sub>4</sub>-P spatial distribution in 2007

the changes in nutrient concentration in the hydro-environment. Localised difference in nutrient concentrations at certain regions in the lake can be seen due to the high resolution mesh and short time steps utilised in the simulation. The simulation in this study could improve further in many aspects, yet its values should be recognised when comparing with existing modelling standards for nutrients studies of Poyang Lake.

### 5.4.4 Effect of Water Levels on Water Quality Variables

The impact of different barrage operational schemes on the lake's water quality can be further demonstrated by investigating the relationship between the water levels and the water quality parameters. In Figure 5.19, the water levels under three different barrage control schemes (S0, S1 and S4) are plotted against three simulated water quality variables (DO, NH<sub>3</sub>-N and TP) as a result of the water control in Poyang Lake. Two locations, Xingzi and Boyang, are used as examples with Xingzi close to the barrage (14 km) at the north of Poyang Lake and Boyang further upstream from the barrage at the east of Poyang Lake (110 km). In each sub-plot, *x*-axis represents the concentration of the water quality variables, *y*-axis indicates the water levels. The colour of the distributions under each scheme follows the same colour coding as previous graphs (S0: black, S1: blue and S4: orange). Each distribution illustrates the concentrations of the water quality variable at a given water level during the one year cycle from January 2008 to January 2009. The overall distributions of each scheme could demonstrate how the changes in water levels correlate with the changes of concentration of respective water quality variable.

The scheme S0 acts as a control in which no barrage operation is simulated. In this scheme, the hydrodynamics of Poyang Lake is at its natural state and the variation of water quality concentrations against water levels is organic. Both schemes S1 and S4 have the barrage operation in effect, with S1 setting higher water level thresholds than S4 in the majority of the dry season. Towards the top of each distribution is an area where all three schemes share similar and overlapping recordings. This is a

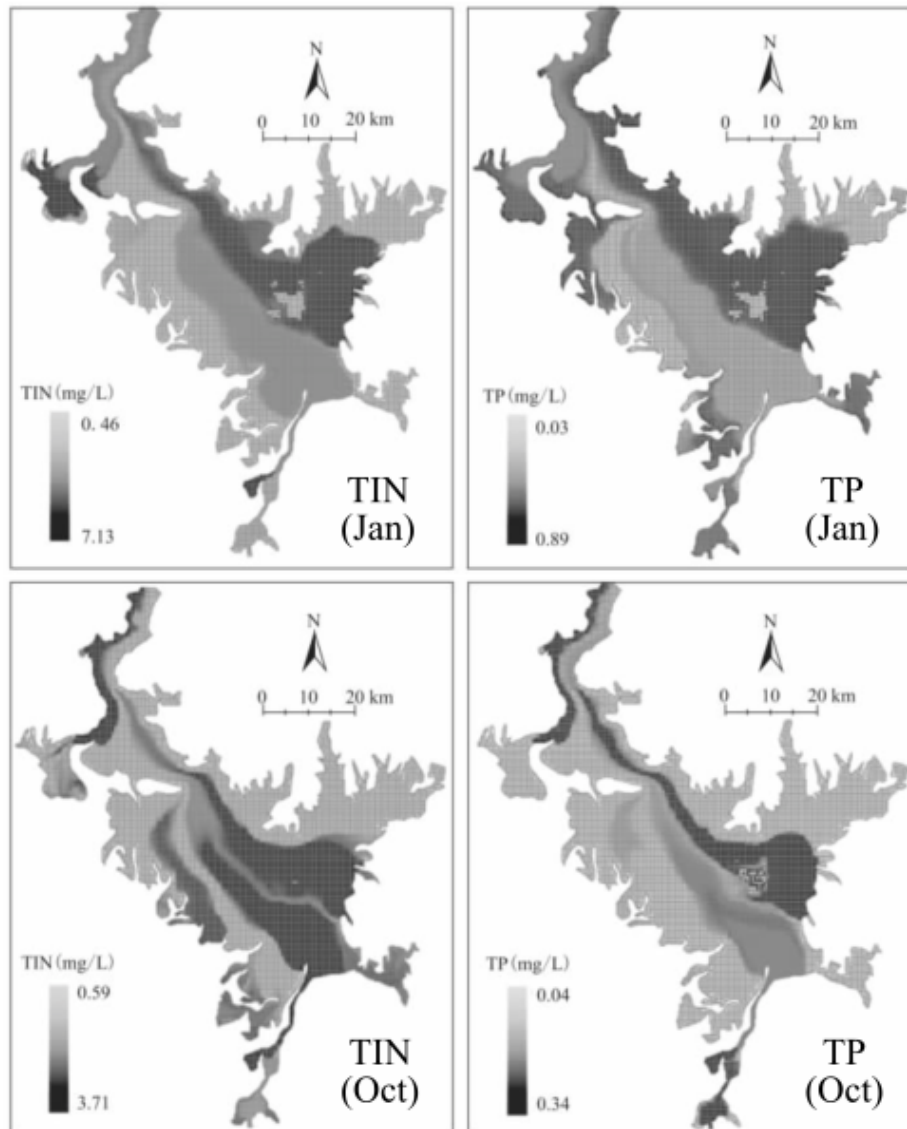


Fig. 5.18 Distribution of monthly-averaged TIN and TP in dry and flat period of Poyang Lake (Source: Hu et al., 2012b)

## Potential Barrage Water Management Schemes for Poyang Lake

---

representation during the flooding season when the water level is high and the barrage is not in operation. As a result, the water levels are at their natural state and all the schemes have identical readings for a certain period in the summer.

In the sub-plots of Figure 5.19, the majority of S0 distribution locates at the bottom among the three schemes. This indicates the scheme having the lowest water levels of the distributions. In addition, the distribution in black is towards the furthest right among the three distributions, as seen in Figures 5.19a, 5.19c, 5.19e and 5.19f and only slightly in Figures 5.19b and 5.19d. This represents the relatively high concentration of S0 at low water levels. As the degree of water level increases due to the implementation of the barrage (S1 and S4), the distribution shows an upward movement due to the increase of water levels. S4 with a mild increase in water levels situates as an orange distribution in the centre of each subplot. S1 with the highest increase in water levels is always among the top of the three schemes as shown by the blue dots. Meanwhile both S1 and S4 distributions exhibit a slight shift towards the left of the plots as they move upwards, indicating a drop in concentration as water levels increase. These characteristics can be seen in various degrees in each subplot.

When comparing the water quality concentrations between the two locations, Boyang recorded generally higher concentrations than Xingzi in all of the three parameters. Despite being further away from the barrage, Boyang's distributions shared similar water levels with their equivalent Xingzi distributions. This demonstrates that the distance away from the barrage in this case has limited effects in reflecting the water levels and water quality concentrations. Factor such as the presence of a pollutant source in the form of an industrial discharge could significantly affect the concentrations in the nearby region. This research focused on the holistic changes in hydraulic and water quality variables of the whole Poyang Lake domain, instead of direct comparison between two locations, to reduce bias and misjudgment on simulation results. Further studies on the identification and modeling of external pollutant sources are recommended to address such issue.

## Potential Barrage Water Management Schemes for Poyang Lake

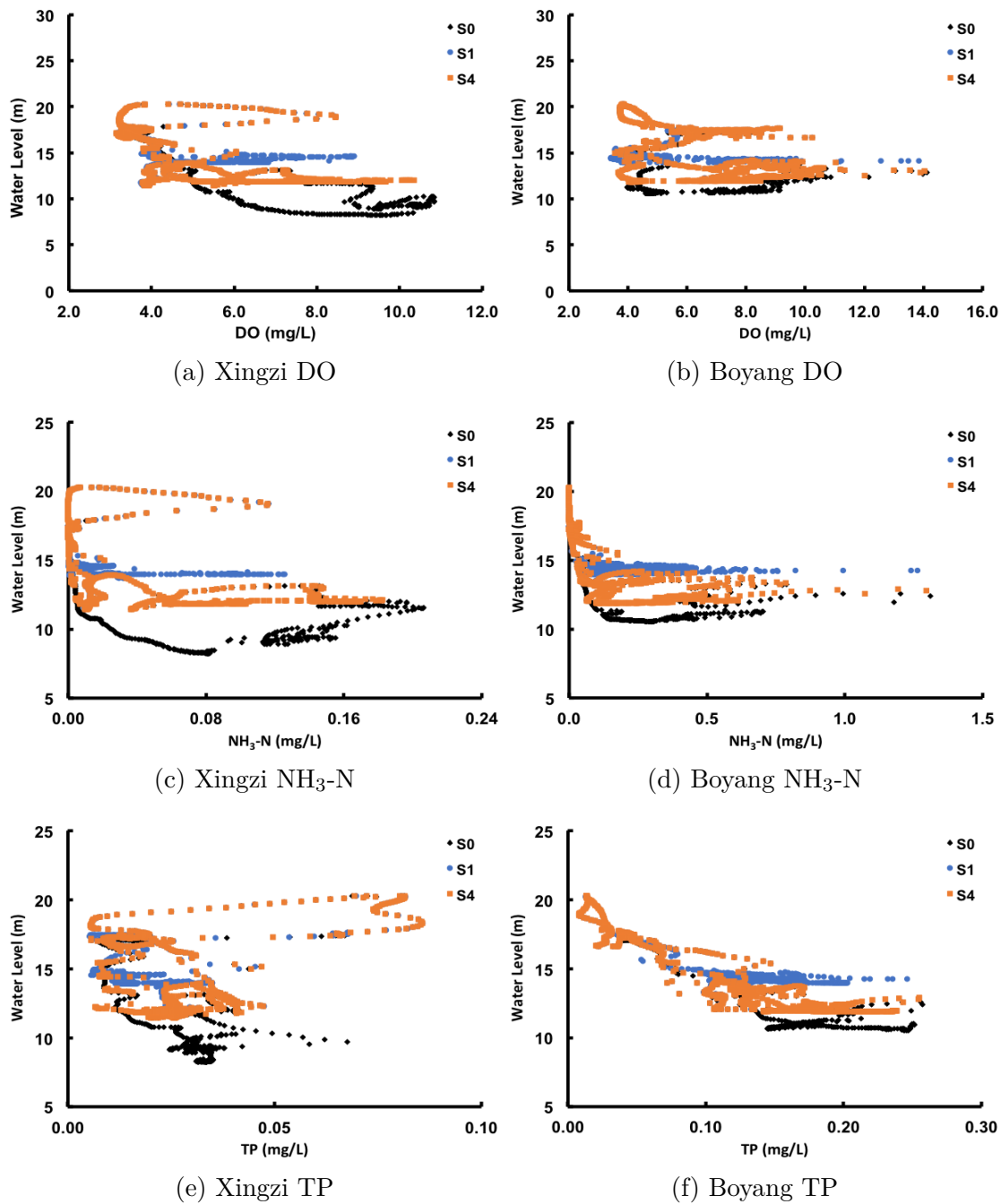


Fig. 5.19 Comparison of water depth ( $z$ ) against water quality variables (DO, NH<sub>3</sub>-N and TP) under different barrage operational schemes at Xingzi and Boyang

### 5.5 Chapter Summary

In this chapter, five barrage operational schemes have been investigated using the numerical model developed. The barrage operational schemes were proposed by local organizations with different aims for the barrage. Their proposals include a series of different water levels control at the barrage throughout the year, which have been translated into inputs for the numerical model. By varying the water levels at the barrage according to the various operational schemes, the barrage effects on the hydrodynamics and water quality of Poyang Lake have been simulated.

For hydrodynamic impacts, the barrage schemes have all demonstrated their capability on increasing water levels and water volume during the dry period. Simulation has shown that the increase of water levels across Poyang Lake is proportional to the rise in the water levels at the barrage. Moreover, the effectiveness of the barrage diminishes as the distance to the barrage increases. The impact of the water environment is further examined by generating the water surface area and water volume of the lake under each scheme. Although the barrage can successfully increase the water levels and alleviate the problem of water shortage and low water levels in dry seasons, the increase in water surface area could potentially destroy wetlands and wildlife habitats that rely on the unique water levels fluctuation nature of the lake.

As for water quality analysis, schemes comparison at locations in Poyang Lake and spatial distribution across the lake domain on three water quality variables (DO,  $\text{NH}_3\text{-N}$  and  $\text{PO}_4\text{-P}$ ) are conducted. Results show that although the barrage schemes are capable to reduce nutrients concentrations ( $\text{NH}_3\text{-N}$  and  $\text{PO}_4\text{-P}$ ) during dry periods through the dilution effect, they also reduce the DO concentration in the lake by hindering water flow and hence prevent current induced reaeration from taking place. DO depletion in the water environment could threaten aquatic wildlife, promote nutrients outburst and trigger eutrophication. The implementation of the barrage could bring both benefits and threats to the ecosystem and all parties involved.

# Chapter 6

## Conclusions

### 6.1 Overview

The aim of this study starts with the development of a numerical model, coupling hydrodynamic and water quality simulations, that can simulate the hydraulic flows and bio-chemical properties of fluctuating water bodies under certain natural lake environment. The model can then be applied to study the hydraulic changes and pollutant behaviours of Poyang Lake, the largest freshwater lake in China. The lake is a central figure in the province that consists of wetland habitats for aquatic wildlife and migrating species, provides freshwater sources to nearby population, facilitates economic and transport activities in the region and shares a close river-lake relationship with Yangtze River, the longest river in Asia. This case study is of great research interests given the lake's recent struggle with the decline of water levels and deterioration of water quality, due to climate change and anthropogenic activities. The numerical model developed in this study can be used to evaluate the potential impact of a proposed engineering control in the form of a barrage on the hydro-environment of Poyang Lake and to offer stakeholders and local governing authorities the scientific analysis of the externalities the engineering control project might bring.

### 6.1.1 Problems and Modeling in Freshwater Environment

This thesis begins with Chapter 1 providing an introduction of the current global water crisis and the importance of lake and river studies towards sustainable development in modern societies. Understanding the background and conditions of the planet's freshwater bodies helps build the foundation of this research to study current river and lake problems that have huge corresponding impacts on the water environment, natural ecosystem and human communities.

Chapter 2 presents a literature review relating to the studies of lakes and rivers using numerical modeling. The development of methods and numerical models used for hydrodynamic modeling and water quality modeling on shallow water environments are examined respectively. The overview of such review suggests that although the field of hydro-environment modeling is rapidly maturing, continuous advancement in model efficiency and computing powers is needed to tackle water problems that are also growing in scale and complexity. Cross-scale coupling between the estuaries and the ocean, multi-phase flow and multi-model ensembles are some of the ongoing development that could assist the numerical simulation in hydro-environment. Combination of different model functions is critical to balance out efficiency and accuracy in modeling. Tailoring and streamlining the models to the specific problems at the given situations remains the key for scientists and engineers moving forward. The review consolidates this research's direction in developing a coupled numerical model that can efficiently simulate the hydro-environment of a large freshwater lake.

An overview of the literature describing Poyang Lake, the subject of our case study, is also presented. The background, significance and characteristics of the lake are being documented. These include the lake's geographical information, economic and ecological conditions, hydraulic and hydrological characteristics and relationship with the Yangtze River and the Three Gorges Dam. The challenges of earlier and prolonged low water levels periods during winter seasons as well as the deterioration of

## Conclusions

---

water quality in the water bodies have been explored. The proposal and the status of the potential Poyang Lake barrage project is also being introduced. Existing research on the hydrodynamic and water quality modeling of Poyang Lake is summarized with the idea that both the data collection and numerical modeling of the subject lack holistic directions, results validation and systematic approach. The limited amount of accessible numerical water quality modeling research on Poyang Lake's recent challenges further prompts the current research on attempting to model pollutant concentrations in the lake and to investigate the potential impact of the barrage on them.

### 6.1.2 Developing the Coupled Numerical Model

In Chapter 3, the basic theories and principles behind the numerical hydrodynamic and water quality models are detailed. The governing equations that describe the water flow and solute transport behaviours in shallow water environments are present in 3-D, 2-D and 1-D scenarios. Numerical methods used in solving these complex equations are also mentioned respectively. For water quality modeling, the conventional bio-chemical processes that focus on the dissolved oxygen, nitrogen and phosphorus in the water environment are explained. These components are key parameters for water quality modeling due to their interlinking relationship and their significant role in regulating wildlife habitats and sustaining organisms growth in the water environment. Extreme irregularities of these components such as low oxygen content and high nutrients level could cause catastrophic hazards such as eutrophication and death of aquatic wildlife in the waters. The formulation of each bio-chemical processes and the representation of their components with respects to one-dimensional and multi-dimensional water quality models are demonstrated. The methodology established in this chapter builds the theoretical foundation for the numerical models in this study.

Chapter 4 dissects the different module structure in the model and demonstrates the various parameters and considerations in setting up the model to successfully simulate the water environment of Poyang Lake. For 1-D simulation, an in-house hydrodynamic

## Conclusions

---

model and the WASP water quality model are used to cover the majority of the middle and lower reach of Yangtze River which includes Poyang Lake and its catchment and river networks. The coverage of an extensive area around Poyang Lake allows a reliable estimation of the water levels, water flows and pollutant concentrations entering Poyang Lake. The 1-D simulation results are translated into the boundary conditions in the multi-dimensional simulation, which is conducted on the MIKE modelling platform and focuses along the main channel and central region of the Poyang Lake domain. Main components used in the model setup such as the unstructured mesh, boundary conditions, initial conditions, control parameters and potential assumptions are discussed. In between multi-dimensional simulations, an investigation is conducted to prove that the 2-D simulation is as accurate as the 3-D simulation in modeling the shallow water environment of Poyang Lake. Hence a decision to proceed with 2-D simulation in subsequent analysis is made for more efficient computational usage and shorter simulation time.

Field-measured data of Poyang Lake provided by the local water authorities and research bodies were used to validate the models. The 1-D hydrodynamic model produced very good results that match the field-measured data from 2004 to 2013. However, the 1-D water quality model did not perform as well and for some of the water quality variables such as ammoniacal nitrogen and total phosphorus, the performance of the model could be unsatisfactory. The generated 2008 results from the 2-D hydrodynamic model showed good coherence with the field-measured data of the same period. Meanwhile, the simulated 2-D velocity flow field in both the wet and dry season matches well with the actual flow characteristics of Poyang Lake in respective periods. For the validation with the 2-D water quality simulation, although most of the variables follow the trend of the field data, the statistical indices show that for water quality variables such as dissolved oxygen and total phosphorus in some locations the model performance is not satisfactory. Discrepancies occur due to inconsistent and disconnected field-measured data, which are understandable given the difficulties and costs in regular data sampling of a big scale lake. Overall, the coupled 2-D model

performs fairly in simulating the hydrodynamic and water quality of Poyang Lake and the aim of developing a numerical model for the simulation of hydro-environment of Poyang Lake has been achieved.

### 6.1.3 Evaluating the Engineering Control of the Barrage

The validated numerical model is applied to examine the impact of different barrage operational schemes on Poyang Lake in Chapter 5. These five operational schemes, proposed by entities including the local province government, water conservation committee and research institute, suggest different targeted water levels at the barrage during various flowing periods throughout the year. The control of water levels, achieved by the opening and closing of the sluice gates, at the barrage would translate into water level changes in the whole of Poyang Lake domain. The operational patterns of the five schemes in the form of varying water levels are entered into the numerical model as boundary conditions at the location of the barrage from 2005 to 2008.

The five schemes (S1-S5) differ by their extent of water level control at the barrage. During the dry periods, the degree of water level rise proposed by the schemes go in descending order of  $S1 > S5 > S3 > S2 > S4 > S0$ , with a reference scheme (S0) acting as a control with no barrage implementation.

In terms of hydrodynamic impact, the schemes have all demonstrated their effectiveness on rising water levels in the winter months. The increase of water levels across the lake is proportional to the rise in water levels at the barrage based on respective schemes. In addition, the effect of the barrage weakens as the distance from the barrage increases. Increase in water surface area could potentially overflow wetlands and wildlife habitats, as well as reducing water exchange in the lake and accumulate nutrients in the long term.

In terms of the impact on water quality, the five schemes are able to reduce the nutrients concentrations in Poyang Lake during the dry period by increasing the

## Conclusions

---

water levels and water volume, resulting in the dilution effect. For both  $\text{NH}_3\text{-N}$  and  $\text{PO}_4\text{-P}$ , their concentrations are below the usual values under the operations of the five schemes. The difference in the degree of reduction depends on the amount of water levels increments. The greater the increase in water levels, the lower the nutrients concentration. This is an encouraging sign showing that the barrage could positively tackle the pollution issues in the Poyang Lake region during dry seasons. However, the rise in water levels also trigger a reduction in DO concentration due to lower water exchange and slow water flow. Current induced reaeration in the lake is hindered and this will lead to potential hazards for aquatic wildlife and the ecosystem in the long term with the occurrence of oxygen depletion in the water.

Based on the results of the simulation, it is clear that the implementation of the barrage control will bring positive impact but also negative externalities to the Poyang Lake environment. Scheme 1 and 5 with the largest increase in water levels demonstrated the biggest impact on increasing water volume and reducing nutrients concentrations in the lake. Nonetheless, increasing water surface area and reducing water level fluctuation in the lake will diminish flow rate and velocities, leading to longer retention time for pollutants. Concerns on the flooding of wetland areas and wildlife habitats, as well as the change in hydraulic behaviours in downstream regions along the Yangtze River will also need to be considered and addressed accordingly. The barrage control scheme is preferable only when the benefits and drawbacks of all parties involved are evaluated and optimised, based on the purpose of the engineering case in concern and the interests of the stakeholders.

## 6.2 Discussion and Remarks

The scope of this research is finite. It is important to realize that this study is conducted under the constraints of resources and time, so that not every aspect of this work could be practically covered in the most comprehensive manners. Under the constraint of data availability, assumptions and adjustments were made in areas that are not controllable within the capacity of this study.

### 6.2.1 Data and Simulation Validity

The premise of the numerical models and simulations in this study is built on data provided by the local water authorities, hydrological bureaus and research institutes in China. The data contain topographic elevation map and measured terrain information dated 2008. The substantial amount of sand dredging, land reclamation and reservoirs construction in Poyang Lake in recent decade have facilitated sediment movement in the region. Coupling with the reducing sediment influx from the five rivers and the Yangtze River, the lake has become an erosional system that is undergoing significant topographical changes. The comparison between different operational barrage scheme was performed for the year 2007 due to restricted data availability. Although the model simulations have produced sound results, the target period in which the schemes are based on has undermined the validity of the analysis to a certain degree. With the simulations and barrage schemes analysis carried out using data in the late 2000s and early 2010s, the difference between the assumptions made and actual reality will be huge by the time the barrage is constructed (e.g. in the 2020s).

The issue of this study subject to obsolete data and outlook is also applicable to other aspects associated with Poyang Lake. One of the aspects include China's views and policies on the management and conversation of water environment, as well as those on the urban and economic development of the Poyang Lake region. Although due to limited scope these topics are not discussed in this study, alteration or implementation

## Conclusions

---

of new policies could potentially lead to changes in the inputs and priorities of the numerical models when considering Poyang Lake's water environments and challenges. For example, the amendment of water quality standards and tightening of policies on wastewater treatment control in China could change the ways in which water quality is evaluated in Poyang Lake and modify the amount of pollutant loadings being set at the boundaries in this research. Similarly, uncertainties in the future projections of climate change will create further unpredictability in the estimation of hydrological and water quality behaviours in water environments using numerical models. The unpredictable nature of the social, political, economic and meteorological aspects of any national and international water issues will always challenge the assumptions and data used in research and possibly change the results and conclusion of one's analysis.

### 6.2.2 Accuracy of Data and Assumptions

The availability and comprehensiveness of the field-measured data pose as a limitation to this study. It is generally difficult to collect lake environment data in developing countries or large scale ecosystem because of poor monitoring and low accessibility. The quality and integrity of the measurements are debatable as they are often inconsistent among sampling done by different research groups and institutes. As a result, the field-measured data used in this work, in particularly those related to water quality, are fragmented in context and temporally irregular.

Means of going around the scarce field data often introduce errors and inaccuracy in the modeling. Interpolation is often used to compute the complete data set needed for model inputs. Validation becomes difficult when the field data points are spread apart with abnormality. All of these create naturally inherited flaws in the numerical models that will accumulate as the model develops into higher order and complexity. Although in this study these errors and inaccuracies are within acceptable limits, as proven by the satisfactory validation results, a comprehensive set of well measured field-measured data is still preferred, which could provide concrete guideline in the

## Conclusions

---

specification of concentrations, loadings and initial conditions at the model boundaries. Moreover, many of the parameters in the model are globally assumed as constants by engineering judgment or referencing to values used by other research studying similar environments. This is unreasonable as parameters such as those related to reaeration and phosphorus exchange with bed in the model are dynamic coefficient varied across the lake. In reality, they can be affected by other factors such as light, temperature, flow regime and nutrient content. Although it is impractical to assign detailed dynamic values to each parameter over the whole simulation domain, simplified constants and their values should not be overlooked and taken for granted in every simulation.

### 6.2.3 Modeling the Environment of the Lake

Due to the complexity of the natural systems, hydro-environmental modeling is always an approximation of the real world. While balancing out between modeling complexity and problem representation, it is undeniable that the numerical model developed in this study has its shortcomings when modeling Poyang Lake's water environment. The hydro-environmental model could always consider modeling extra elements to become more representative of the actual environment. In terms of hydraulic modeling, several elements such as wind forcing, ice coverage, tidal potential, higher order numerical solving methods and in depth hydrological and atmospheric modeling with infiltration, precipitation and evaporation data could be included. The environmental elements that have not been considered in this study include transport of sedimentation, nutrients flux between the water bodies and bed sediment, occurrence of eutrophication, point source pollution, dynamic kinetic modeling for the lake's microorganisms and the barrage's influence on fish, plants and migratory bird's habitats and growth. These components of the water environment are not considered in this research due to scope constraints, limited data support, insufficient knowledge of the processes and high requirement and complication in modeling resources. Nonetheless, the knowledge and data of these processes in the water environment are essential.

### 6.3 Future Work

Several areas of future work are evident from the research presented. These areas include additional focus on sediment related experiments and modeling, improvement on data comprehensiveness and reliability, strengthening of research collaboration with a more open and systematic approach and advancement of modern technology and alternative solutions. These areas could provide stronger support for the modeling and analysis of Poyang Lake's hydro-environment.

The next viable step for this research is to incorporate the sediment in Poyang Lake into the numerical model. The integration includes the modeling of the physical movement of sediments in the region and the exchange of nutrient via adsorption and desorption with the sediment particles. Sediment interaction with the water bodies and their intake and release of nutrients are yet to be included as an internal pollutant source in the water quality modeling of Poyang Lake. The accumulation of nutrients, especially for TP, should be reflected in the numerical model in the future. Extensive sampling and laboratory experiments need to be carried out with sediments and nutrients to provide extensive understanding of the bio-chemical processes relating to sediments and their characteristics in the Poyang Lake environment.

Furthermore, the modeling of the barrage could be further developed. The barrage specification can be modeled into the study as a physical structure that reacts with the hydrodynamics of the lake. The operation of the opening and closing of the sluice gates could also be modeled with more control. This study does not include the control of individual sluice gates at the barrage. Focus is put on achieving a certain water level at a particular time of the year. In the future the sluice gates can be implemented into the model as individual units. By having direct control of the opening and closing of sluice gates, numerous other barrage operational schemes can be explored. The barrage in the model could offer an extra level of complexity for the users with partially open and close sluice gates at any portion. This will result in many new management plans

## Conclusions

---

and scenarios that could help explore further in tackling the water quantity and quality issues of Poyang Lake.

Another topic for exploration will be the local changes in hydrodynamics and pollutant concentration within the Poyang Lake domain. In this research, both the modeling and evaluation are performed with regards to the whole of Poyang Lake. More specific analysis could be performed at particular region and smaller areas in the lake at which a certain river inflow or pollutant source dominates. This will provide more localized results with higher resolution that will be beneficial when decision makers and stakeholders are focusing on the circumstances of one town or one power plant within the Poyang Lake region.

Meanwhile, the modeling of Poyang Lake environment could be enhanced by improving the comprehensiveness and accuracy of the data. The data used in this study is as accurate as it could be, available directly from the local water authorities in Poyang Lake. Nonetheless, the data is imperfect and often lacks consistency with irregular sampling intervals. The validation in this research is therefore proved to be challenging. The model could be calibrated and validated more fittingly to the lake environment by the improvement of the accuracy and completeness of the field-measured data. This can be achieved by promoting data sharing among researchers and increasing transparency on the data collection processes. A shared database with information including the meteorological data, remote sensing images, digital elevation maps and field-measured hydraulic and water quality data of Poyang Lake would effectively facilitate research work and modeling. For example, pollution related information such as the discharge details and location of the upstream pollutant sources, waste treatment plants and animal farms could allow better approximation of pollutant influx in the water quality model.

In addition, the correctness of the field-measured data should be ensured to help identifying the causes of the mismatch between measured and modelled data. Higher

## Conclusions

---

temporal resolution in topographical comparisons and more advanced measurements in higher spatial and temporal resolution would allow for the improvement of the modelling ability and evaluation. The accuracy of the field data can be improved by a regulated sampling procedures with standardized practices and equipment. The frequency and locations in which the measurements are taken should also be strictly managed by a central research authority. Under the era of rapid technology advancement, researchers could utilize the use of drones in collecting field data under fierce weather and at remote location that are not easily accessible to man.

Rapid advancement in modern technology is where the current topic can draw inspiration from in the future. For example, the amount of data processed within a lake environment could increase tremendously with the use of a neural network, which could be applied for modeling of gigantic database with multiple variables. The neural network could be utilized for hydrodynamic and water quality model simulation at a larger scale with quicker calculation and higher accuracy. Alternative solution in contrast to hard engineering resolutions should also be explored. Bioremediation, which utilizes microbes in treating contaminants in soil and water, is a rising method that could be explored in the context of lake and river pollution. Advanced technology and computational power can also be applied to the water management aspect of this study. Automated sensing and management system could be implemented to control the barrage operation with direct response to real-time situations in the lake region. This can help to provide a more adaptive and suitable water management approaches for Poyang Lake, upgrading from the predetermined and inflexible barrage control schemes.



# References

- Akima, H. (1970). A New Method of Interpolation and Smooth Curve Fitting Based on Local Procedures. *Journal of the Association for Computing Machinery*, 17(4):589–602.
- Alosairi, Y., Pokavanich, T., and Alsulaiman, N. (2018). Three-dimensional hydrodynamic modelling study of reverse estuarine circulation: Kuwait Bay. *Marine Pollution Bulletin*, 127:82–96.
- Ambrose, R., Wool, T., and Martin, J. (1993). The Water Quality Analysis Simulation Program WASP5 Model Documentation and User Manuals. Technical report, US Environmental Protection Agency, Athens, Georgia.
- American Water Works Association (2013). Nitrification Prevention and Control in Drinking Water - AWWA Manual M56. Technical report, American Water Works Association.
- Arega, F. and Sanders, B. F. (2004). Dispersion Model for Tidal Wetlands. *Journal of Hydraulic Engineering*, 130(8):739–754.
- Babu, M., Vethamony, P., and Desa, E. (2005). Modelling tide-driven currents and residual eddies in the Gulf of Kachchh and their seasonal variability: A marine environmental planning perspective. *Ecological Modelling*, 184(2-4):299–312.
- Baptista, A. M., Zhang, Y., Chawla, A., Zulauf, M., Seaton, C., Myers III, E. P., Kindle, J., Wilkin, M., Burla, M., and Turner, P. J. (2005). A cross-scale model for 3D baroclinic circulation in estuary–plume–shelf systems: II. Application to the Columbia River. *Continental Shelf Research*, 25(7-8):935–972.
- Barber, R. W. and Volakos, N. P. (2005). Modelling Depth-integrated Pollution Dispersion In The Gulf Of Thermaikos Using A Lagrangian Particle Technique. *WIT Transactions on Ecology and the Environment*, 80:173–184.
- Barré de Saint-Venant, A. (1871). Théorie du mouvement nonpermanent des eaux, avec application aux crues des rivières et à l’introduction des marées dans leur lit. *Comptes Rendus de l’Académie des Sciences*, 73:147–154.
- Boussinesq, J. (1897). *Théorie de l’écoulement tourbillonnant et tumultueux des liquides dans les lits rectilignes a grande section*, volume 1. Paris, Gauthier-Villars et fils, Paris.
- Burn, D. H. and McBean, E. A. (1985). Optimization Modeling of Water Quality in an Uncertain Environment. *Water Resources Research*, 21(7):934–940.

## References

---

- Cai, X. and Ji, W. (2009). Wetland hydrologic application of satellite altimetry - A case study in the Poyang Lake watershed. *Progress in Natural Science*, 19(12):1781–1787.
- Cai, Y., Sun, G., and Liu, B. (2005). Mapping of water body in Poyang Lake from partial spectral unmixing of MODIS data. *International Geoscience and Remote Sensing Symposium (IGARSS)*, 7:4539–4540.
- Caissie, D. (2006). The thermal regime of rivers: a review. *Freshwater Biology*, 51(8):1389–1406.
- Camp, T. R. (1963). *Water and Its Impurities*. Reinhold Publishing, New York.
- Cao, X. and Zhang, H. (2006). Commentary on Study of Surface Water Quality Model. *Journal of Water Resources and Architectural Engineering*, 4(4):18–21.
- Chao, X., Jia, Y., Shields, F. D., Wang, S. S., and Cooper, C. M. (2010). Three-dimensional numerical simulation of water quality and sediment-associated processes with application to a Mississippi Delta lake. *Journal of Environmental Management*, 91(7):1456–1466.
- Chen, B., Wang, P., and Zhang, H. (2016). The Review of Nitrogen and Phosphorus Pollution in Poyang Lake Water. *Journal of Jiangxi Normal University (Natural Science)*, 40(4):437–441.
- Chen, J., Wu, X., Wang, Z., and Zhu, J. (2012). Establishment of fundamental geographic information system and associated key technologies for Poyang Lake wetland. *Geomatics and Information Science of Wuhan University*, 37(8):888–896.
- Cheng, S.-c. and Ru, B. (2003). The characteristics of the lake current of Poyang Lake. *Jiangxi Hydraulic Science & Technology*, 29(2):105–108.
- Chiesa, M., Mathiesen, V., Melheim, J. A., and Halvorsen, B. (2005). Numerical simulation of particulate flow by the Eulerian–Lagrangian and the Eulerian–Eulerian approach with application to a fluidized bed. *Computers & Chemical Engineering*, 29(2):291–304.
- Chung, T. (2010). *Computational Fluid Dynamics*. Cambridge University Press, New York, second edition.
- Cole, T. and Well, S. (2006). CE-QUAL-W2: A two-dimensional, laterally averaged, Hydrodynamic and Water Quality Model, Version 3.5. Technical report, US Army Engineering and Research Development Center, Vicksburg.
- Constable, T. W. and McBean, E. A. (1979). Kalman Filter Modeling of the Speed River Quality. *Journal of the Environmental Engineering Division*, 105(5):961–978.
- Courant, R., Friedrichs, K., and Lewy, H. (1967). On the Partial Difference Equations of Mathematical Physics. *IBM Journal of Research and Development*, 11(2):215–234.
- Cui, L., Qiu, Y., Fei, T., Liu, Y., and Wu, G. (2013). Using remotely sensed suspended sediment concentration variation to improve management of Poyang Lake, China. *Lake and Reservoir Management*, 29(1):47–60.

## References

---

- Cui, L., Wu, G., and Liu, Y. (2009). Monitoring the impact of backflow and dredging on water clarity using MODIS images of Poyang Lake, China. *Hydrological Processes*, 23(2):342–350.
- Dai, X., Wan, R., and Yang, G. (2015). Non-stationary water-level fluctuation in China's Poyang Lake and its interactions with Yangtze River. *Journal of Geographical Sciences*, 25(3):274–288.
- Darwish, M. and Moukalled, F. (2003). TVD schemes for unstructured grids. *International Journal of Heat and Mass Transfer*, 46(4):599–611.
- Davison, N. (2014). The drying up of China's largest freshwater lake. [Online; Accessed on 2015-04-04]. <https://www.chinadialogue.net/article/show/single/en/6626-The-drying-up-of-China-s-largest-freshwater-lake>.
- Deltares (2014). Delft3D-FLOW Hydro-Morphodynamics User Manual. Technical report, Deltares, Delft.
- Deng, X., Zhao, Y., Wu, F., Lin, Y., Lu, Q., and Dai, J. (2011). Analysis of the trade-off between economic growth and the reduction of nitrogen and phosphorus emissions in the Poyang Lake Watershed, China. *Ecological Modelling*, 222(2):330–336.
- DHI (2017a). MIKE 11 WQ Templates Scientific Documentation. Technical report, Danish Hydraulic Institute, Hørsholm, Denmark.
- DHI (2017b). MIKE 21 & MIKE 3 Flow Model Advection-Dispersion Module Scientific Description. Technical report, Danish Hydraulic Institute, Hørsholm, Denmark.
- DHI (2017c). MIKE 21 & MIKE 3 Flow Model FM Hydrodynamic and Transport Module Scientific Documentation. Technical report, Danish Hydraulic Institute, Hørsholm, Denmark.
- DHI (2017d). MIKE 21 & MIKE 3 Flow Model FM: MIKE ECO Lab Module Short Description. Technical report, Danish Hydraulic Institute, Hørsholm, Denmark.
- DHI (2017e). MIKE ECO Lab Water Quality Templates Scientific Description. Technical report, Danish Hydraulic Institute, Hørsholm, Denmark.
- Di Toro, D. M., O'Connor, D. J., and Thomann, R. V. (1971). A Dynamic Model of the Phytoplankton Population in the Sacramento—San Joaquin Delta. In J. D. Hem, editor, *Nonequilibrium Systems in Natural Water Chemistry*, chapter 5, pages 131–180. American Chemical Society.
- Dobbins, W. E. (1964). BOD and Oxygen Relationship in Streams. *Journal of the Sanitary Engineering Division*, 90(3):53–78.
- Donea, J., Huerta, A., Ponthot, J.-P., and Rodríguez-Ferran, A. (2004). Arbitrary Lagrangian-Eulerian Methods. In Stein, E., de Borst, R., and Hughes, T. J., editors, *Encyclopedia of Computational Mechanics*, chapter 14, pages 1–25. John Wiley & Sons, Ltd, first edition.

## References

---

- Ekebjærg, L. and Justesen, P. (1991). An explicit scheme for advection-diffusion modelling in two dimensions. *Computer Methods in Applied Mechanics and Engineering*, 88(3):287–297.
- Encyclopaedia Britannica (2018). Three Gorges Dam. [Online; Accessed on 2018-08-28]. <https://www.britannica.com/topic/Three-Gorges-Dam>.
- Engel, B., Storm, D., White, M., Arnold, J., and Arabi, M. (2007). A Hydrologic/Water Quality Model Application Protocol. *Journal of the American Water Resources Association*, 43(5):1223–1236.
- European Commission (1998). Council Directive 98/83/EC. *Official Journal of the European Communities*, 330:32–54.
- Falconer, R. A. (1991). Review of Modelling Flow and Pollutant Transport Processes in Hydraulic Basins. In Wrobel L.C. and Brebbia C.A., editors, *Water Pollution: Modelling, Measuring and Prediction*, pages 3–23. Springer, Dordrecht.
- Fang, H., Dai, D., Li, S., He, G., and Huang, L. (2016). Forecasting Yangtze finless porpoise movement behavior using an Eulerian–Eulerian-diffusion method (EEDM). *Ecological Engineering*, 88:39–52.
- Feng, L., Hu, C., Chen, X., Cai, X., Tian, L., and Gan, W. (2012). Assessment of inundation changes of Poyang Lake using MODIS observations between 2000 and 2010. *Remote Sensing of Environment*, 121:80–92.
- Finlayson, M., Harris, J., McCartney, M., Young, L., and Chen, Z. (2010). Report on Ramsar visit to Poyang Lake Ramsar site. Technical report, Ramsar Convention.
- Fredsøe, J. (1984). Turbulent Boundary Layer in Wave-current Motion. *Journal of Hydraulic Engineering*, 110(8):1103–1120.
- Ganju, N. K., Brush, M. J., Rashleigh, B., Aretxabaleta, A. L., del Barrio, P., Grear, J. S., Harris, L. A., Lake, S. J., McCardell, G., O’Donnell, J., Ralston, D. K., Signell, R. P., Testa, J. M., and Vaudrey, J. M. P. (2016). Progress and Challenges in Coupled Hydrodynamic-Ecological Estuarine Modeling. *Estuaries and Coasts*, 39(2):311–332.
- Gao, G., Ruan, R., and Ouyang, Q. (2010). Water quality status and changing trend in Poyang Lake. *Journal of Nanchang Institute of Technology*, 29(4):50–53.
- Gao, J. H., Jia, J., Kettner, A. J., Xing, F., Wang, Y. P., Xu, X. N., Yang, Y., Zou, X. Q., Gao, S., Qi, S., and Liao, F. (2014). Changes in water and sediment exchange between the Changjiang River and Poyang Lake under natural and anthropogenic conditions, China. *Science of the Total Environment*, 481(1):542–553.
- Gao, W., Gao, B., Yan, C., and Liu, Y. (2016). Evolution of anthropogenic nitrogen and phosphorus inputs to Poyang Lake Basin and its effect on water quality of lake. *Acta Scientiae Circumstantiae*, 36(9):3137–3145.
- Gough, D. I. (1969). Incremental stress under a two-dimensional artificial lake. *Canadian Journal of Earth Sciences*, 6(5):1067–1075.

## References

---

- Gross, E. S., Koseff, J. R., and Monismith, S. G. (1999). Evaluation of Advective Schemes for Estuarine Salinity Simulations. *Journal of Hydraulic Engineering*, 125(1):32–46.
- Gualtieri, C., Gualtieri, P., and Doria, G. P. (2002). Dimensional Analysis of Reaeration Rate in Streams. *Journal of Environmental Engineering*, 128(1):12–18.
- Guildford, S. J., Hendzel, L. L., Kling, H. J., Fee, E. J., Robinson, G. G. C., Hecky, R. E., and Kasian, S. E. M. (1994). Effects of Lake Size on Phytoplankton Nutrient Status. *Canadian Journal of Fisheries and Aquatic Sciences*, 51(12):2769–2783.
- Gündüz, O. (2004). *Coupled Flow and Contaminant Transport Modeling in Large Watersheds*. PhD thesis, Georgia Institute of Technology, USA.
- Guo, H., Hu, Q., and Jiang, T. (2008). Annual and seasonal streamflow responses to climate and land-cover changes in the Poyang Lake basin, China. *Journal of Hydrology*, 355(1-4):106–122.
- Guo, H., Hu, Q., Zhang, Q., and Feng, S. (2012a). Effects of the Three Gorges Dam on Yangtze River flow and river interaction with Poyang Lake, China: 2003-2008. *Journal of Hydrology*, 416-417:19–27.
- Guo, Y., Lou, F., Lou, P., and Yang, X. (2012b). Studies of Poyang Lake Water Environment Dynamics and its Mechanisms. Technical report, Jiangxi Province Poyang Lake Water Bureau; Hohai University.
- Guo, Z., Shi, B., and Zheng, C. (2002). A coupled lattice BGK model for the Boussinesq equations. *International Journal for Numerical Methods in Fluids*, 39(4):325–342.
- Gurumoorthi, K. and Venkatachalapathy, R. (2017). Hydrodynamic modeling along the southern tip of India: A special emphasis on Kanyakumari coast. *Journal of Ocean Engineering and Science*, 2(4):229–244.
- Hakim, B. A., Wibowo, M., Kongko, W., Irfani, M., Hendriyono, W., and Gumbira, G. (2015). Hydrodynamics Modeling of Giant Seawall in Semarang Bay. *Procedia Earth and Planetary Science*, 14:200–207.
- Hamrick, J. M. (1992). A Three-Dimensional Environmental Fluid Dynamics Computer Code : Theoretical and computational aspects. Technical report, Virginia Institute of Marine Science.
- Hannoun, I., List, E. J., Kavanagh, K. B., Chiang, W.-L., Ding, L., Preston, A., Karafa, D., and Rackley, I. (2006). Use of ELCOM and CAEDYM for Water Quality Simulation in Boulder Basin. *Proceedings of the Water Environment Federation*, 2006(9):3943–3970.
- Hartanto, I., Beevers, L., Popescu, I., and Wright, N. (2011). Application of a coastal modelling code in fluvial environments. *Environmental Modelling & Software*, 26(12):1685–1695.

## References

---

- Higashino, M., Gantzer, C. J., and Stefan, H. G. (2004). Unsteady diffusional mass transfer at the sediment/water interface: Theory and significance for SOD measurement. *Water Research*, 38(1):1–12.
- Hirsch, C. (1990). *Numerical computation of internal and external flows*. John Wiley & Sons, Ltd, West Sussex, England.
- Hu, C., Lou, Q., Ding, W., and Zhou, W. (2012a). Study on the retention effect of nitrogen and phosphorus nutrients in Poyang Lake. *Environmental Pollution & Control*, 34(9):1–4.
- Hu, C. and Ruan, B. (2011). Study on key technologies of Poyang Lake Water Control Project. *Journal of China Institute of Water Resources and Hydropower Research*, 9(4):243–248.
- Hu, C., Shi, W., Hu, L., and Zhou, W. (2012b). Simulation study on the impact of Poyang Lake hydro-junction projects on nitrogen and phosphorus nutrient in lake region. *Resources and Environment in the Yangtze Basin*, 21(6):749–755.
- Hu, M., Yuan, J., Lu, F., Li, R., and Xu, X. (2012c). Frequency and causes characteristics of nitrogen and phosphorus pollution in typical section of Poyang Lake. *Journal of Water Resources & Water Engineering*, 23(1):14–17.
- Hu, Q., Feng, S., Guo, H., Chen, G., and Jiang, T. (2007). Interactions of the Yangtze river flow and hydrologic processes of the Poyang Lake, China. *Journal of Hydrology*, 347(1-2):90–100.
- Huang, G., Falconer, R. A., and Lin, B. (2018). Evaluation of E.coli losses in a tidal river network using a refined 1-D numerical model. *Environmental Modelling & Software*, 108:91–101.
- Huang, G., Xu, X., Ding, H., Chen, Q., and Cui, Y. (2011). Study of the impact of Poyang Lake barrage project on the lake region's water quality. Technical report, Research Center for Eco-Environmental Science, Chinese Academy of Science; Jiangxi Province Institute of Water Sciences, Beijing, China.
- Huang, J., Gao, J., and Zhang, Y. (2015a). Combination of artificial neural network and clustering techniques for predicting phytoplankton biomass of Lake Poyang, China. *Limnology*, 16(3):179–191.
- Huang, J., Wang, X., Xi, B., Xu, Q., Tang, Y., Jia, K., Huo, S., Da, A., Gao, R., Liu, H., Li, X., Liu, M., and Mao, J. (2015b). Long-term variations of TN and TP in four lakes fed by Yangtze River at various timescales. *Environmental Earth Sciences*, 74(5):3993–4009.
- Hui, F., Xu, B., Huang, H., Yu, Q., and Gong, P. (2008). Modelling spatial-temporal change of Poyang Lake using multitemporal Landsat imagery. *International Journal of Remote Sensing*, 29(20):5767–5784.
- Jafari, M. and Khayamian, T. (2008). Direct determination of ammoniacal nitrogen in water samples using corona discharge ion mobility spectrometry. *Talanta*, 76(5):1189–1193.

## References

---

- Jawahar, P. and Kamath, H. (2000). A High-Resolution Procedure for Euler and Navier–Stokes Computations on Unstructured Grids. *Journal of Computational Physics*, 164(1):165–203.
- Jørgensen, S. E. (1979). *Handbook of environmental data and ecological parameters*. Pergamon Press, Oxford, UK.
- Jones, O., Zyserman, J. A., and Wu, Y. (2014). Influence of Apparent Roughness on Pipeline Design Conditions Under Combined Waves and Current. In *ASME 2014 33rd International Conference on Ocean, Offshore and Arctic Engineering*, page 8, San Francisco, USA. ASME.
- Kannel, P. R., Kanel, S. R., Lee, S., Gan, T. Y., Kanel, S. R., Lee, Y.-S., and Gan, T. Y. (2011). A Review of Public Domain Water Quality Models for Simulating Dissolved Oxygen in Rivers and Streams. *Environmental Modeling and Assessment*, 16(2):183–204.
- Kernkamp, H., van Dam, A., Stelling, G., and de Goede, E. (2011). Efficient scheme for the shallow water equations on unstructured grids with application to the Continental Shelf - Semantic Scholar. *Ocean Dynamics*, 61(1175-1188).
- Kong, J., Xin, P., Shen, C.-J., Song, Z.-Y., and Li, L. (2013). A high-resolution method for the depth-integrated solute transport equation based on an unstructured mesh. *Environmental Modelling & Software*, 40:109–127.
- Körner, S., Das, S. K., Veenstra, S., and Vermaat, J. E. (2001). The effect of pH variation at the ammonium/ammonia equilibrium in wastewater and its toxicity to *Lemna gibba*. *Aquatic Botany*, 71(1):71–78.
- Lai, G., Pan, R., and Huang, X. (2011a). Research and Development of Poyang Lake Hydrodynamic Modeling System Based on MapWinGIS. *Journal of Geo-Information Science*, 13(4):447–454.
- Lai, G., Wang, P., and Li, L. (2016). Possible impacts of the Poyang Lake (China) hydraulic project on lake hydrology and hydrodynamics. *Hydrology Research*, 47(51):187–205.
- Lai, X., Huang, Q., Zhang, Y., and Jiang, J. (2014a). Impact of lake inflow and the Yangtze River flow alterations on water levels in Poyang Lake, China. *Lake and Reservoir Management*, 30(4):321–330.
- Lai, X., Jiang, J., and Huang, Q. (2012). Water storage effects of Three Gorges project on water regime of Poyang lake. *Journal of Hydroelectric Engineering*, 31(6):132–148.
- Lai, X., Jiang, J., Huang, Q., and Xu, L. (2011b). Two-dimensional numerical simulation of hydrodynamic and pollutant transport for Lake Poyang. *Journal of Lake Science*, 23(6):893–902.
- Lai, X., Jiang, J., Liang, Q., and Huang, Q. (2013). Large-scale hydrodynamic modeling of the middle Yangtze River Basin with complex river–lake interactions. *Journal of Hydrology*, 492:228–243.

## References

---

- Lai, X., Liang, Q., Jiang, J., and Huang, Q. (2014b). Impoundment Effects of the Three-Gorges-Dam on Flow Regimes in Two China's Largest Freshwater Lakes. *Water Resources Management*, 28(14):5111–5124.
- Laval, B. and Hodges, B. R. (2000). The CWR Estuary and Lake Computer Model ELCOM User Guide. Technical report, Centre for Water Research, The University of Western Australia, Perth, Australia.
- Legates, D. R. and McCabe, G. J. (1999). Evaluating the use of “goodness-of-fit” Measures in hydrologic and hydroclimatic model validation. *Water Resources Research*, 35(1):233–241.
- Li, J. (2014). Troubled waters: huge Poyang Lake dam 'back on the agenda'. [Online; Accessed on 2015-04-04]. <http://www.scmp.com/news/china/article/1580458/troubled-waters-huge-poyang-lake-dam-back-agenda>.
- Li, M. and Xu, K. (2007). Long-term variations in dissolved silicate, nitrogen, and phosphorus flux from the Yangtze River into the East China Sea and impacts on estuarine ecosystem. *Estuarine, Coastal and Shelf Science*, 71(1-2):3–12.
- Li, R.-D. and Liu, J.-Y. (2002). Wetland vegetation biomass estimation and mapping from Landsat ETM data: a case study of Poyang Lake. *Journal of Geographical Sciences*, 2(1):35–41.
- Li, T. (2008). Crisis at Poyang Lake. [Online; Accessed on 2015-04-05]. <https://www.chinadialogue.net/homepage/show/single/en/1846-Crisis-at-Poyang-Lake>.
- Li, X., Zhang, Q., Xu, C. Y., and Ye, X. (2015a). The changing patterns of floods in Poyang Lake, China: characteristics and explanations. *Natural Hazards*, 76(1):651–666.
- Li, Y., Acharya, K., and Yu, Z. (2011). Modeling impacts of Yangtze River water transfer on water ages in Lake Taihu, China. *Ecological Engineering*, 37(2):325–334.
- Li, Y. and Yao, J. (2015). Estimation of Transport Trajectory and Residence Time in Large River–Lake Systems: Application to Poyang Lake (China) Using a Combined Model Approach. *Water*, 7(10):5203–5223.
- Li, Y., Zhang, Q., and Yao, J. (2015b). Investigation of Residence and Travel Times in a Large Floodplain Lake with Complex Lake-River Interactions: Poyang Lake (China). *Water*, 7(5):1991–2012.
- Li, Y., Zhang, Q., Yao, J., Li, X., and Xu, X. (2012). An Integrated Hydrological Model for Poyang Lake Watershed, China. In *2012 2nd International Conference on Remote Sensing, Environment and Transportation Engineering*, pages 1–4. IEEE.
- Li, Y., Zhang, Q., Yao, J., Werner, A., and Li, X. (2014). Hydrodynamic and Hydrological Modeling of the Poyang Lake Catchment System in China. *Journal of Hydrologic Engineering*, 19(3):607–616.
- Liang, D., Chong, K., Thusyanthan, N., and Tang, H. (2012). Thermal imaging study of scalar transport in shallow wakes. *Journal of Hydrodynamics, Ser. B*, 24(1):17–24.

## References

---

- Liang, D., Wang, X., Bockelmann-Evans, B. N., and Falconer, R. A. (2013). Study on nutrient distribution and interaction with sediments in a macro-tidal estuary. *Advances in Water Resources*, 52:207–220.
- Liang, D., Wang, X., Falconer, R. A., and Bockelmann-Evans, B. N. (2010). Solving the depth-integrated solute transport equation with a TVD-MacCormack scheme. *Environmental Modelling & Software*, 25(12):1619–1629.
- Liang, D. and Wu, X. (2014). A random walk simulation of scalar mixing in flows through submerged vegetations. *Journal of Hydrodynamics, Ser. B*, 26(3):343–350.
- Liang, J., Yang, Q., Sun, T., Martin, J. D., Sun, H., and Li, L. (2015). MIKE 11 model-based water quality model as a tool for the evaluation of water quality management plans. *Journal of Water Supply: Research and Technology—AQUA*, 64(6):708.
- Lin, B. and Falconer, R. A. (1997). Tidal Flow and Transport Modeling Using ULTIMATE QUICKEST Scheme. *Journal of Hydraulic Engineering*, 123(4):303–314.
- Lindim, C., Pinho, J., and Vieira, J. (2011). Analysis of spatial and temporal patterns in a large reservoir using water quality and hydrodynamic modeling. *Ecological Modelling*, 222(14):2485–2494.
- Liu, K., Ni, Z., Wang, S., and Ni, C. (2015). Distribution characteristics of phosphorus in sediments at different altitudes of Poyang Lake. *China Environmental Science*, 35(3):856–861.
- Liu, W., Chan, W., and Tsai, D. D. (2016). Three-dimensional modeling of suspended sediment transport in a subalpine lake. *Environmental Earth Sciences*, 75(2):173.
- Liu, Y., Wu, G., and Zhao, X. (2013). Recent declines in China’s largest freshwater lake: trend or regime shift? *Environmental Research Letters*, 8(1):014010.
- Lu, J., Qi, H., Chen, X., Chen, L., Sauvage, S., and Sanchez-Perez, J.-M. (2015). Validation of Hydrodynamic Model by Remote Sensing Data for China’s Largest Freshwater Lake. In *2015 IEEE International Geoscience and Remote Sensing Symposium (IGARSS)*, pages 2504–2507. IEEE, New York.
- Luo, M., Li, J., Cao, W., and Wang, M. (2008). Study of heavy metal speciation in branch sediments of Poyang Lake. *Journal of Environmental Sciences*, 20(2):161–166.
- Luo, Y., Wu, H., Li, Y., Wan, Z., Zhang, Q., Jia, J., Xiao, N., and Jiangxi Environmental Monitoring Center (2014). The Study on the Pollutant of Flux of Lake Inflow in Poyang Lake Basin. *Jiangxi Science*, 32(5):587–605.
- Lv, T. and Wu, C. (2013). Study on Coupling Degree and Optimal Path between Land Water Resources and Economic Development in Poyang Lake Ecological Economical Zone. *International Journal of Environmental Science & Development*, 4(5):569.
- Ma, G., Wang, S., Wang, Y., Zuo, D., Yu, Y., and Xiang, B. (2015). Temporal and spatial distribution characteristics of nitrogen and phosphorus and diffuse source pollution load simulation of Poyang Lake Basin. *Acta Scientiae Circumstantiae*, 35(5):1285–1291.

## References

---

- Mahanty, M., Mohanty, P., Pattnaik, A., Panda, U., Pradhan, S., and Samal, R. (2016). Hydrodynamics, temperature/salinity variability and residence time in the Chilika lagoon during dry and wet period: Measurement and modeling. *Continental Shelf Research*, 125(8):28–43.
- Manning, R. (1891). On the Flow of Water in Open Channels and Pipes. *Transactions of the Institution of Civil Engineers of Ireland*, 20:161–207.
- Marsooli, R., Orton, P. M., Georgas, N., and Blumberg, A. F. (2016). Three-dimensional hydrodynamic modeling of coastal flood mitigation by wetlands. *Coastal Engineering*, 111:83–94.
- Mehta, B. M., Ahlert, R. C., and Yu, S. L. (1975). Stochastic variation of water quality of the Passaic River. *Water Resources Research*, 11(2):300–308.
- Meselhe, E. A. and Holly Jr., F. M. (1997). Invalidity of Preissmann Scheme for Transcritical Flow. *Journal of Hydraulic Engineering*, 123(7):652–655.
- MET Office (2013). The impact of climate, population, and carbon dioxide on water resources. [Online; Accessed on 2015-04-09]. <https://www.metoffice.gov.uk/research/news/2013/impacts-on-water-resource>.
- Ministry of Environmental Protection (2002). Environmental quality standards for surface water of People’s Republic of China. Technical report, Ministry of Ecology and Environmental of the People’s Republic of China.
- Morales-Hernández, M., Lacasta, A., Murillo, J., and García-Navarro, P. (2017). A Large Time Step explicit scheme (CFL>1) on unstructured grids for 2D conservation laws: Application to the homogeneous shallow water equations. *Applied Mathematical Modelling*, 47:294–317.
- Moriasi, D., Arnold, J., Van Liew, M., Bingner, R., Harmel, R., and Veith, T. (2007). Model evaluation guidelines for systematic quantification of accuracy in watershed simulations. *Transactions of the ASABE 2007*, 50(3):885–900.
- Nakamura, Y. and Stefan, H. G. (1994). Effect of Flow Velocity on Sediment Oxygen Demand: Theory. *Journal of Environmental Engineering*, 120(5):996–1016.
- Nash, J. and Sutcliffe, J. (1970). River flow forecasting through conceptual models part I - A discussion of principles. *Journal of Hydrology*, 10(3):282–290.
- National Geographic (2010). Freshwater Crisis. [Online; Accessed on 2019-07-19]. <https://www.nationalgeographic.com/environment/freshwater/freshwater-crisis/>.
- Novak, P., Guinot, V., Jeffrey, A., and Reeve, D. E. (2010). *Hydraulic Modelling: An Introduction: Principles, Methods and Applications*. CRC Press, Abingdon.
- O’Connor, D. and Thomann, R. (1972). Water Quality Models: Chemical, Physical and Biological Constituents. In *Estuarine Modeling: An Assessment*, chapter 702/71, pages 102–169. EPA Water Pollution Control Research Series 16070.

## References

---

- O'Connor, D. J. (1967). The temporal and spatial distribution of dissolved oxygen in streams. *Water Resources Research*, 3(1):65–79.
- O'Connor, D. J. and Dobbins, W. E. (1956). The Mechanics of Reaeration in Natural Streams. *Journal of the Sanitary Engineering Division*, 82(6):1–30.
- Orlob, G. T. (1983). *Mathematical Modeling of Water Quality: Streams, Lakes, and Reservoirs*. John Wiley & Sons, Ltd, Bath.
- Ou, M., Zhou, W., and Hu, C. (2012). Chlorophyll-a's Spatial Distribution and Relationship with Nitrogen and Phosphorus in Poyang Lake. *Acta Agriculturae Boreali-occidentalis Sinica*, 21(6):162–166.
- Padgett, W. J. and Rao, A. N. (1979). Estimation of BOD and DO Probability Distribution. *Journal of the Environmental Engineering Division*, 105(3):525–533.
- Peeters, F. and Hofmann, H. (2015). Length-scale dependence of horizontal dispersion in the surface water of lakes. *Limnology and Oceanography*, 60(6):1917–1934.
- Peucker, T. K., Fowler, R. J., Little, J. J., and Mark, D. M. (1978). The triangulated irregular network. In American Society of Photogrammetry, editor, *Digital Terrain Models Symposium*, pages 516–532, Falls Church, VA, USA.
- Preissmann, A. (1961). Propagation des intumescences dans les canaux et rivières. In *1st Congress of the French Association for Computation (AFCALTI)*, Grenoble, France.
- Qi, H., Lu, J., Chen, X., Sauvage, S., and Sanchez-Pérez, J.-M. (2016). Water age prediction and its potential impacts on water quality using a hydrodynamic model for Poyang Lake, China. *Environment Science Pollution Research*.
- Qi, S. and Liao, F. (2013). A study on the scheme of water level regulation of the Poyang Lake hydraulic project. *Acta Geographica Sinica*, 68(1):118–126.
- Qian, K., Liu, X., and Chen, Y. (2016). Effects of water level fluctuation on phytoplankton succession in Poyang Lake, China – A five year study. *Ecohydrology & Hydrobiology*, 16(3):175–184.
- Ranasinghe, R., Larson, M., and Savioli, J. (2010). Shoreline response to a single shore-parallel submerged breakwater. *Coastal Engineering*, 57(11-12):1006–1017.
- Renardy, M. (2009). Ill-posedness of the Hydrostatic Euler and Navier–Stokes Equations. *Archive for Rational Mechanics and Analysis*, 194(3):877–886.
- Richtmyer, R. D. (1957). *Difference methods for initial-value problems*. Interscience Publishers, New York.
- Ritter, A. and Muñoz-Carpena, R. (2013). Performance evaluation of hydrological models: Statistical significance for reducing subjectivity in goodness-of-fit assessments. *Journal of Hydrology*, 480:33–45.
- Rodi, W. (1984). *Turbulence models and their application in hydraulics: a state of the art review*. International Association for Hydraulic Research, Delft, The Netherlands.

## References

---

- Roe, P. (1981). Approximate Riemann solvers, parameter vectors, and difference schemes. *Journal of Computational Physics*, 43(2):357–372.
- Samaras, A. G., Gaeta, M. G., Moreno Miquel, A., and Archetti, R. (2016). High-resolution wave and hydrodynamics modelling in coastal areas: operational applications for coastal planning, decision support and assessment. *Hazards Earth Syst. Sci.*, 16:1499–1518.
- Shankman, D., Keim, B. D., and Song, J. (2006). Flood frequency in China’s Poyang Lake region: trends and teleconnections. *International Journal of Climatology*, 26(9):1255–1266.
- Siegle, E., Huntley, D. A., and Davidson, M. A. (2007). Coupling video imaging and numerical modelling for the study of inlet morphodynamics. *Marine Geology*, 236(3-4):143–163.
- Sleigh, P., Gaskell, P., Berzins, M., and Wright, N. (1998). An unstructured finite-volume algorithm for predicting flow in rivers and estuaries. *Computers & Fluids*, 27(4):479–508.
- Smagorinsky, J. (1963). General Circulation Experiments with the Primitive Equations. *Monthly Weather Review*, 91(3):99–164.
- Sokolova, E., Pettersson, T. J., Bergstedt, O., and Hermansson, M. (2013). Hydrodynamic modelling of the microbial water quality in a drinking water source as input for risk reduction management. *Journal of Hydrology*, 497:15–23.
- Soldatova, E., Guseva, N., Sun, Z., Bychinsky, V., Boeckx, P., and Gao, B. (2017). Sources and behaviour of nitrogen compounds in the shallow groundwater of agricultural areas (Poyang Lake basin, China). *Journal of Contaminant Hydrology*, 202:59–69.
- Song, Y. and Haidvogel, D. (1994). A Semi-implicit Ocean Circulation Model Using a Generalized Topography-Following Coordinate System. *Journal of Computational Physics*, 115(1):228–244.
- Streeter, H. and Phelps, E. B. (1925). A Study of the Pollution and Natural Purification of the Ohio River. Technical report, United States Public Health Service.
- Sun, B., Zhang, L., Yang, L., Zhang, F., Norse, D., and Zhu, Z. (2012). Agricultural non-point source pollution in China: Causes and mitigation measures. *Ambio*, 41(4):370–379.
- Sun, S., Chen, H., Ju, W., Song, J., Zhang, H., Sun, J., and Fang, Y. (2013). Effects of climate change on annual streamflow using climate elasticity in Poyang Lake Basin, China. *Theoretical and Applied Climatology*, 112(1-2):169–183.
- Swinehart, D. F. (1962). The Beer-Lambert Law. *Journal of Chemical Education*, 39(7):333.

## References

---

- Symonds, A. M., Vijverberg, T., Post, S., Van der Spek, B.-J., Henrotte, J., and Sokolewicz, M. (2016). Comparison between MIKE21 FM, Delft3D and Delft3D FM Flow models of Western Port Bay, Australia. *Coastal Engineering Proceedings*, 1(35):11.
- Tan, G., Tan, M., Long, X., and Xing, G. (2008). Impact of the Jiangxi Five Rivers System on Poyang Lake's Ecosystem. Technical report, Jiangxi Province Water Bureau; Jiangxi Province Academy of Science.
- Tan, G., Zhou, Z., Wu, J., Wang, S., Li, M., Wang, H., Wu, M., and Deng, Y. (2014). Poyang Lake Water Environment Surface Water Quality Monitoring Site Optimization. Technical report, Jiangxi Province Poyang Lake Water Bureau.
- Tang, C., Yi, Y., Yang, Z., and Cheng, X. (2014). Water pollution risk simulation and prediction in the main canal of the South-to-North Water Transfer Project. *Journal of Hydrology*, 519(B):2111–2120.
- Thayer, R. P. and Krutchkoff, R. G. (1967). Stochastic Model for BOD and DO in Streams. *Journal of the Sanitary Engineering Division*, 93(3):59–72.
- Thomas, L. (1949). Elliptic Problems in Linear Differential Equations over a Network. Technical report, Columbia University, New York.
- Tim, U. S. and Jolly, R. (1994). Evaluating Agricultural Nonpoint-Source Pollution Using Integrated Geographic Information Systems and Hydrologic/Water Quality Model. *Journal of Environment Quality*, 23(1):25.
- Tufford, D. L. and McKellar, H. N. (1999). Spatial and temporal hydrodynamic and water quality modeling analysis of a large reservoir on the South Carolina (USA) coastal plain. *Ecological Modelling*, 114(2-3):137–173.
- UN POPIN (1994). Population and Water Resources (contrib. by FAO). [Online; Accessed on 2015-04-09]. <http://www.un.org/popin/fao/water.html>.
- UNESCO (1981). Tenth report of the Joint Panel on Oceanographic. Technical report, United Nations Educational, Scientific and Cultural Organization, Paris, France.
- US EPA (2015). Water Resources Impacts & Adaptation. [Online; Accessed on 2015-04-09]. <http://www.epa.gov/climatechange/impacts-adaptation/water.html>.
- US EPA (2018). Effects of Acid Rain. [Online; Accessed on 2018-09-06]. <https://www.epa.gov/acidrain/effects-acid-rain>.
- van Vliet, M. T. H., Yearsley, J. R., Franssen, W. H. P., Ludwig, F., Haddeland, I., Lettenmaier, D. P., and Kabat, P. (2012). Coupled daily streamflow and water temperature modelling in large river basins. *Hydrology and Earth System Sciences*, 16(11):4303–4321.
- van Vossen, B. (2000). Horizontal Large Eddy Simulation; Evaluation of Computations with DELFT3D-FLOW. Technical report, Delft University of Technology, The Netherlands, Delft.

## References

---

- Vested, H. J., Justesen, P., and Ekebjærg, L. (1992). Advection-dispersion modelling in three dimensions. *Applied Mathematical Modelling*, 16(10):506–519.
- Wang, H., Wu, M., Deng, Y., Tang, C., and Yang, R. (2014a). Surface water quality monitoring site optimization for poyang lake, The largest freshwater lake in China. *International Journal of Environmental Research and Public Health*, 11(11):11833–11845.
- Wang, H., Zhang, L., Yao, X., Xue, B., and Yan, W. (2017). Dissolved nitrous oxide and emission relating to denitrification across the Poyang Lake aquatic continuum. *Journal of Environmental Sciences*, 52:130–140.
- Wang, H., Zhou, Y., and Wang, X. (2015a). Algal growth simulation post water regulation in a river-connected lake. In *PROCEEDINGS OF THE 2015 INTERNATIONAL FORUM ON ENERGY, ENVIRONMENT SCIENCE AND MATERIALS*, volume 40, pages 1049–1054.
- Wang, J., Chen, Z., and Wu, J. (2004). Stream water quality models and its developing trend. *Journal of Anhui Normal University*, 27(3):242–247.
- Wang, M., Hu, C., and Zhou, W. (2008a). Concentration variations of N and P in Poyang Lake during high water period with analysis on their sources. *Resources and Environment in the Yangtze Basin*, 17(1):139–142.
- Wang, M., Zhou, W., and Hu, C. (2008b). Status of nitrogen and phosphorus in waters of Lake Poyang Basin. *Journal of Lake Science*, 20(3):334–338.
- Wang, P., Lai, G., and Huang, X. (2014b). Simulation of the impact of Lake Poyang Project on the dynamic of lake water level. *Journal of Lake Sciences*, 26(1):29–36.
- Wang, P., Lai, G., and Li, L. (2015b). Predicting the Hydrological Impacts of the Poyang Lake Project Using an EFDC Model. *Journal of Hydrologic Engineering*, 20(12):1–10.
- Wang, Q., Li, S., Jia, P., Qi, C., and Ding, F. (2013). A review of surface water quality models. *The Scientific World Journal*, 2013(Article ID 231768):7.
- Wang, X., Hao, F., Cheng, H., Yang, S., Zhang, X., and Bu, Q. (2011). Estimating non-point source pollutant loads for the large-scale basin of the Yangtze River in China. *Environmental Earth Sciences*, 63(5):1079–1092.
- Wang, Y., Jiang, Y., Liao, W., Gao, P., Huang, X., Wang, H., Song, X., and Lei, X. (2014c). 3-D hydro-environmental simulation of Miyun reservoir, Beijin. *Journal of Hydro-environment Research*, 8(4):383–395.
- WantChinaTimes (2012). Jiangxi proposes dam on Poyang Lake to cope with drought. [Online; Accessed on 2015-04-09]. <http://www.wantchinatimes.com/news-subclass-cnt.aspx?id=20121005000030&cid=1505>.
- Wei, Y., Zhang, J., Zhang, D., Tu, T., and Luo, L. (2014). Metal concentrations in various fish organs of different fish species from Poyang Lake, China. *Ecotoxicology and Environmental Safety*, 104(1):182–188.

## References

---

- Welander, P. (1968). Wind-driven circulation in one- and two-layer oceans of variable depth. *Tellus*, 20(1):1–16.
- Westerink, J. J., Luettich, R. A., Feyen, J. C., Atkinson, J. H., Dawson, C., Roberts, H. J., Powell, M. D., Dunion, J. P., Kubatko, E. J., and Pourtaheri, H. (2008). A Basin-to Channel-Scale Unstructured Grid Hurricane Storm Surge Model Applied to Southern Louisiana. *Monthly Weather Review*, 136(3):833–864.
- Wetzel, R. G. (2001). *Limnology : Lake and River Ecosystems*. Academic Press, San Diego, third edition.
- White, F. M. (2008). Pressure Distribution in a Fluid. In 2, editor, *Fluid Mechanics*, chapter 2, pages 63–107. McGraw-Hill, New York, 7 edition.
- WHO (2014). Climate change and health. [Online; Accessed on 2015-04-09]. <http://www.who.int/mediacentre/factsheets/fs266/en/>.
- Wolanski, E., Mazda, Y., and Ridd, P. (1992). Mangrove hydrodynamics. In Robertson, A. and Alongi, D., editors, *Tropical Mangrove Ecosystems, Volume 41*, chapter 3, pages 43–62. American Geophysical Union (AGU).
- World Bank (2015a). Water and Climate Change. [Online; Accessed on 2015-04-09]. <http://water.worldbank.org/topics/water-resources-management/water-and-climate-change>.
- World Bank (2015b). Water Resources Management Overview. [Online; Accessed on 2017-12-17]. <http://www.worldbank.org/en/topic/waterresourcesmanagement/overview>.
- Wu, G. and Liu, Y. (2015). Capturing variations in inundation with satellite remote sensing in a morphologically complex, large lake. *Journal of Hydrology*, 523(4):14–23.
- Wu, Z. (2014). *The Influence of River-lake Relation Change on the Poyang Lake Sediments Nitrogen/Phosphorus Form and Release Risk*. PhD thesis, Nanchang University.
- Wu, Z., Lai, X., Zhang, L., Cai, Y., and Chen, Y. (2014). Phytoplankton chlorophyll a in Lake Poyang and its tributaries during dry, mid-dry and wet seasons: a 4-year study. *Knowledge and Management of Aquatic Ecosystems*, 412(06):1–13.
- WWF China (2014). WWF Suggests to Suspend the Poyang Lake Water Control Project. [Online; Accessed on 2015-04-04]. <https://en.wwfchina.org/?5121/WWF-Suggests-to-Suspend-the-Poyang-Lake-Water-Control-Project>.
- WWF UK (2015). Rivers and lakes - Protecting our freshwater ecosystems. [Online; Accessed on 2015-04-04]. [http://www.wwf.org.uk/what\\_we\\_do/rivers\\_and\\_lakes/](http://www.wwf.org.uk/what_we_do/rivers_and_lakes/).
- WWF UK (2018). Protecting our rivers, lakes and freshwater. [Online; Accessed on 2015-04-04]. <https://www.wwf.org.uk/what-we-do/area-of-work/protecting-our-rivers-lakes-and-freshwater>.

## References

---

- Xiang, S. and Zhou, W. (2011). Phosphorus forms and distribution in the sediments of Poyang Lake, China. *International Journal of Sediment Research*, 26(2):230–238.
- Xie, H., Wang, P., and Huang, H. (2013). Ecological Risk Assessment of Land Use Change in the Poyang Lake Eco-economic Zone, China. *International Journal of Environmental Research and Public Health*, 10(1):328–346.
- Xu, A. (2012). China alters controversial Poyang dam plan. [Online; Accessed on 2015-04-04]. <http://www.ecns.cn/2012/02-06/7550.shtml>.
- Xu, C., Zhang, J., Bi, X., Xu, Z., He, Y., and Gin, K. Y.-H. (2017). Developing an integrated 3D-hydrodynamic and emerging contaminant model for assessing water quality in a Yangtze Estuary Reservoir. *Chemosphere*, 188:218–230.
- Yang, Y., Gao, B., Hao, H., Zhou, H., and Lu, J. (2017). Nitrogen and phosphorus in sediments in China: A national-scale assessment and review. *Science of The Total Environment*, 576:840–849.
- Yao, M., Lin, J., Liu, M., and Xu, Y. (2012). Detection of chromium in wastewater from refuse incineration power plant near Poyang Lake by laser induced breakdown spectroscopy. *Applied Optics*, 51(10):1552–1557.
- Ye, X., Zhang, Q., Bai, L., and Hu, Q. (2011). A modeling study of catchment discharge to Poyang Lake under future climate in China. *Quaternary International*, 244(2):221–229.
- Ye, X., Zhang, Q., Liu, J., Li, X., and Xu, C. Y. (2013). Distinguishing the relative impacts of climate change and human activities on variation of streamflow in the Poyang Lake catchment, China. *Journal of Hydrology*, 494:83–95.
- Yih, S.-M. and Davidson, B. (1975). Identification in nonlinear, distributed parameter water quality models. *Water Resources Research*, 11(5):693–704.
- Yoshioka, H. and Unami, K. (2013). A cell-vertex finite volume scheme for solute transport equations in open channel networks. *Probabilistic Engineering Mechanics*, 31(1):30–38.
- Yu, Z., Chen, X., Zhou, B., Tian, L., Yuan, X., and Feng, L. (2012). Assessment of total suspended sediment concentrations in Poyang Lake using HJ-1A/1B CCD imagery. *Chinese Journal of Oceanology and Limnology*, 30(2):295–304.
- Zhang, L., Yao, X., Tang, C., Xu, H., Jiang, X., and Zhang, Y. (2016). Influence of long-term inundation and nutrient addition on denitrification in sandy wetland sediments from Poyang Lake, a large shallow subtropical lake in China. *Environmental Pollution*, 219:440–449.
- Zhang, P., Lu, J., Feng, L., Chen, X., Zhang, L., Xiao, X., and Liu, H. (2015a). Hydrodynamic and Inundation Modeling of China's Largest Freshwater Lake Aided by Remote Sensing Data. *Remote Sensing*, 7(4):4858–4879.

## References

---

- Zhang, Q., Li, L., Wang, Y. G., Werner, A. D., Xin, P., Jiang, T., and Barry, D. A. (2012a). Has the Three-Gorges Dam made the Poyang Lake wetlands wetter and drier? *Geophysical Research Letters*, 39(20).
- Zhang, Q. and Werner, A. D. (2015). Hysteretic relationships in inundation dynamics for a large lake–floodplain system. *Journal of Hydrology*, 527:160–171.
- Zhang, Q., Ye, X., Werner, A. D., Li, Y., Yao, J., Li, X., and Xu, C. (2014). An investigation of enhanced recessions in Poyang Lake: Comparison of Yangtze River and local catchment impacts. *Journal of Hydrology*, 517:425–434.
- Zhang, R., Qian, X., Yuan, X., Ye, R., Xia, B., and Wang, Y. (2012b). Simulation of Water Environmental Capacity and Pollution Load Reduction Using QUAL2K for Water Environmental Management. *International Journal of Environmental Research and Public Health*, 9(12):4504–4521.
- Zhang, S., Jiang, Y., Liu, X., and Wang, H. (2011). Study on dispatching scheme of Water Control Project in Poyang Lake and its influence on water resources and flood control. *Journal of China Institute of Water Resources and Hydropower Research*, 9(4):257–261.
- Zhang, Y. and Baptista, A. M. (2008). SELFE: A semi-implicit Eulerian–Lagrangian finite-element model for cross-scale ocean circulation. *Ocean Modelling*, 21(3–4):71–96.
- Zhang, Z., Chen, X., Xu, C. Y., Hong, Y., Hardy, J., and Sun, Z. (2015b). Examining the influence of river-lake interaction on the drought and water resources in the Poyang Lake basin. *Journal of Hydrology*, 522:510–521.
- Zhao, D. H., Shen, H. W., Tabios, G. Q., Lai, J. S., and Tan, W. Y. (1994). Finite-Volume Two-Dimensional Unsteady-Flow Model for River Basins. *Journal of Hydraulic Engineering*, 120(7):863–883.
- Zhao, G., Hörmann, G., Fohrer, N., Zhang, Z., and Zhai, J. (2010). Streamflow trends and climate variability impacts in Poyang Lake basin, China. *Water Resources Management*, 24(4):689–706.
- Zheleznyak, M. J., Demchenko, R. I., Khursin, S. L., Kuzmenko, Y. I., Tkulich, P. V., and Vitiuk, N. Y. (1992). Mathematical modeling of radionuclide dispersion in the Pripyat-Dnieper aquatic system after the Chernobyl accident. *Science of The Total Environment*, 112(1):89–114.
- Zhen, L., Li, F., Huang, H., Dilly, O., Liu, J., Wei, Y., Yang, L., and Cao, X. (2011). Households’ willingness to reduce pollution threats in the Poyang Lake region, southern China. *Journal of Geochemical Exploration*, 110(1):15–22.
- Zheng, L., Chen, C., and Zhang, F. Y. (2004). Development of water quality model in the Satilla River Estuary, Georgia. *Ecological Modelling*, 178(3-4):457–482.

## References

---

- Zhu, G., Qin, B., Gao, G., Zhang, L., and Fan, C. (2004). Fractionation of phosphorus in sediments and its relation with soluble phosphorus contents in shallow lakes located in the middle reaches of Changjiang River, China. *Acta Scientiae Circumstantiae*, 24(3):381–388.
- Zhu, J. and Xu, W. (1992). River network water quality model and its parameter modeling. *Journal of Hohai University*, 20(1):16–21.